

Ⓟ

F-82

PAN

**NUCLEATE POOL BOILING OF LIQUIDS  
AND  
THEIR MIXTURES AT SUBATMOSPHERIC PRESSURES**

A THESIS

*submitted in fulfilment of the  
requirements for the award of the degree*

*of*  
**DOCTOR OF PHILOSOPHY**  
*in*  
**CHEMICAL ENGINEERING**



ROORKEE CENTRAL  
178309  
11-5-85

By

**Mrs. SHASHI KRISHNA PANDEY**

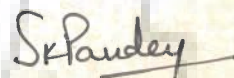


**DEPARTMENT OF CHEMICAL ENGINEERING  
UNIVERSITY OF ROORKEE  
ROORKEE-247667 (India)  
August, 1982**

## Candidate's Declaration

I hereby certify that the work which is being presented in the thesis entitled "*Nucleate Pool Boiling of Liquids and their Mixtures at Subatmospheric Pressures*" in fulfilment of the requirements for the award of the degree of **DOCTOR OF PHILOSOPHY** submitted in the Department of Chemical Engineering of the University is an authentic record of my own work carried out during a period from July 30, 1979 to August 16, 1982 under the supervision of Dr. B.S. Varshney and Dr. P.R. Sharma.

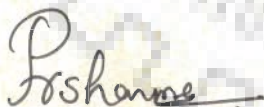
The matter embodied in this thesis has not been submitted by me for the award of any other degree.



*Sh. Pandey*

(Mrs. SHASHI KRISHNA PANDEY)

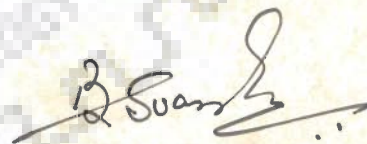
This is to certify that the above statement made by the candidate is correct to the best of our knowledge.



*P. Sharma*

(P. R. SHARMA)

Lecturer,  
Chemical Engineering Department,  
University of Roorkee,  
Roorkee-247667 (India)



*B. S. Varshney*

(B. S. VARSHNEY)

Professor & Head,  
Chemical Engineering Department,  
University of Roorkee,  
Roorkee-247667 (India)

August 16, 1982

## A B S T R A C T

The present investigation pertains to the experimental research work related to the nucleate boiling heat transfer from a horizontal 410 ASIS stainless steel cylinder to the pool of saturated liquids, and to their binary liquid mixtures both at atmospheric and subatmospheric pressures. The pure liquids used for the investigation are distilled water, ethanol, methanol and isopropanol, and the binary liquid mixtures having varying concentrations of ethanol-water, methanol-water and isopropanol-water mixtures. The heat flux ranges from  $9,618 \text{ W/m}^2$  to  $31,354 \text{ W/m}^2$  and the system pressure from  $25.33 \text{ kN/m}^2$  to  $98.63 \text{ kN/m}^2$ .

Since this investigation aims to obtain experimental data for the pool boiling of pure liquids and their binary mixtures, an experimental facility was carefully designed and raised. The experimental set-up includes provisions for the measurement of concentration of the binary liquid mixtures, electrical energy input to the heating surface, pressure over the liquid pool and temperatures of the heating surface and the boiling liquid.

The copper-constantan thermocouples measure the temperatures of the heating surface and the boiling liquid. The heating surface temperature is

measured circumferentially at the top-, the side-, and the bottom- positions at a given plane. The specially home-made travelling thermocouple probes measure the liquid bulk temperature at the three locations corresponding to the surface thermocouple positions. The surface temperature is corrected by subtracting the temperature drop across the wall thickness. From the readings of the corrected surface and the corresponding liquid temperatures, local values of  $\Delta t$  are calculated for the top-, the side-, and the bottom- positions of the heating surface. Using the 'mechanical quadrature' technique, the average values of  $\Delta T$  are obtained to calculate average heat transfer coefficient,  $\bar{h}$  over the circumference.

The concentration of the boiling binary liquid mixture,  $X$  is determined by drawing the liquid sample from the liquid sampling unit and then comparing its refractive index with the calibration curve. The refractrometer used was supplied by M/s Carl Zeiss Jena Co., West Germany. The liquid concentration is checked at several intervals of time during a given test run for a given mixture composition. The concentration in the vapour phase,  $Y$  in equilibrium with the liquid phase concentration,  $X$  is obtained from the literature.

The experimental data for the pool boiling of pure liquids at atmospheric as well as at subatmospheric pressures corroborate the validity of the well-established

relationship between the heat transfer coefficient and the heat flux for high pressures, i.e.,  $h \propto q^{0.7}$ . However, the relationship between the boiling heat transfer coefficient and the pressure for the subatmospheric pressures differs from that at high pressures. In fact, the boiling heat transfer coefficient varies with the pressure raised to the power of 0.32 for the data conducted at subatmospheric pressures, i.e.  $h \propto P^{0.32}$ .

The heat transfer data for the boiling of ethanol, methanol and isopropanol do not deviate amongst themselves, whereas they differ considerably from those of distilled water.

The experimental data for the pool boiling of pure liquids as used in this investigation and those of earlier investigators conducted on widely differing heating surfaces for the liquids possessing differing physico-thermal properties for subatmospheric pressures are correlated by the following equation within  $\pm 15$  per cent deviation :

$$\frac{\bar{h}^*}{\bar{h}_1^*} = \left( \frac{P}{P_1} \right)^{0.32}$$

where  $\bar{h}^* = (\bar{h}/q^{0.7})$ , represents a ratio of average heat transfer coefficient to heat flux raised to the power of 0.7, and  $P$  is the system pressure. The subscript, 1 corresponds to 'reference' pressure for which the value

of  $\bar{h}_1^*$  is known for a given liquid and heating surface. However, in the present investigation the 'reference' pressure chosen is one atmosphere. With the knowledge of  $\bar{h}_1^*$  and  $P_1$ , the above correlation readily determines the value of  $\bar{h}^*$  at any subatmospheric pressure for the same boiling liquid and the heating surface. Further, the above correlation is useful to check the consistency of boiling heat transfer data for a given liquid and heating surface at subatmospheric as well as atmospheric pressures.

Since this correlation is for the data conducted for different liquids on the heating surfaces possessing differing surface characteristics at subatmospheric pressures, an implication of this is that the effect of the surface-liquid combination is the same for all the pressures,  $P \ll 1$  atmosphere. It is important to note that the data for the pool boiling of liquids at high pressures could not be correlated by a correlation of the aforesaid type. This is due to the fact that the effect of surface-liquid combination is not the same for all the pressures,  $P > 1$  atmosphere.

The experimental data of binary liquid mixtures for subatmospheric pressures on a given heating surface are also correlated by the relationships :  $h \propto q^{0.7}$  and  $h \propto P^{0.32}$  which are applicable for the boiling of pure liquids. The data analysis of binary liquid mixtures shows that they are satisfied by the following correlation within  $\pm 15$  per cent like for pure liquids:

$$\frac{h^*}{h_1^*} = \left(\frac{P}{P_1}\right)^{0.32}$$

where the terms have their same meaning as described for the correlation for the pure liquids.

The addition of more volatile component to the water shows that the boiling heat transfer coefficient of the binary liquid mixture decreases upto a certain concentration, beyond which it increases. The concentration at which the heat transfer coefficient is minimum corresponds to a maximum value of [Y-X]. It is 31.10 wt. per cent ethanol, 30.80 wt. per cent methanol, and 22.5 wt. per cent isopropanol for ethanol-water, methanol-water and isopropanol-water mixtures respectively. This behaviour is shown at all the subatmospheric pressures studied. It may be noted that the actual heat transfer coefficient for any concentration of the binary liquid mixtures studied is less than the weighted heat transfer coefficient calculated from the heat transfer coefficients of the mixture in their pure states and the concentration of the mixture. This is a consistent behaviour for all the pressures investigated.

The experimental data of all the binary liquid mixtures studied lead to correlations within  $\pm 15$  per cent as follows :

(a) For the values of  $X'$  ;  $0 < X' \leq 22.0$

$$\bar{Nu}^* \left(\frac{P_1}{P}\right)^{0.32} = 3.70 \times 10^{-2} (X')^{-0.60}$$

(b) For the values of  $X'$  ;  $30.0 \leq X' \leq 78.0$

$$\bar{Nu}^* \left(\frac{P_1}{P}\right)^{0.32} = 2.51 \times 10^{-4} (X')^{0.90}$$

In the above equations  $\bar{Nu}^*$  represents the average value of the normalised Nusselt number given by the quantity

$\frac{\bar{h}}{k} \sqrt{\frac{\sigma}{(\rho_l - \rho_v)g}}$  where  $\sigma$  is the surface tension;  $k$ , the thermal conductivity of the boiling mixture;  $\rho_l$ , the liquid density and  $\rho_v$ , the vapour density.

$P$  represents the system pressure;  $P_1$ , the 'reference' pressure and  $X'$ , the wt. per cent of more volatile component in the liquid phase.

These correlations provide a procedure for calculating the boiling heat transfer coefficient of a binary liquid mixture for the aforesaid concentrations,  $X'$  at subatmospheric and atmospheric pressures on a given heating surface.



## A C K N O W L E D G E M E N T S

• The author expresses her deep sense of gratitude and indebtedness to Dr. B.S. Varshney, Professor and Head, Chemical Engineering Department and Dr. P.R. Sharma, Lecturer, Chemical Engineering Department, University of Roorkee, Roorkee, for their excellent guidance, lasting encouragement and wholehearted co-operation throughout the course of this work. Their efforts in going through the manuscript and suggestions for its improvement are gratefully acknowledged.

The author deeply appreciates the constant encouragement, help and technical discussions at various stages of the work with her husband, Shri K.S. Pandey, Research Scholar under Quality Improvement Programme in Department of Metallurgy, University of Roorkee, Roorkee.

Sincere thanks are due to Dr. S.C. Gupta, Reader in Chemical Engineering Department, University of Roorkee, Roorkee, for his help and co-operation.

Thanks are also due to Shri Chandrahas Tyagi, Lecturer in Mechanical Engineering Department, Institute of Paper Technology, Saharanpur, University of Roorkee, for his enthusiastic association and help during the initial stages of the work.

Special thanks are due to

Quality Improvement Programme, a Scheme run by Government of India to provide facilities for higher studies to Engineering Faculty ;

Thiru C. Aranganayagam, Education Minister, Tamil-Nadu and Chairman of Regional Engineering College, Tiruchirapalli, for sponsorship under Quality Improvement Programme ;

Prof. P.S. Manisundaram, Formerly Principal, Regional Engineering College, Tiruchirapalli, presently Vice-Chancellor, University of Tiruchirapalli, Tamil-Nadu, for sponsorship and help ;

Dr. S.H. Ibrahim, Professor and Head, Chemical Engineering Department, and Dr. C.R. Kandaswamy, Professor, Mechanical Engineering Department, Regional Engineering College, Tiruchirapalli, for their co-operation ;

Author's colleauges, Dr. V.R. Arunachalam and Dr. P. Subramanian, Assistant Professors and Dr. S. Sundaram, Lecturer, Chemical Engineering Department, Regional Engineering College, Tiruchirapalli, for persistent encouragement in completing this task ;

Miss Jyoti Lata Pandey, Research Scholar, Department of Metallurgy, University of Roorkee, Roorkee, for her assistance in checking the manuscript ;

Dr. S.D. Bhattacharya, Reader and Shri T.N.S. Mathur, Lecturer, Chemical Engineering Department, University of Roorkee, Roorkee, for their help ;

Shri Sunredra Singh, S.L.T., for the electrical circuits and instrumentation ;

Shri Jugendra Singh, S.L.T., for his help in fabricating equipment ;

Shri Abdul Aziz, L.A., for his assistance in commissioning the experimental set-up ;

Shri Harbans Singh, L.A., for his help during the experimentation ;

Shri Atam Prakash and Shri Y.P. Arora for their skillful draftsmanship ;

Shri V.P. Kaushish for excellent typing ;

and finally to her parents and sons for inspiration and affection.

# C O N T E N T S

	Page
ABSTRACT	i
ACKNOWLEDGEMENTS	vii
CONTENTS	x
LIST OF FIGURES	xii
LIST OF TABLES	xx
NOMENCLATURE	xxi
CHAPTER 1 INTRODUCTION	1
CHAPTER 2 LITERATURE REVIEW	6
2.1 Introduction	6
2.2 Empirical correlations for binary liquid mixtures	7
2.3 Theoretical models for bubble growth rates in binary liquid mixtures	42
CHAPTER 3 EXPERIMENTAL SET-UP	65
3.1 Design considerations	65
3.2 Description of the experimental set-up	69
3.3 Instrumentation and calibration	83
CHAPTER 4 EXPERIMENTAL PROCEDURE	89
4.1 Testing of experimental set-up	89
4.2 Operating procedure	90
4.3 Consistency of experimental data	93

Contents (contd.)		Page
CHAPTER 5	RESULTS AND DISCUSSION	97
5.1	Limitations of data processing	100
5.2	Nucleate pool boiling of pure liquids	103
5.3	Variation of $(\bar{h}^*/\bar{h}_1^*)$ with $P/P_1$ for subatmospheric pressure	129
5.4	Variation of $(\bar{h}^*/\bar{h}_1^*)$ with $P/P_1$ for superatmospheric pressure	132
5.5	Nucleate pool boiling of binary liquid mixtures	136
5.6	Variation of $\bar{h}^*/\bar{h}_1^*$ with $P/P_1$ for subatmospheric pressure	175
5.7	Generalised correlation	181
CHAPTER 6	CONCLUSIONS AND RECOMMENDATIONS	187
APPENDIX A	ANALYSIS OF ERRORS	194
APPENDIX B	TABULATION OF EXPERIMENTAL DATA	201
APPENDIX C	EVALUATION OF PHYSICO-THERMAL PROPERTIES	307
APPENDIX D	SAMPLE CALCULATIONS	329
	REFERENCES	337

## LIST OF FIGURES

	Page	
Fig. 2.1	Vapour-liquid concentration difference and heat transfer coefficient of benzene-toluene[60]	38
Fig. 2.2	Experimental data of van Wijk et al [97] for nucleate boiling of mixture	47
Fig. 2.3	Vapour bubble growth rate as a function of concentration of mixture (X, ethanol concentration) [103]	57
Fig. 3.1	Schematic diagram of experimental set-up	70
Fig. 3.2	Photographic view of experimental set-up	71
Fig. 3.3	Details of test vessel	73
Fig. 3.4	Photographic view of test vessel and auxiliary equipment	74
Fig. 3.5	Heat transfer surface and thermocouples layout	76
Fig. 3.6	Stabilized power supply system	84
Fig. 3.7	Details of selector switch and thermocouple assembly	86
Fig. 3.8	Comparison of experimental refractive index with values in literature [119] for pure liquids at 15°C	88
Fig. 4.1	Calibration curve for ethanol-water mixtures at 15°C	94

List of Figures (Contd.)	Page
Fig. 4.2 Calibration curve for methanol-water mixtures at 15°C	95
Fig. 4.3 Calibration curve for isopropanol-water mixtures at 15°C	96
Fig. 5.1 Variation of heat transfer coefficient with heat flux for distilled water at atmospheric and subatmospheric pressure	104
Fig. 5.2 Variation of heat transfer coefficient with heat flux for ethanol at atmospheric and subatmospheric pressure	105
Fig. 5.3 Variation of heat transfer coefficient with heat flux for methanol at atmospheric and subatmospheric pressure	106
Fig. 5.4 Variation of heat transfer coefficient with heat flux for isopropanol at atmospheric and subatmospheric pressure	107
Fig. 5.5 Heat transfer coefficient - heat flux relationship for isopropanol at 98.63 kN/m <sup>2</sup>	112
Fig. 5.6 Heat transfer coefficient - heat flux relationship for methanol at 66.64 kN/m <sup>2</sup>	113
Fig. 5.7 Variation of heat transfer coefficient with heat flux on a horizontal brass cylinder at 61.25 kN/m <sup>2</sup>	116
Fig. 5.8 Variation of heat transfer coefficient with heat flux for pure liquids at 98.63 kN/m <sup>2</sup>	117
Fig. 5.9 Variation of heat transfer coefficient with heat flux for pure liquids at 66.64 kN/m <sup>2</sup>	118

List of Figures (Contd.)	Page
Fig. 5.10 Variation of heat transfer coefficient with heat flux for pure liquids at $50.65 \text{ kN/m}^2$	119
Fig. 5.11 Variation of heat transfer coefficient with heat flux for pure liquids at $33.32 \text{ kN/m}^2$	120
Fig. 5.12 Variation of heat transfer coefficient with heat flux for pure liquids at $25.33 \text{ kN/m}^2$	121
Fig. 5.13 Variation of heat transfer coefficient with pressure for pure liquids	123
Fig. 5.14 Variation of heat transfer coefficient with pressure for distilled water on different heating surfaces	126
Fig. 5.15 Variation of $\bar{h}^*/\bar{h}_1^*$ with $P/P_1$ for pure liquids at subatmospheric pressures	130
Fig. 5.16 Variation of $\bar{h}^*/\bar{h}_1^*$ with $P/P_1$ for pure liquids at high pressures	133
Fig. 5.17 Variation of heat transfer coefficient with heat flux for 11.86 wt. % ethanol in ethanol-water mixture at atmospheric and subatmospheric pressure	138
Fig. 5.18 Variation of heat transfer coefficient with heat flux for 31.10 wt. % ethanol in ethanol-water mixture at atmospheric and subatmospheric pressure	139
Fig. 5.19 Variation of heat transfer coefficient with heat flux for 71.88 wt. % ethanol in ethanol-water mixture at atmospheric and subatmospheric pressure	140



List of Figures (Contd.)	Page
Fig. 5.20 Variation of heat transfer coefficient with heat flux for 8.56 wt. % methanol in methanol-water mixture at atmospheric and subatmospheric pressure	141
Fig. 5.21 Variation of heat transfer coefficient with heat flux for 30.80 wt. % methanol in methanol-water mixture at atmospheric and subatmospheric pressure	142
Fig. 5.22 Variation of heat transfer coefficient with heat flux for 64.00 wt. % methanol in methanol-water mixture at atmospheric and subatmospheric pressure	143
Fig. 5.23 Variation of heat transfer coefficient with heat flux for 15.00 wt. % isopropanol in isopropanol-water mixture at atmospheric and subatmospheric pressure	144
Fig. 5.24 Variation of heat transfer coefficient with heat flux for 22.50 wt. % isopropanol in isopropanol-water mixture at atmospheric and subatmospheric pressure	145
Fig. 5.25 Variation of heat transfer coefficient with heat flux for 77.00 wt. % isopropanol in isopropanol-water mixture at atmospheric and subatmospheric pressure	146
Fig. 5.26 Heat transfer coefficient - heat flux relationship for 19.3 wt. % water in water-ethylene glycol mixture on different heating surfaces at $98.63 \text{ kN/m}^2$	149

List of Figures (Contd.)	Page
Fig. 5.27    Variation of heat transfer coefficient with heat flux for ethanol-water mixtures at $66.64 \text{ kN/m}^2$	150
Fig. 5.28    Variation of heat transfer coefficient with heat flux for methanol-water mixtures at $33.32 \text{ kN/m}^2$	151
Fig. 5.29    Variation of heat transfer coefficient with heat flux for isopropanol-water mixtures at $98.63 \text{ kN/m}^2$	152
Fig. 5.30    Variation of normalised heat transfer coefficient with wt. % of ethanol for ethanol-water mixtures	155
Fig. 5.31    Variation of normalised heat transfer coefficient with wt. % of methanol for methanol-water mixtures	156
Fig. 5.32    Variation of normalised heat transfer coefficient with wt. % of isopropanol for isopropanol-water mixtures	157
Fig. 5.33    Variation of normalised heat transfer coefficient with wt. % of more volatile component for binary liquid mixtures at $33.32 \text{ kN/m}^2$	159
Fig. 5.34    Plot of (Y-X) vs X or X' for ethanol-water mixtures	161
Fig. 5.35    Plot of (Y-X) vs X or X' for methanol-water mixtures	162
Fig. 5.36    Plot of (Y-X) vs X or X' for isopropanol-water mixtures	163
Fig. 5.37    Variation of heat transfer coefficient with wt. % of water in binary liquid mixtures at $22.45 \times 10^3 \text{ W/m}^2$ [126]	165

List of Figures (Contd.)	Page
Fig. 5.38 Variation of normalised heat transfer coefficient with pressure for distilled water, ethanol and ethanol-water mixtures	166
Fig. 5.39 Variation of normalised heat transfer coefficient with pressure for ethanol-water mixtures	167
Fig. 5.40 Variation of normalised heat transfer coefficient with pressure for distilled water, methanol and methanol-water mixtures	169
Fig. 5.41 Variation of normalised heat transfer coefficient with pressure for methanol-water mixtures and distilled water	170
Fig. 5.42 Variation of normalised heat transfer coefficient with pressure for distilled water, isopropanol and isopropanol-water mixtures	171
Fig. 5.43 Variation of normalised heat transfer coefficient with pressure for isopropanol-water mixtures	172
Fig. 5.44 Variation of $\bar{h}^*/\bar{h}_1^*$ with $P/P_1$ for ethanol and ethanol-water mixtures	177
Fig. 5.45 Variation of $\bar{h}^*/\bar{h}_1^*$ with $P/P_1$ for methanol and methanol-water mixtures	178
Fig. 5.46 Variation of $\bar{h}^*/\bar{h}_1^*$ with $P/P_1$ for isopropanol and isopropanol-water mixtures	179
Fig. 5.47 Variation of $\bar{h}^*/\bar{h}_1^*$ with $P/P_1$ for pure liquids and alcohol -water mixtures	180

List of Figures (Contd.)	Page
Fig. 5.48 Plot of $\bar{Nu}^*(P_1/P)^{0.32}$ vs $X'$ for ethanol-water mixtures	182
Fig. 5.49 Plot of $\bar{Nu}^*(P_1/P)^{0.32}$ vs $X'$ for methanol-water mixtures	183
Fig. 5.50 Plot of $\bar{Nu}^*(P_1/P)^{0.32}$ vs $X'$ for isopropanol-water mixtures	184
Fig. 5.51 Plot of $\bar{Nu}^*(P_1/P)^{0.32}$ vs $X'$ for alcohol-water mixtures	185
Fig. C.1 Variation of liquid and vapour densities with saturation temperature for pure liquids	308
Fig. C.2 Variation of surface tension and viscosity with saturation temperature for pure liquids	309
Fig. C.3 Variation of thermal conductivity with saturation temperature for pure liquids	310
Fig. C.4 Variation of latent heat of vaporization and saturation pressure with saturation temperature for pure liquids	311
Fig. C.5 Variation of specific heat with saturation temperature for pure liquids	312
Fig. C.6 Variation of mole per cent of ethanol in vapour phase with saturation pressure for ethanol-water mixtures	317
Fig. C.7 Variation of saturation pressure with saturation temperature for ethanol-water mixtures	318
Fig. C.8 Variation of liquid and vapour densities of ethanol-water mixtures with saturation temperature	319

List of Figures (Contd.)	Page
Fig. C.9 Variation of surface tension and thermal conductivity with saturation temperature for ethanol-water mixtures	320
Fig. C.10 Variation of mole per cent of methanol in vapour-phase with saturation pressure for methanol-water mixtures	321
Fig. C.11 Variation of saturation pressure with saturation temperature for methanol-water mixtures	322
Fig. C.12 Variation of liquid and vapour densities of methanol-water mixtures with saturation temperature	323
Fig. C.13 Variation of surface tension and thermal conductivity with saturation temperature for methanol-water mixtures	324
Fig. C.14 Variation of mole per cent of isopropanol in vapour phase with saturation pressure for isopropanol-water mixtures	325
Fig. C.15 Variation of saturation pressure with saturation temperature for isopropanol-water mixtures	326
Fig. C.16 Variation of liquid and vapour densities of isopropanol-water mixtures with saturation temperature	327
Fig. C.17 Variation of surface tension and thermal conductivity with saturation temperature for isopropanol-water mixtures	328

## LIST OF TABLES

	Page	
Table 2.1	Values of constant $A_0$ for binary mixtures in Equation (2.21)	20
Table 2.2	Average absolute deviations of correlations [36-38] with data of Clements and Colver [39]	24
Table 2.3	Values of constant E in Equation (2.31)	27
Table 5.1	Parameters for saturated nucleate pool boiling studies	97
Table 5.2	Parameters for earlier studies in nucleate pool boiling of pure liquids	114
Table 5.3	Values of constant, $C_1$ in Equation (5.3) for pure liquids at subatmospheric pressures	128
Table 5.4	Values of constant, $C_1$ in Equation (5.3) for pure liquids at high pressures	135
Table 5.5	Values of constant, $C_{m1}$ in Equation (5.7) for binary liquid mixtures at subatmospheric pressures	173

## N O M E N C L A T U R E

$A$	heat transfer area	$m^2$
$C$	constant of proportionality as defined in Equation (5.2)	
$C_1$	constant of proportionality as defined in Equation (5.3)	
$C_m$	constant of proportionality as defined in Equation (5.5)	
$C_{m1}$	constant of proportionality as defined in Equation (5.7)	
$d$	diameter of the heating surface	$m$
$d_h$	diameter of the circle passing through the centre of the thermocouple hole as defined in Equation (D.2)	$m$
$d_i$	inside diameter of the heating surface	$m$
$d_o$	outside diameter of the heating surface	$m$
$D$	Laplace constant	$m$
$D_b$	diameter of the bubble at departure	$m$
$f$	bubble emission frequency	$s^{-1}$
$g$	acceleration due to gravity	$m/s^2$
$h$	heat transfer coefficient	$W/m^2 K$
$\bar{h}$	average heat transfer coefficient	$W/m^2 K$
$h^*$	normalised heat transfer coefficient ( $h/q^{0.7}$ )	$W^{0.3}/m^{0.6} K$
$\bar{h}^*$	normalised average heat transfer coefficient at a pressure ( $\bar{h}/q^{0.7}$ )	$W^{0.3}/m^{0.6} K$
$k$	thermal conductivity of pure liquids	$W/m K$
$k_m$	thermal conductivity of binary liquid mixture	$W/m K$

$\ell$	length of the heating surface	m
M	average molecular weight of the binary liquid mixture	kg/kg mole
P	pressure	N/m <sup>2</sup>
$\Delta P$	pressure difference	N/m <sup>2</sup>
q	heat flux	W/m <sup>2</sup>
$R_{\min}$	minimum radius of curvature of a nucleation site	m
S	surface area of a spherical bubble	m <sup>2</sup>
$S_0$	surface area of a spherical bubble at base	m <sup>2</sup>
T	temperature	K or °C
$\bar{T}$	average temperature	K or °C
$\Delta T$	temperature difference, ( $T_w - T_\ell$ )	K or °C
$\overline{\Delta T}$	average temperature difference	K or °C
$\Delta T_w$	wall superheat ( $T_w - T_s$ )	K or °C
$\overline{\Delta T}_w$	average wall superheat	K or °C
$\delta T_w$	temperature drop across the wall as defined in Equation (D.1)	K or °C
X	mole per cent of more volatile component of binary mixture in liquid-phase	
$X'$	weight per cent of more volatile component of binary mixture in liquid-phase	
Y	mole per cent of more volatile component of binary mixture in vapour-phase	
y	mole fraction of more volatile component of binary mixture in vapour phase	



## Greek Symbols

$\sigma$	surface tension	N/m
$\rho$	density	Kg/m <sup>3</sup>
$\lambda$	latent heat of vaporization	J/Kg
$\mu$	dynamic viscosity	N s/m <sup>2</sup>
$\nu$	kinematic viscosity	m <sup>2</sup> /s
$\alpha$	thermal diffusivity, $k/C\rho$	m <sup>2</sup> /s
$\beta$	contact angle	rad.
$\theta$	time	s
$\eta$	refractive index	

## Dimensionless Modulii

Ja Jakob number

$$\frac{C_l \rho_l \Delta T_w}{\rho_v \lambda}$$

$\overline{Nu}$  Average Nusselt number

$$\frac{\overline{h}}{k} \sqrt{\frac{\sigma}{(\rho_l - \rho_v)g}}$$

## Subscripts

$l$  liquid

$v$  vapour

$w$  wall

## C H A P T E R - 1

### INTRODUCTION

Nucleate pool boiling heat transfer finds wide applications in process, power, refrigeration, and allied industries. This has prompted many research workers to undertake investigations related to different aspects of boiling heat transfer, namely ; the boiling curve, the bubble dynamics on the heating surface including the number of nucleation sites, bubble growth rates, the bubble departure diameter, the bubble emission frequency and many others. In fact these studies contribute immensely to our knowledge to understand the boiling heat transfer process scientificall. However, much more research inputs are needed to exploit these areas of research for better understanding of the subject.

The knowledge of boiling heat transfer pertaining to the determination of the parametric effects of the heat flux, the system pressure, the physico-thermal properties of boiling liquids and the heating surface characteristics on the pool boiling heat transfer coefficient is of immediate applications for the design of the evaporators, the reboilers, the vapourisers, and many other alike heat transfer equipment of industrial importance. Consequently, a large number of experimental data have been conducted for the boiling

of water on widely differing heating surfaces generally for high pressures. These data have resulted in obtaining a plethora of correlations for calculating the pool boiling heat transfer coefficient incorporating the effect of heat flux, pressure, properties of boiling liquid and surface-liquid combination factor. In fact, no generalised correlation for pool boiling heat transfer exists. Besides, different investigators have used different dimensionless groups in their respective correlations. In addition to this, the surface-liquid combination factor is another parameter which has unique value depending upon the system used. The research inputs of different investigators, one by one, have failed to generalise the values of surface-liquid combination factor.

The above mentioned observations corroborate the fact that the boiling heat transfer at high pressure still needs further investigations to evolve a generalised correlation like other convective heat transfer processes.

Further, a survey of the literature shows that the experimental data for the boiling of liquids other than water on widely differing heating surfaces at subatmospheric pressures are scarce. It may be noted that the correlations for the boiling of liquids at high pressures are inadequate to correlate the data conducted at low pressures. Hence, there is an absolute need to investigate the pool boiling heat

transfer data for organic liquids at low pressures, especially at subatmospheric pressures, then to establish the functional relationship relating heat transfer coefficient to heat flux, pressure and physico-thermal properties of boiling liquids. There is also a need to scrutinise the value of the constant appearing in the correlation for heat transfer coefficient which incorporates the effect of heating surface characteristics and the boiling liquid enveloping the heating surface.

The nucleate pool boiling heat transfer data and the design correlation for the calculation of heat transfer coefficient for the binary liquid mixtures represent another need-based research area which is of paramount importance in process industries. This has its distinct applications in the design of reboilers, evaporators and vapourisers. This may be noted that, in absence of any experimental data, the design engineer has been calculating the weighted heat transfer coefficient for any concentration of the binary mixture from the knowledge of the heat transfer coefficients of the constituents of the liquid mixture in their pure state. The recent studies, though not enough, indicate that the weighted heat transfer coefficient is much different from the actual experimental values. A review of the literature suggests that there is almost a vacuum of the experimental data for the boiling of different binary liquid mixtures, especially for the subatmospheric pressures. Obviously, the literature is almost devoid

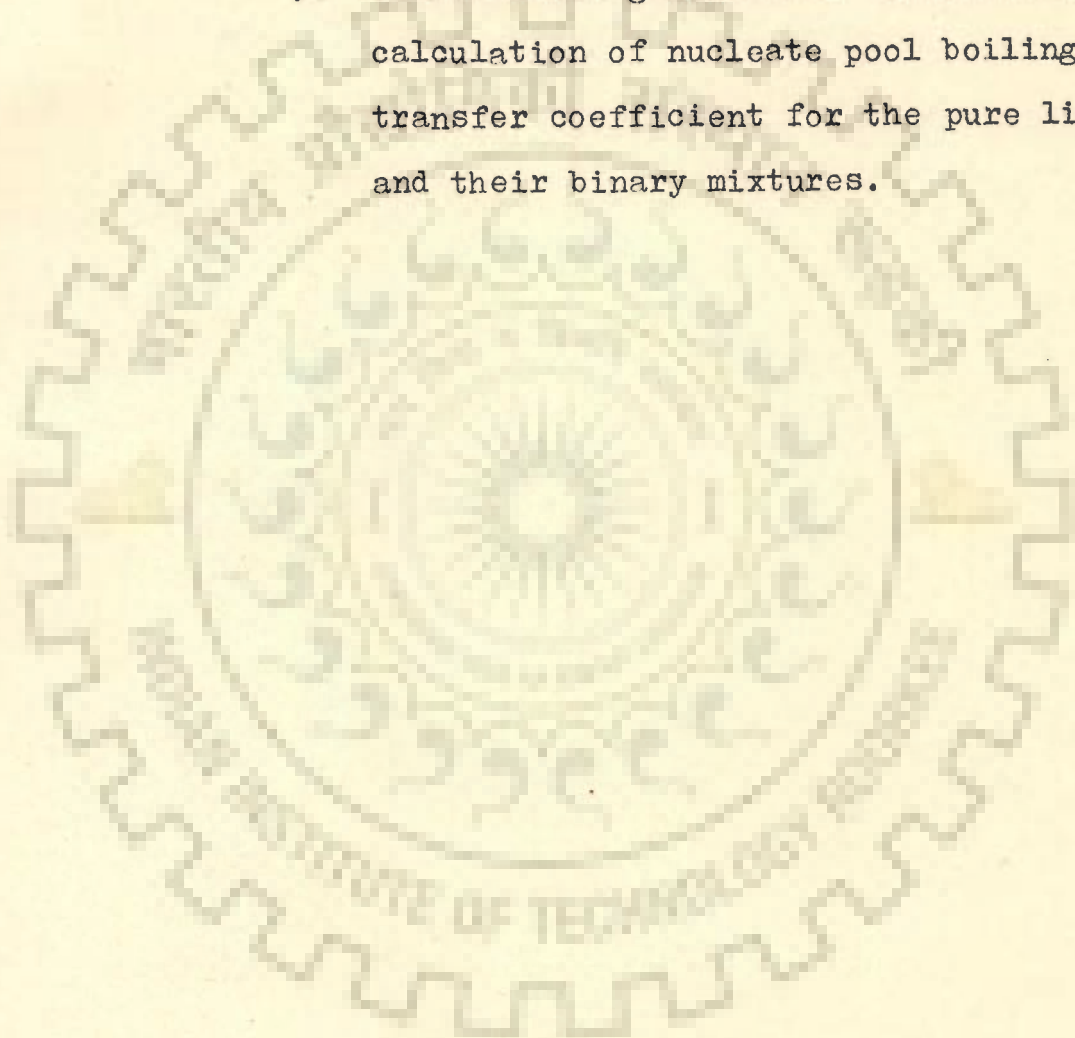
of the pertinent information relating the pool boiling heat transfer coefficient of the binary liquid mixture to the heat flux, the pressure, the physico-thermal properties, and the heating surface characteristics. This demands a relevant investigation leading to suitable design correlation to be employed for the design of evaporators, reboilers, vapourisers, and alike process equipment.

Considering the above mentioned observations, the present investigation was planned with the following objectives :

1. To raise an experimental set-up for carrying out the nucleate pool boiling heat transfer data at atmospheric and subatmospheric pressures for the liquids and their binary liquid mixtures.
2. To obtain experimental data for the nucleate pool boiling of pure liquids at atmospheric and subatmospheric pressures for water and alcohols; ethanol, methanol and isopropanol.
3. To generate experimental data for the nucleate pool boiling heat transfer coefficient of aqueous binary alcohol mixtures both for atmospheric and subatmospheric pressures and thereby to determine the effect of concentration of binary liquid mixtures on

the boiling heat transfer coefficient.

4. To ascertain the effect of surface-liquid combination for the boiling of pure liquids and aforesaid binary liquid mixtures at atmospheric and subatmospheric pressures.
5. To recommend generalised correlation for the calculation of nucleate pool boiling heat transfer coefficient for the pure liquids and their binary mixtures.



## CHAPTER - 2

### LITERATURE REVIEW

#### 2.1 INTRODUCTION

Nucleate pool boiling of binary and polynary liquid mixtures is an important field of research from the view point of its ultimate application in improving the design of heat transfer equipment largely employed in chemical and allied industries. The aim in itself is difficult to achieve firstly, because of the difficulties inherited in understanding the complicated nature of the boiling process and then extending this information successfully to the practical problems. Literature is almost silent except a few exceptions [1-7], with regard to study the overall performance of such piece of equipment where nucleate boiling of binary and multicomponent liquid mixtures is encountered. However, large efforts have been made mainly in two directions : (i) experimental studies to generate data and proposing the empirical correlations to evaluate heat transfer coefficients and critical heat fluxes (ii) theoretical studies to understand the basic principles involved in bubble growth rates and bubble emission frequencies in nucleate pool boiling of pure and binary liquid mixtures.

This chapter reviews, in brief, the published literature on the above two aspects for the boiling of binary liquid mixtures excluding the studies regarding critical heat fluxes. Exhaustive literature review for nucleate pool boiling of pure liquids has been reported recently by Sharma [8] and it is not intended to repeat the survey again. However, in view of the above mentioned objectives, some of the empirical correlations and studies on bubble growth rates for pure liquids have been mentioned, wherever necessary.

## 2.2 EMPIRICAL CORRELATIONS FOR BINARY LIQUID MIXTURES

Probably the earliest work in the area of nucleate pool boiling of binary liquid mixtures is attributed to Cryder and Finalborgo [9]. In their efforts to generate the experimental data for pool boiling of pure liquids at subatmospheric pressures they have taken a binary mixture and two aqueous solutions. The binary mixture was 26 wt. % glycerol in water-glycerol and aqueous solutions were 10 wt.% sodium sulfate and 24 wt.% sodium chloride. The saturation temperature of water-glycerol ranged from  $68.88^{\circ}\text{C}$  to  $113.3^{\circ}\text{C}$  and heat flux from  $8141 \text{ W/m}^2$  to  $41,868 \text{ W/m}^2$ .

Bonilla and Perry [10] are the pioneer investigators who took as many as six binary mixtures of water-ethanol, water-acetone, water-butanol, ethanol-butanol



ethanol-acetone and butanol-acetone with a fairly wide range of composition. A horizontal chromium plate was used as a heating surface. In some of their mixtures, Bonilla and Perry [10] have found a maximum heat flux in nucleate boiling exceeding somewhat than that of either of the pure components. However, no systematic investigation about the influence of concentration was made and the increase of maximum heat flux mentioned by them was very moderate.

Cichelli and Bonilla [11] investigated mixtures of water-ethanol and propane- n-heptane boiling on a horizontal copper chrome-plated plate heated electrically. They took 33 wt. % and 80 wt. % propane-n-heptane mixtures and conducted experiments at high pressures ranging from 4 to 32 bars. The heat flux ranged from  $2.9075 \times 10^3$  to  $5.815 \times 10^5$  W/m<sup>2</sup>. They proposed the following equations for calculating heat transfer coefficient :

$$h = 1.07 q^{0.7} \left( \frac{P}{17.93} \right)^{0.53} \quad \dots(2.1)$$

$$h = 19 q^{0.7} P^{0.62} \quad \dots(2.2)$$

It is interesting to note that both the above equations contain no concentration terms.

Bonilla and Eisenberg [12] conducted experimental data on water-styrene and water-butadiene mixtures. These data are useful for rubber industries.

Bonnet and Gerster [1] took mixtures of  $C_4$ -hydrocarbons and furfural and conducted experiments on these systems at atmospheric pressure.

Kirschbaum [13,14] in two separate investigations employed three binary mixtures; water-ethanol, benzene-toluene and water-glycerol. He has found that in 20 wt. % solution of glycerol in water the overall heat transfer coefficient was raised by a factor of two as compared with pure water at the same degree of wall superheat,  $\Delta T = 20^\circ C$ . He obtained this maxima also for a 50 wt. % solution of glycerol. He attributes this behaviour to foaming. No sufficient data are, however, given to conclude that why the maximum heat flux was reached in this case.

Chernobylskii and Lukach [15] calculated the heat transfer coefficient during boiling of two binary mixtures viz. benzene-toluene and ethanol-water of varying compositions. They conducted their experiments at atmospheric pressure and in the heat flux range  $18.61 \times 10^3$  to  $15.12 \times 10^4$   $W/m^2$ . The results for these binary mixtures were expressed in the conventional form i.e.  $h = c q^n$ . The values of  $c$  and  $n$  vary with concentration of the more volatile component in the mixture.

Chi-Fang-Lin et al [16] undertook an investigation for nucleate pool boiling of liquid binary mixtures of ethanol-water and benzene-toluene at subatmospheric

pressures. The value of the pressure ranged from 200 to 760 mm Hg. They worked at relatively low values of heat flux ranging from 4652 to 46520 W/m<sup>2</sup>. The concentration range was wide in their investigation. The concentration of ethanol in ethanol-water were 5, 25, 60 and 91.8 per cent by weight and that of benzene in benzene-toluene mixtures were 8, 12, 25, 50, 75, 88 and 100 wt. per cent. They calculated the experimental values of heat transfer coefficient and correlated their data by modifying Kruzhilin's equation [17] within  $\pm 10$  per cent deviation as given below :

$$Nu_B = 0.71 Pr^{0.45} Kq^{0.57} Ku^{0.33} \dots(2.3)$$

where  $Ku = \frac{1}{Kt}$  and  $Kt$  is criterion for bubble break-off frequency and  $Kq = Re.Pr.Kt$

A good deal of experimental work was conducted by Sternling and Tichacek [18] to determine the heat transfer coefficient in pool boiling for fourteen saturated binary mixtures at atmospheric conditions. The mixtures chosen for investigation were both ideal solutions or mixtures with strong positive and negative deviations from Raoult's law. All the mixtures had a wide boiling range of at least 90°C. They used the same thin stainless steel tubing of diameter 4.51 mm for all the experiments. Heating was done by alternating current. The compositions and heat fluxes used were of very wide range unlike other earlier investigators.

For all the binary mixtures, heat transfer coefficient at a given heat flux decreased markedly with the addition of a more volatile component until a specific composition was attained. At this composition a turnaround was observed and heat transfer coefficients started increasing. This turnaround behaviour has been attributed to the change in bubble dynamics with the addition of more volatile component in a pure liquid.

Huber and Hoehne [19] studied the pool boiling of benzene, diphenyl and benzene-diphenyl mixtures at pressures more than atmospheric ( $93.08 \times 10^3$  to  $3368 \times 10^3 \text{ N/m}^2$ ) boiling on a 9.525 mm O.D. horizontal tube. They correlated their experimental heat transfer coefficients with the correlations proposed for pure liquids by Rohsenow [20,21], Gilmour [22] and Levy [23]. They observed that the wall superheat in the boiling benzene-diphenyl mixture was found to be two or three times those of pure liquids at all pressures.

Palen and Small [2] were probably the first to propose a correlation for calculating heat transfer coefficient for binary mixtures. They proposed that the heat transfer coefficient for binary mixtures should be calculated for the equivalent pure liquid multiplied by a correction factor,  $f$ , given by;

$$f = \exp [-0.015(T_{\text{sat},\infty} - T_{\text{sat},y=x_{\infty}})] \quad \dots(2.4)$$

where  $T_{\text{sat}, y=x_{\infty}}$  is the dew point of a vapour of the same composition as the bulk liquid and  $T_{\text{sat}, \infty}$  is the dew point of the vapour in equilibrium with the bulk liquid, i.e. the bulk liquid bubble point.

Tolubinskii and Ostrovskii [24] undertook an investigation to measure the vapour bubble growth rate in pool boiling of ethanol-water and ethanol-butanol mixtures at atmospheric pressure. They reported that the vapour bubble growth decreased with increase in the difference of concentrations of more volatile component in vapour and liquid phases. The experimental values of Nusselt number for the ethanol-water mixture were correlated by

$$\text{Nu}_B = 75 \text{Kq}^{0.7} \text{Pr}^{-0.2} [1-(Y-X)]^{1.85} \quad \dots(2.5)$$

Afgan [25] conducted experiments for boiling of ethanol, benzene and their mixtures on a cylindrical tube of diameter 5.12 mm heated by direct-current. The pressure varied from 6 atm to 15 atm. He correlated the pure component data with the equation :

$$\text{Nu} = 9.44 \times 10^{-4} \text{Re}^{0.7} \text{Kp}^{0.7} \text{Pr}^{0.35} \quad \dots(2.6)$$

where  $\text{Kp}$  is the criterion for pressure term.

The bubble departure diameter in the above equation is that of Fritz [26].

For mixtures, Afgan used weight fractions of 0.1, 0.2, 0.5, 0.8 and 0.9. For constant heat flux, he noted that plots of heat transfer coefficient against concentration showed maxima and minima. These roughly corresponded, respectively, with minima and maxima of the absolute values of the differences of equilibrium concentration in the two phases, i.e.  $(Y-X)$  where  $Y$  is the vapour concentration in equilibrium with  $X$ . It may be noted that  $(Y-X)$  is related simply to  $\Delta T_b / G_d$  where  $G_d$  is the vaporised molar fraction of the liquid near the surface. On the basis of this observation Afgan suggested that the mixture data could be correlated by a single equation of the form of Equation (2.6) but with a multiplier which depends on  $(Y-X)$ . This multiplier was found to be given by

$$9.44 \times 10^{-4} [1 - K(Y-X)] \quad \dots(2.7)$$

which reduces to  $9.44 \times 10^{-4}$  for pure substances and azeotropic mixtures. According to Afgan the value of  $K$  depends on the particular components of a mixture.

Ivanov [27] studied the boiling heat transfer of refrigerant mixtures of F-12 and F-22 for heat fluxes varying from 2,000 to 25,000  $W/m^2$  and temperature from 240 K to 293 K. The experimental data showed a minimum value of heat transfer coefficient between 15 to 35 per cent concentration of less volatile component, F-22. Ivanov has employed the method of

corresponding state which was suggested by Borishanskii [28] for boiling of liquids in their pure state. He recommends the following equation for computing heat transfer coefficient :

$$\frac{h/q^{0.75}}{h^*/q^{0.75}} = f \left( \frac{P}{P^*} \right) \quad \dots(2.8)$$

where  $P^* = 0.03 P_c^S$

$P_c^S$  is the pseudocritical pressure of the mixture and can be calculated as below taking into account the relative volatility

$$P_c^S = (P_c)_{F-12} + \Psi [(P_c)_{F-22} - (P_c)_{F-12}] \quad \dots(2.9)$$

$\Psi$  is the relative volatility and is given by

$$\Psi = \frac{Y_{F-22} [1 - X_{F-22}]}{X_{F-22} [1 - Y_{F-22}]} \quad \dots(2.10)$$

and  $P_c$  is the critical pressure.

Klimenko and Kozitskii [29] took an investigation to calculate heat transfer coefficients during the boiling of light hydrocarbon mixtures. They correlated heat transfer coefficient in terms of critical properties of the hydrocarbon mixture and heat flux. Their equation is as follows :

$$h = 320 \left[ P_{\text{crit}}^{0.3} T_{\text{crit}}^{-0.85} M_{\text{crit}}^{-0.15} \right] \left[ 0.62 + 3.0 P_m / T_{\text{crit}} \right] F^{-m} q^{0.7} \dots (2.11)$$

where  $F$  is a function for multicomponent mixtures, subscript  $m$  refers to mean value.

Filatkin [30], in his paper, studied the heat transfer to water-ammonia solution in pool boiling on a horizontal tube 28 mm diameter and 450 mm long. He plotted the heat transfer coefficient as a function of the liquid-phase concentration and heat flux as parameter. He observed that the solution with an ammonia concentration of approximately 0.4 has the minimum heat transfer coefficient. One of the reasons attributed to this reduction in heat transfer coefficient is that as the concentration difference between the vapour and liquid phase (the quantity,  $Y-X$ ) increases the number of nucleation sites decrease and so the heat transfer coefficient. The larger the difference in concentration ( $Y-X$ ) the larger the minimum radius of the cavity from which a vapour bubble may originate, grow and finally depart. This is attributed to the minima in heat transfer coefficient.

Based on the theory of similarity, Filatkin proposed the following correlation :

$$\frac{h}{k} \sqrt{\frac{\sigma}{(\rho_l - \rho_v)}} = D \left( \frac{\alpha}{D} \right)^{0.45} \left[ \frac{C (\sigma^{0.5} T_s \rho_l (\rho_l - \rho_v)^{0.5})}{J (\lambda \rho_v)^2} \right]^{0.33} \left[ \frac{J \rho_v \lambda q}{T_s k (\rho_l - \rho_v)} \right]^n \dots (2.12)$$



Equation (2.12) is applicable for the following conditions :

(i)  $Pr = 1.3$  to  $4.8$

(ii) 
$$\frac{C_p \sigma^{0.5} T_s p (p - p_v)^{0.5}}{J (\lambda p_v)^2} = 1.0 \times 10^{-4} \text{ to } 206.0 \times 10^{-4}$$

(iii) 
$$\frac{J p_v \lambda q}{T_s k (p - p_v)} = 0.3 \text{ to } 40.4$$

The values of  $n$  and  $D$  are calculated by the following equations :

$$n = 0.70 - 0.24 (Y-X) \quad \dots(2.13)$$

$$D = 0.083 + 0.33 (Y-X) \quad \dots(2.14)$$

Filatkin [30] concluded that the effect of Prandtl number on heat transfer coefficient is less noticeable. He also concluded that the pressure appears to increase the system heat transfer coefficient at low rate.

Tolubinskii and Ostrovskii [31] studied the mechanism of heat transfer in nucleate pool boiling of binary mixtures. They generated data for heat transfer coefficients, bubble departure diameters and bubble frequencies for boiling of methanol-water, ethanol-water, ethanol-n-butanol and ethanol-benzene on a stainless steel tube of diameter 4.5 mm heated by direct current. They indicated that the presence of mixtures affect the nucleation site density in comparison to pure

liquids and showed that for a given heat flux,  $h$ ,  $D_b$  and the product  $fD_b$  attains a minima when  $(Y-x)$  is at its maxima.

With the aid of dimensional analysis and ethanol-water experimental data over the entire range of concentration they recommended the following equation for product  $fD_b$  and Nusselt number :

$$(fD_b)_m = [(fD_b)_{\text{water}}(1-x'_{\infty}) + (fD_b)_{\text{ethanol}} x'_{\infty}] \left[ 1 - \frac{(Y'_{\infty} - x'_{\infty})^2}{Y'_{\infty}(1-x'_{\infty})} \right]^{1.15} \dots(2.15)$$

$$\text{Nu} = \left\{ \frac{q}{\lambda F_v [(fD_b)_{\text{water}}(1-x'_{\infty}) + (fD_b)_{\text{ethanol}} x'_{\infty}]} \right\}^{0.7} \left\{ \frac{c_l \mu_l}{k_l} \right\}^{-0.2} \left[ 1 - \frac{(Y'_{\infty} - x'_{\infty})^2}{Y'_{\infty}(1-x'_{\infty})} \right]^{1.6} \dots(2.16)$$

where,

$x'_{\infty}$  is mass fraction in liquid phase far from bubble

$Y'_{\infty}$  is equilibrium mass fraction in vapour far from bubble

The above equations are, thus, not general for all mixtures and even for ethanol-water, their use require prior information for the determination of  $fD_b$  factor for pure components.

Stephen and Körner [32] developed another empirical correlation for calculating heat transfer coefficients based on their extensive experimental work on seventeen different binary mixtures for pressures ranging from 1 to 10 bar. They undertook a thermodynamic analysis to find necessary free energy of formation for a bubble in a mixture growing in superheated liquid of infinite extent. Their expression for free energy of formation is :

$$\Delta G^+ = \frac{16\pi}{3} \sigma^3 \frac{(\bar{V}_V - \bar{V}_L)^2}{(\Delta T_{\text{sat}})^2 \left[ \frac{\bar{h}_V - \bar{h}_L}{T_{\text{sat}}} + \left\{ (y^* - x) \left( \frac{\partial^2 \bar{G}}{\partial x^2} \right)_{T,P} \frac{\Delta x}{\Delta T_b} \right\} \right]^2} \dots (2.17)$$

where  $\bar{V}_V$  and  $\bar{V}_L$  are molar volumes,  $\bar{h}_V$  and  $\bar{h}_L$  are molar enthalpies of vapour and liquid respectively,  $\Delta x$  is change of concentration and  $\Delta T_b$  is change in saturation temperature due to change of concentration.

Certain important conclusions arise from an inspection of the group  $(y^* - x) \left( \frac{\partial^2 \bar{G}}{\partial x^2} \right) \frac{\Delta x}{\Delta T_b}$  of Equation (2.17). By applying Konovalov's rule (the vapour is richer than the liquid with which it is in equilibrium in that component by addition of which to the system the vapour pressure is raised) one can deduce that  $y^* - x$  and  $\frac{\Delta x}{\Delta T_b}$  are always of opposite sign and the basic rules of thermodynamic equilibrium (Stephen and Körner assumed the mixture to be in thermodynamic equilibrium) predict that  $\left( \frac{\partial^2 \bar{G}}{\partial x^2} \right)_{T,P}$  is always positive.

Thus the above term is always negative for all mixtures and the free energy change is increased in mixtures resulting in the increase of work for the formation of vapour bubbles and hence decreasing the heat transfer coefficient.

From this reasoning Stephan and Körner [32] argued that where the ideal heat transfer coefficient is obtained as a linear function of mole fraction, the actual coefficient will be less by an amount proportional to  $(y^* - x)$ . Thus these investigators developed their correlation in the following form :

$$\frac{\Delta T_{\text{sat},w}}{\Delta T_{\text{sat},w,\text{ideal}}} = 1 + \theta \quad \dots(2.18)$$

where

$$\Delta T_{\text{sat},w,\text{ideal}} = x_{\infty} \Delta T_{\text{sat},w,A} + (1-x_{\infty}) \Delta T_{\text{sat},w,B} \quad \dots(2.19)$$

$\Delta T_{\text{sat},w,A}$  and  $B$  are the wall superheats for pure components boiling on the same surface and at the same heat flux as the mixture in question.

$\Delta T_{\text{sat},w}$  is actual wall superheat for the mixture in question

and  $\theta$  represents the deviation from the ideal situation due to mass transfer resistance and is related to the concentration difference by

$$\theta = A ( y^* - x ) \quad \dots(2.20)$$

where  $A$  is a function of pressure and is different for every binary mixture.

Stephan and Körner using published data from a variety of sources found the following expression to evaluate  $A$  :

$$A = A_0 (0.88 + 0.12P) \quad \dots(2.21)$$

where  $P$  is in bar and  $A_0$  is a constant which depends only on the nature of the two components and is independent of concentration. Table 2.1 shows their calculated values as reported by Stephan and Körner [32]:

Table 2.1 : Values of constant,  $A_0$  for some Binary Mixtures in Equation (2.21)

Binary Mixture	$A_0$
Acetone - Ethanol	0.75
Acetone - Butanol	1.18
Acetone - Water	1.40
Ethanol - Benzene	0.42
Ethanol - Cyclohexane	1.31
Ethanol - Water	1.21
Benzene - Toluene	1.44
Heptane - Methylcyclohexane	1.95
Isopropanol - Water	2.04
Methylethyl Ketone - Toluene	1.32
Methanol - Benzene	1.08
Methanol - Amyl alcohol	0.80
n-propanol - water	3.29
Methylethylketone - Water	1.21
Water - Glycol	1.47
Water - Pyridine	3.56
Water - Glycerine	1.50

Stephan and Körner tested their correlation for above mentioned 17 binary mixtures by taking  $A_0$  values as listed above and pressures 1 to 10 bar. They concluded that their data can be represented with an average quadratic deviation of  $\pm 8.6$  per cent. Using a generalised value of  $A_0$  equal to 1.53 for the same mixtures, they found an average quadratic deviation of 15 per cent and hence recommended this value when no other is available.

Tolubinskiĭ and Ostrovskii [33] undertook an investigation to understand the heat transfer mechanism to saturated boiling water-glycerine mixtures at atmospheric pressure. The glycerine concentration was taken upto 96 wt. per cent. It was observed that with increasing glycerine concentration upto 70 wt. per cent the bubble departure diameter,  $D_b$  increased slightly and bubble emission frequency,  $f$  reduced. For glycerine concentration greater than 70 wt. per cent, both the bubble departure diameter and frequency fell rapidly.

Contrary to low-boiling liquids, it was observed in this case that there is continuous reduction in the value of heat transfer coefficient with increase in glycerine concentration and no intermediate minima is observed even upto 96 wt. per cent glycerine.

Takeda et al [34] conducted experiments with pure water, methanol, ethanol, MEK and acetone and with mixtures of water and the later four organics on a

copper plate and a thin platinum wire (0.2 mm diameter). They produced a correlation based on dimensional analysis. In their correlation they have taken the variables for mixtures same as that for pure liquids. Hence their correlation for all the boiling data is :

$$\left( \frac{\rho_v \lambda}{C_\lambda \rho_\lambda \Delta T_{\text{sat}}} \right) \left( \frac{C_\lambda \mu_\lambda}{k_\lambda} \right)^{0.67}$$

$$= 1.00 \times 10^{-2} \left( \frac{D_b \cdot q \cdot \rho_\lambda}{\mu_\lambda \lambda \rho_v} \right)^{-0.35} \left( \frac{p^2}{g \sigma \rho_\lambda} \right)^{0.25}$$

$$\text{St} \cdot \text{Pr}^{0.67} = 1.00 \times 10^{-2} \text{Re}^{-0.35} \cdot \text{II}^{0.25} \dots (2.22)$$

In the above equation  $D_b$  is given by Fritz [26]. Takeda et al have plotted  $\text{St} \cdot \text{Pr}^{0.67} \cdot \text{II}^{-0.25}$  vs  $\text{Re}$  for their own data and data of different investigators [10,11]. They have not indicated the magnitude of the scatter of their data on the plot. However, there seems to be some deviation and probably this is attributed to the omission of any parameters which take into account the effect of mixture properties.

Wright et al [35] conducted experiments for nucleate and film boiling heat transfer to the pure ethane and ethylene and their mixtures containing 0.25, 0.50 and 0.75 mole fraction of ethylene. The test-section was a direct-current heated, gold-plated tube of diameter 20.6 mm and length 89 mm. They conducted their experiments at atmospheric ( $9.807 \times 10^4 \text{ N/m}^2$ ) and subatmospheric ( $7.355 \times 10^4 \text{ N/m}^2$ ) pressures. The data

were compared with the correlations of Borishanskii et al [36], Kutateladze [37] and McNelly [38] which were all devised for pure coolants. Borishanskii et al correlation correlated the data with an average deviation of 48.7 per cent while both Kutateladze and McNelly correlation with an average deviation of 42 per cent. A least square fit of the data showed that the best correlation was obtained by modifying the equation of Rohsenow [20] in the following form :

$$\frac{q}{\lambda} \frac{D_b}{\mu_l} = 683.3 \left[ \frac{C_l \Delta T}{\lambda} \left( \frac{T}{F_r} \right)^{1.18} \right]^{1.243} \dots (2.23)$$

where  $D_b$  is bubble departure diameter given by Fritz [26].

Clements and Colver [39] extended their work [35] for saturated boiling of propane, n-butane and n-pentane, and of mixtures of propane with n-butane and n-pentane on the test section described above [35]. They also extended the range of pressure upto  $3 \times 10^6$  N/m<sup>2</sup>. From the experimental data they prepared plots of wall superheat vs concentration for each heat flux and observed that the position of the maxima is roughly coinciding with that of maximum  $(Y_{\infty}^* - X_{\infty})$ , that means the value of heat transfer coefficient is minimum at maximum  $(Y_{\infty}^* - X_{\infty})$ . The data for these liquids were also compared with the above mentioned correlations [36-38] and average absolute deviation are shown below in Table 2.2.



Table 2.2 : Average Absolute Deviations of Correlations [36-38] with Data of Clements and Colver[39]

Correlation	Pure Components	Mixtures	
	%	Unmodified %	Modified %
Borishanskii et al [36]	39.9	266.9	96.9
Kutateladze [37]	42.5	92.7	37.8
McNelly [38]	33.1	101.3	30.3

From the above Table it is clear that McNelly correlation [38] gives the best results. However, for binary mixture these equations are not adequate which is evident by the results shown in the above Table. To correlate the data for binary mixtures with the help of these equations Clements and Colver [39] modified these equations by introducing the term relative volatility,  $\alpha_{\infty}$ , which takes into account the mass transfer resistance effects.  $\alpha_{\infty}$  is defined as :

$$\alpha_{\infty} = \frac{Y_{\infty}^* (1-x_{\infty})}{X_{\infty} (1-y_{\infty}^*)} \dots(2.24)$$

A least square fit of the data showed that the best correlation was obtained by introducing into each of the basic equations, the term  $\alpha_{\infty}^{-0.5}$ . Thus modified correlations are as follows :

Modified Borishanskii et al correlation ;

$$\frac{q D_b}{k \Delta T_w} = 8.7 \times 10^{-4} \alpha_{\infty}^{-0.5} \left[ \frac{q D_b}{\alpha \rho_v \lambda} \right]^{0.7} \left[ \frac{P D_b}{\sigma} \right]^{0.7} \dots (2.25)$$

Modified Kutateladze correlation ;

$$\frac{q D_b}{k \Delta T_w} = 7.0 \times 10^{-4} \alpha_{\infty}^{-0.5} \left[ \frac{q D_b}{\alpha \rho_v \lambda} \right]^{0.7} \left[ \frac{P D_b}{\sigma} \right]^{0.7} \left[ \frac{C \mu_{\ell}}{k_{\ell}} \right]^{-0.35} \dots (2.26)$$

Modified McNelly correlation ;

$$\frac{q d}{k \Delta T_w} = 0.255 \alpha_{\infty}^{-0.5} \left[ \frac{q d}{\lambda \mu_L} \right]^{0.69} \left[ \frac{P d}{\sigma} \right]^{0.31} \left[ \frac{\rho_{\ell}}{\rho_v} - 1 \right]^{0.33} \left[ \frac{C \mu_{\ell}}{k_{\ell}} \right]^{0.69} \dots (2.27)$$

In Equation (2.27),  $d$  is a characteristic dimension of the heating surface.

With these modified correlations, Clements and Colver [39] correlated their data and observed that modified forms of the Kutateladze and McNelly equations predict the data for mixtures as accurate as the original equations predict for pure liquids.

Calus and Rice [40] undertook a comprehensive investigation for pool boiling of binary liquid mixtures. They obtained pool boiling data for 7 concentrations of isopropanol in water and 9 concentrations of acetone in water, as well as for 3 pure components. The heat transfer surface was a nickel-aluminium-alloy wire of 0.315 mm diameter and 89 mm test-section length, heated by direct current. They used a different wire taken from the same spool with its diameter 0.315 mm and the test-section length 72.6 mm for acetone-water mixtures.

Calus and Rice observed that the growth rate equations of Scriven [41] and van Stralen [42-45] for a bubble growing in an infinite volume of superheated liquid are the same and these equations can be transformed into the following more convenient form :

$$R = \left(\frac{12}{\pi}\right)^{0.5} \frac{\Delta T \alpha^{0.5} t^{0.5}}{\frac{\rho_v \lambda}{\rho_l c_l} \left[ 1 - (y^* - x) \left(\frac{\alpha}{D}\right)^{0.5} \left(\frac{c_l}{\lambda}\right) \left(\frac{dT_{sat}}{dx}\right) \right]} \quad \dots(2.28)$$

Calus and Rice argued that the contents of the square bracket in the denominator of the above equation form a correction due to simultaneous heat and mass transfer. The mass diffusion is a considerably slower process than the heat diffusion and hence the dimensionless ratio  $(\alpha/D)^{0.5}$  in Equation (2.28) is a measure of the additional resistance to heat transfer, the term  $(y^* - x)$  indicates the driving force for that diffusion.

In order to incorporate suitable correction factor to pure liquids for the determination of binary heat transfer coefficients, two factors were tried :

$$1 - (y^* - x) \left(\frac{\alpha}{D}\right)^{0.5} \left(\frac{c_l}{\lambda}\right) \left(\frac{dT}{dx}\right) \quad \dots(2.29)$$

and

$$1 + (y^* - x) \left(\frac{\alpha}{D}\right)^{0.5} \quad \dots(2.30)$$

It was found by these investigators that the correction factor given by Equation (2.30) corresponds very closely with the variation in the Nusselt number. Thus the final

form of the correlation for binary liquid mixtures included the heat and mass transfer term  $1+(y^*-x)(\frac{\alpha}{D})^{0.5}$  in the Borishanskii - Minchenko correlation [36] modified earlier by Rice and Calus [46]

$$\left[ \frac{Nu}{K_P^{0.7}} \right] \left[ \frac{T_s}{T_{sw}} \right]^4 = E \left[ \frac{Pe}{1+(y^*-x)(\frac{\alpha}{D})^{0.5}} \right]^{0.7} \dots(2.31)$$

Calus and Rice determined the value of E in the above equation for their own data (binary as well as pure liquids) and those for Sternling and Tichacek [18] data for aqueous solutions of glycol and glycerol. Table 2.3 gives the values of E for these liquids :

Table 2.3 : Values for Constant E in Equation (2.31)

System	Heat transfer Surface	Constant E in Equation(2.31)
Isopropanol-Water	Nickel-aluminium alloy, 'Wire 200' [40]	$5.8 \times 10^{-4}$
Acetone-Water	Nickel-aluminium alloy, 'Wire 24' [40]	$4.7 \times 10^{-4}$
Water-Glycerol	Stainless steel hypodermic tubing [18]	$12.2 \times 10^{-4}$
Water-Glycol	Stainless steel hypodermic tubing [18]	$11.4 \times 10^{-4}$
Seven single component liquids	Nickel-aluminium alloy [46]	$6.3 \times 10^{-4}$

An inspection of the above Table shows that unique values of  $E$  hold over these ranges, and that the values were roughly the same as for the pure components on very similar wires. This confirms that it is the surface which is an important part in the surface-liquid combination factor. The slight difference in the multipliers for the mixtures from the  $6.3 \times 10^{-4}$  which applied to the wire as used for the pure liquids was attributed to the different degrees of aging of the surfaces. With these values of  $E$  for Sternling and Tichacek data [18], Equation (2.31) correlated their 85 per cent of the experimental data points within  $\pm 20$  per cent accuracy limits. This error is mainly for the less concentrated solutions and this discrepancy was attributed to larger error in the extrapolated values of mass diffusivity for these less concentrated solutions.

Isshiki and Nikai [47] conducted experiments on nucleate pool boiling of binary mixtures of water-ethanol, water-ethylene glycol and water-n-butanol. They have determined characteristic nucleate boiling curves and burnout heat fluxes for these mixtures. From these results they have confirmed that there exists a minimum heat transfer coefficient at a certain concentration, and that more than twice the value of the burnout heat flux for pure liquids can be obtained at a very low concentration of the more volatile component. In order to explain these results they developed a one-dimensional

model of heat and mass transfer on bubble growth in a binary liquid mixture. From this model, they concluded that the temperature of the vapour-liquid interface is higher than the saturation temperature of the bulk liquid mixture and that the temperature difference between superheated bulk and vapour-liquid interface (effective superheat) has a minimum value at a certain concentration.

Tolubinskiy et al [48] studied the effect of pressure on the boiling heat transfer rate in water-ethanol mixtures, at pressures upto 15 bars and over the entire range of concentrations. The mixture under study was boiled in a vertical test element consisting of a stainless steel tube heated by direct current. The heat flux density,  $q$  at the heated section was varied from  $0.5 \times 10^4$  to  $0.8 \times 10^6$  W/m<sup>2</sup>. Observations were carried out with the various values of heat flux density and it was found by monitoring the mixture composition before and after the experiments that it remained constant during the experiments.

Tolubinskiy et al observed that boiling of water-ethanol mixtures at elevated pressures involves the same mechanism as boiling at atmospheric pressure i.e. reduction in the heat transfer rate in the range of maximum excess concentration ( $y^* - x$ ) of the low-boiling temperature component as a result of simultaneous reduction in the rate of growth of vapour bubbles and in the number of effective nucleation sites as compared

with pure components. Consequently, the boiling of binary mixtures at elevated pressures involves the same regularities as at atmospheric pressure. This made it possible to use an empirical expression for the boiling heat transfer coefficient for mixtures at atmospheric pressure for the case at hand, by supplementing it by a term which provides allowance for the pressure :

$$h_{\text{mix}} = \left\{ [A_{h.b}(1-x') + A_{\lambda.b}x'] - \frac{A_{h.b}}{A_{\lambda.b}} \right\} \Delta x^{0.7} P^n q^{0.7} \dots(2.32)$$

For the water-ethanol mixtures under study  $A_{h.b} = 3.05P^{0.2}$ ,  $A_{\lambda.b} = 1.5P^{0.4}$ ,  $n=0.4$ . The above correlation correlated the bulk of the data within  $\pm 20$  per cent.

In an attempt to modify the earlier correlations proposed by Stephan and Körner [32] and Calus and Rice [40], Calus and Leonidopoulos [49] have carried out an extensive investigation for pool boiling data for pure n-propanol, pure water and their eleven mixtures at atmospheric pressure. Like previous studies of Calus and Rice [40,46] the test-section in this study [49] was also a nickel-aluminium alloy wire, which was stabilized by an annealing process and by prolonged boiling. The diameter and length of the wire were 0.3 mm and 72.6 mm respectively.

The main purpose of the work of Calus and Leonidopoulos [49] was to modify the constant A in Equation (2.20) given by Stephan and Körner [32].

Stephan and Körner have stated that the value of  $A$  can be regarded as constant for the entire range of concentrations in the case of mixtures having a vapour-liquid equilibrium relationship approaching ideal behaviour. But it is observed and also indicated by Stephan and Körner themselves that to treat  $A$  as a constant is a major approximation for the binary mixtures behaving as highly non-ideal. The binary mixtures of n-propylalcohol and water chosen by Calus et al is an example having a highly non-ideal vapour-liquid equilibrium relationship. In view of this, it was thought necessary to modify the existing correlation of Stephan and Körner [32].

Calus and Leonidopoulos [49], based on the analytical work of Scriven [41], van Stralen [42-45] and Stephan and Körner [32] successfully replaced constant  $A$  in Equation (2.20) in terms of the vapour-liquid equilibrium relationship, the transport properties and the thermodynamic properties of the binary mixture. Thus their final correlation emerges in the following form :

$$\Delta T = (\Delta T_1 x_1 + \Delta T_2 x_2) \left[ 1 + (x - y^*) \left( \frac{\alpha}{D} \right)^{0.5} \left( \frac{C}{\lambda} \right) \left( \frac{dT}{dx} \right) \right] \dots (2.33)$$

where  $\Delta T$ ,  $\Delta T_1$  and  $\Delta T_2$  are the  $(T_{\text{wall}} - T_{\text{sat}})$  differences for the mixture of concentration  $x$ , for the pure component 1 and for the pure component 2, respectively,



required for obtaining the same heat flux. All the quantities in Equation (2.33) are based on the weight fraction concentrations. The use of above equation requires knowledge of the variation of the factor

$[(x-y^*)(\frac{\alpha}{D})^{0.5}(\frac{C}{\lambda})(\frac{dT}{dx})]$  with concentration. The gradient of the boiling point curve,  $\frac{dT}{dx}$ , was obtained by fitting a polynomial to the curve  $T=f(x)$  and subsequently differentiating it with respect to  $x$ .

The specific feature of the Equation (2.33) is that it has no experimental constants and can be used to predict either nucleate boiling heat transfer coefficients or boiling curves for binary liquid mixtures provided the boiling curves for the pure components, obtained on the same heat transfer surface are available. Although the variable factor  $[(x-y^*)(\frac{\alpha}{D})^{0.5}(\frac{C}{\lambda})(\frac{dT}{dx})]$  is strictly applicable to the process of a bubble growing in an infinite superheated liquid, the Equation (2.33) was successful in correlating 84 experimental data points for nucleate pool boiling of n-propylalcohol-water mixtures on a heat transfer surface within  $\pm 16.6$  per cent, indicating that analytical work of Scriven [41] for vapour bubble growing in a superheated infinite liquid is adequately helpful for vapour bubble growing on a heat transfer surface.

In another study Tolubinskii et al [50] studied boiling heat transfer rate from benzene-ethanol mixtures as a function of pressure. The experimental study was

carried out over the pressure range of 1-18 bars, heat flux densities of  $10^4$  to  $3.5 \times 10^5$  W/m<sup>2</sup> and concentrations of 0-100 per cent. The mixtures boiled on a vertical stainless steel element, 4.5/0.3 mm in diameter and 50 mm long, directly heated by direct current. For this system, two minima of heat transfer coefficient in the region of extremal values of  $(y^*-x)$  and an intermediate maximum at the azeotropic composition of the binary mixture were observed.

Ohnishi and Tajima [51] undertook an investigation to study the pool boiling heat transfer to lithium bromide-water solutions at subatmospheric pressures. The work is being reported in this literature review because it pertains to subatmospheric pressures. The boiling was carried out on a 20 mm diameter and 150 mm long horizontal copper cylinder finished with 0.5 grade emery paper. The pressure varied from 30 mm Hg to 300 mm Hg, the concentration 0 to 55 wt. per cent lithium bromide, and the heat flux 0 to  $3.489 \times 10^4$  W/m<sup>2</sup>. Ohnishi and Tajima have shown variation in boiling curves with pressure and concentration and made following conclusions:

- (i) The heat transfer coefficient for lithium bromide solution is fairly small than that of pure water at all the pressures investigated.
- (ii) The boiling phenomena is least affected by changing the pressure in the concentration range of 30-55 per cent, whereas the boiling

phenomena of lithium bromide-water solution are largely affected by the change in concentration at a given pressure.

- (iii) The boiling phenomena of lithium bromide-water solution are scarcely affected by the conditions of the heating surface.

Ohnishi and Tajima were able to correlate their experimental data by the Nishikawa-Yamagata [52] equation within the limits of error  $\pm 20$  per cent.

Chashchin et al [53] investigated experimentally the effect of some organic alcohols namely; propyl, butyl, amyl, octyl, polyvinyl and glycerine when added to water, on heat transfer during boiling. The experiments were carried out on a set-up consisting of an air-tight vessel with 5 litres capacity. They studied the dependence of the heat transfer coefficient on the concentration of each additive, number of carbon atoms and hydroxyl groups in an alcohol molecule. They found that the dependence of heat transfer coefficient on concentration for all additives has an extremal character. Optimum concentrations and corresponding maximum value of the heat transfer coefficient were determined for each additive.

Styushin and Astaf'ev [54] have studied the effect of diffusion processes on boiling of solutions. They have demonstrated some of the special characteristics of the dependence of the heat transfer coefficient on

the concentration of solutions and the process parameters.

Kravchenko et al [55] have suggested the equations for calculating boiling heat transfer coefficients for light hydrocarbons and ethylene-ethane mixtures.

Yusufova and Chernyakhovskiy [56] have presented the experimental investigation for heat transfer in pool boiling of six binary mixtures over wide range of pressure and concentration. The mixtures investigated were, benzene-toluene, benzene-isooctane, acetone-water, benzene-xylene, methylethylketone-water and acetone-methylethylketone . They have examined the data in view of current knowledge of boiling heat transfer.

Styushin and Astaf'ev [57] have made the analysis regarding the dependence of heat transfer coefficient on the concentration of the low boiling component in binary mixtures. They have studied three binary mixtures, water-ammonium hydroxide, ethanol-benzene and water-n-propanol. They have also analysed the position of maximum on heat transfer coefficient-composition curve in accordance to the equilibrium data of these mixtures.

Thome and Bold [58] have studied the nucleate pool boiling in cryogenic binary mixtures. They obtained the pool boiling curves for liquid nitrogen, argon and their mixtures at 1 atm and 1.3 atm pressures. They observed a minimum heat flux in the mixtures and compared their results with the existing correlations

of Happel and Stephan [59] and Calus and Leonidopoulos [49] but neither is found satisfactory.

Happel [60] has recently studied heat transfer during boiling of binary mixtures in the regimes of both nucleate and film boiling. In this survey the work pertaining to nucleate boiling will only be discussed. Happel has conducted measurements of boiling heat transfer with mixtures of benzene-toluene, ethanol-benzene and water-isobutanol in a pressure range of 0.5-2 bar as well as with refrigerants in a pressure range of 0.5-30 bar. The test surface was a pure nickel horizontal tube having an outside diameter of 14 mm. The integrated roughness of the tube was 0.43  $\mu\text{m}$ . Provision was made to heat the tube both by the electricity and passing a hot stabilized fluid through the tube.

Happel has discussed, in brief, the mechanism of nucleate pool boiling in binary liquid mixtures. He reaffirmed that in boiling of mixtures, there is mass transfer of the volatile fraction through the mixture to the growing bubble in addition to heat transfer. As a result of this diffusion resistance, the heat transfer coefficient for the mixture is reduced. He concluded that larger the concentration difference  $(Y-X)$ , Stronger is the reduction in heat transfer coefficient. The reduction of heat transfer as compared with that for pure substances can be represented in terms of a simple power law of  $(Y-X)$  as follows :

$$\frac{h_{\text{eff}}}{h_{\text{id}}} = 1 - K_{\text{st}}[Y-X]^n \quad \dots(2.34)$$

where,  $h_{\text{eff}}$  is the effective heat transfer coefficient and  $h_{\text{id}} = h_{10}(1-X) + h_{20} X \quad \dots(2.35)$

thus  $h_{\text{id}}$  (id for ideal) should be obtainable from the values of the pure components  $h_{10}$  and  $h_{20}$ .

$K_{\text{st}}$  depends only on the substance and on the pressure. For a given pressure the values of  $K_{\text{st}}$  and  $n$  can be determined by experiments at only two different mixture compositions.

The behaviour, viz., that the location of the lowest heat transfer coefficient coincides with that of the largest concentration difference is shown clearly in Figure 2.1 for the system benzene-toluene and for a heat flux of  $q = 10^5 \text{ W/m}^2$ .

For the benzene-toluene system at atmospheric pressure the experimental values of  $K_{\text{st}}=1.5$  and  $n = 1.4$ .

An inspection of Figure 2.1 shows that at higher pressures there is a steeper drop in the value of  $h_{\text{eff}}$ . According to Grigoryev[61], nucleus density generally increases with pressure because the work that must be done to form a viable bubble increases with pressure, calling for larger heat transfer. However, in a mixture, as the concentration difference increases, the heavier, less volatile fraction exhibits a stronger

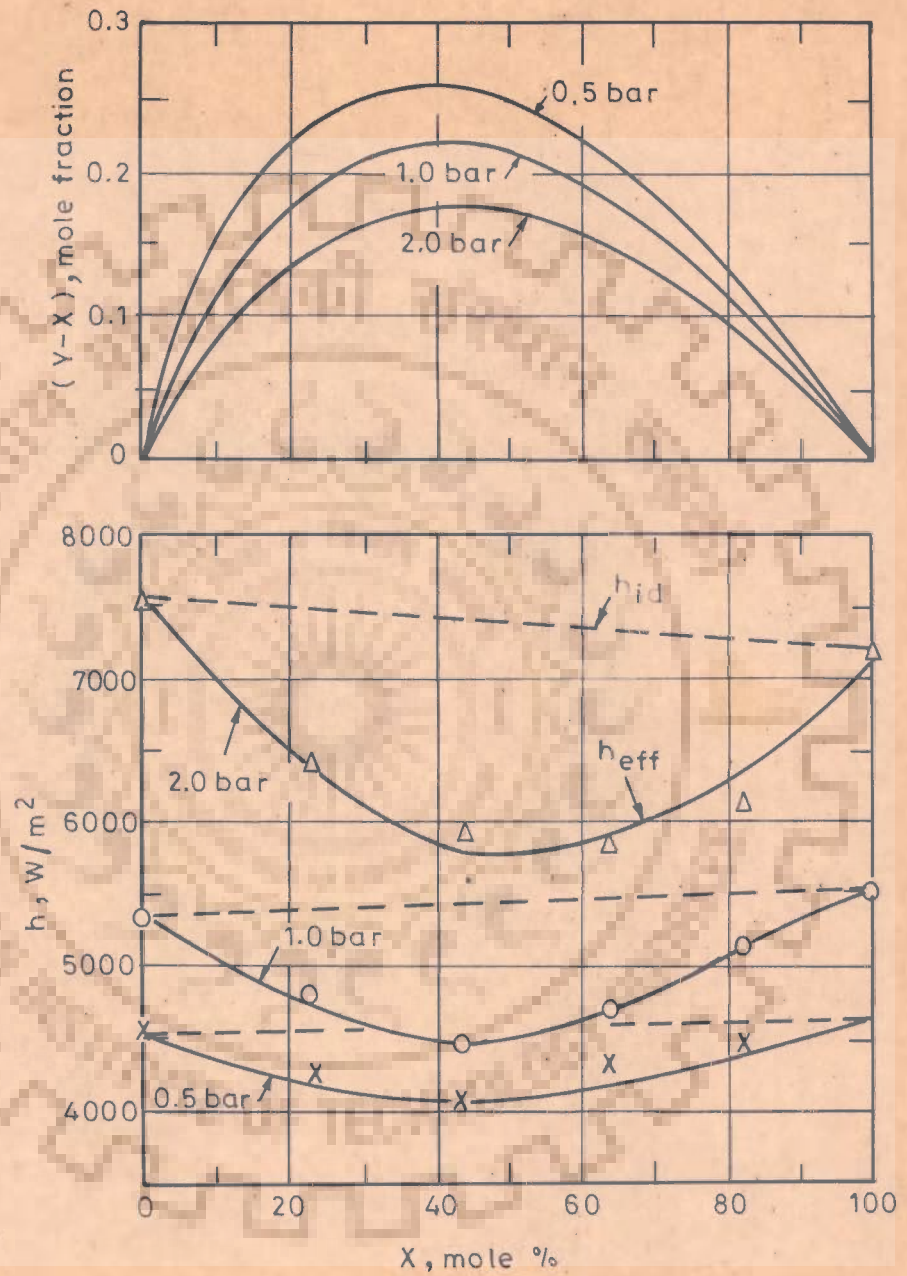


Fig.2.1-Vapour-liquid concentration difference and heat transfer coefficient of benzene-toluene [60]

tendency to accumulate at the wall. This means that the energy necessary for the formation of a viable nucleus increases and the nucleus density again decreases. This effect apparently predominates at higher pressures, which explains the relatively strong reduction of heat transfer at high pressures as compared to that at lower pressures, with the concentration difference (Y-X) being equal.

Von Hoffman [62] has dealt with pool boiling of nitrogen, methane, ethane and mixtures of nitrogen-methane and methane-ethane at different pressures. The heat transfer surface was a horizontal plane copper disk. He has analyzed the results for pure liquids as well as their binaries.

Stephan and Preusser [63] studied heat transfer in nucleate boiling of 16 binary and 25 ternary compositions consisting of acetone, methanol and water. In their experiments, they used a horizontal Nickel tube of 14 mm O.D., 550 mm length and a mean roughness of about 0.25  $\mu\text{m}$ . Experiments on pool boiling of mixtures mostly conducted on miscible binary mixtures close to atmospheric pressure, clearly indicate a reduction in heat transfer as compared with that for pure substances. This effect is explained by the more ready evaporation of the volatile fraction in binary mixtures which creates a concentration difference between the liquid and the vapour bubble, thus building up a diffusion resistance in addition to



the thermal resistance. Thermodynamic equilibrium has been assumed at the interface between vapour bubbles and liquid and, therefore, Gibbs potential in binary mixtures proves also to be larger than that of a hypothetical reference mixture. This reference mixture has been defined by authors [63] to have the same thermodynamic properties as the real binary mixture but vanishing difference in composition between liquid and vapour phase.

In binary mixtures, the reduction in heat transfer coefficients depends on the difference in the mole fractions between both phases. It increases with the difference in mole fractions and vanishes at azeotropic points. Empirical correlations on pool boiling heat transfer in binary mixtures, therefore, usually contain  $(x-y^*)$  as one of the most relevant parameters [25,49].

Stephan and Preusser [63] have plotted the heat transfer coefficients of binary mixture acetone-methanol against the composition for a heat flux of  $10^5 \text{ W/m}^2$ . From this plot, they concluded that the heat transfer coefficients are smaller than those for the reference mixture and also smaller than the heat transfer coefficients of the pure components. The later conclusion confirms the observations of Bonilla and Perry [10].

Stephan and Preusser [64,65] in these investigations attempted to calculate the boiling heat transfer coefficient of ternary mixtures from the data of pure components and binary mixtures. They have conducted the experiments with two ternary mixtures of organic components and of binary mixtures at atmospheric pressure boiling on a horizontal nickel tube. They have recommended that for rough estimation, the heat transfer in the boiling of ternary mixtures can be calculated from the data of corresponding binary mixtures with the expanded formulation of the correlation of Stephan and Körner [32] for binary mixtures. Further, an equation is derived for heat transfer in the boiling of mixtures, in which the non-linear variation of the material properties has been taken into account.

Stephan and Abdelsalam [66] attempted to present guidelines for predicting heat transfer coefficients in natural convection boiling. In order to establish correlations with wide application, the methods of regression analysis were applied to nearly 5000 existing experimental data points for natural convection boiling heat transfer. As demonstrated by the analysis, these data can best be represented by subdividing the substances into four groups depending upon their physico-thermal properties. The four groups were water, hydrocarbons, cryogenic fluids and refrigerants. Each set of group employed a different set of dimensionless numbers to

correlate the data for the calculation of approximate value of heat transfer coefficient.

### 2.3 THEORETICAL MODELS FOR BUBBLE GROWTH RATES IN BINARY LIQUID MIXTURES

There exists a large number of theoretical papers on the growth of vapour bubbles in pure boiling liquids [67-95], but relatively lesser number of publications [41-45, 96-114] have appeared in the literature on the vapour bubble growth rates in binary liquid mixtures. This Section reviews, in brief, the bubble growth rates in nucleate pool boiling of binary liquid mixtures only.

Scriven [41] is the first investigator who has comprehensively developed a theoretical model on the dynamics of vapour bubble growth rates both for pure and binary liquid mixtures. Starting with the fundamental equations of continuity, motion, energy flow and mass flow, he derived a relationship from which the bubble radius of a spherical symmetry in a quiescent superheated liquid of infinite extent can be calculated as a function of time. To facilitate the solution of the equations he made number of simplifying assumptions :

- (i) Newtonian liquid
- (ii) liquid of constant density
- (iii) viscous, inertia and surface energy terms are neglected

- (iv) energy is transferred to the bubble by ordinary conduction alone
- (v) mass is transferred by ordinary diffusion with constant mass diffusivity value
- (vi) two component system having constant physico-thermal properties in both the liquid and vapour phase
- (vii) heat of mixing of two components is negligible
- (viii) specific heat capacities of both the components are equal
- (ix) vapour-liquid equilibrium relationship is linear and equilibrium is assumed at the interface.

The governing differential equations are sufficiently complex and the bubble growth rates cannot be represented by an analytical solution of the equations in closed form. Scriven [41] reported his final results in the following form :

$$R = 2\beta \sqrt{\alpha \theta} \quad \dots(2.36)$$

where, R is bubble radius,  $\beta$  is growth constant;

$\alpha$ , thermal diffusivity and  $\theta$ , time co-ordinate.

The above equation is applicable to situations with large superheats. The value of  $\beta$  is defined approximately by the following expression :

$$\beta \equiv \left[ \left( \frac{2}{\pi} \right) \left\{ \frac{\Delta T_{\text{sat}}}{P_v \left[ \frac{\lambda}{C_l} - (y' P_l - C_{\infty}) \sqrt{\alpha/D} / \left( \frac{\partial C}{\partial T} \right)_P \right]} \right\} \right]^{0.5}; \beta \gg 0, w \ll 1 \quad \dots(2.37)$$

where  $y'$  is mass fraction in vapour phase,  $C_{\infty}$  is mass

concentration at large value of radial co-ordinate,  $D$  is mass diffusivity and  $w = \frac{P_v}{P}$ .

An expression for radius  $R$  is given by :

$$R \cong \left(\frac{12}{\pi}\right)^{0.5} \left[ \frac{\Delta T_{\text{sat}} (P \lambda C k \theta)^{0.5}}{P_v \left\{ \lambda + \frac{[(y' P - C_{\infty}) R_g T_{\text{sat}}^2 (1 - \alpha_{\infty})]}{C_{\infty} \lambda_1 [M_2 C_{\infty} + (P \lambda - C_{\infty}) M_1]} [1 + \alpha_{\infty} \cdot \frac{\lambda_2 (P \lambda - C_{\infty})}{\lambda_1 C_{\infty}}] \sqrt{\frac{P C k}{D}} \right\}} \right] \dots (2.38)$$

where  $R_g$  is gas constant,  $\alpha_{\infty}$  is relative volatility,  $\lambda_1$  and  $\lambda_2$  are latent heat of vaporisation of solute and solvent,  $M_1$  and  $M_2$  are molecular weights of solute and solvent.

The latent heat is taken to be a linear function of concentration.

Scriven [41] concludes that lower the concentration of volatile material or the mass diffusivity, the greater is the superheat required to attain a given bubble growth constant.

Using numerical techniques, Scriven suggested value of  $\beta$  for two mixtures, ethylene glycol-water and glycerol-water at atmospheric pressure.

van Stralen and his associates [96-98] started working in the area of pool boiling of binary mixtures around 1956. Probably the basic aim of their study was to obtain the suitable parameters so that the peak heat

flux could be increased considerably by adding an appropriate quantity of some suitable component to the pure liquid. In one of their earliest work [96], they studied boiling of water-methylethylketone mixtures (0, 4.2, 20, 52, 88.5 and 100 wt. per cent of MEK) on 99.99 per cent pure platinum wire of diameter 0.2 mm and on a nichrome wire of 0.8 mm heated by direct current. These investigators observed that with increasing concentration of MEK a gradual shift of the curves to lower heat transfer occurred, except for the 4.2 and 20 wt. per cent mixtures, where a noticeably high maximum heat flux of 2.5 and 2.0 times that of water was found. This higher heat flux was obtained at the same temperature of the heating surface as for water, or alternatively, the same heat flux was obtained at a lower surface temperature. The same behaviour was observed with all the heating wires used by them. This peculiar behaviour was attributed to characteristic properties of the liquid mixtures themselves and not of different metals and alloys of which wires were made.

In continuation to above work [96] van Wijk and co-workers [97] studied maximum heat flux in nucleate boiling for mixtures of water with acetone, methylethylketone, alcohols ranging in molar mass from ethanol to n-octanol, and ethylene glycol respectively. They also used mixtures of dioxane with methanol and of 2-chloroethanol with di-iso-propylether. They examined boiling curves and critical heat fluxes. In all these cases the bulk liquid were at saturation temperatures. Figure 2.2

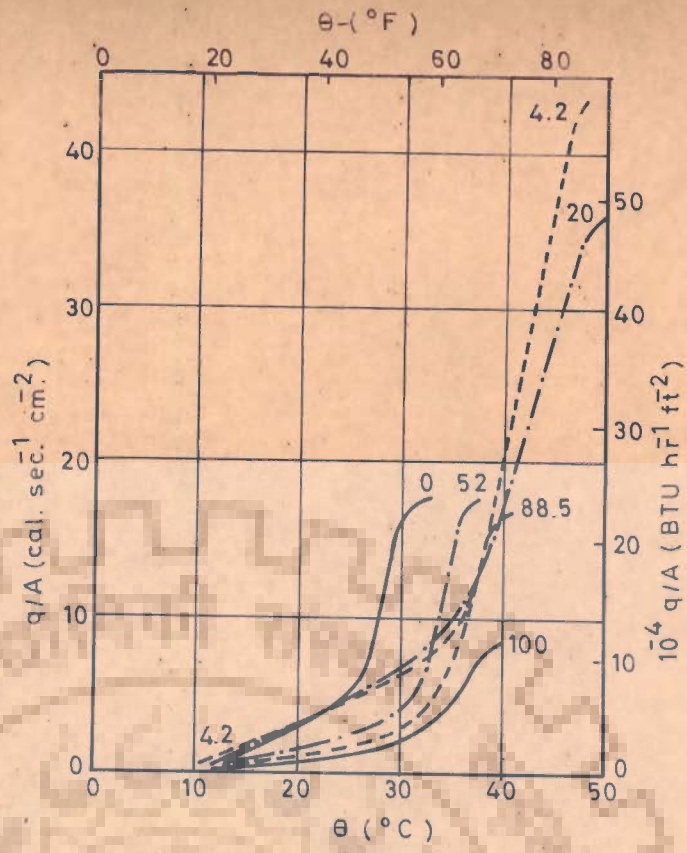
depicts the boiling curve for water-MEK mixture which is typical for mixtures. The pattern of the curve shows the considerably reduced heat transfer rates in a 4.2 wt. per cent aqueous solution of MEK as compared with that in pure water. It is also seen that the critical heat flux shows a pronounced maximum at this concentration. In all mixtures (for other liquids) a maximum value of critical heat flux for nucleate boiling occurs at a certain concentration.

The occurrence of the maxima is explained qualitatively by van Wijk et al and the explanation is as follows : the liquid layer at the bubble boundary becomes richer than at the bulk in the heavier component due to the preferential stripping of the lighter component. Hence the bubble point at the bubble boundary is higher than in the bulk and the wire superheat relative to saturation at the boundary is less than that relative to the saturation in the bulk. If the bulk of the liquid is of composition  $x_{\infty}$  and a molar fraction  $G_d$  of the liquid near the surface is vaporized, a material balance gives :

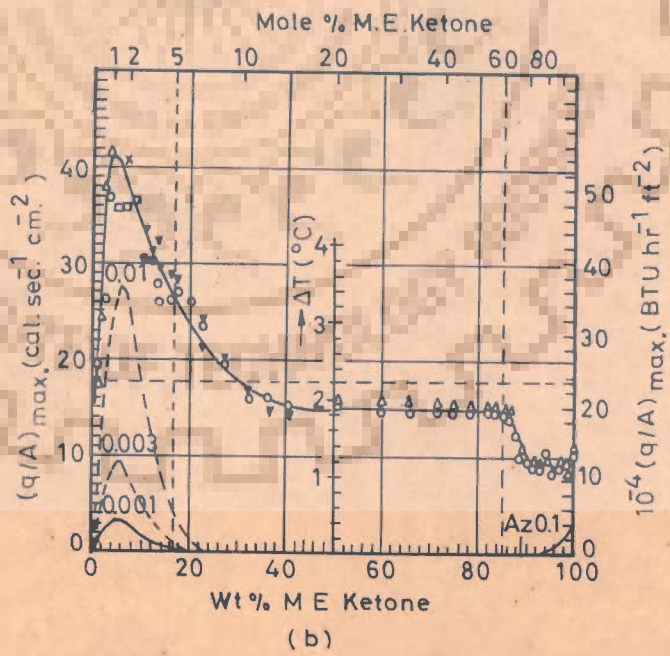
$$(1-G_d)x + G_d y = x_{\infty} \quad \dots(2.39)$$

and for equilibrium flash vaporization one has

$$y = Kx \quad \dots(2.40)$$



(a)  
 Water-methylethylketone: Heat flux  $q/A$  for convection and nucleate boiling as a function of temperature difference  $\theta$  between heating surface and liquid. The figures near the curves denote % by weight methylethylketone



(b)  
 Water methylethylketone: Maximum heat flux  $q/A$  as a function of composition. Measurements carried out with the same wire are represented by the same figures Az azeotrope. The dotted vertical lines indicate the boundaries of the region of demixing at azeotropic boiling point. The other curves represent  $\Delta T$  as a function of composition for a constant vaporized molar fraction  $G_d$ .  $\Delta T$  is the difference between dew temperature of the vapour bubbles and boiling temperature of the original liquid. The numbers near these curves are the values of  $G_d$ .

Fig.2.2-Experimental data of van Wijk et al [97] for nucleate boiling of mixture



From Equations (2.39) and (2.40)

$$x = \frac{x_{\infty}}{1 + (K-1) G_d} \quad \dots(2.41)$$

and

$$y = \frac{K x_{\infty}}{1 + (K-1) G_d} \quad \dots(2.42)$$

where  $x$  and  $y$  are the mole fractions in the liquid layer adjacent to the bubble and within it, respectively.  $K$  is the equilibrium constant for the more volatile component.

The concentration in the liquid layer adjacent to the bubble has been assumed constant. The customary assumptions of equilibrium at the interface and uniform concentration within the bubble have also been made.

The temperature in the bubble and its boundary is the dew point of a vapour of concentration  $y$ , equal to the bubble point of a liquid of concentration  $x$ . Since  $x < x_{\infty}$  the bubble point of the liquid adjacent to the bubble is greater than that of the original bulk, liquid by an amount  $\Delta T_b$ . This difference depends on  $G_d$  and is the "reduction of available superheat" which causes the reduction in heat transfer efficiency. This is at a maximum, in a solution of MEK in water when  $x_{\infty}$  is 0.042.

In the same year van Stralen [98] studied the effect of reduced pressures on boiling of pure liquids and aqueous mixture containing 4.1 wt. per cent methylethylketone. He observed that the rate of heat transfer decreased with decreasing pressure as a consequence

of increasing average size of vapour bubbles both in pure as well binary water-MEK mixtures. He also noted that the value of maximum heat flux for 4.1 wt. per cent MEK exceed considerably in comparison to the corresponding value in water at all the pressure investigated by them. In the same investigation they have also shown systematically the effect of composition on maximum value of heat flux at different pressures. The systems taken were water-MEK, water-acetone, water-ethanol, water-1-propanol and water-1-butanol at several reduced pressures. In all mixtures a maximum value of the maximum heat flux occurred at a certain low concentration of organic compound which was approximately independent of pressure. The absolute values of the maxima decreased with decreasing pressure. Not only the absolute values of the maxima in nucleate boiling heat flux increased gradually with pressure, but even the ratio of these maxima to maximum value in water at the same pressure decreased with decreasing pressure.

In next series of his papers van Stralen [42-44] undertook an extensive theoretical investigations on the growth rate of vapour bubbles on a superheated heating surface. He investigated both pure liquids and binary liquid mixtures. In this series the author has modified the previous theories proposed by van Wijk et al [97], Scriven [41] and Bruijn [99] concerning the growth rate of free spherical vapour bubbles in uniformly superheated binary mixtures.

The heat flow to the bubble required for vaporization during rapid initial bubble growth has been derived from the excess enthalpy of the equivalent conduction layer at the heating surface built up in the delay period. Heat passes from this layer into the bubble by ordinary conduction only. This thermal boundary layer is pushed away periodically from the wall due to the generation of succeeding bubbles on nucleation sites.

The radius of the bubble is governed by an equation of the form :

$$R = C_1 \nu_0 e^{0.5} \quad \dots(2.43)$$

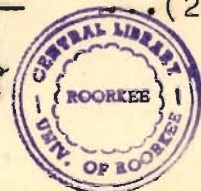
where  $\nu_0$  is superheating of the heating surface. The growth rate Equation (2.43) is applicable both for pure liquids and binary liquid mixtures. The constant  $C_1$ , bubble growth constant, is different for these two cases.

For a free bubble growing in an infinite volume of superheated pure liquid  $C_1$  is given by :

$$C_1 = \left(\frac{12}{\pi}\right)^{0.5} \left[ \frac{\alpha_l^{0.5}}{\left(\frac{P_v \lambda}{P_l C_l}\right)} \right] \quad \dots(2.44)$$

For binary mixtures the growth constant  $C_1$ , for a constant liquid superheating, depends on the concentration of the more volatile component according to the expression:

$$C_1 = \left(\frac{12}{\pi}\right)^{0.5} \frac{\alpha_l^{0.5}}{\left\{ \frac{P_v}{P_l} \left[ \frac{\lambda}{C_l} + \left(\frac{\alpha_l}{D_l}\right)^{0.5} \frac{\Delta T_b}{G_d} \right] \right\}} \quad \dots(2.45)$$



where  $D_{\ell}$  is mass diffusivity,  $\Delta T_b$  is change of saturation temperature due to change of concentration.

Equation (2.45) shows that for a maximum value of  $\Delta T_b/G_d$  the value of  $C_1$  is minimum or the growth rate is minimum. This occurs, usually, at a small concentration of more volatile component. The maximum reduction in the bubble growth rate and consequently, the maximum reduction of bubble departure size results in maximum reduction of heat transfer coefficient at a given heat flux. A relationship between  $\Delta T_b/G_d$  and mass fraction of more volatile component in original liquid in a binary mixture has been derived from equilibrium data in the following form :

$$\frac{\Delta T_b}{G_d} = - x_0 \left\{ K(x_0) - 1 \right\} \left( \frac{dT}{dx} \right)_{x=x_0} \dots (2.46)$$

where  $K = y/x$  is equilibrium constant of more volatile component in binary mixture.

The experimentally determined growth of bubbles adhering to a platinum wire in water, water-MEK and water-1-butanol mixtures was found to agree well with the theoretical prediction given by Equation (2.45).

In an analytical study Grigoryev [100] investigated how  $R_{\min}$ , the minimum radius of curvature of a nucleation site on a heating surface, is affected in a binary liquid mixture. He did a detailed thermodynamic analysis of the problem.

The value of  $R_{\min}$  is given by the following expression

$$R_{\min} = \frac{2\sigma}{\left(\frac{dP}{dT}\right)_{\text{sat}} (T_w - T_s)} \quad \dots(2.47)$$

For pure coolants  $\left(\frac{dP}{dT}\right)_{\text{sat}}$  is calculated conveniently by Clausius-Clapeyron equation. For mixtures,  $\left(\frac{dP}{dT}\right)_{\text{sat}}$  changes not only with temperature but also with composition unlike pure liquids. Using thermodynamic analysis, Grigoryev evaluated the quantity  $\left(\frac{dP}{dT}\right)_{\text{sat}}$  for binary liquid mixtures. Some of his steps are reproduced below.

The vapour pressure as a function of temperature and liquid composition for a binary system is expressed as follows :

$$\left[ (V_v - V_l) - (Y-X) \left(\frac{\partial V}{\partial X}\right)_{T,P} \right] dP = \left[ \frac{\partial^2 G}{\partial X^2} \right] (Y-X) dx + \left[ (S_v - S_l) - (Y-X) \left(\frac{\partial S}{\partial X}\right)_{T,P} \right] dT \quad \dots(2.48)$$

Imposing the following conditions on Equation (2.48) much away from the critical point

$$(V_v - V_l) \gg (Y-X) \left(\frac{\partial V}{\partial X}\right)_{T,P}$$

and

$$(S_v - S_l) \gg (Y-X) \left(\frac{\partial S}{\partial X}\right)_{T,P}$$

the above equation reduces to :

$$(V_v - V_l) dP = \left[ \frac{\partial^2 G}{\partial X^2} \right] (Y-X) dx + (S_v - S_l) dT \quad \dots(2.49)$$

or

$$\left(\frac{dP}{dT}\right)_{\text{sat}} = \left[\frac{\partial^2 G}{\partial x^2}\right] \left[\frac{Y-X}{V_v - V_l}\right] \left[\frac{dX}{dT}\right] + \frac{S_v - S_l}{V_v - V_l} \quad \dots(2.50)$$

From Equations (2.47) and (2.50) one obtains ;

$$R_{\min} = \frac{2\sigma}{\left[\left(\frac{S_v - S_l}{V_v - V_l}\right) + \left(\frac{\partial^2 G}{\partial x^2}\right) \left(\frac{Y-X}{V_v - V_l}\right) \left(\frac{dX}{dT}\right)\right]} [T_w - T_s] \quad \dots(2.51)$$

Equation (2.51) reduces to be applicable for a pure liquid by setting the quantity  $\left[\left(\frac{\partial^2 G}{\partial x^2}\right) \left(\frac{Y-X}{V_v - V_l}\right) \left(\frac{dX}{dT}\right)\right]$  as zero. Thus this quantity represents that  $R_{\min}$  in case of binary systems depends upon the concentration of boiling mixture. Grigoryev analyzed this quantity in detail. He concluded, for the conditions far away from the critical point that (i) the term  $(Y-X/V_v - V_l)$  is always positive for non-azeotropic binary mixture whereas for azeotropic mixtures it is positive upto the point of azeotrope and negative beyond it, (ii) the sign of quantity  $\left(\frac{\partial^2 G}{\partial x^2}\right) \left(\frac{dX}{dT}\right)$  is understood by Steronkin [101] analysis.

$$\left(\frac{\partial^2 G}{\partial x^2}\right) \left(\frac{dX}{dT}\right) = \frac{Q_{12}}{T} \left\{ \frac{\lambda_{LB} - \lambda_{HB}}{Q_{12}} + \frac{(\Delta V)_{HB} - (\Delta V)_{LB}}{V_{12}} \right\} \quad \dots(2.52)$$

$Q_{12}$  is differential latent heat of vaporization. For the state of system far from critical point

$(\lambda_{LB} - \lambda_{HB})/Q_{12} \gg [(\Delta V)_{HB} - (\Delta V)_{LB}]/V_{12}$  and Equation (2.52) reduce to :

$$\left(\frac{\partial^2 G}{\partial X^2}\right) \left(\frac{dX}{dT}\right) = \frac{\lambda_{LB} - \lambda_{HB}}{T} \dots(2.53)$$

Thus the sign of the above term depends upon the difference of values of latent heat of vaporization of more volatile component ( $\lambda_{HB}$ ) and less volatile component ( $\lambda_{LB}$ ) in the mixture. He concluded that the sign of this term does not change over the whole concentration range.

From the above discussion it follows that the quantity  $\left[\left(\frac{\partial^2 G}{\partial X^2}\right)\left(\frac{Y-X}{V_v - V_l}\right)\left(\frac{dX}{dT}\right)\right]$  may have either a positive sign or a negative sign. The effect of sign before this quantity on  $R_{min}$  is discussed as follows for non-azeotropic mixtures only.

- a. If the sign is positive, then an increase in the value of (Y-X) will activate a greater number of nuclei by making smaller ones active. This, in turn, will increase the rate of vapour bubble formation and as a consequence of it heat transfer coefficient will be enhanced.
- b. If the sign is negative, then an increase in the value of (Y-X) will activate only the limited number of sites and heat transfer rates will decrease.

Yatabe and Westwater [102] studied photographically the bubble growth rates and bubble emission frequencies for ethanol-water and ethanol-isopropanol mixtures. Motion pictures were taken at terminal speeds of 5,300 frames/sec

with a magnification of four diameters on 100 ft rolls of 16 mm film. Boiling took place at atmospheric pressure at three different artificial nucleation sites of about 0.01 inch size located on a vertical copper surface superheated by 3.8°C. Bubble frequencies were as high as 179/sec.

Scriven's [41] analysis was used to correlate the experimental data. The growth constant  $\beta$  in Equation (2.36) for the two mixtures; isopropanol-ethanol and ethanol-water, at a superheat of 3.8°C were computed. For each bubble the growth data were fitted to the following equation :

$$R = a t^n \quad \dots(2.54)$$

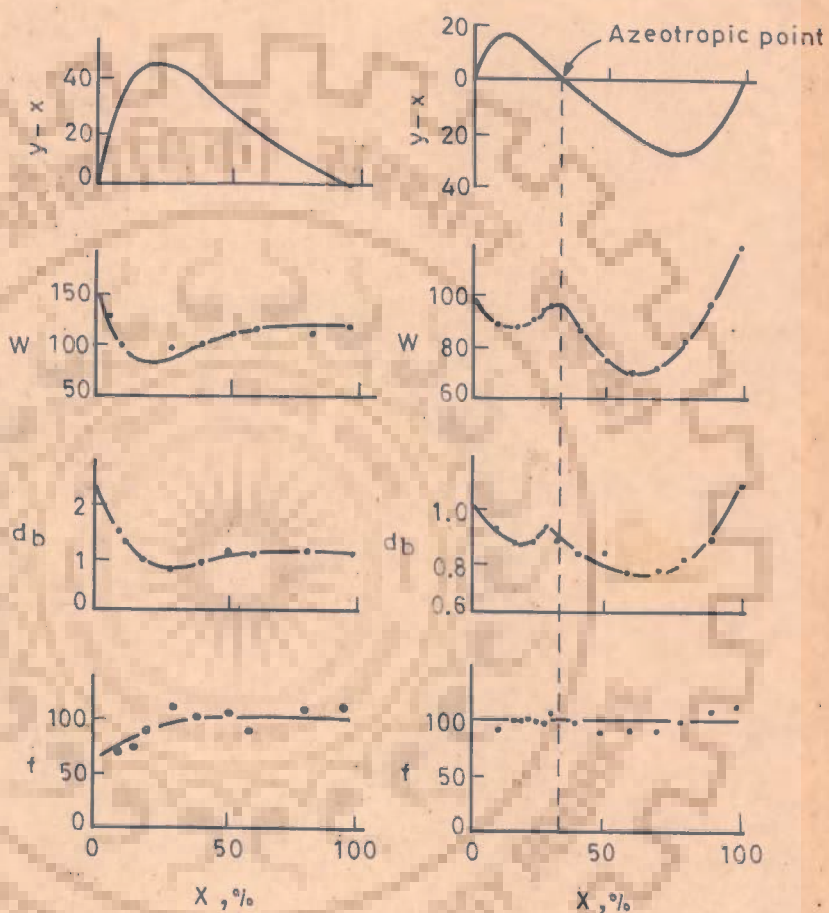
The best fit values of arbitrary coefficient 'a' and exponent n were determined graphically. The significant fact is that for all bubbles, measured, n is below 0.5 value predicted by Scriven's theory. The average value of n are 0.27 for ethanol-isopropanol mixtures and 0.32 for ethanol-water mixtures. Thus they concluded that bubble diameters varied approximately with the 0.3 power of time rather than the 0.5 power predicted by the Scriven model [41]. The experimental growth coefficients for ethanol isopropanol varied with composition as expected, but the data were 15 per cent above the predicted values. The experimental growth coefficients for ethanol-water were higher than predicted values from 0 to 100 per cent, depending on the composition, the geometry of the nucleation site, and whether early or late portions of



the growth curve were examined. A predicted minimum in the coefficient at 7 wt. per cent ethanol for ethanol-water system was not detected. This minima, in fact, occurs at 31 wt. per cent ethanol in ethanol-water mixture as observed in the present investigation.

Tolubinskii et al [103] have conducted photographic study on the mechanism of boiling of binary mixtures. They used water-glycerine and ethanol-water mixtures for their studies. The former system is without the azeotropic point and the latter is with the azeotropic point. They have shown the effect of concentration of more volatile component on the rate of vapour bubble growth. This is reproduced in Figure 2.3. Following conclusions can be drawn from this figure :

1. There exists a pronounced relationship between the average growth rate of vapour bubbles,  $w$ , bubble departure diameter,  $D_b$  and the quantity  $(Y-X)$ .
2. For non-azeotropic system the rate of vapour bubble growth,  $w$ , is found to decrease with the increase in concentration of more volatile component upto a certain concentration. Beyond this concentration it begins to increase. The concentration at which the rate of bubble growth is minimum corresponds to a maximum value of  $(Y-X)$ . The quantity  $(Y-X)$  is playing an important role in the growth rate of binary mixtures. The bubble departure diameter,  $D_b$  also exhibits the similar behaviour i.e. the reduced bubble growth rates result in smaller bubble departure diameter.



(a) Ethanol-water

(b) Ethanol-benzene

Fig.2.3-Vapour bubble growth rate as a function of concentration of mixture ( $X$ , ethanol concentration) [103]

This conclusion has also been drawn by van Stralen [42-44]. A similar conclusion can also be drawn from the work of Hatton and Hall [104] who have investigated the bubble growth rates and departure sizes by considering both static and dynamic forces acting on the bubble.

3. With the azeotropic point there are two minima corresponding to two external points on the curve  $(Y-X) = f(x)$  and an intermediate maximum at the azeotropic point.

Rehm [105] has investigated the bubble growth parameters in saturated and subcooled nucleate boiling of water and aqueous solutions of sucrose and n-propanol with the aid of high speed photography. He qualitatively analyzed the forces which influence bubble growth and separation. He concluded that highly viscous sucrose solutions produced small, short lived bubbles while low-surface tension n-propanol solutions produced bubbles much larger than those obtained in pure water.

In next series of papers van Stralen [106, 107] has reviewed the existing theories [41, 68 and 69] concerning spherically symmetric growth of free bubbles in uniformly superheated liquids. He also conducted experimental investigations [107] with high speed motion picture camera for growth rate of bubbles, generated at a moderate heat flux density. The boiling was taking place on an electrically heated platinum wire immersed in water,

water-MEK and water-n-butanol solutions. In his theoretical analysis he showed that Equation (2.45) can be obtained from the Seriven [41] model for pure coolants by an analogy of heat and mass transfer. In doing this he replaced  $T$  by  $x$ ,  $\alpha_L$  by  $D_L$ ,  $\Delta T_{\text{sat},\infty}$  by  $x_\infty - x$ ,  $\lambda/C_\ell$  by  $y-x$  and  $\beta$  by  $(\alpha_\ell/D_\ell)^{0.5} \beta$ . He concluded that the experimental values of the growth constants for ascending released bubbles for above mentioned aqueous solutions are generally in quantitative agreement with theoretical predictions.

van Ouwerkerk [108] studied hemispherical bubble growth in a binary mixture. He showed that a vapour bubble at a liquid-solid interface in the binary mixture grows without changing its shape and its dimensions increase proportionately with the square root of the growth time. This growth process controlled both the transport of heat and matter, is described by a self-similar solution. Analysis shows the reduction in growth rate, relative to a pure liquid, to be the same as a first approximation as the reduction for a free spherical bubble. The dry area in the microlayer under the bubble can be much smaller in a binary mixture than in a pure liquid and this influences the peak heat flux which can be attained in nucleate boiling.

van Stralen et al [109] have studied the combined effect of relaxation and evaporation microlayers during bubble growth rates in pure and binary liquid mixtures. They used Pohlhausen's equation to determine the initial

thickness of the evaporating microlayer beneath a hemispherical vapour bubble on a superheated horizontal wall. Microlayer thickness is proportional to the square root of the distance to the nucleation site during early bubble growth, while a linear relationship exists during advanced growth.

A heat and mass diffusion-type solution is derived for advanced bubble growth, which accounts for the interaction of the mutually dependent contributions due to relaxation microlayer (around the bubble-dome) and the evaporation microlayer. The entire bubble behaviour during adherence is determined by a combination of this asymptotic solution and the Rayleigh solution, which governs early growth.

The proposed final bubble growth equation, which is valid both in pure liquids and in binary mixtures during the entire adherence time is assumed to be of the following form :

$$R(t) = \frac{R_1(t) R_2(t)}{R_1(t) + R_2(t)} \quad \dots(2.55)$$

where  $R = R^*/2^{1/3}$ , equivalent spherical bubble radius and  $R^*$  is radius of hemispherical bubble.

$R_1$  is equivalent bubble radius according to modified Rayleigh solution and  $R_2$  is equivalent bubble radius according to total diffusion (combined evaporation and relaxation microlayer).

$R_1(t)$  and  $R_2(t)$  are given by Equations (62) and (63) of Reference [109].

At low concentrations of the more volatile component in binary systems, the dominating influence of mass diffusion is demonstrated by the following effects :

(i) asymptotic bubble growth is slowed down substantially, (ii) the formation of dry areas beneath bubbles is prevented, even at subatmospheric pressure, (iii) the lower part of the bubble is contracted, (iv) the evaporation microlayer contribution to bubble growth is negligible at atmospheric and at elevated pressures.

Tolubinskii [110] has recommended to compute the average growth rate of vapour bubbles by employing the theory of similitude equations. The equation allows to calculate the heat transfer in the boiling of a variety liquids.

van Stralen et al [111] have investigated experimentally the growth rate of vapour bubbles during nucleate boiling of aqueous binary systems at subatmospheric pressures. They have investigated water-ethanol mixture (upto 31 wt. per cent ethanol at pressures between 4.08 to 6.65 kPa with corresponding Jakob number ranging from 1989 to 1075), water-1-butanol (upto 2.4 wt. per cent 1-butanol at pressures between 3.60 - 4.08 kPa with corresponding Jakob number ranging from 2760 to 1989) and water-2-butanone (upto 15 wt. per cent 2-butanone at pressures between 7.31-9.07 kPa with corresponding Jakob number ranging from 1519-683).

Recently Shock [112] has analyzed two different theories responsible for heat transfer in nucleate boiling in binary mixtures. According to the first theory the bubble growth rate in binary mixtures is different than pure liquids because of the additional mass transfer resistance i.e. interdiffusion of the species. And according to the second theory, the different mechanism in binary and pure liquids is due to differences in the superheat required to initiate bubble growth rate due to changes in the parameters governing the saturation pressure-temperature relationship. With the help of theoretical analysis and his experimental data [113] on convective boiling of ethanol-water mixtures in heated channels Shock [112] has found that the latter theory can not be defended successfully. However, he has shown that in aqueous systems there may be an increase in the superheat required for the onset of nucleate boiling due to the effects of the change in wetting characteristics for organic solvents at low concentrations. Based on the experimental data of other investigators, Shock has shown that the diffusion resistance which is found once boiling has commenced still plays a significant role in the reduction in heat transfer in aqueous systems and it is presumed to be the controlling factor in non-aqueous systems.

Zijl et al [114] have investigated the combined inertia and diffusion controlled growth and implosion

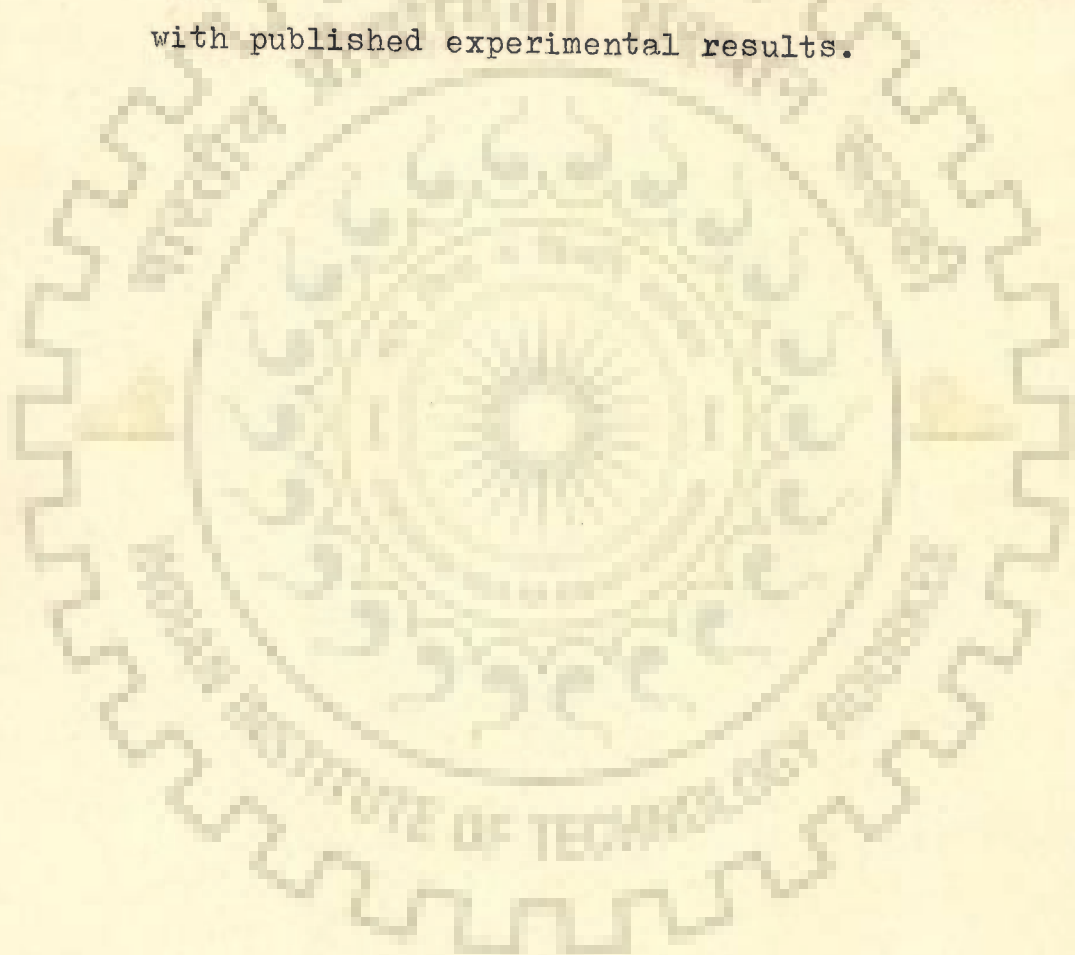
of a spherical vapour bubble in an initially uniformly superheated and supersaturated infinitely extended liquid. The equations and solutions are presented with sufficient generality to provide a basic understanding of growth and implosion of vapour bubbles **under** most complicated physical conditions.

Zijl et al [115] have given global numerical solutions of growth and departure of a vapour bubble at a horizontal superheated wall in a pure liquid and a binary mixture. Integral forms of the heat transport equations have been solved by use of series expansions, obtained by the theory of fractional derivatives. The global orthogonal collocation method has been applied for the potential flow around the bubble. In this way a set of only eight or ten ordinary differential equations have to be integrated by computer. The results following from prescribed initial temperature distributions, are in quantitative agreement with experimental data, obtained in water and aqueous binary mixtures boiling at subatmospheric pressures.

Pinnes and Mueller [116] analyzed the homogeneous vapour nucleation and superheat limits to multicomponent liquid mixtures. They distinguished the multicomponent liquid mixtures with that of single component case in two ways. Both these results from the unequal volatilities of the species, one is that the vapour phase may contain several components, the other is that nucleation formation



alters the composition of the nearby liquid. They incorporated these two features into the classical theory of homogeneous nucleation to yield a general theory applicable to multicomponent liquids. The theory was applied to binary hydrocarbon mixtures by using an equation of state extrapolated into the metastable region. Superheat limits thus calculated were compared with published experimental results.



## C H A P T E R - 3

### EXPERIMENTAL SET-UP

#### 3.1 DESIGN CONSIDERATIONS

Basic objective of the present investigation was to obtain experimental data of heat transfer from a horizontally placed cylindrical surface submerged into the pool of boiling liquids and their binary mixtures with distilled water at atmospheric and subatmospheric pressures. Several factors were considered for the design, the fabrication and the commissioning of the experimental set-up. They are as follows :

- Heat transfer surface
- Surface and liquid thermocouples
- Power supply
- Condenser unit
- Vacuum unit
- Composition of the boiling liquid mixtures.

The above design considerations are discussed hereunder :

##### 3.1.1 Heat Transfer Surface

In a closed circuit experimental facility, where the vapours are continuously generated from the pool of boiling liquid at the heating surface, condensed in

condensers and fed back to the pool of liquid as shown in Figure 3.1, the location of heat transfer surface in the vessel is an important design consideration. This is because of the fact that the heat transfer surface is not to be disturbed by the flow of incoming mass of the condensate. Besides this, the boiling phenomenon should not be affected adversely due to the penetration of the condensate through the pool which condenses on the inside surface of the top cover of the test vessel. To meet this effectively, the heat transfer surface was placed in such a position so that it had sufficient liquid height above and beneath it.

### 3.1.2 Surface and Liquid Thermocouples

For a heating surface diameter as used in the present investigation there exists a variation in surface temperature around its circumference. Therefore, one of the important design requirements is to determine the location of surface thermocouples. A scrutiny of the bubble dynamics on such a large diameter heating surface demands a minimum number of three thermocouples placed at the top-, at the side- and at the bottom-positions of the heating surface. Therefore, three thermocouples were placed at  $90^\circ$  apart from each other. The placement of thermocouples at three circumferential positions is helpful in calculating local values of heat transfer coefficients. These three values are also sufficient to apply mechanical quadrature [117]

method to determine average value of surface temperature and heat transfer coefficient.

Another consideration was the location of liquid thermocouple probes. The liquid thermocouples were placed by the side of the respective surface thermocouple positions. Their readings were used to calculate the degree of wall superheat at three locations and consequently the local heat transfer coefficients. At this stage it was also required to decide as to how much they should be away from the heating surface. In fact, to monitor the bulk temperature of the pool, the probe should be placed outside the zone of the superheated liquid layer enveloping the heat transfer surface. This was ensured by varying the position of the liquid thermocouple probe away from the heating surface to a position beyond which no change in liquid temperature was observed. As a matter of fact the thickness of the superheated liquid layer changes with the parameters [118] namely; heat flux, pressure and physico-thermal properties of the boiling liquid. Therefore, the movable liquid thermocouple probes were installed.

### 3.1.3 Power Supply

An accurate heat transfer study demands a stabilized and modulated supply of heat flux so that the minor power fluctuations should not disturb the energy input and thereby the steady state boiling heat

transfer data. Adequate measures were included in the experimental facility to achieve this.

#### 3.1.4 Condenser Unit

As mentioned earlier, it is necessary for a closed circuit experimental facility to return the vapours back to the vessel from the condenser. To meet this requirement and to maintain the steady state conditions, the rate of condensation must be equal to the rate of evaporation. This was ensured by installing a large size condenser unit. It is important to mention that in the absence of adequate condensation of the vapours, the following difficulties are likely to arise :

- (i) Decrease in the liquid level above the heating surface
- (ii) Variation in the composition of the binary mixtures, and
- (iii) Fluctuations in the system pressure.

Thus, in order to overcome the above difficulties, an effective condensation unit was designed and employed.

#### 3.1.5 Vacuum Unit

One of the aims in the present investigation was to obtain experimental data for nucleate pool boiling of organic liquid mixtures at subatmospheric pressures as low as  $12 \text{ kN/m}^2$ . Therefore, a suitable vacuum unit

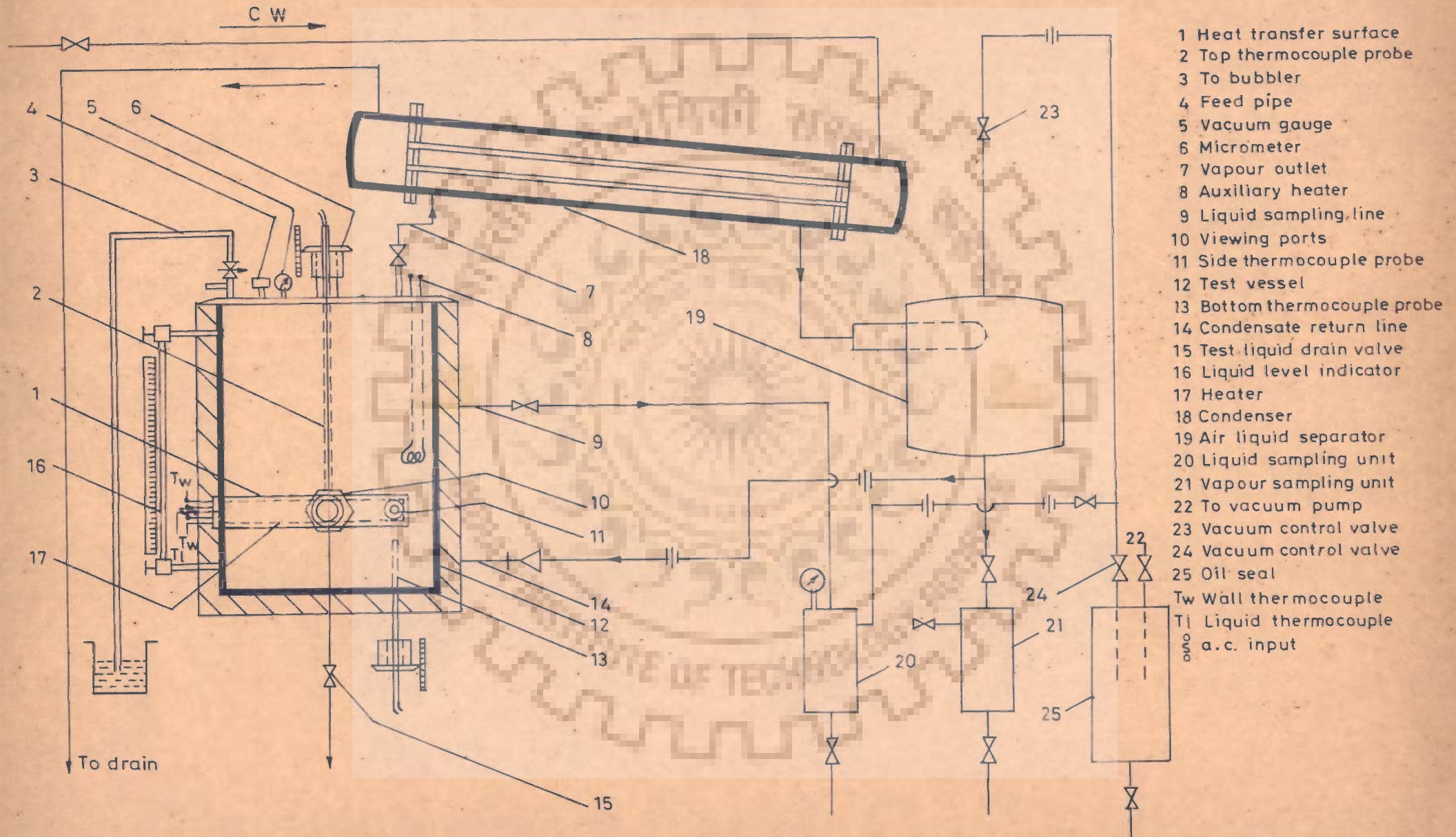
system was designed which could handle the moisture and the organic vapours successfully.

### 3.1.6 Composition of the Boiling Liquid Mixtures

While conducting experimental data for binary mixtures it was necessary to maintain the composition of the pool at a given value throughout the experimentation. Therefore, a care was exercised to recycle all the condensing vapours back to the vessel to avoid any variation in composition of the boiling liquid mixtures. Provision was made to draw and analyse the liquid and vapour samples at a given time interval to check the composition. These samples were collected in ground glass bottles placed in an ice box to avoid any flashing.

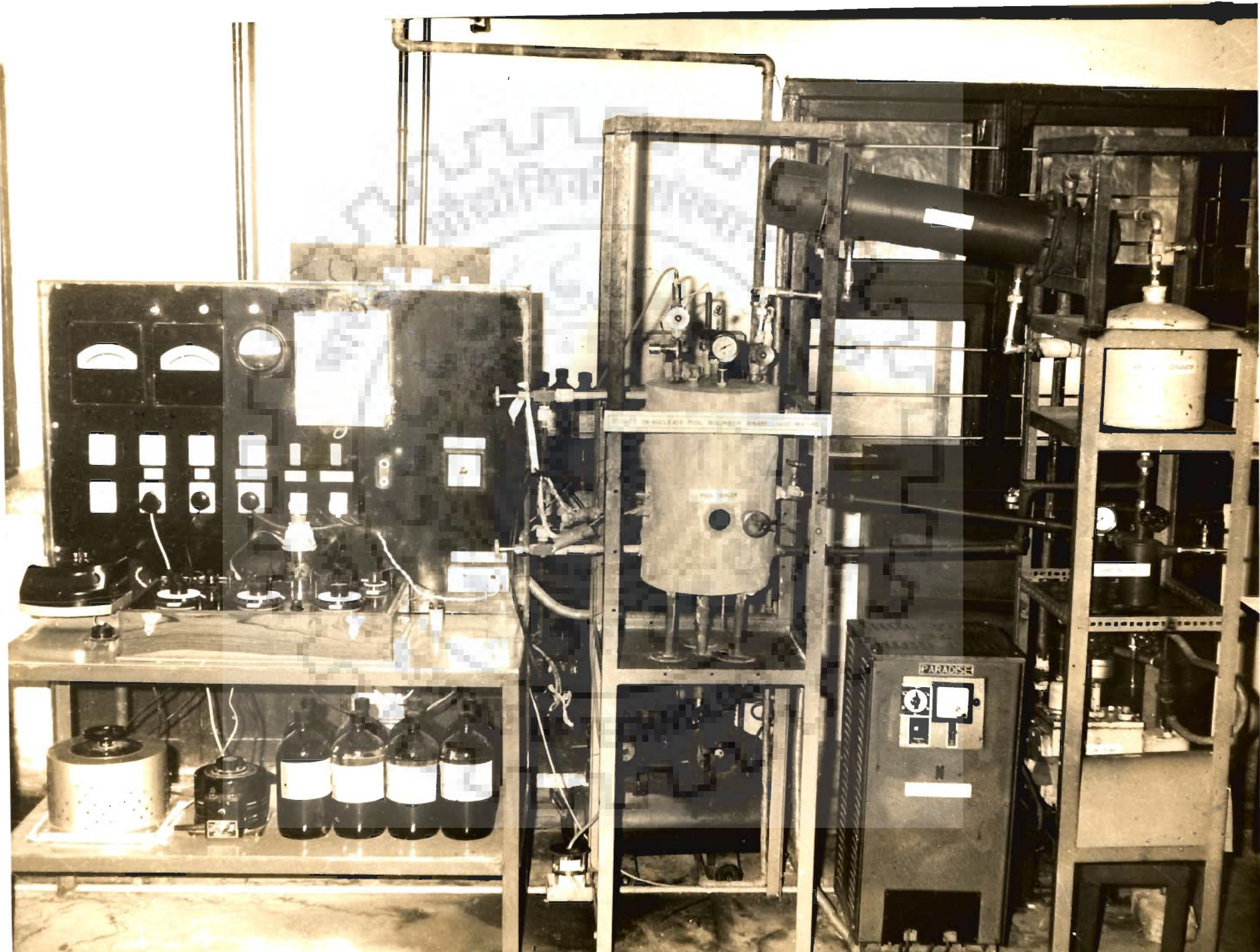
## 3.2 DESCRIPTION OF THE EXPERIMENTAL SET-UP

Keeping in view the above considerations an experimental facility to obtain data for nucleate pool boiling of binary liquid mixtures at atmospheric and subatmospheric pressures was designed, fabricated and commissioned. The schematic diagram and photograph of the experimental facility are shown in Figures 3.1 and 3.2 respectively.



- 1 Heat transfer surface
- 2 Top thermocouple probe
- 3 To bubbler
- 4 Feed pipe
- 5 Vacuum gauge
- 6 Micrometer
- 7 Vapour outlet
- 8 Auxiliary heater
- 9 Liquid sampling line
- 10 Viewing ports
- 11 Side thermocouple probe
- 12 Test vessel
- 13 Bottom thermocouple probe
- 14 Condensate return line
- 15 Test liquid drain valve
- 16 Liquid level indicator
- 17 Heater
- 18 Condenser
- 19 Air liquid separator
- 20 Liquid sampling unit
- 21 Vapour sampling unit
- 22 To vacuum pump
- 23 Vacuum control valve
- 24 Vacuum control valve
- 25 Oil seal
- $T_w$  Wall thermocouple
- $T_l$  Liquid thermocouple
- a.c. input

Fig.3.1-Schematic diagram of experimental set-up





### 3.2.1 Test Vessel

Figures 3.3 and 3.4 show the details of the test vessel and mountings on it. The test vessel was stainless steel cylinder of 270 mm diameter and 470 mm height with a flat top and dished bottom. The top cover had a vacuum gauge (5) to measure the vacuum in the vessel a movable thermocouple probe (2) to monitor liquid temperature above the heating surface and an auxiliary heater (8). Also, it had provisions for charging the vessel, (4) with test liquid and a valve (3) to pass on the dissolved air to the bubbler (19) and a vapour pipe line (7) for carrying vapours to the condenser. The heat transfer surface (1) was inserted in the test vessel from its side and installed horizontally at a submergence depth of about 280 mm from the top. This submergence depth was in accordance with the design considerations as discussed in Section 3.1. The details of socket (3), checknut (2) and gasket (4) for securing the heating surface in the horizontal position are shown in Figure 3.5. Liquid level indicator (16) helped to know the height of the liquid in the vessel as shown in Figure 3.3.

To facilitate the visual observations for bubble initiation, growth and departure on the heat transfer surface, two diametrically opposite view ports (10) were located at the front- and rear-side of the test vessel. The front-side was provided with a thermocouple probe (11) to record the liquid temperature at the side-position

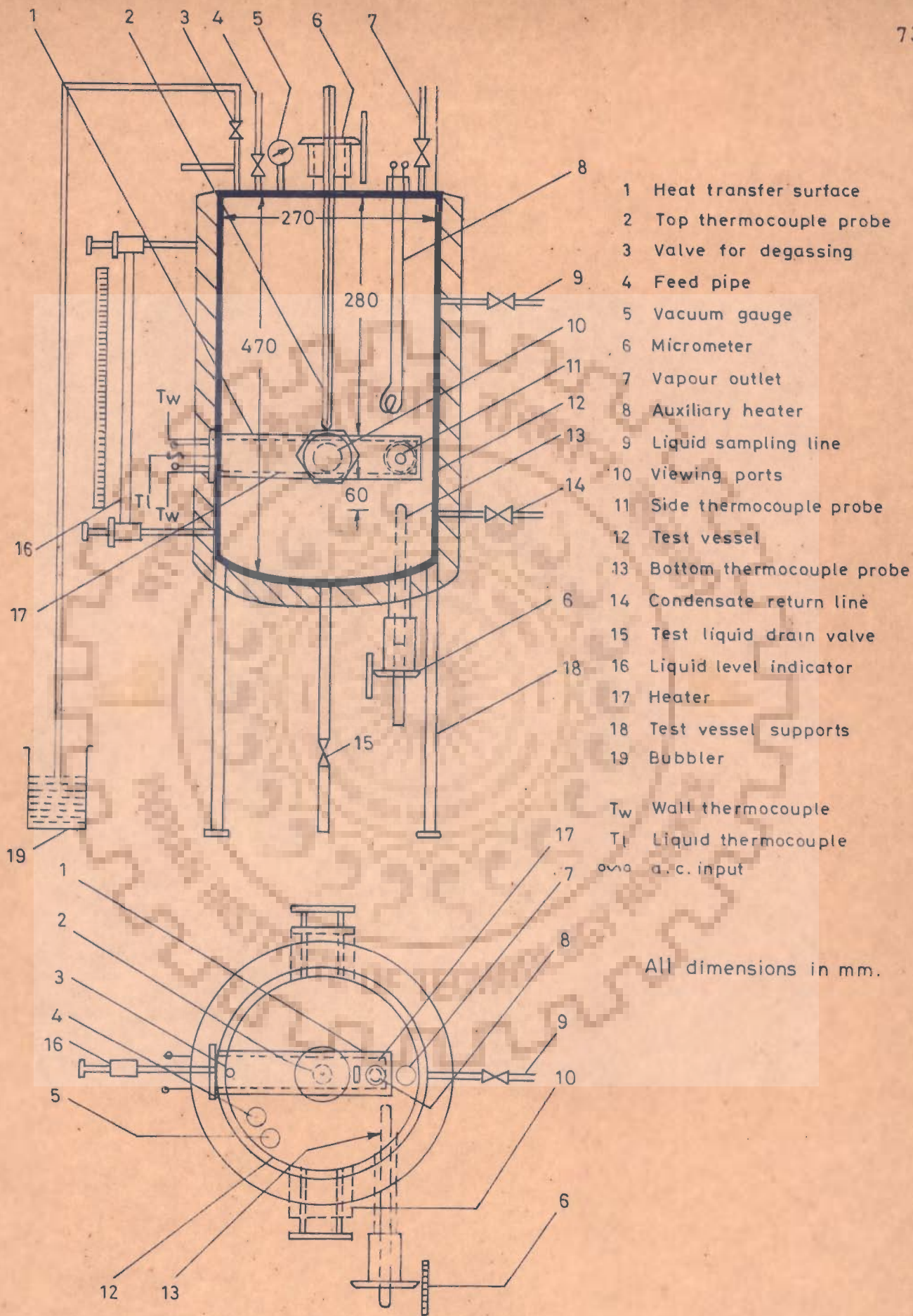


Fig.3.3 - Details of test vessel

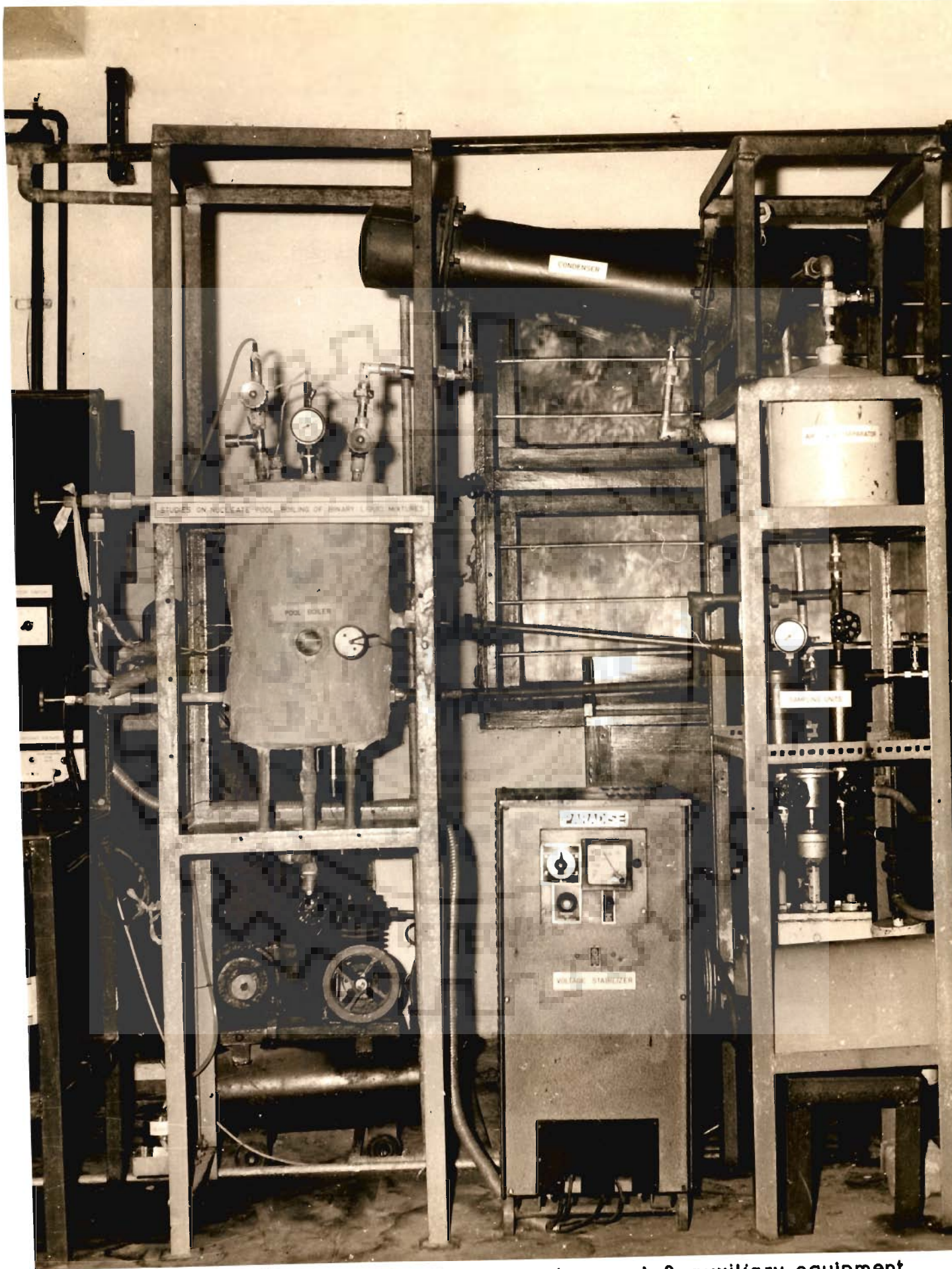


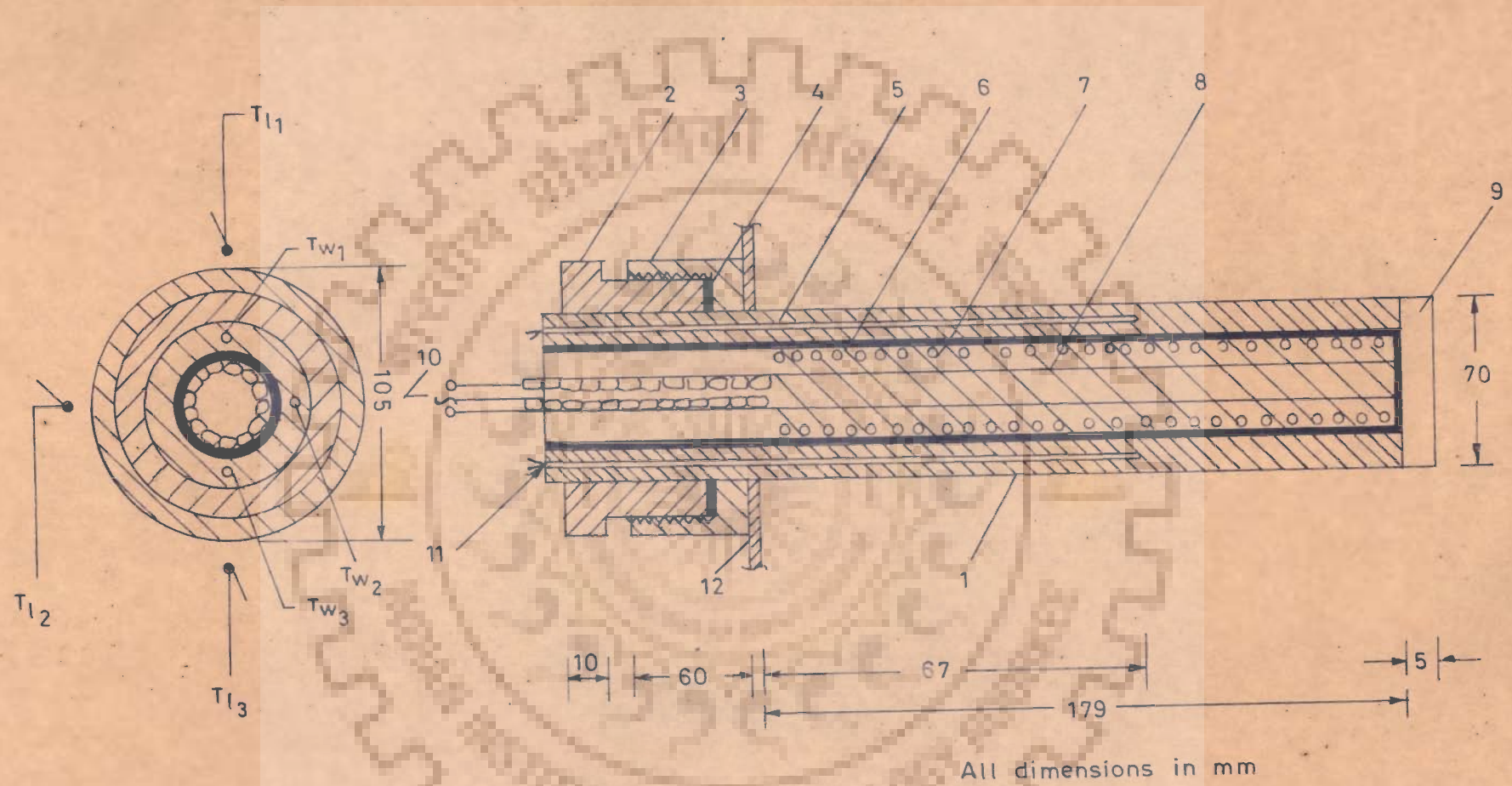
Fig.3.4-Photographic view of test vessel & auxiliary equipment.

of the heating surface. The dished bottom had the provision for discharging the liquid through a valve (15) and a thermocouple probe (13) to record the liquid temperature below the heat transfer surface. To fully satisfy the design consideration as detailed in Section 3.1 i.e., the incoming mass of liquid from the separator (19) should not disturb the vicinity of the heating surface, the condensate return line (14) had its entry sufficiently below the heating surface as shown in Figure 3.1. This distance was found to be 60 mm from the bottom of the heat transfer surface. Further, this distance was sufficient since the condensate from the separator to the vessel was cooler in comparison to the boiling liquid inside the vessel and hence remains at the bottom for sometime before it reattains the same thermodynamic state as that of the pool of liquid. Pipe line (9) connects the liquid sampling unit (20) with the test vessel.

To minimize the heat losses to surroundings, the vessel body was thoroughly insulated by means of asbestos followed by glass-wool and then 85 per cent magnesia powder.

### 3.2.2 Heat Transfer Surface

Figure 3.5 shows details of the heat transfer surface. It consists of a 410 ASIS grade stainless-steel hollow cylinder having 70 mm O.D., 4 mm wall



- |                         |                   |                           |
|-------------------------|-------------------|---------------------------|
| 1 Heat transfer surface | 6 Mica insulation | 11 Thermocouple leads     |
| 2 Check nut             | 7 Heating element | 12 Test vessel wall       |
| 3 Socket                | 8 Porcelain core  | $T_l$ Liquid thermocouple |
| 4 Gasket                | 9 End plate       | $T_w$ Wall thermocouple   |
| 5 Thermocouple          | 10 Electric leads |                           |

Fig.3.5-Heat transfer surface and thermocouples layout

thickness and 179 mm effective heating length and heat transfer area  $3.93 \times 10^{-2} \text{ m}^2$ . Its outer surface was uniformly machined and smoothed by set of emery papers (1/0, 2/0, 3/0 and 4/0) and finally cleaned by acetone. It was then fitted to the test vessel with the help of a stainless steel socket (3) welded on the body of the vessel (12). A checknut (2) along with a lead gasket (4) helped in making the whole assembly leak-proof.

The heat transfer surface was heated by an electric heater (7) placed in it. A cartridge heater was fabricated for a maximum value of heat flux upto  $35,000 \text{ W/m}^2$ . The heating element was Kanthal A-1 grade of 16 gauge wire of a maximum current carrying capacity of 13 amperes. This heating element was electrically insulated with fish spine type of porcelain beads. It was wound carefully on a 16 mm porcelain rod. This was then thoroughly wrapped with glass tape and a thin mica sheet (6) to provide complete safety against any electric leakage. The entire assembly was then carefully inserted in the hollow portion of the heat transfer surface, suitable electric connections (10) were provided at the open end of the heating surface. The heat losses from this end were reduced to minimum by covering this end thoroughly with glass-wool.

The three thermocouples at the top- at the side- and at the bottom- positions of the heating surface,  $90^\circ$

apart from each other were placed in the holes (11) in the wall thickness of the heating surface. Utmost precaution was observed in drilling these holes of diameters slightly greater than 24 gauge - the diameter of the thermocouple wires. The axial length of these holes was 127 mm. Calibrated fibre-glass insulated copper-constantan thermocouple wires of 24 gauge were inserted in these holes to monitor the surface temperatures.

### 3.2.3 Liquid Thermocouple Probes

As required in Section 3.1 for the calculation of local values of heat transfer coefficient at three locations in the pool, movable liquid thermocouple probes (2,11,13) were provided corresponding to the respective positions of surface thermocouples as shown in Figure 3.3. These probes could traverse in the pool of boiling liquid so as to record the temperature of the liquid lying in the close vicinity of the heating surface right upto the bulk of boiling liquid. The bulk liquid temperature was measured at the distance sufficiently away from the superheated liquid layer. These thermocouple assemblies are depicted in Figures 3.3 and 3.4.

### 3.2.4 Degassing Facility

The air dissolved in the liquid, if any, was to be removed prior to conducting the experiments.

The presence of non-condensable gases affects the temperature needed to initiate bubble growth from the irregularities on the heating surface and thereby heat transfer data.

In order to get rid of the above difficulty a degassing facility was used. Prior to each experiment the liquid was heated to its boiling point by means of auxiliary heater (8). This heating caused the dissolved gases to bubble out of the liquid. These gases were then forced out of the system by closing all other valves (4,7,9 and 14), except the valve (3) in the pipe line connected to bubbler (19) as shown in Figure 3.3. The bubbler consisted of a beaker filled with the same liquid as in the test vessel. It was connected to the test vessel with a polythene tube.

The remaining dissolved gases, if any, were removed out of the system in the air-liquid separator as described in Section 3.2.6.

### 3.2.5 External Condenser

The vapours from the pool of boiling liquid passed through a pipe line (7) to a water cooled condenser (18) as shown in Figures 3.1 and 3.4. The condenser was designed and fabricated so as to cause adequate condensation for the vapours of all the liquids investigated for a heat load of 2.5 kW and placed in inclined position. However, the heat load for which



data were conducted did not exceed 1.3 kW.

The condenser was a single pass shell and tube heat exchanger of shell diameter 112 mm and tube diameter 12.7 mm. The total number of tubes were 12 having length of 400 mm each. The material of construction for both shell and tubes was stainless steel. The condensing vapours routed through the shell side while the cooling water through the tube side. The baffles were provided in the shell side. The condenser was kept pitched towards the air-liquid separator (19) as shown in Figure 3.1. This facilitated the flow of the condensate to the separator without any hold up of it in the condenser (18)

### 3.2.6 Air-Liquid Separator

The purpose of incorporating air-liquid separator (19) in the experimental set-up was to provide an additional facility to remove non-condensable gases which could not be removed during the degassing operation. Besides, some air is likely to infiltrate into the system. To remove these non-condensables from the system, air-liquid separator (19) was placed between condenser and vacuum unit as depicted in Figures 3.1 and 3.2. The air-liquid mixture after condenser enters into the separator tangentially. The separated non-condensables passed to the vacuum pump through the pipe (23) at the top of the separator and thus thrown out to the atmosphere, while the condensate returned

back to the pool of liquid through a pipe (14) provided at the bottom of the separator.

### 3.2.7 Vacuum Pump Assembly

A 'HV' series Hindustan Rotary two-stage oil immersed type vacuum pump was used with a suction capacity of  $1.25 \times 10^{-3} \text{ m}^3/\text{s}$ . The pump was driven by a 0.37 kW motor having 1450 rpm. One of the essential features of the pump was an Air Ballast which enabled the pump to attain high vacuum even when a lot of moisture and organic vapours were sucked in by the pump. Drops of water particles which were released under high compression ratio, of the order of 1:700, collected underneath the main valves were completely eliminated by the introduction of fresh atmospheric air through the Air-Ballast vent. Thus the pump satisfied the demand of handling moisture and organic vapours. To minimize the entry of moisture and organic vapours in the pump, silica gel was used in the suction inlet. An oil seal (25) was also provided for this purpose as shown in Figures 3.1 and 3.4. High vacuum of the order of 730 mm Hg was obtained from this pump. To check the back flow of oil into the experimental apparatus, valves (23, 24) were installed at suitable positions. Vacuum was regulated by means of a fine needle valve (23).

### 3.2.8 Sampling Units

As mentioned in Section 3.1 that for the prediction of heat transfer coefficients in binary liquid mixtures, it is essential to maintain the composition of the pool constant throughout the experimentation. Therefore, two sampling units were included in this experimental facility for drawing out the samples of boiling liquid and the vapours in equilibrium with the liquid for analysis to check the constancy of composition. These sampling units (20,21) were small vessels made of stainless steel. Liquid sampling unit (20) was directly connected to the pool of the boiling liquid with a liquid sampling line (9) and vapour sampling unit (21) to the condensate line (14) from the separator as depicted in Figures 3.1 and 3.4. A separate vacuum line was provided for both these units with necessary valves as shown in Figures 3.1 and 3.2. This enabled the units to operate either under subatmospheric or atmospheric pressure conditions, without disturbing rest of the system. A separate vacuum gauge was provided for these units. Samples were withdrawn from the dished bottom of the vessels (20,21) and collected in ground glass bottles placed in an ice-box to avoid any evaporation of the liquids.

### 3.2.9 Power Supply System

Figure 3.6 shows the complete details of the electric circuit for the supply of stabilized and modulated low-voltage power to the heat transfer surface. Single-phase 230 volt, 50 c/s a.c. power was supplied to an automatic servomotor controlled voltage stabiliser supplied by M/s Paradise Co. The stabilised voltage was then supplied to the primary of an autotransformer of 15 amperes rating. This autotransformer modulated the electric power input to the heater for desired value of heat flux. Low resistance, thick copper conductors were used for power supply between the autotransformer and the heater.

## 3.3 INSTRUMENTATION AND CALIBRATION

### 3.3.1 Heat Flux Measurement

The power supplied to the heat transfer surface was measured by means of calibrated precision grade voltmeter and ammeter having accuracy within  $\pm 1$  per cent. The voltmeter and ammeter were calibrated against the Substandard Voltmeter and Ammeter. The range of voltmeter was 0 - 250 volts and that of ammeter was 0 - 15 amperes. The readings of the voltmeter and the ammeter were noted in order to calculate the power input to the heating element. The power divided by the effective area of heat transfer surface represented

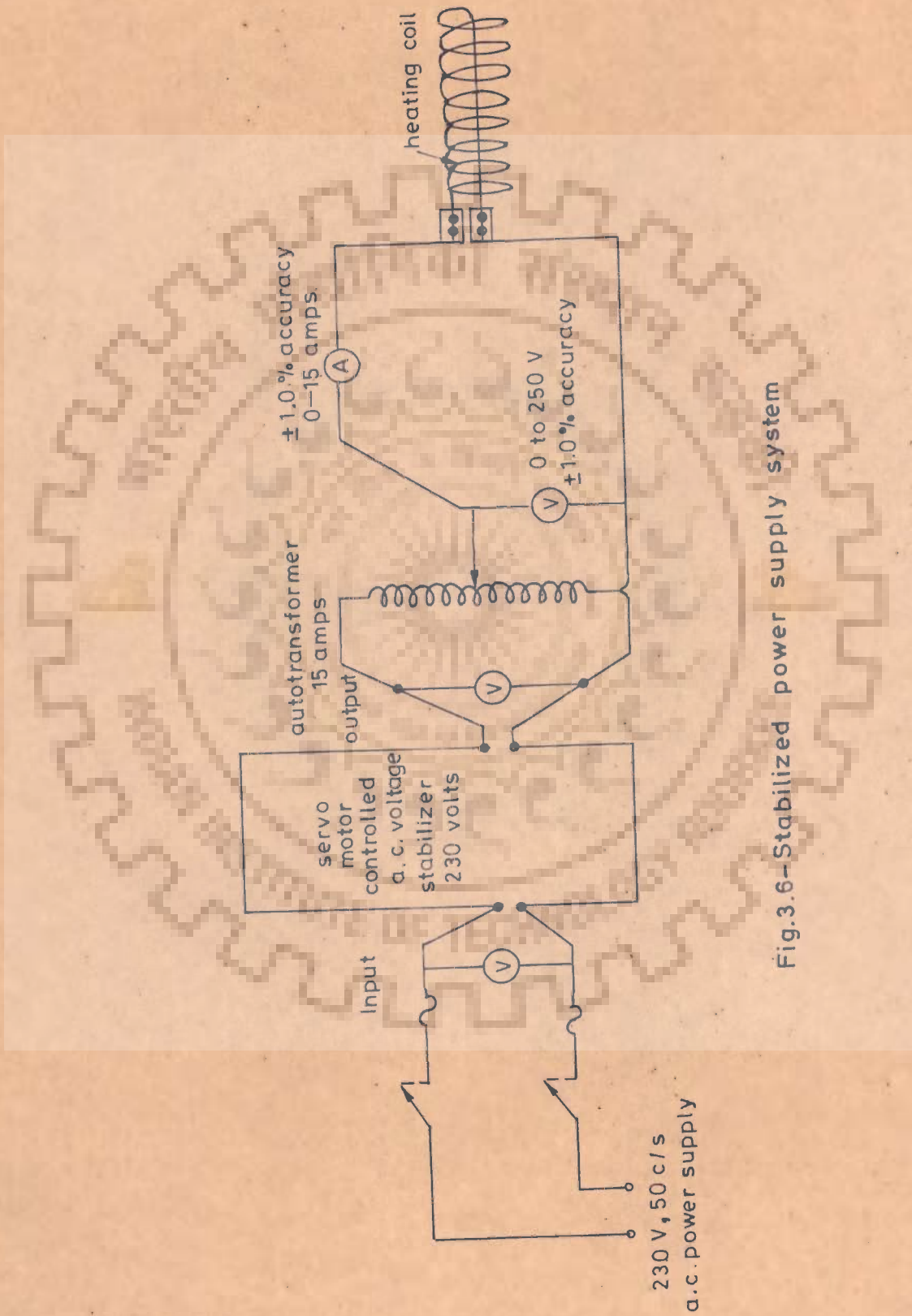


Fig.3.6--Stabilized power supply system

the heat flux. Different values of heat flux were obtained by the autotransformer as already mentioned above.

### 3.3.2 e.m.f. Measurement of Thermocouples

The electro-motive force of thermocouples was measured with the help of a Vernier potentiometer supplied by M/s Elfo Scientific Instruments and a sensitive spot reflecting galvanometer supplied by M/s Osaw and Co. The range of the potentiometer was 0 to 1.901 volts with a least count of 0.1 microvolt and accuracy 0.01 per cent. The power supply to the potentiometer was given by a constant d.c. voltage source of 2.25 volts by connecting this source at the correct terminals of the potentiometer. A standard cell having fixed voltage of 1.0186 volts was connected to the potentiometer for its standardisation. To provide required reference temperature of  $0^{\circ}\text{C}$  a melting-ice bath was used as a cold junction. A multi-point selector switch supplied by M/s Toshniwal and Co. was used to connect the thermocouples to the potentiometer as shown in Figure 3.7.

The surface and liquid thermocouples were calibrated before their insertion in the experimental facility. The thermocouples were calibrated by means of immersing their hot junction in different pure liquids of known boiling points at atmospheric pressure.

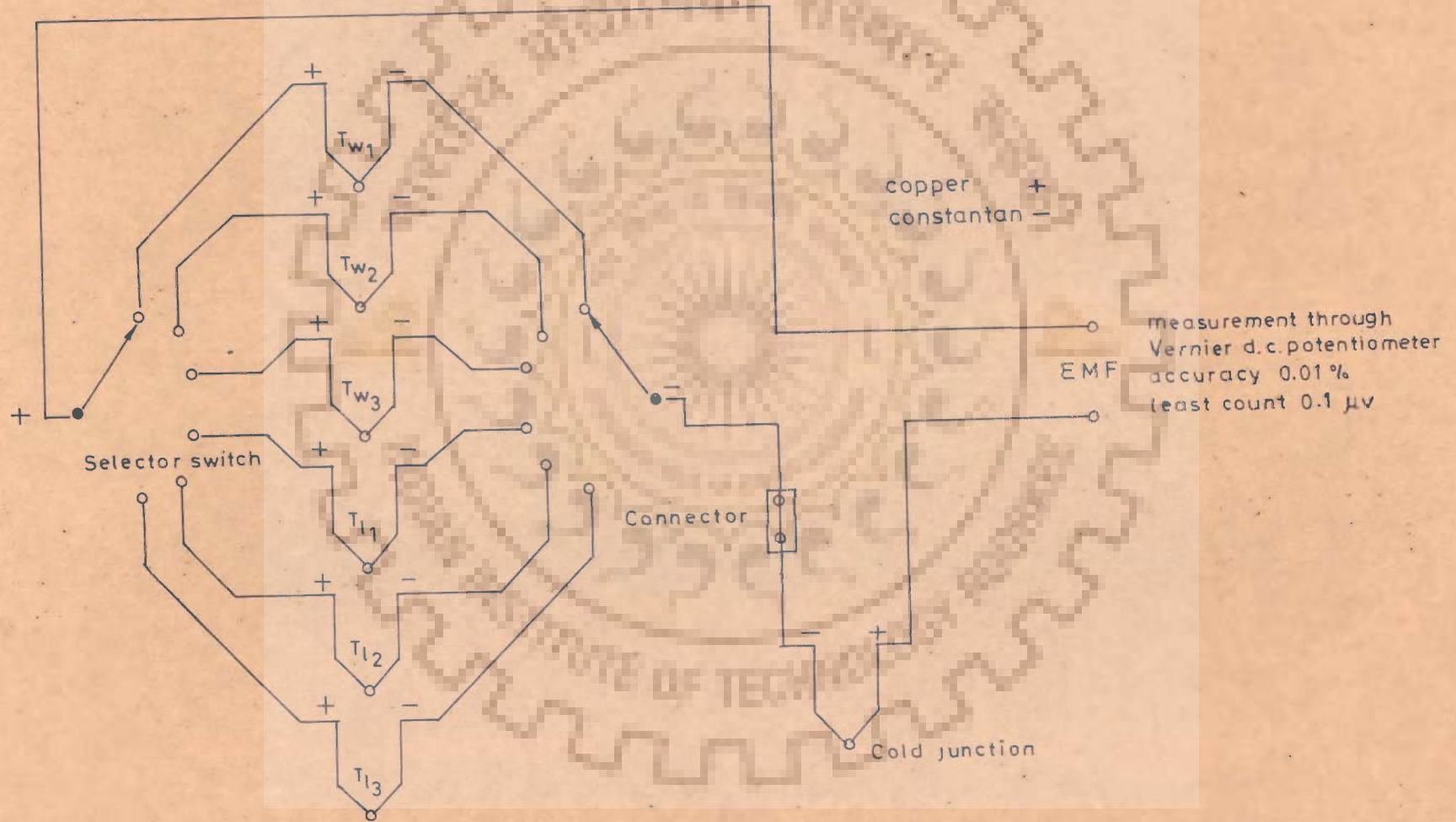


Fig.3.7-Details of selector switch and thermocouple assembly

The e.m.f. of thermocouples were recorded by the arrangement described above. A mercury in-glass thermometer of accuracy  $0.05^{\circ}\text{C}$  was also placed in the boiling liquids to compare the readings of thermocouples. The e.m.f. recorded by thermocouples compared with the respective boiling points of four pure liquids showed a maximum deviation of  $\pm 0.1$  per cent. The readings of thermocouples and thermometer were also within a maximum deviation of  $\pm 0.1$  per cent.

### 3.3.3 Concentration Measurement

The concentration of binary liquid mixtures was measured by using a calibrated precision grade refractrometer supplied by M/s Carl Zeiss Jena Co. The accuracy of the instrument was measured by comparing the refractive index values of four pure liquids as mentioned above at  $15^{\circ}\text{C}$  with those available in literature [119] as shown in Figure 3.8. The accuracy obtained in the refractive index measurement was within  $\pm 0.02$  per cent.

### 3.3.4 Vacuum Measurement

Vacuum was measured by placing two calibrated precision grade vacuum gauges. One of them was mounted on the top of the test vessel and other on liquid sampling unit as shown in Figures 3.1 and 3.4.



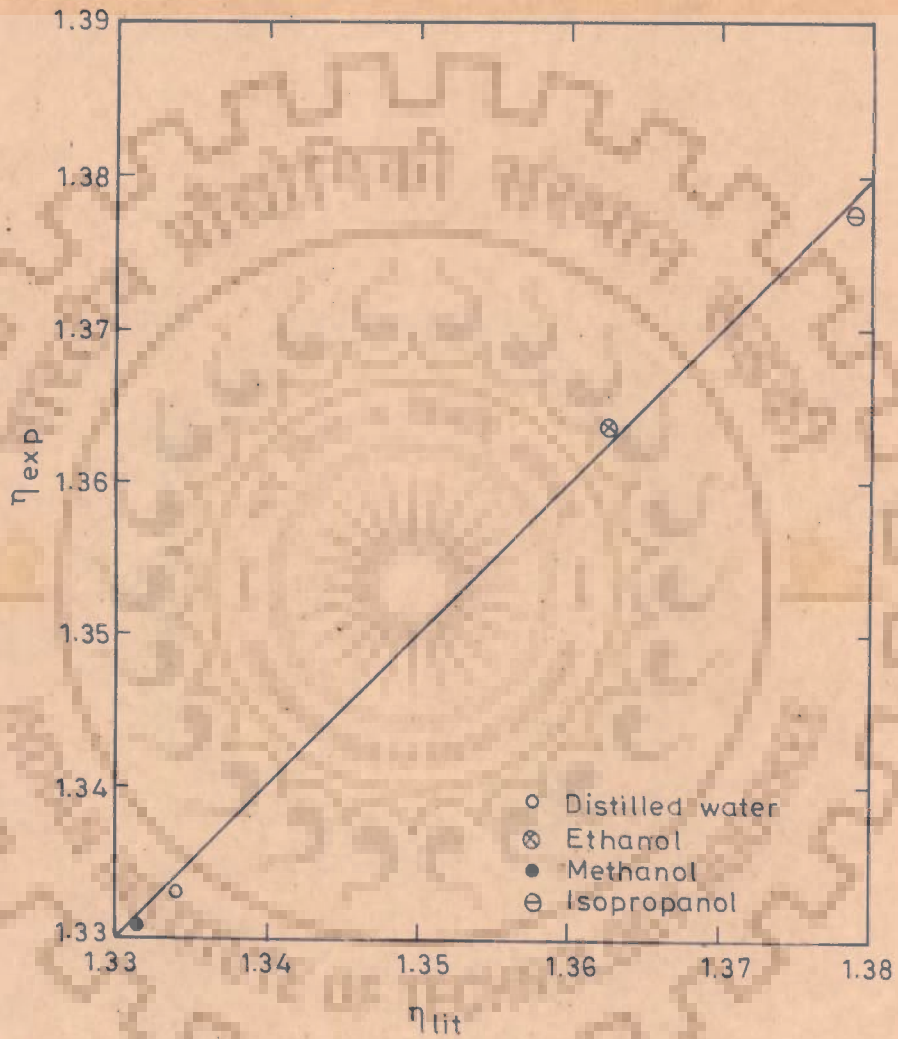


Fig.3.8-Comparison of experimental refractive index with values in literature [119] for pure liquids at 15°C.

## CHAPTER - 4

### EXPERIMENTAL PROCEDURE

#### 4.1 TESTING OF EXPERIMENTAL SET-UP

To obtain the reliable experimental data the facility was subjected to the following tests :

The objective of the present investigation was to obtain nucleate pool boiling data at subatmospheric pressure. Therefore, experimental facility was tested for vacuum integrity. This was done in two steps : Firstly, the facility was charged with compressed air at a pressure of  $680 \text{ kN/m}^2$  and left for 48 hours. No change in pressure gauge reading was observed. Then it was evacuated till the vacuum gauge registered a reading of  $95 \text{ kN/m}^2$  and this was also left for 48 hours. No change in the vacuum gauge reading was observed. Both these tests ensured the vacuum integrity of the experimental facility.

In addition to the above test the condenser (18) was ensured against liquid interchange between the test-liquid side and the coolant side.

Tests were also conducted to check against any electric leakage. All electrical connections were earthed for the safe operation of the facility.

## 4.2 OPERATING PROCEDURE

The following procedure was used for obtaining the experimental data :

### 4.2.1 Stabilization of the Heat Transfer Surface

Before conducting the series of experimental runs it was necessary to age and stabilize the heat transfer surface. This was done as follows : the surface was submerged in the pool of liquid for a period of 48 hours followed by a boiling of 12 hours. Steady state was allowed to reach and the surface temperatures were recorded. The surface was again kept submerged in the pool of liquid for 72 hours followed by another 12 hours of boiling at similar experimental conditions. Surface temperatures were then recorded and compared with previous values. The discrepancy in these data were observed. The procedure was repeated till the data were reproducible after several days of aging and several hours of boiling. This reproducibility of the data ensured the stabilization of the heat transfer surface.

This procedure was repeated for each new liquid chosen for experimentation.

#### 4.2.2 Cleaning and Charging

Prior to charging the system with new liquid, the system was thoroughly cleaned for the traces of the previous liquid. This was accomplished by flushing all the components of the experimental facility with compressed air. The heat transfer surface was then rinsed with distilled water, acetone and finally with the liquid under investigation. The test vessel was then filled with the liquid upto a given level.

#### 4.2.3 Removal of Dissolved Air from the Test Liquid

As discussed in Section 3.2.4 degassing of the test-liquid was necessary to obtain reliable experimental data. This was done by heating the liquid to its boiling point. With continued boiling, the dissolved air started coming out of the liquid. This was indicated by the bubbling taking place in the beaker (19) filled with test liquid. During boiling all the valves (4,7,9, 14), except valve (3), were closed as depicted in Figure 3.1. When bubbling ceased, valve (3) was closed and valve (7) was opened.

#### 4.2.4 Experimentation

After removing the last traces of dissolved air the facility was set for the experimental parameters namely; heat flux and pressure for a given liquid. These parameters were varied systematically. The vacuum

in the facility was created by switching on the vacuum pump and manipulating the control valves (23, 24) as shown in Figure 3.1. When the desired vacuum was maintained, the control valves were closed and vacuum pump switched off. The required heat flux was then modulated by means of an autotransformer. After adjusting these parameters the experiment was allowed to run for 1 to 2 hours till the thermal equilibrium was attained. Under these conditions, there was no change in surface and liquid temperatures with time. For all the data a steady state of one hour was observed. At equilibrium, the readings of surface and liquid thermocouples, ammeter, voltmeter and vacuum gauge were recorded and also the barometric pressure.

While conducting experiments with binary liquid mixtures the samples of liquid and vapour in equilibrium with it were taken periodically from respective sampling units (20, 21) as shown in Figure 3.1. Their refractive indices were measured with the help of a refractometer to know the liquid and vapour compositions. Since the refractive index is sensitive to temperature, the samples on collecting from the experimental facility were kept in ground glass bottles immersed in a constant temperature bath at  $0^{\circ}\text{C}$ . The samples were then analysed in the Instrumentation Laboratory where the room temperature is maintained at  $15^{\circ}\text{C}$ .

To obtain the calibration curves, known compositions of alcohol-water mixtures were prepared and their refractive indices were measured. These values are plotted against composition for ethanol-water, methanol-water and isopropanol-water mixtures in Figures 4.1 through 4.3 respectively. These plots served as reference curves for evaluating compositions of liquid and vapour samples drawn during experimentation.

The next run was conducted by changing the heat flux value for the same pressure and liquid. Similar experimental runs were conducted for all the heat flux values as given in Table 5.1. For all the runs, this procedure was also followed for other pressures for the pure liquids; distilled water, ethanol, methanol and isopropanol and their aqueous binary mixtures. The details of experimental parameters are given in Table 5.1.

#### 4.3 CONSISTENCY OF EXPERIMENTAL DATA

Several experimental runs are repeated to check the consistency of experimental data and it was found that the data were reproducible within the allowable experimental errors of 1.5 per cent. This shows that the data points were not erratic. However, these data have not been included in the thesis.

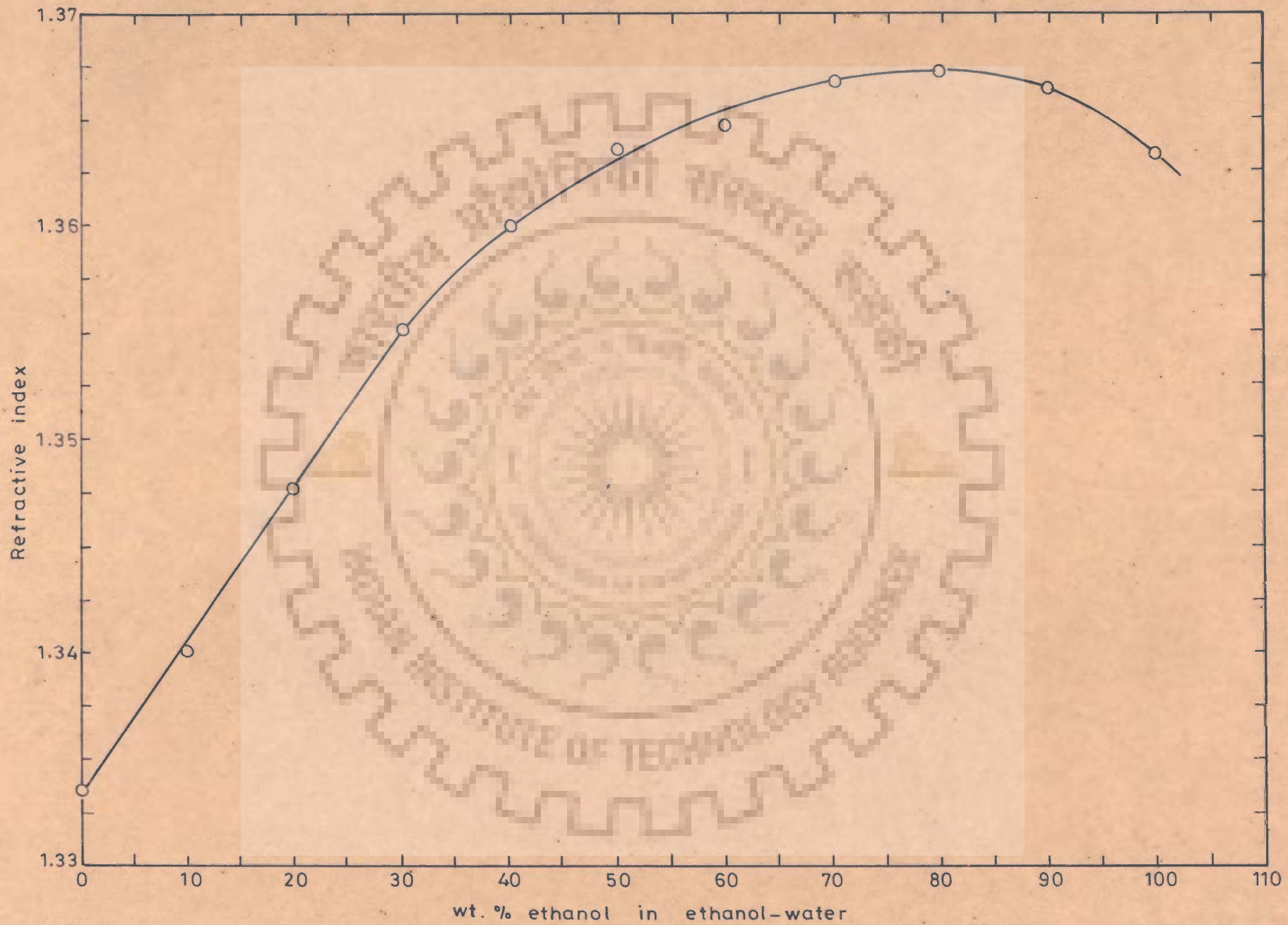


Fig.4.1-Calibration curve for ethanol-water mixtures at 15°C

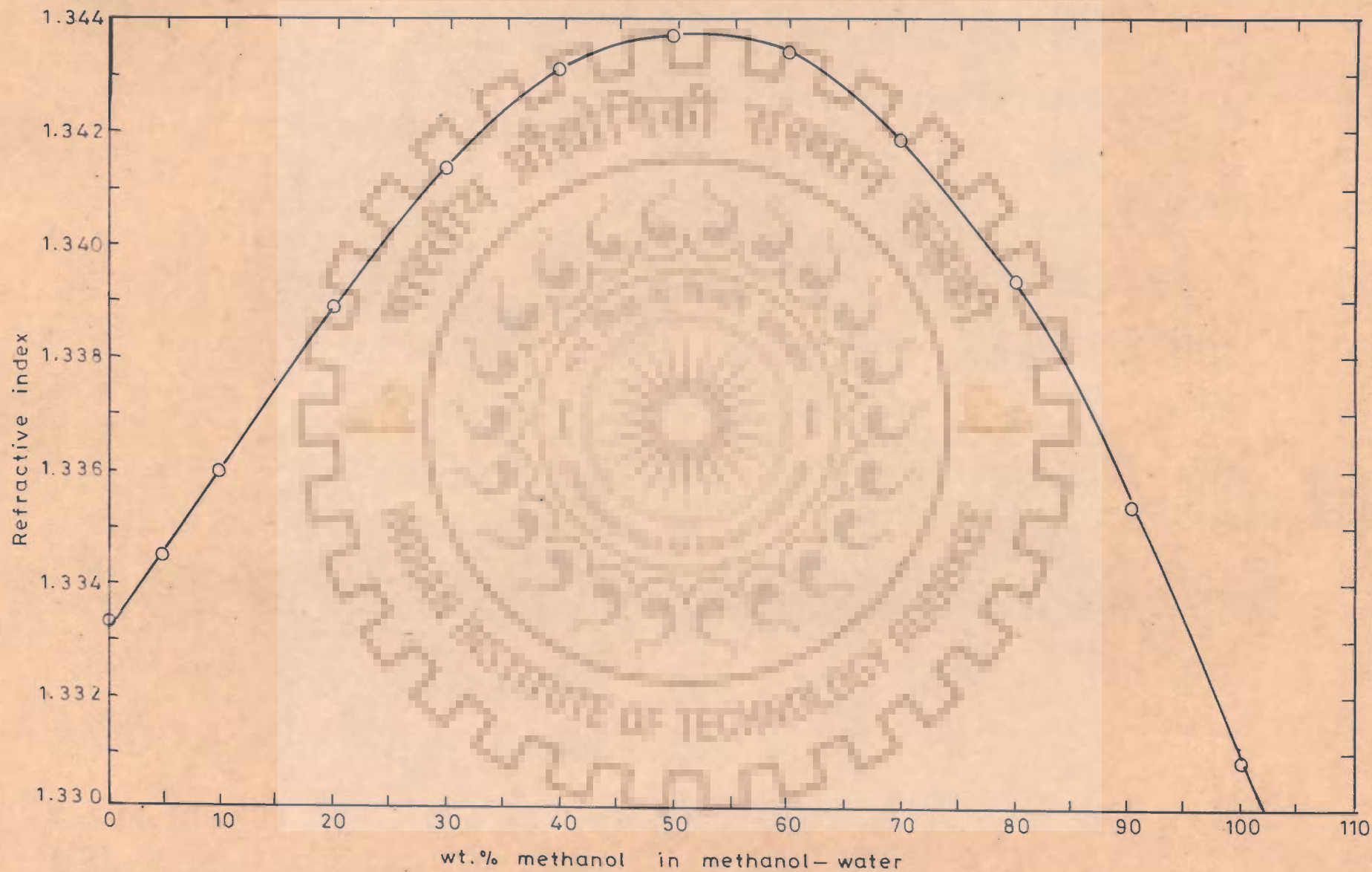


Fig.4.2- Calibration curve for methanol-water mixtures at 15°C



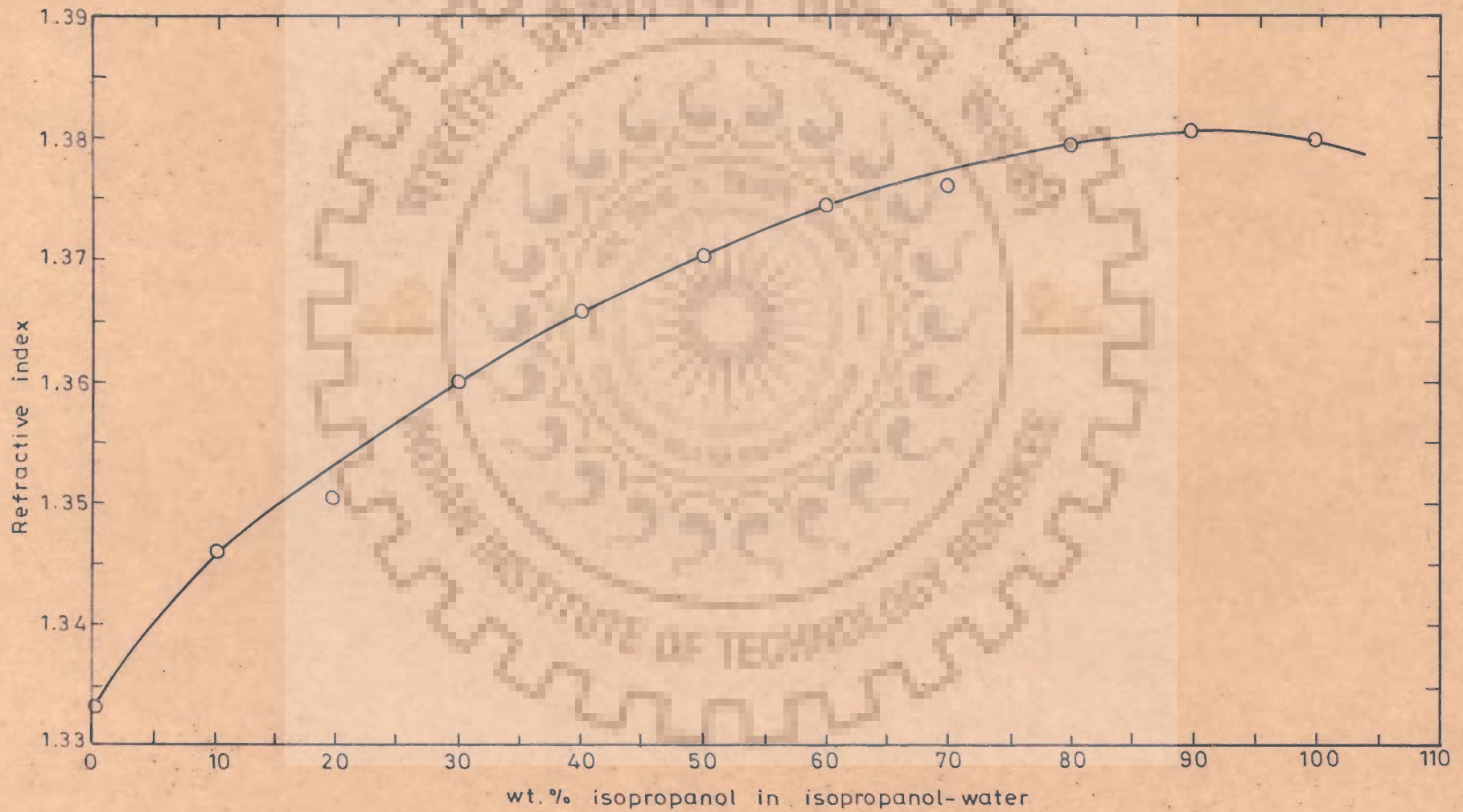


Fig.4.3-Calibration curve for isopropanol-water mixtures at 15°C

## CHAPTER - 5

### RESULTS AND DISCUSSION

Present investigation pertains to boiling heat transfer from a horizontally placed cylindrical surface, submerged in a pool of saturated liquids and their mixtures. These studies were carried out at low heat flux under the atmospheric and the subatmospheric pressures.

Table 5.1 enlists liquids and their binary mixtures alongwith the range of experimental parameters. The heating surface used for the present study was a 410 ASIS grade stainless steel cylinder.

In all 468 data points for the saturated pool boiling studies were obtained and subsequently analyzed. They are recorded in Tables B-1 to B-21 of Appendix-B.

Table 5.1 : Parameters for Saturated Nucleate Pool Boiling Studies

System No.	Boiling liquid	Heat flux, $W/m^2$	Pressure, $kN/m^2$
1	Distilled water	9618, 12621, 16489, 20356 and 24911	98.63, 66.64, 50.65, 33.32 and 25.33
2	Ethanol	9975, 12865, 16947, 20611, 25191 and 26740	98.63, 61.31, 47.98, 33.32 and 25.33

System No.	Boiling liquid	Heat flux, $w/m^2$	Pressure, $kN/m^2$
3	Ethanol-Water Mixture		
(i)	11.86 wt. per cent ethanol	9975, 13028, 16532, 20865 and 25471	98.63, 61.31, 42.45, 36.0 and 28.0
(ii)	22.12 wt. per cent Ethanol	10064, 13232, 16419, 20865, 26219 and 30229	98.63, 66.64, 53.52, 33.32 and 21.33
(iii)	31.10 wt. per cent Ethanol	9975, 13028, 16718, 20865, 25191 and 30534	98.63, 66.64, 50.65, 33.32 and 22.66
(iv)	39.00 wt. per cent Ethanol	10153, 13028, 16947, 20611, 25751 and 30534	98.63, 66.64, 47.98, 35.99 and 25.33
(v)	52.30 wt. per cent Ethanol	10153, 13130, 17674, 21120, 25611 and 30229	98.63, 66.64, 46.65, 33.32 and 22.66
(vi)	71.88 wt. per cent Ethanol	13232, 16489, 19824, 26219 and 30534	98.63, 69.31, 47.98, 33.32 and 18.66
4	Methanol	9618, 12621, 16260, 20356 and 24911	98.63, 66.64, 50.65, 34.65 and 25.33
5	Methanol-Water Mixtures		
(i)	8.56 wt. per cent Methanol	9618, 12824, 16489, 20356 and 25050	98.63, 66.64, 50.65, 33.32 and 25.33
(ii)	16.50 wt. per cent Methanol	9618, 12926, 16489, 20356 and 24911	98.63, 66.64, 50.65, 33.32 and 25.33
(iii)	30.80 wt. per cent Methanol	9618, 12824, 16489, 20611 and 25239	98.63, 66.64, 50.65, 33.32 and 29.32
(iv)	43.24 wt. per cent Methanol	9440, 12417, 16031, 19847 and 25191	98.63, 66.64, 50.65, 33.32 and 25.33
(v)	64.00 wt. per cent Methanol	9618, 9975, 12824, 16489, 20611, 24631 and 30534	98.63, 66.64, 49.32, 33.32 and 26.66

System No.	Boiling liquid	Heat Flux, W/m <sup>2</sup>	Pressure, kN/m <sup>2</sup>
6	Isopropanol	9657, 9975, 12784, 16305, 20865 and 25191	98.63, 69.31, 47.98, 34.66 and 12.66
7	Isopropanol-Water Mixtures		
(i)	15.00 wt. per cent Isopropanol	9975, 12947, 16718, 20865 and 25191	98.63, 73.98, 49.32, 33.32 and 25.33
(ii)	22.50 wt. per cent Isopropanol	9975, 13771, 17041, 20611, 25471 and 29924	98.63, 66.64, 53.32, and 34.66
(iii)	31.25 wt. per cent Isopropanol	16718, 20611, 24631, 29425 and 31354	98.63, 61.31, 50.65, 34.66 and 25.33
(iv)	37.00 wt. per cent Isopropanol	16947, 20865, 25191 and 30840	98.63, 63.98, 50.65, 33.32 and 25.33
(v)	59.00 wt. per cent Isopropanol	9975, 10959, 13232, 16718, 20865 and 25191	98.63, 65.31, 50.65, 34.66 and 25.33
(vi)	77.00 wt. per cent Isopropanol	9975, 13603, 16489, 20611, 22494 and 25191	98.63, 66.64, 50.65, 33.32 and 25.33

It may be noted that the actual values of heat flux are given in Appendix-B for each of the pressures investigated.

All the test runs of Appendix-B contain temperatures at the top-, the side-, and the bottom-positions of the heating surface and their corresponding liquid temperatures, heat flux, and system pressure.

Besides, the conduction correction for wall temperature, the temperature difference between wall and liquid and the local and the average heat transfer coefficients are also included. The average value of temperature difference,  $\overline{\Delta T}$  over the circumference at a given plane was calculated by the method of mechanical quadrature [117]. To obtain the average value of temperature difference, the wall temperature was corrected by considering the wall temperature drop as discussed in Appendix-D, and the average heat transfer coefficient was calculated from the following equation :

$$\bar{h} = \frac{q}{\overline{\Delta T}} \quad \dots(5.1)$$

### 5.1 LIMITATIONS OF DATA PROCESSING

The constraints involved while processing the data were as follows :

1. The direct measurement of temperature along the circumference of the heating surface at a given plane was not feasible because of the fact that it involved the installation of thermocouples on the outer surface of the heating surface, which, in turn, led to fabricational difficulties and possibilities of interference with boiling phenomenon. Therefore, the temperature measurement at a given plane was carried out by placing the

thermocouples in between the inner and the outer surfaces of the heat transfer surface at the top-, the side-, and the bottom-positions as detailed in Figure 3.5. To determine the temperatures corresponding to these positions at the outer surface, Fourier's conduction equation was used to calculate the temperature drop assuming that the heat flow in axial direction was negligibly small. This was a valid assumption as the thickness of the cylinder-wall was much smaller than its length. The temperature drop across the wall was subtracted from the measured values of the surface temperatures to obtain the corrected wall temperatures,  $T_w$ .

2. The average values of temperature difference,  $\overline{\Delta T}$ , were calculated from the  $\Delta T$  values at the three positions as mentioned above. The value of  $\Delta T$  at a particular location was the corrected wall temperature minus the corresponding liquid temperature. This average temperature difference was, further, used to calculate the value of average heat transfer coefficients.
3. The physico-thermal properties of binary liquid mixtures were calculated at their saturation temperatures corresponding to the pressures. The properties of these mixtures were not available

in the literature over the experimental range used in the present investigation. Therefore, the methods, discussed in Appendix-C, were devised and first tested for the available values to calculate the physico-thermal properties of binary liquid mixtures which showed a  $\pm 5$  per cent deviation, hence they have been used to predict the properties with confidence.

4. The heat flux was limited to  $30,000 \text{ W/m}^2$  due to the current carrying capacity of the resistance wire, Kanthal-Al grade of 16 gauge which was used as heating element in the form of a coil.
5. Experimental data of other investigators are not available in the literature for binary mixtures for the similar conditions of heat flux and pressure as employed in the present study. Therefore, the generalised correlations are based on the data of present investigation only.
6. Methanol and isopropanol were of Analar grade as supplied by Chemical Division of Glaxo Laboratories Limited, Bombay (India). Their boiling points were measured under atmospheric pressure. A deviation of  $+2^\circ\text{C}$  was noticed in their saturation temperatures as against the reported values by the Suppliers. However, for

processing the data, the temperatures recorded by the thermocouple were accepted. This was also followed in case of ethanol.

## 5.2 NUCLEATE POOL BOILING OF PURE LIQUIDS

Nucleate pool boiling heat transfer is largely affected by the parameters, namely; heat flux, system pressure, physico-thermal properties of boiling liquids, and heating surface characteristics. The parametric effects of these variables are discussed in the subsequent Sections.

### 5.2.1 Effect of Heat Flux on Heat Transfer Coefficient

Figures 5.1 to 5.4 represent the log-log plots, demonstrating the effect of heat flux on the average value of the heat transfer coefficient for distilled water, ethanol, methanol and isopropanol, respectively with pressure as parameter. From these figures the following salient features emerge out :

1. Heat transfer coefficient increases linearly with heat flux, showing a slope of 0.7, for all the boiling liquids. This unique characteristic is exhibited both for the atmospheric and the subatmospheric pressures. This can be explained as follows :



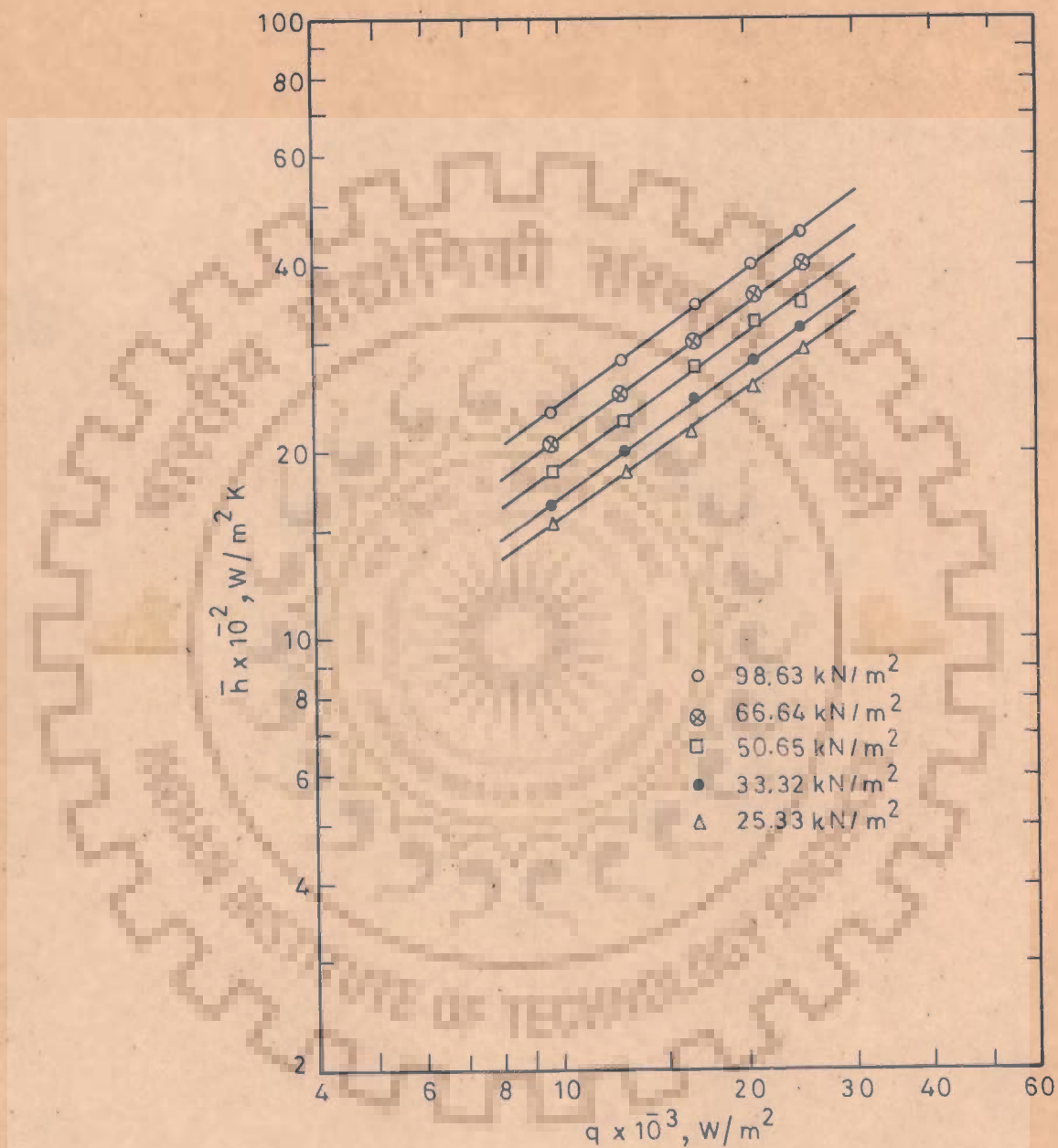


Fig.5.1- Variation of heat transfer coefficient with heat flux for distilled water at atmospheric and subatmospheric pressure

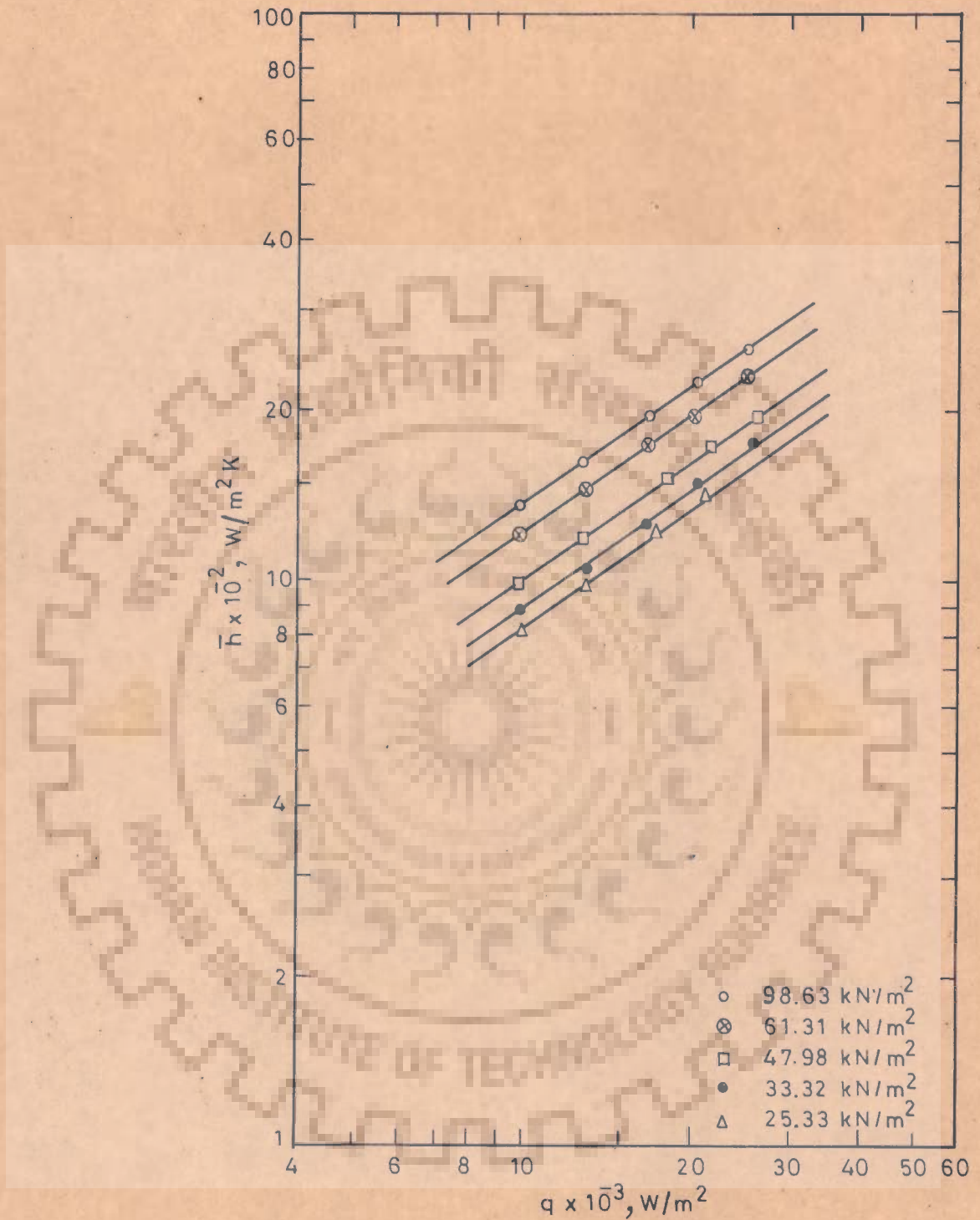


Fig.5.2-Variation of heat transfer coefficient with heat flux for ethanol at atmospheric and subatmospheric pressure

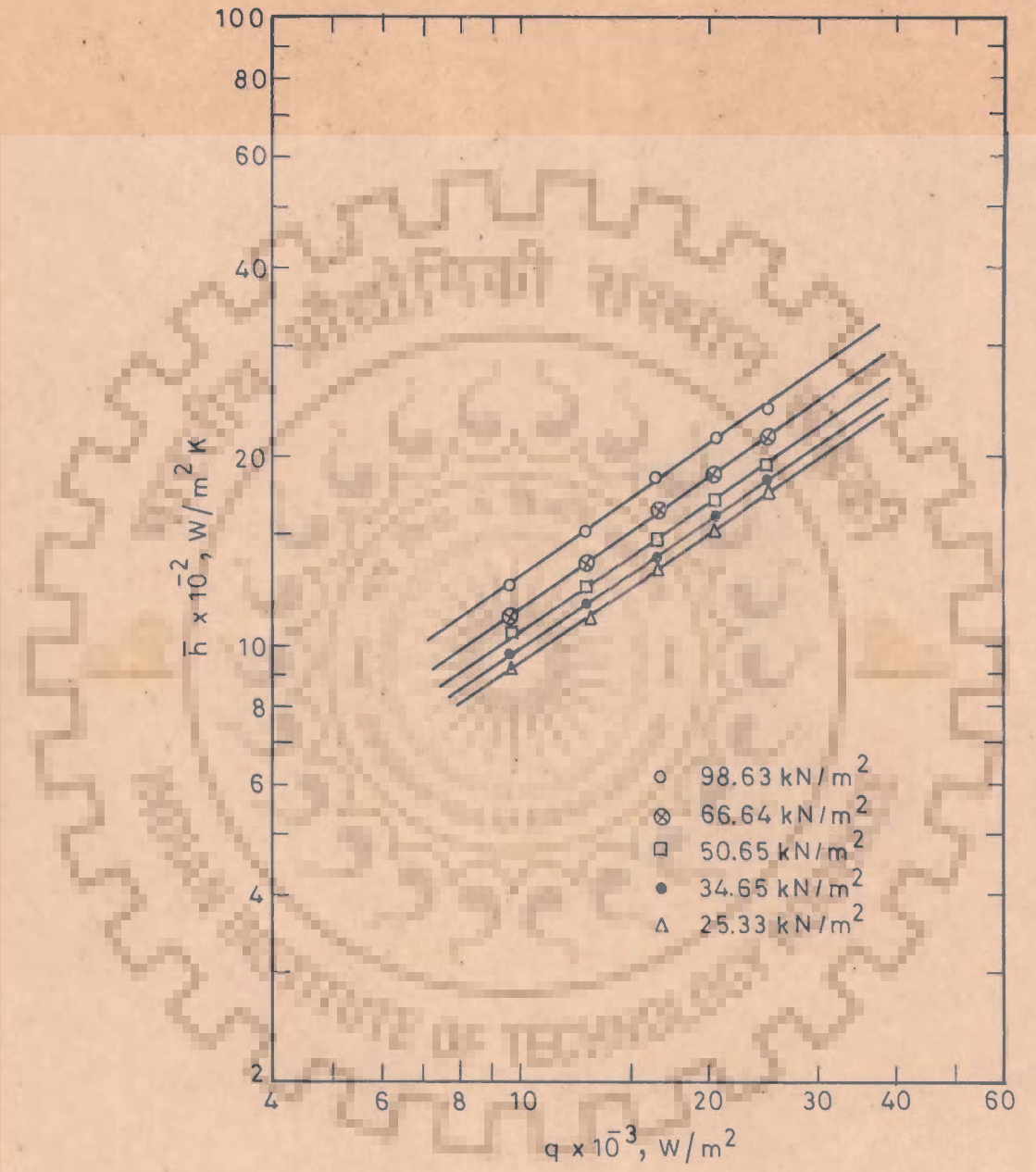


Fig.5.3-Variation of heat transfer coefficient with heat flux for methanol at atmospheric and subatmospheric pressure

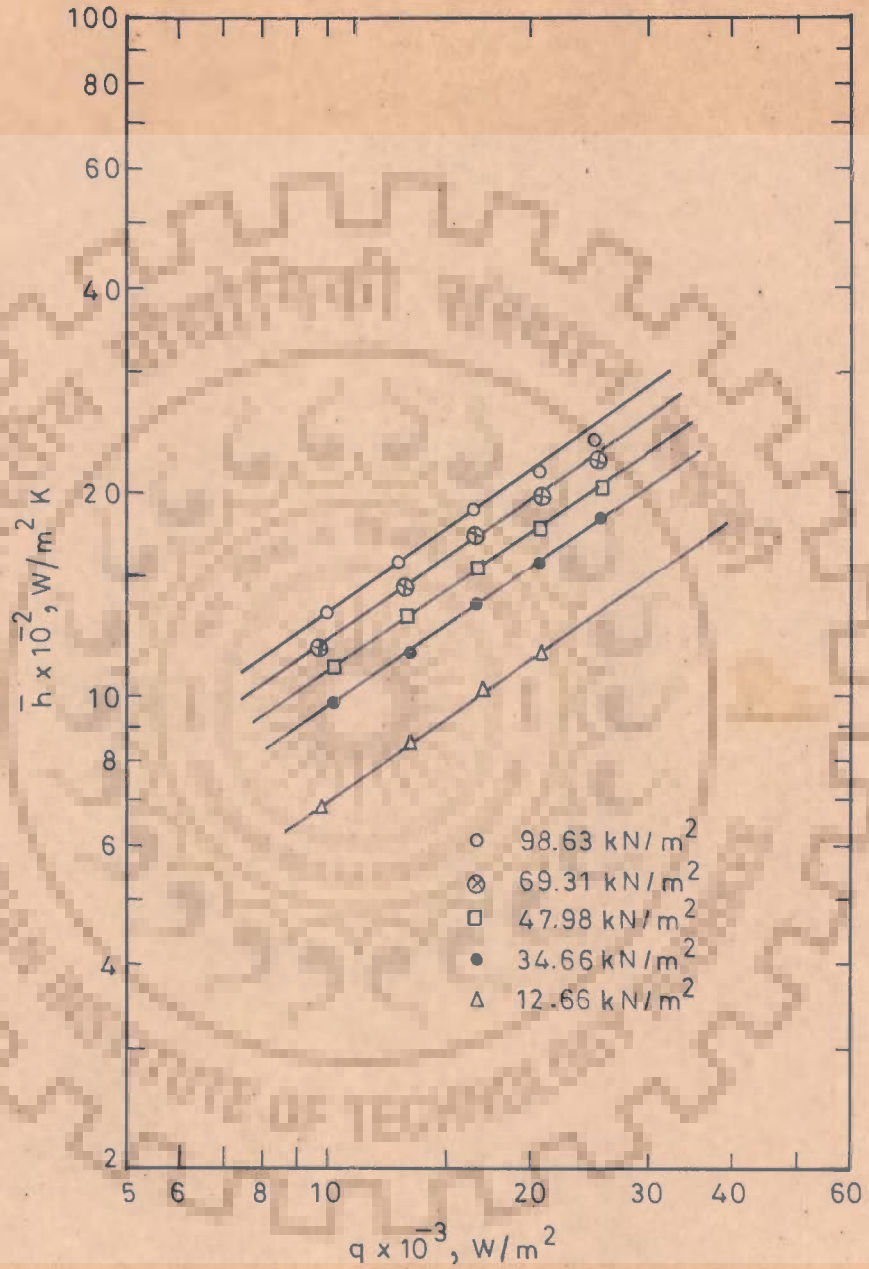


Fig.5.4-Variation of heat transfer coefficient with heat flux for isopropanol at atmospheric and subatmospheric pressure

With an increase in the value of heat flux for a liquid at a constant pressure, there is an increase in the number of active nucleation sites,  $n$  on the heating surface and thereby the bubble emission frequency,  $f$ . The strong dependency of the number of nucleation sites on heat flux is a well-established fact as shown by several investigators [120-122].

The increase in the bubble emission frequency with heat flux has been demonstrated by Sharma and Varshney [123] who have recommended following expressions for calculating bubble emission frequency, from a heat transfer surface submerged in a pool of liquid, for different values of Jakob number :

(a) For  $Ja \leq 100$

$$f = \frac{1}{\frac{[133.3/P]^2 [\sigma / (\rho_l - \rho_v) g]}{\pi \alpha_l Ja^2} + \frac{0.867}{\alpha_l} \left[ \frac{k_l \Delta T_w}{q} \right]^2} \dots (A)$$

(b) For  $Ja > 100$

$$f = \frac{1}{\frac{[133.3/P]^2 [\sigma / (\rho_l - \rho_v) g]}{25 \alpha_l Ja^{3/2}} + \frac{0.867}{\alpha_l} \left[ \frac{k_l \Delta T_w}{q} \right]^2} \dots (B)$$

In fact, first term in the denominator of Equations (A and B) represents the growth period and the second term, the waiting period. Both the Equations (A and B) clearly indicate that the bubble emission frequency depends upon the heat flux and physico-thermal properties of the bulk liquid. Thus, for a given pressure an increase in the value of heat flux reduces the magnitude of the waiting period. As a consequence of this the bubble emission frequency increases. It may be noted that Körner and Photiadis [124] have also established that the frequency of bubble generation increased strongly with heat flux. Similar results are reported by Saini [93].

Further, Wiebe and Judd [118] relates the heat transfer coefficient to number of nucleation active sites,  $n$  and bubble emission frequency,  $f$  as follows :

$$h \propto (nf)^a$$

Hence the above explains the increase in heat transfer coefficient when the heat flux is raised.

2. Another noticeable phenomenon observed from these plots is that the increase in pressure results in shifting the lines to the left indicating that the heat transfer coefficient increases for a given value of heat flux. The enhancement in heat transfer coefficient with respect to increasing the values of pressure is due to the reduction in surface tension of the liquid. As the surface tension is reduced the nucleation sites having smaller radii, not being active at lower pressures, become active causing more induced turbulence in the boiling liquid. In fact, the work required to form a vapour bubble on a heating surface is given by the following equations :

$$\text{Work} = \sigma S \left[ 1 - \frac{S}{S^0} (1 - \cos \beta) \right]$$

This equation indicates that the work required for the formation of a vapour bubble decreases as the value of surface tension decreases. Therefore, with the increase in pressure for a given heat flux, more number of the bubbles will be formed, thereby causing more induced turbulence. As a consequence of it, the heat transfer coefficient increases. Mathematically,

these plots can be expressed by the following empirical relationship :

$$\bar{h} = C q^{0.7} \quad \dots(5.2)$$

where the constant,  $C$ , represents a constant of proportionality. In fact, one can not establish its nature, unless the dependence of  $\bar{h}$  on pressure, nature of liquid, and heating surface characteristic is also known.

#### 5.2.2 Effect of Surface Characteristics on Heat Transfer Coefficient

Figures 5.5 and 5.6 are the typical log-log plots of heat transfer coefficient against heat flux for isopropanol and methanol, respectively. These plots were made to understand the effect of heating surface characteristics on heat transfer coefficient.

Figure 5.5 contains the data of present investigation and those of Sternling and Tichacek [18] for the boiling of isopropanol at  $98.63 \text{ kN/m}^2$ . The data for the boiling of methanol at  $66.64 \text{ kN/m}^2$  of present investigation and of Cryder and Finalborgo [9] are shown in Figure 5.6. The heating surfaces used in these investigations were different as given in Table 5.2.

An examination of these figures reveals that all the data points show same functional relationship between heat transfer coefficient and heat flux, i.e.



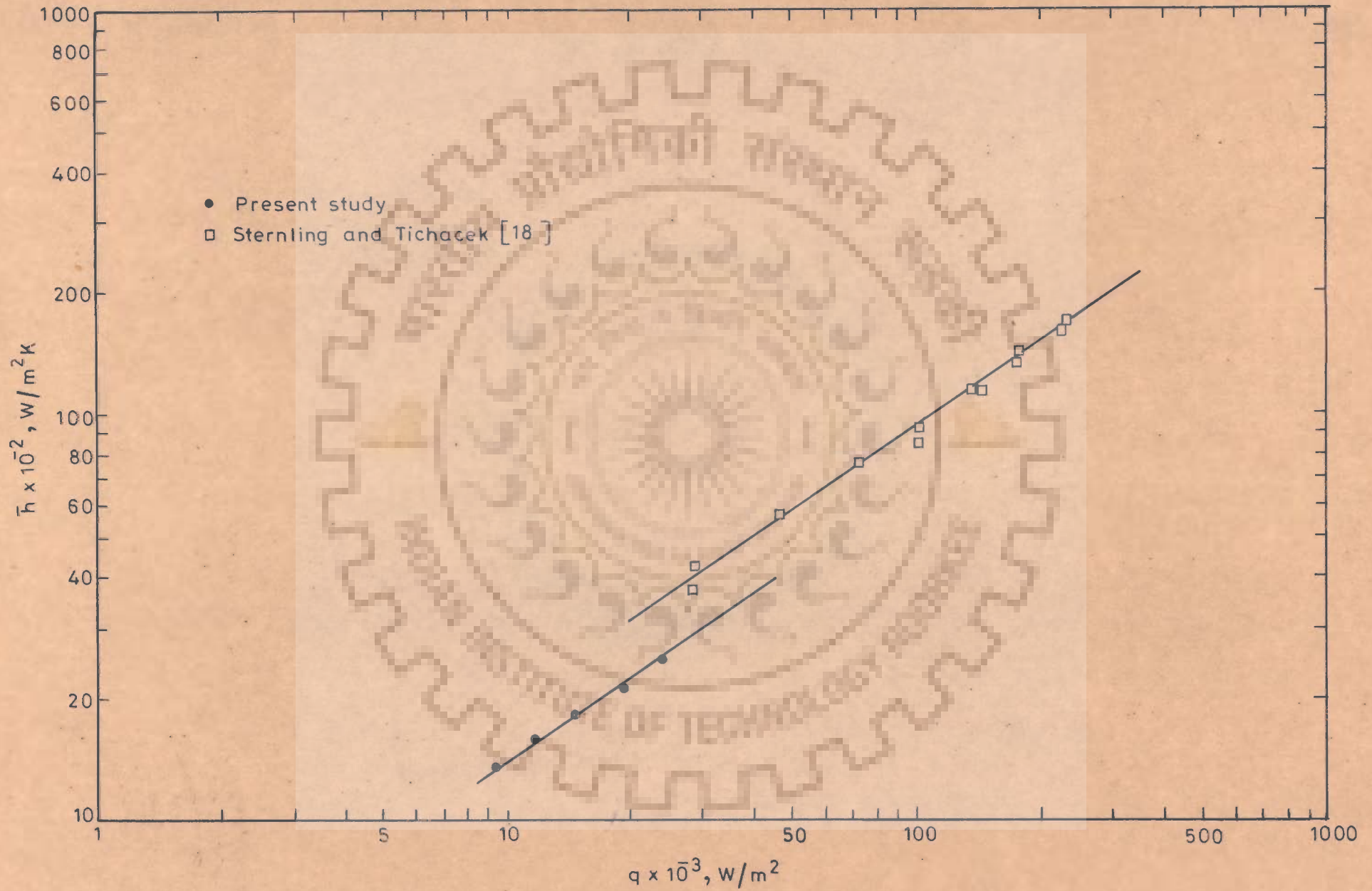


Fig.5.5-Heat transfer coefficient-heat flux relationship for isopropanol at 98.63 kN/m<sup>2</sup>

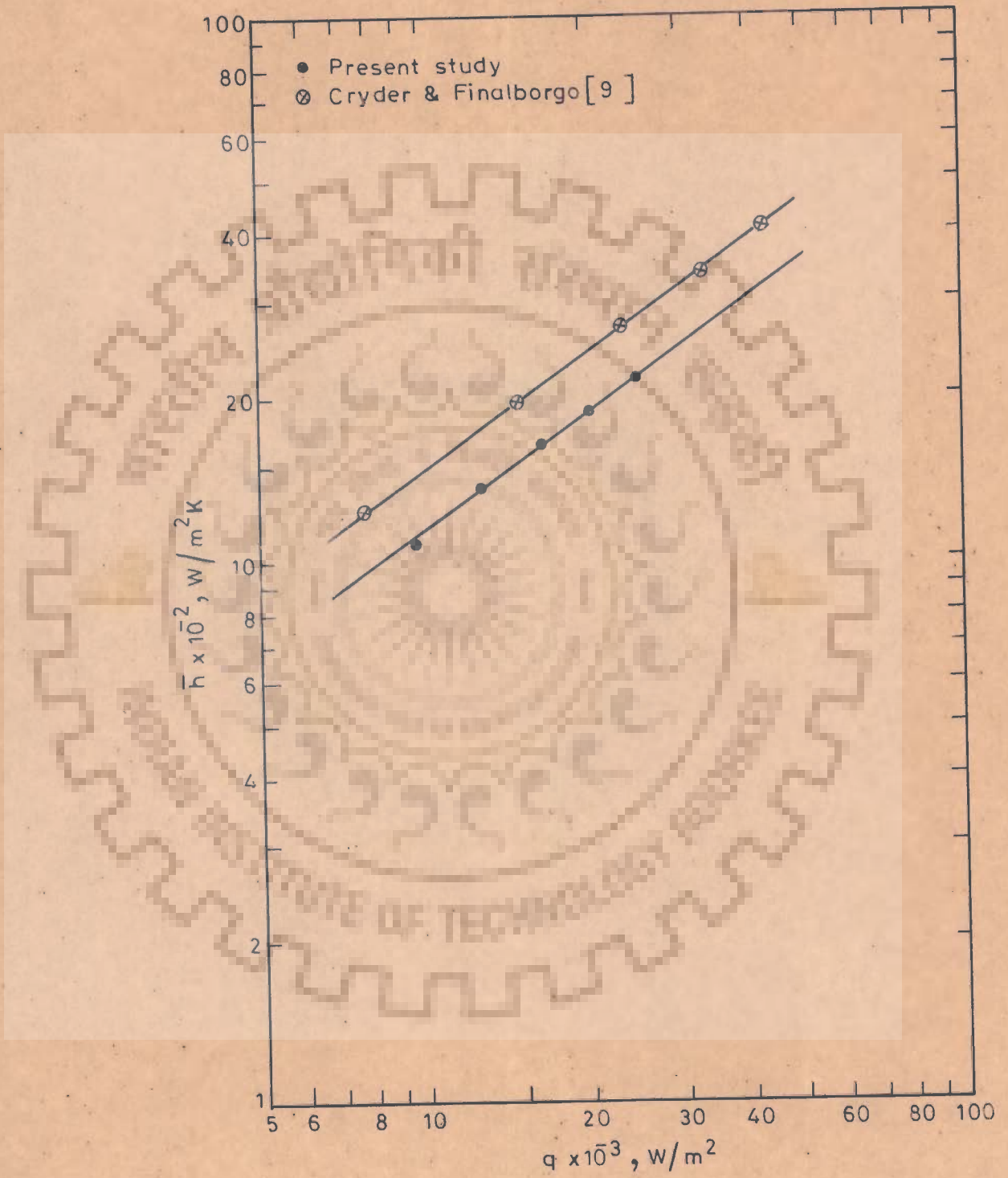


Fig.5.6-Heat transfer coefficient – heat flux relationship for methanol at 66.64 kN/m<sup>2</sup>

$\bar{h} = \text{constant } (q)^{0.7}$ . However, the value of the 'constant' differs widely from one investigation to another. This is attributed to the differing heating surfaces used in these investigations. Finally, it is concluded that the boiling heat transfer data are influenced strongly by the heating surfaces.

Table 5.2 : Parameters for Earlier Studies in Nucleate Pool Boiling of Pure Liquids

S.No.	Boiling liquid	Heat Flux $W/m^2$	Pressure $kN/m^2$	Nature of heating surface	Investigator
1.	Distilled water	6209-46220	1.33-101.30	Copper cylinder	Raben et al [125]
2.	Distilled water Methanol n-Butanol Carbon - Tetrachloride	7808-43543	3.82-101.13	Brass pipe	Cryder and Finalborgo [9]
3.	Isopropanol Methanol	4420-343890	101.30	Stainless steel tube	Sternling and Tichacek [18]
4.	Distilled water Ethanol	140000 - 867500	101.3-5260	Copper plate	Cichelli and Bonilla [11]
5.	Distilled water Ethanol	62340 - 1099030	101.3-7306	Stainless steel cylinder	Borishanskii et al [36]

### 5.2.3 Effect of Boiling Liquids on Heat Transfer Coefficient

Figure 5.7 is a log-log plot of heat transfer coefficient versus heat flux on a given horizontal brass pipe at  $61.25 \text{ kW/m}^2$ , conducted by Cryder and Finalborgo [9]. The distinct lines obtained for distilled water, methanol and carbon tetrachloride having a slope of 0.7 indicate that the effect of boiling liquid on constant  $C$  of Equation (5.2) is appreciable.

Figures 5.8 through 5.12 show the data of present investigation - the heat transfer coefficient as a function of heat flux for distilled water and all the alcohols investigated at atmospheric and subatmospheric pressures. An examination of these Figures reveals one of the distinguishable results of the present work. From these Figures it is clearly seen that all the data points for ethanol, methanol and isopropanol are represented by a single line for a given pressure. This behaviour has been observed both at the atmospheric and the subatmospheric pressures indicating that the proportionality constant,  $C$ , in Equation (5.2) remains constant for all the alcohols under study. This remarkable behaviour may be due to the similar physico-thermal properties of these alcohols. This is clearly seen in Figures C.1 through C.5 of Appendix-C. Due to this, the data for the alcohols investigated have the similar heat transfer behaviour at a given pressure.

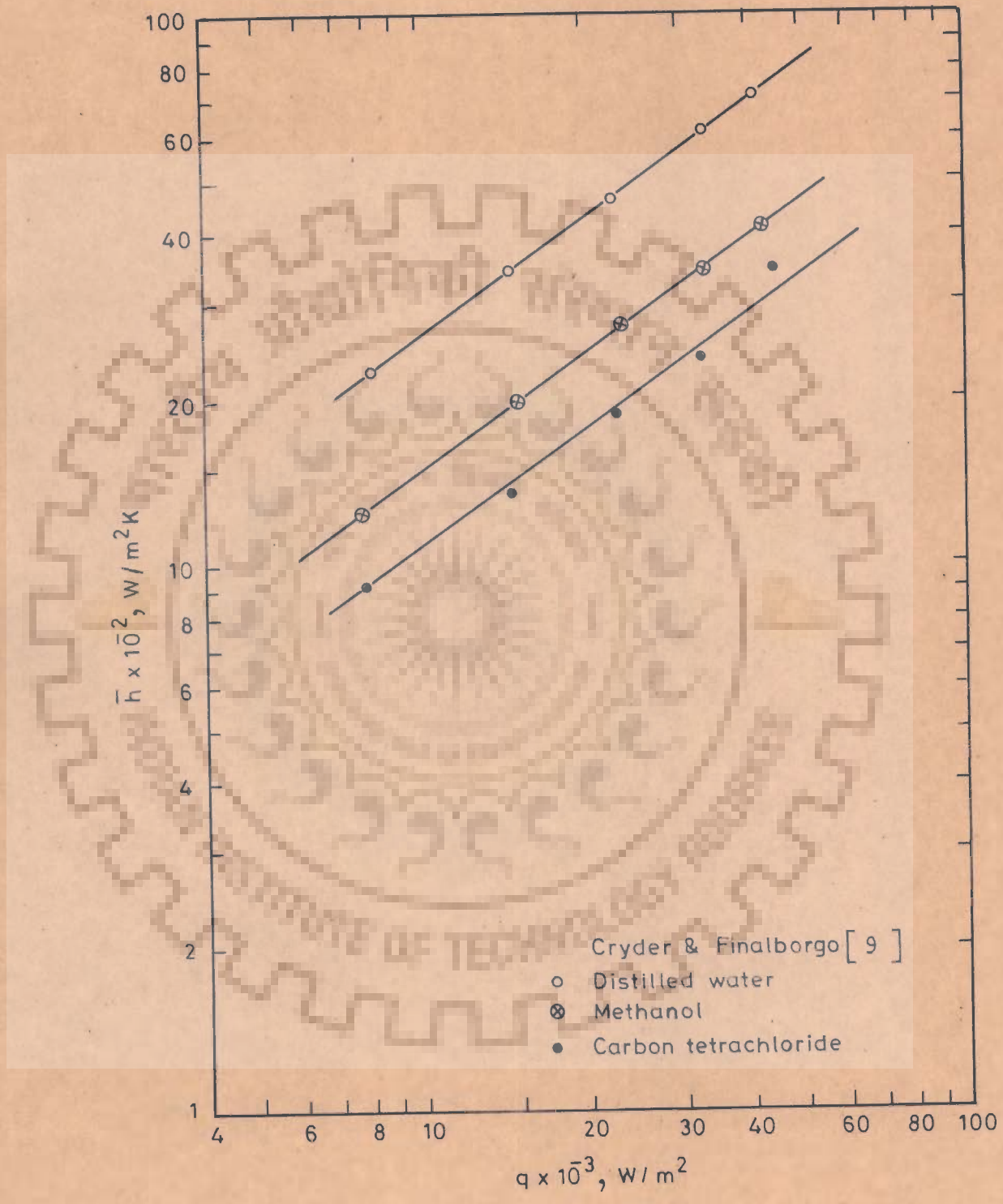


Fig.5.7- Variation of heat transfer coefficient with heat flux on a horizontal brass cylinder at  $61.25 \text{ kN/m}^2$

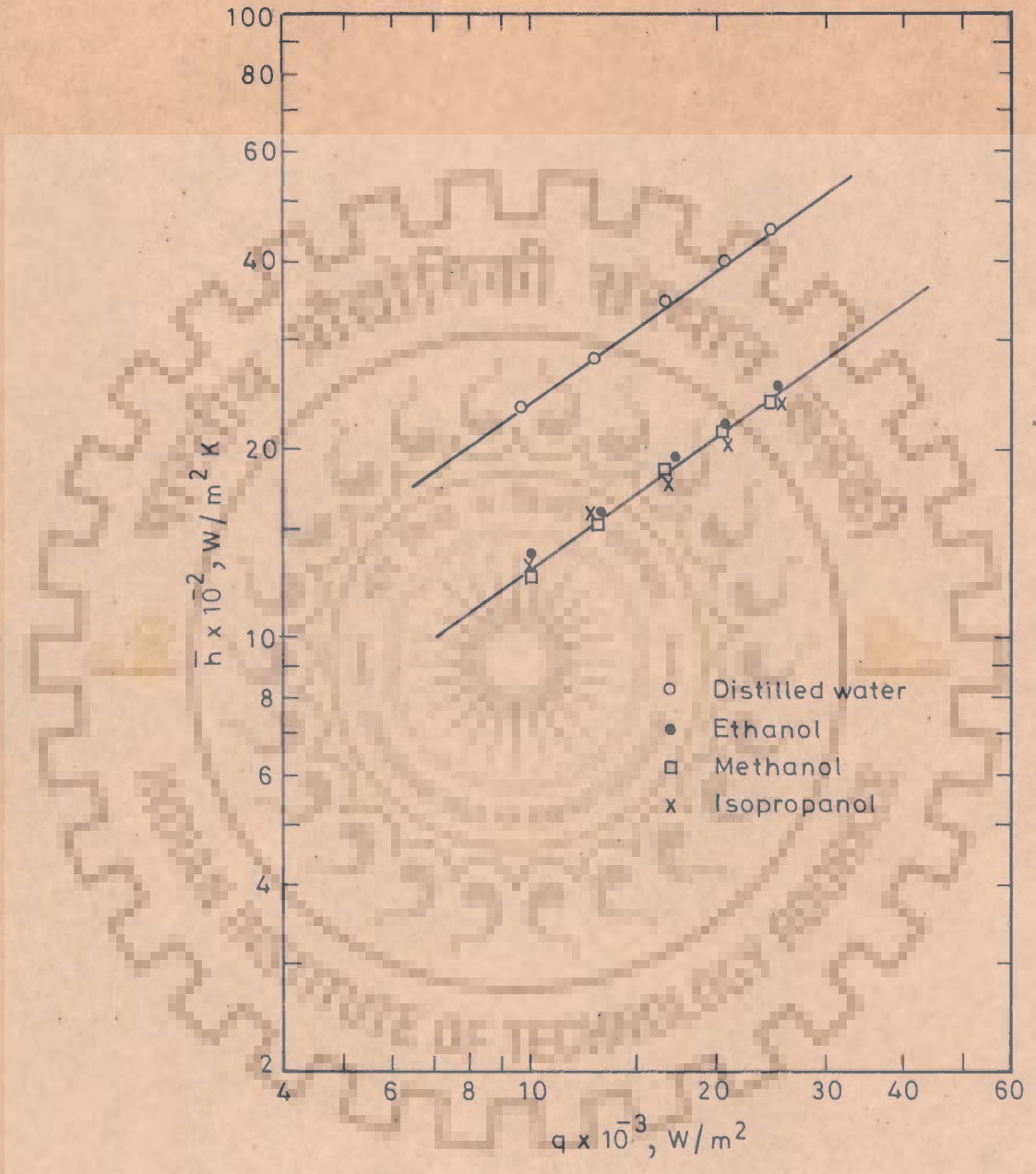


Fig.5.8 -Variation of heat transfer coefficient with heat flux for pure liquids at  $98.63 \text{ kN/m}^2$

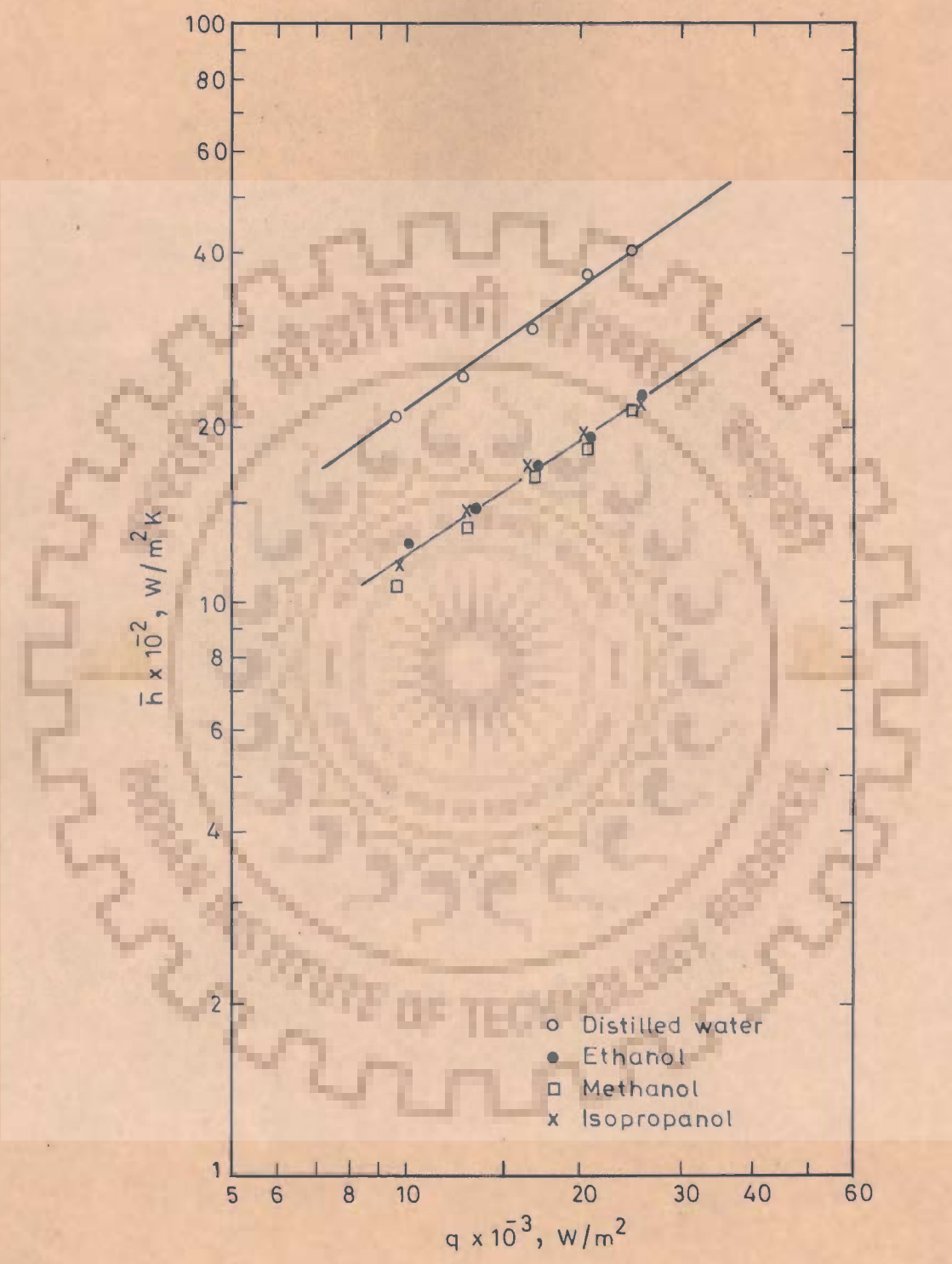


Fig.5.9-Variation of heat transfer coefficient with heat flux for pure liquids at 66.64 kN/m<sup>2</sup>

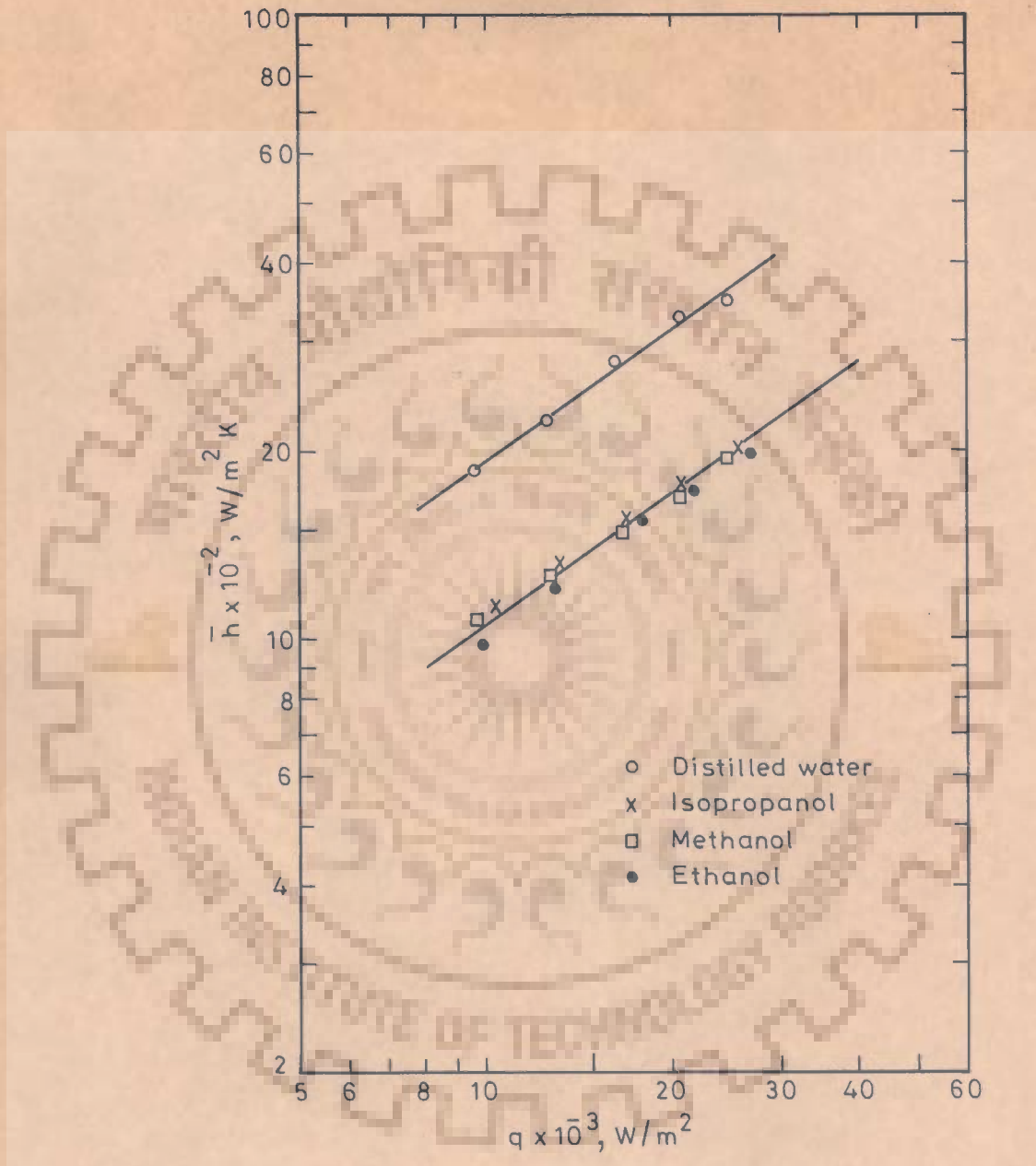


Fig.5.10-Variation of heat transfer coefficient with heat flux for pure liquids at  $50.65 \text{ kN/m}^2$



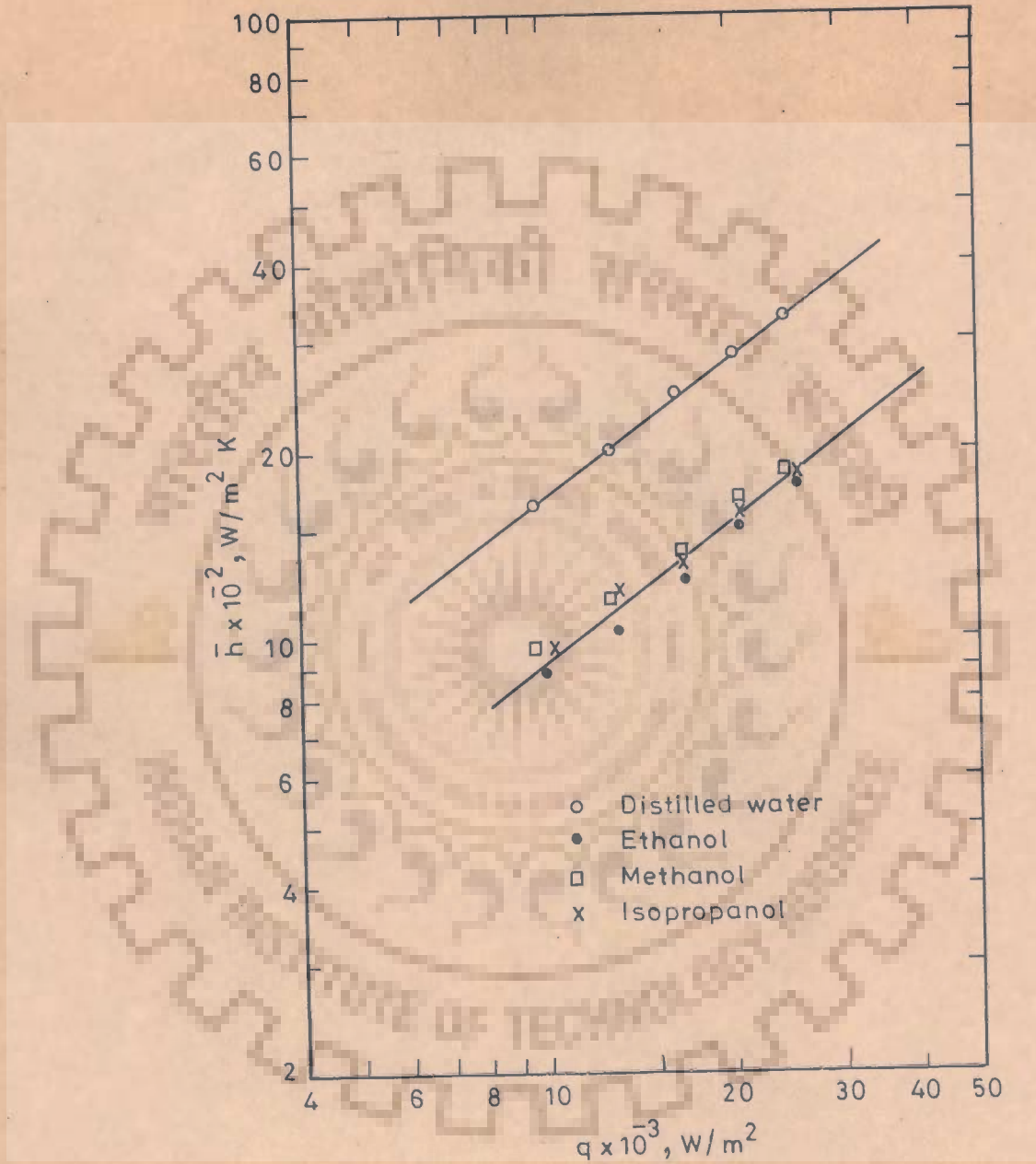


Fig.5.11-Variation of heat transfer coefficient with heat flux for pure liquids at  $33.32 \text{ kN/m}^2$

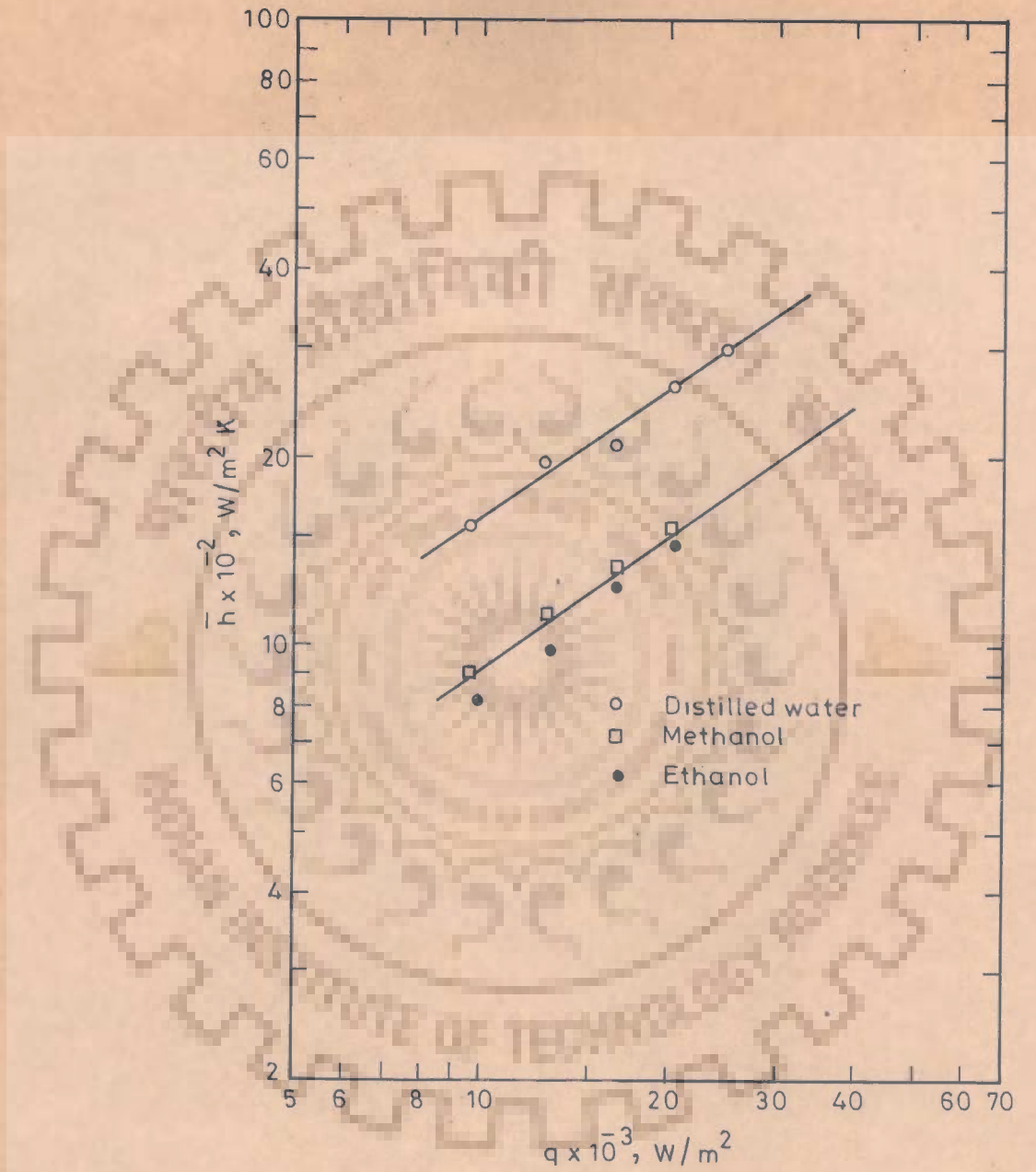


Fig.5.12-Variation of heat transfer coefficient with heat flux for pure liquids at  $25.33 \text{ kN/m}^2$

Further, it is noted that the data points of distilled water differ considerably with those of alcohols. This is not a surprising behaviour, since the properties of water are much different than those of alcohols.

#### 5.2.4 Effect of Pressure on Heat Transfer Coefficient

Figure 5.13 illustrates the variation in  $\bar{h}^*$  with pressure for distilled water, ethanol, methanol and isopropanol. It may be noted that  $\bar{h}^*$  is defined as follows :

$$\bar{h}^* = \bar{h}/q^{0.7}$$

The use of  $\bar{h}^*$  instead of  $\bar{h}$  eliminates one of the operating variables, i.e. heat flux. The value of  $\bar{h}^*$  remains constant with change in heat flux provided there is no change in pressure, heating surface characteristics, and the boiling liquid. The data of all the alcohols investigated merge together and are well-represented by a straight line having a slope of 0.32 for the reasons given in Section 5.2.3. There is a distinct line for distilled water on this plot having the same slope indicating that the heat transfer properties of the water are different than those of alcohols. The variation of heat transfer coefficient with pressure can be empirically represented as follows :

$$\bar{h}^* = c_1 p^{0.32} \quad \dots(5.3)$$

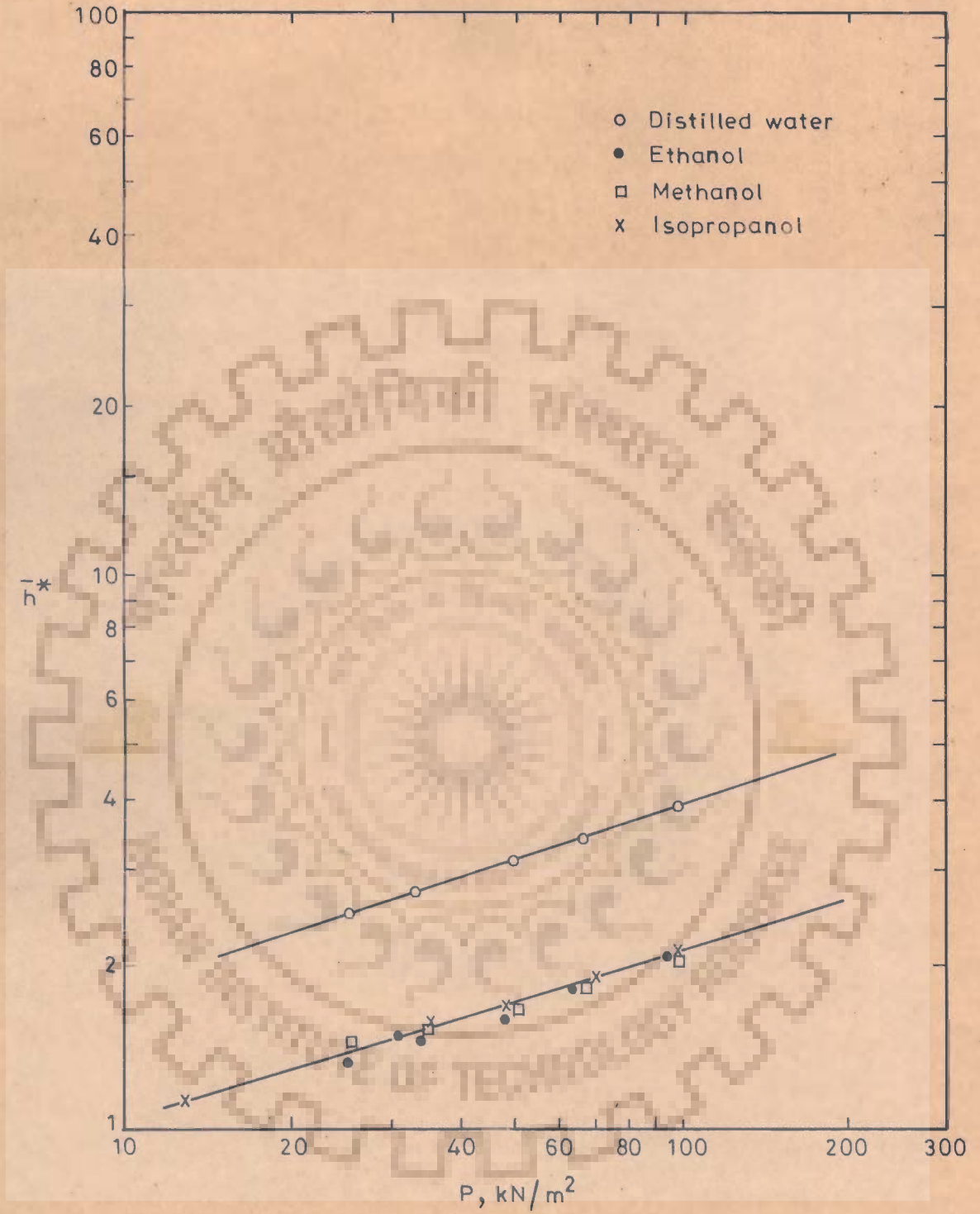


Fig.5.13-Variation of heat transfer coefficient with pressure for pure liquids

where the constant,  $C_1$  is a constant of proportionality. The experimental data correlated by Equation (5.3) were conducted on a given heating surface for distilled water, ethanol, methanol and isopropanol. The data points of ethanol, methanol and isopropanol are represented by a single line, whereas those of water by another line. This finding suggests that the constant,  $C_1$  depends upon the nature of the boiling liquid for a given heating surface.

It may be mentioned here that the value of exponent over pressure as obtained in the present investigation and those proposed by other investigators [16, 121] differs amongst themselves. Chi-Fang-Lin [16] has reported two different values of the exponent, i.e., 0.2 for water and benzene and 0.7 for toluene over the pressure range from 200 mm to 760 mm Hg indicating that the value of exponent can not be treated as a generalized one. Mikheyev [121] has reported this value as 0.15 for the boiling of water in the pressure range from 0.22 to 100 atm. It is important to mention that Mikheyev's correlation is based on the large number of data points at superatmospheric pressure and on limited number of data for subatmospheric pressure. This, in other words, does not represent the behaviour at subatmospheric pressures exclusively. To add to it, Borishanskii et al [36] have established, based on large number of carefully obtained data, that the experimental data for pressures

greater than atmospheric pressure are represented by

$$h^* \propto P^n$$

where the exponent  $n$  is some function of pressure.

Keeping the above in view and the dependence of the present experimental data and those of Cryder and Finalborgo [9] and Raben et al [125] on pressure it can be concluded that heat transfer coefficient varies with pressure raised to the power of 0.32 for the data conducted at the subatmospheric pressures.

In order to show the effect of heating surface characteristics on constant,  $C_1$  of Equation (5.3), data were collected for a given liquid but conducted on different heating surfaces as enlisted in Table 5.2. Figure 5.14 contains this aspect of study. In this figure,  $h^*$  is plotted against pressure for distilled water on log-log plot for the data of Raben et al [125] on a copper cylinder, Cryder and Finalborgo [9] on a brass pipe and present investigation on a stainless steel cylinder. Three different lines having a slope of 0.32 are obtained for different heating surfaces as employed by these investigators, i.e. the constant  $C_1$  is different for different heating surfaces. This clearly demonstrates that the heating surface characteristics also affect the proportionality constant,  $C_1$ , in Equation (5.3) for a given boiling liquid.

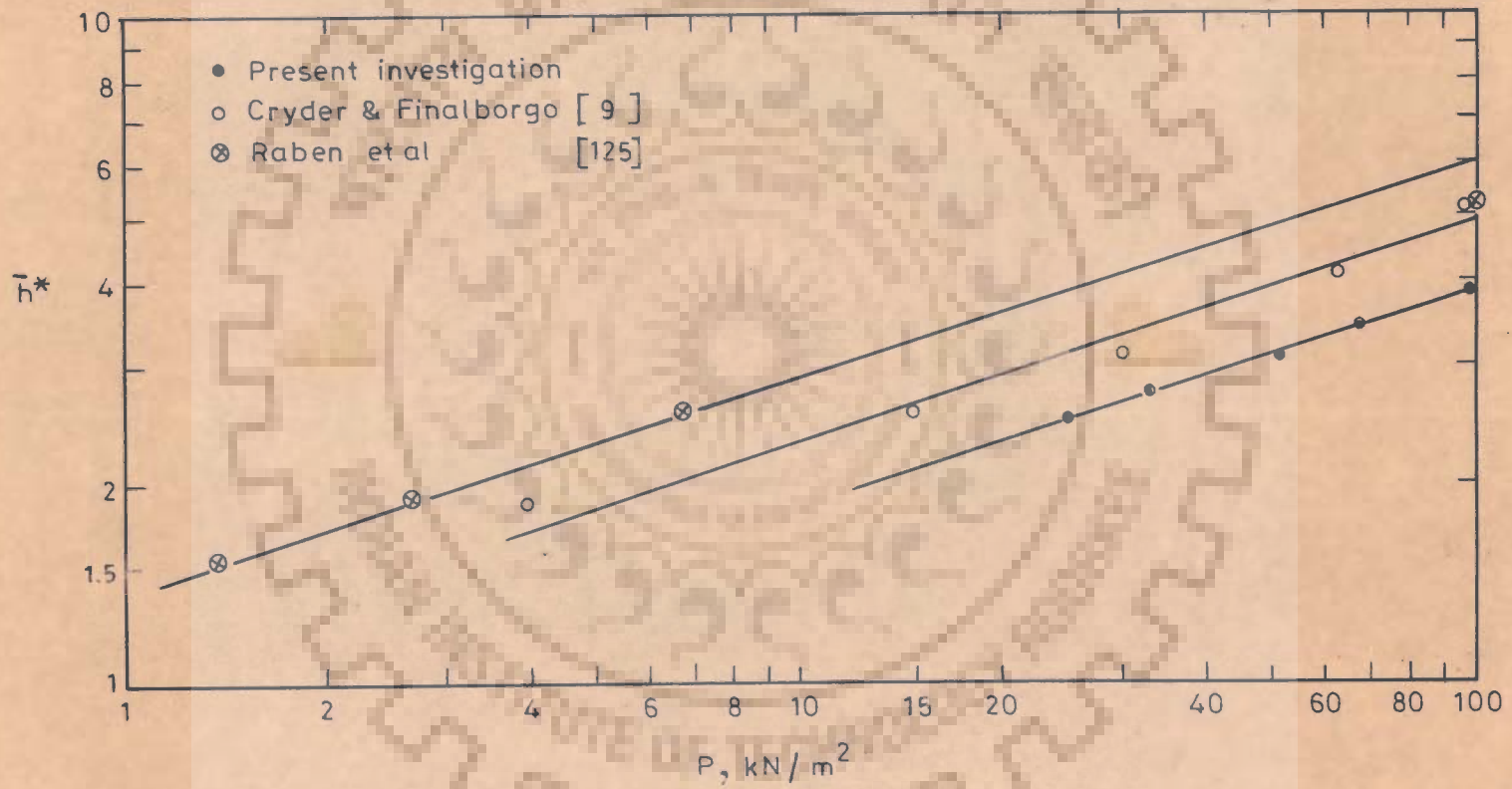


Fig.5.14-Variation of heat transfer coefficient with pressure for distilled water on different heating surfaces

Hence, the results of Figures 5.13 and 5.14 suggest that the constant,  $C_1$  is a function of the nature of boiling liquid and the heating surface characteristic. In fact, this is analogous to 'surface-liquid combination factor',  $C_{sf}$  in the literature [20,21].

The experimental values of constant,  $C_1$  in Equation (5.3) for different investigations were calculated. To show the scatter in the values of constant,  $C_1$ , statistical parameters, namely; Mean ( $\bar{X}$ ), Standard Deviation ( $\sigma$ ) and Coefficient of Variation (C.O.V.) were calculated for each of the liquid as given in Table 5.3. The last column of this Table contains all these values. An inspection of these values shows that the maximum Coefficient of Variation in the values of  $C_1$  for the data of present investigation is 4.55 per cent while those for the data of Cryder and Finalborgo is 7.57 per cent and of Raben et al is 9.66 per cent. Keeping in view the errors involved in conducting boiling heat transfer data these variations are negligibly small ; hence constant,  $C_1$  is practically independent of pressure. In other words it depends upon the nature of boiling liquid and the heating surface characteristics only.



Table 5.3 : Values of Constant,  $C_1$  in Equation (5.3)  
for Pure Liquids at Subatmospheric Pressures

Boiling Liquid	Pressure kN/m <sup>2</sup>	Constant $C_1$	Heating Surface	Investigator	Statistical Parameters for $C_1$
Distilled Water	98.63	0.880	410 ASIS Grade Stainless Steel Cylinder	Present Investigation	$\bar{X} = 0.8802$ $\sigma = 0.0061$ COV = 0.69 %
	66.64	0.882			
	50.65	0.870			
	33.32	0.886			
	25.33	0.883			
Ethanol	98.63	0.490	-do-	-do-	$\bar{X} = 0.4824$ $\sigma = 0.0155$ COV = 3.21%
	61.31	0.502			
	47.98	0.460			
	33.32	0.480			
	25.33	0.480			
Methanol	98.63	0.470	-do-	-do-	$\bar{X} = 0.487$ $\sigma = 0.0222$ COV = 4.55 %
	66.64	0.472			
	50.65	0.473			
	34.65	0.500			
	25.33	0.520			
Isopropandl	98.63	0.470	-do-	-do-	$\bar{X} = 0.4886$ $\sigma = 0.0115$ COV = 2.36 %
	69.31	0.490			
	47.98	0.491			
	34.66	0.490			
	12.66	0.502			
Distilled Water	3.82	1.200	Brass Pipe	Cryder and Finalborgo [9]	$\bar{X} = 1.135$ $\sigma = 0.0626$ COV = 5.51 %
	14.44	1.110			
	29.90	1.060			
	61.25	1.104			
	97.33	1.200			
Methanol	8.40	0.663	-do-	-do-	$\bar{X} = 0.6242$ $\sigma = 0.0248$ COV = 3.97 %
	25.22	0.604			
	40.74	0.608			
	66.27	0.611			
	101.14	0.635			

Boiling Liquid	Pressure kN/m <sup>2</sup>	Constant C <sub>1</sub>	Heating Surface	Investigator	Statistical Parameters for C <sub>1</sub>
n-Butanol	17.93	0.397	Brass pipe	Cryder and Finalborgo [9]	$\bar{X} = 0.3725$
	35.45	0.364			$\sigma = 0.0166$
	52.98	0.368			COV = 4.25 %
	98.94	0.361			
Carbon Tetrachloride	21.25	0.370	-do-	-do-	$\bar{X} = 0.4157$
	30.30	0.420			$\sigma = 0.0315$
	41.98	0.435			COV = 7.57 %
	61.12	0.438			
Distilled Water	1.33	1.223	Copper Cylinder	Raben et al [125]	$\bar{X} = 1.300$
	2.66	1.448			$\sigma = 0.1255$
	6.65	1.358			COV = 9.66 %
	101.30	1.173			
$\bar{X}$ = Mean $\sigma$ = Standard Deviation COV = Coefficient of Variation					

### 5.3 VARIATION OF $(\bar{h}^*/\bar{h}_1^*)$ WITH $(P/P_1)$ FOR SUBATMOSPHERIC PRESSURE

From Table 5.3, it is clearly seen that the constant, C<sub>1</sub> of Equation (5.3) disappears if one represents  $(\bar{h}^*/\bar{h}_1^*)$  as a function of  $(P/P_1)$  for given liquid and heating surface. With this in view, a plot between  $(\bar{h}^*/\bar{h}_1^*)$  and  $(P/P_1)$  is drawn in Figure 5.15. This plot correlates excellently the data of present investigation for the four pure liquids,

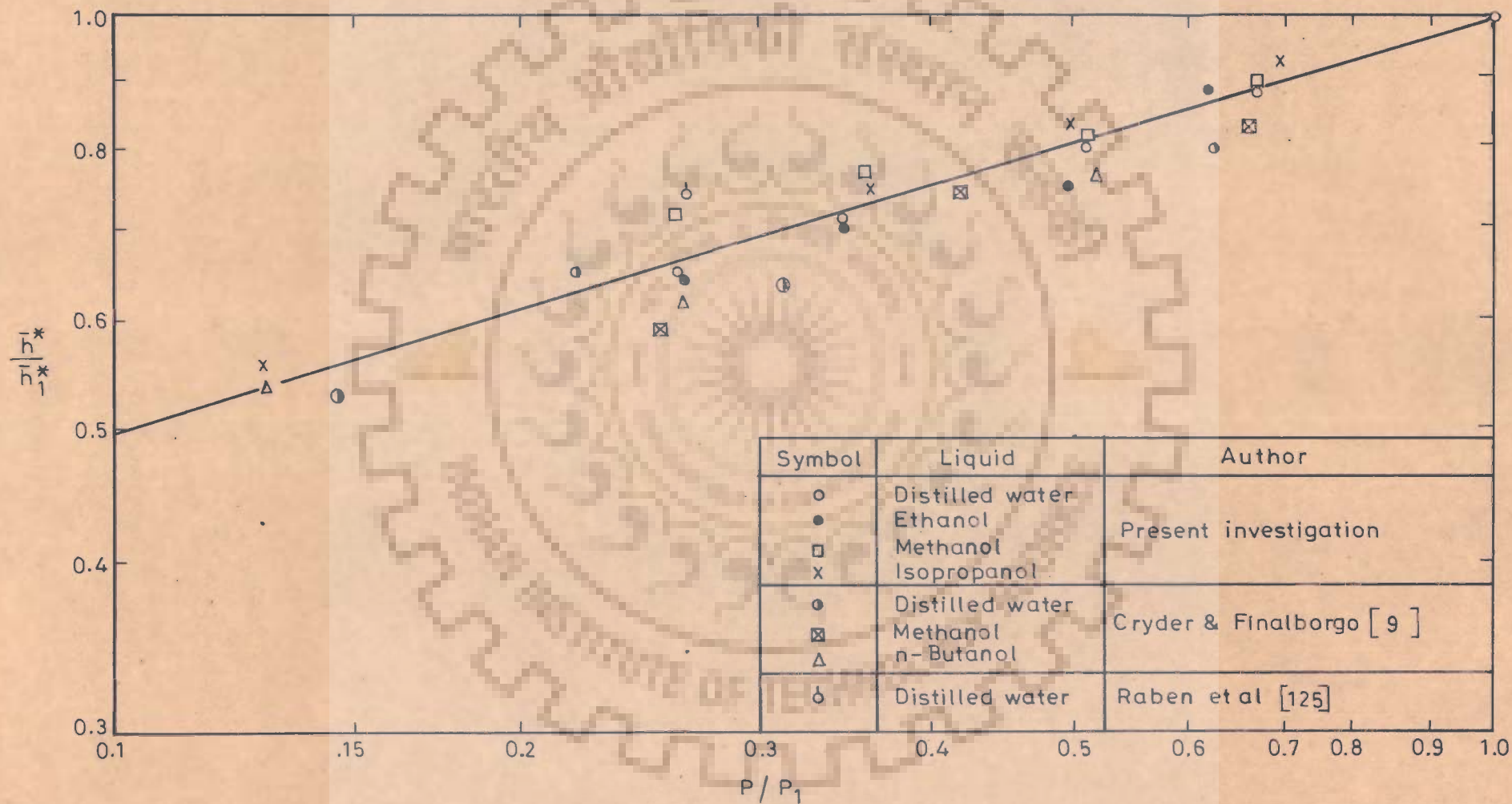


Fig.5.15-Variation of  $\frac{h}{h_1^*}$  with  $P/P_1$  for pure liquids at subatmospheric pressures

obtained on 410 ASIS stainless steel cylinder, and also the data of other investigators, namely; Cryder and Finalborgo [9] for distilled water, methanol and n-butanol conducted on a brass pipe, and Raben et al [125] for distilled water obtained on a copper cylinder. All these data are for subatmospheric pressures. Further, the plot shows that the data of all the investigators are correlated within  $\pm 15$  per cent deviation by the following empirical relationship :

$$\frac{h^*}{h_1^*} = \left( \frac{P}{P_1} \right)^{0.32} \quad \dots(5.4)$$

where subscript '1' denotes a reference pressure for which the value of boiling heat transfer coefficient is known for a given heating surface and the liquid.

It is important to restate that Equation (5.4) has succeeded in correlating all the experimental data of present and earlier investigators at atmospheric and subatmospheric pressures implying that constant,  $C_1$  of Equation (5.3) cancels out. In other words, the constant,  $C_1$  does not depend upon the pressure for the data conducted for atmospheric and subatmospheric pressures.

Thus, the above correlation offers the following advantages :

- a. It is useful to predict the values of heat transfer coefficient for pressures ( $P < 98.63$  kN/m<sup>2</sup>) other than reference pressure, for a given

heating surface and boiling liquid from the knowledge of heat transfer coefficient for the same heating surface and liquid at the reference pressure.

- b. The correlation can be used to check the consistency of the experimental data of the boiling binary liquid mixtures conducted on a given heating surface for atmospheric and subatmospheric pressures.

A similar attempt was made for the data taken for pressures greater than atmospheric pressure as given in the following Section.

#### 5.4 VARIATION OF $(\bar{h}^*/\bar{h}_1^*)$ WITH $(P/P_1)$ FOR SUPERATMOSPHERIC PRESSURE

Figure 5.16 shows the plot of  $(\bar{h}^*/\bar{h}_1^*)$  against  $(P/P_1)$  for the data of Borishanskii et al [36], and Cichelli and Bonilla [11] for the superatmospheric pressures. Unlike the nature of the plot in Figure 5.15, Figure 5.16 illustrates a wide scatter amongst the data points of the liquids, conducted on differing heating surfaces. The scatter in the data points is random, implying that there is a non-linear relationship between  $(\bar{h}^*/\bar{h}_1^*)$  and  $(P/P_1)$ . It is important to recall the findings of Borishanskii et al [36] as mentioned in Section 5.2.4, that the heat transfer coefficient

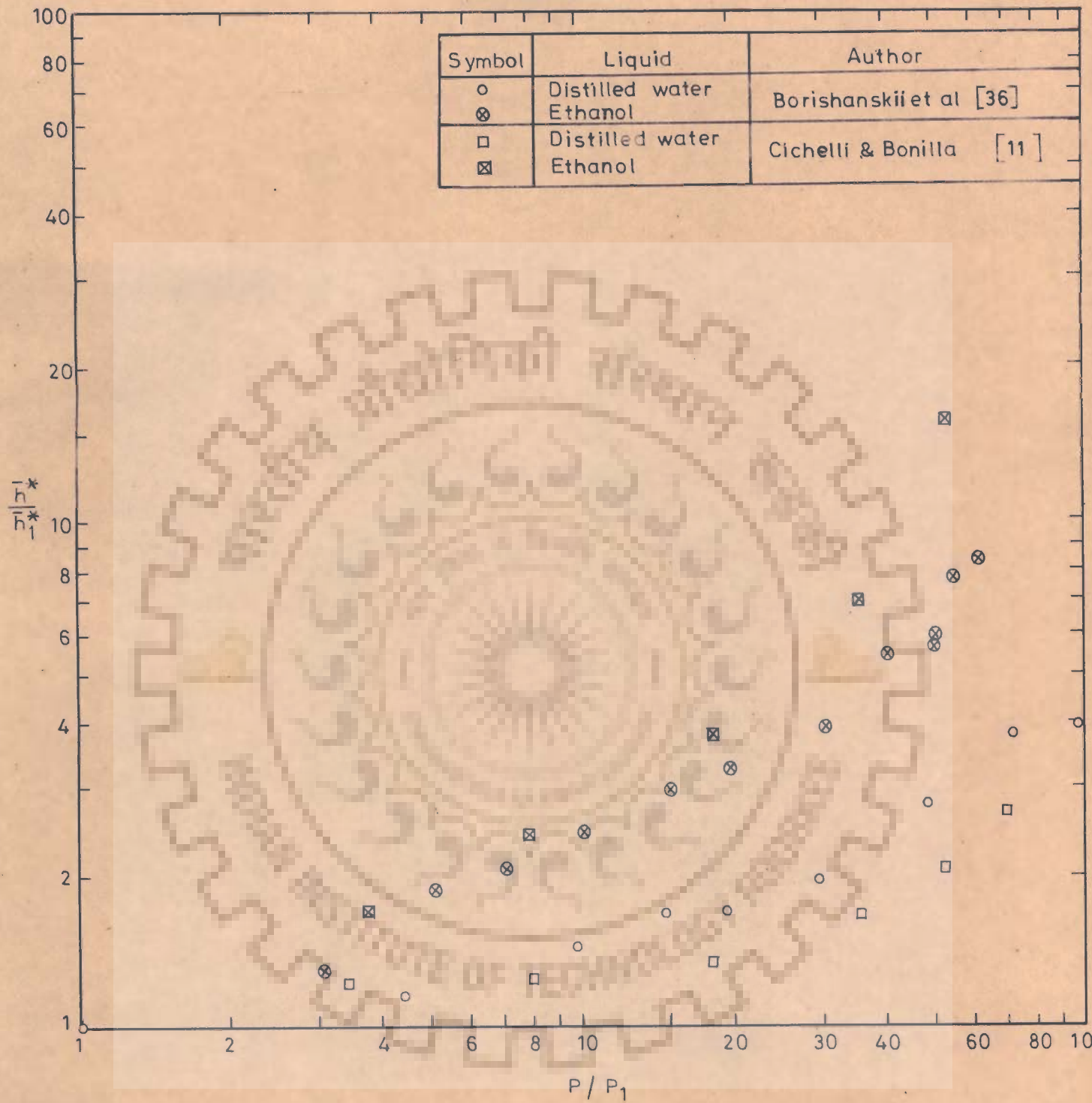


Fig.5.16-Variation of  $\bar{h}^*/\bar{h}_1^*$  with  $P/P_1$  for pure liquids at high pressure

changes with pressure as follows :

$$h \propto P^n$$

for pressure exceeding 1 atmosphere. However, the exponent,  $n$  does not possess a constant value unlike for the data taken for subatmospheric pressures. Further, the exponent,  $n$  is some function of pressure itself. Hence, the data for superatmospheric pressures are not correlated by Equation (5.4).

From the above it is concluded that the constant,  $C_1$  of Equation (5.3) does not disappear if the ratios of  $\bar{h}^*/\bar{h}_1^*$  are plotted against  $P/P_1$ , implying that the value of  $C_1$  for superatmospheric boiling data is a function of pressure also unlike the data for subatmospheric pressures.

The experimental values of constant,  $C_1$  in Equation (5.3) for the superatmospheric boiling data for the investigators [36,11] were calculated and are given in Table 5.4.

The statistical parameters were calculated and are given in Table 5.4 itself. The large value of coefficient of variation as large as 67.09 per cent sufficiently proves that the values of constant,  $C_1$  cannot be accepted as independent of pressure for a given boiling liquid and heating surface. In other words, it is a function of system pressure also, in addition to nature of boiling liquid and heating surface characteristics.

Table 5.4 : Values of Constant,  $C_1$  in Equation (5.3) for Pure Liquids at High Pressures

Boiling Liquid	Pressure kN/m <sup>2</sup>	Constant $C_1$	Heating Surface	Investigator	Statistical Parameters for Constant $C_1$
Distilled Water	101.3	0.728	Copper Plate	Cichelli and Bonilla [11]	$\bar{X} = 0.500$ $\sigma = 0.125$ COV = 25.02 %
	344.7	0.604			
	799.8	0.466			
	1827.1	0.387			
	3550.8	0.392			
	5267.6	0.426			
	6998.2	0.497			
Ethanol	101.3	0.343	-do-	-do-	$\bar{X} = 0.6656$ $\sigma = 0.4466$ COV = 67.09 %
	379.2	0.412			
	792.0	0.428			
	1827.0	0.518			
	3564.0	0.767			
	5274.0	1.526			
Distilled Water	101.0	0.752	Stain- less steel Cylinder	Borishanskii et al [36]	$\bar{X} = 0.6985$ $\sigma = 0.273$ COV = 39.09 %
	451.1	0.545			
	980.7	0.527			
	1480.8	0.536			
	1941.8	0.491			
	2942.1	0.505			
	4903.5	0.597			
	7306.1	0.721			
	9806.9	0.684			
	14710.4	0.898			
19613.8	1.428				



Boiling Liquid	Pressure kN/m <sup>2</sup>	Constant C <sub>1</sub>	Heating Surface	Investigator	Statistical Parameters for Constant C <sub>1</sub>
Ethanol	98.1	0.511	Stainless Steel Cylinder	Borishanskii et al [36]	$\bar{X} = 0.7274$ $\sigma = 0.2173$ COV = 29.88 %
	301.1	0.468			
	500.2	0.576			
	696.3	0.567			
	990.5	0.596			
	1471.0	0.633			
	1941.8	0.638			
	2942.1	0.669			
	3942.4	0.853			
	4903.5	0.833			
	4942.7	0.856			
	5344.8	1.102			
	5943.0	1.155			

$\bar{X}$  = Mean

$\sigma$  = Standard Deviation

COV = Coefficient of Variation

### 5.5 NUCLEATE POOL BOILING OF BINARY LIQUID MIXTURES

The literature survey of Chapter 2 has amply shown that the pool boiling for binary liquid mixtures is more complex than that for pure liquids. In fact, it is affected by the composition of the vapours in equilibrium with that of the boiling liquid, besides the heat flux, the system pressure, the heating surface characteristics, and the physico-thermal properties of the boiling liquid mixture. The effects of these parameters on the boiling

heat transfer of binary liquid mixtures are given in subsequent Sections.

The range of the heat flux, the pressure and the compositions of the binary liquid mixtures, for which the data were conducted, are given in Table 5.1, while the experimental data in Appendix-B. It may be pointed out that ethanol-water and isopropanol-water systems form azeotropic mixtures. However, the present investigation did not cover the azeotropic compositions for conducting the experimental data.

The physico-thermal properties of the binary liquid mixtures are compiled in Appendix-C.

#### 5.5.1 Effect of Heat Flux on Heat Transfer Coefficient

Figures 5.17 through 5.25 represent the typical log-log plots showing the effect of heat flux on heat transfer coefficient for different compositions of ethanol-water, methanol-water, and isopropanol-water mixtures with system pressures as parameter. From these plots the following characteristic points emerge out :

- a. The heat transfer coefficient changes linearly with the heat flux with a slope of 0.7 similar to that for pure liquids for all the pressures studied. This behaviour is well-represented by the following mathematical expression :

$$\bar{h} = C_m q^{0.7} \quad \dots(5.5)$$

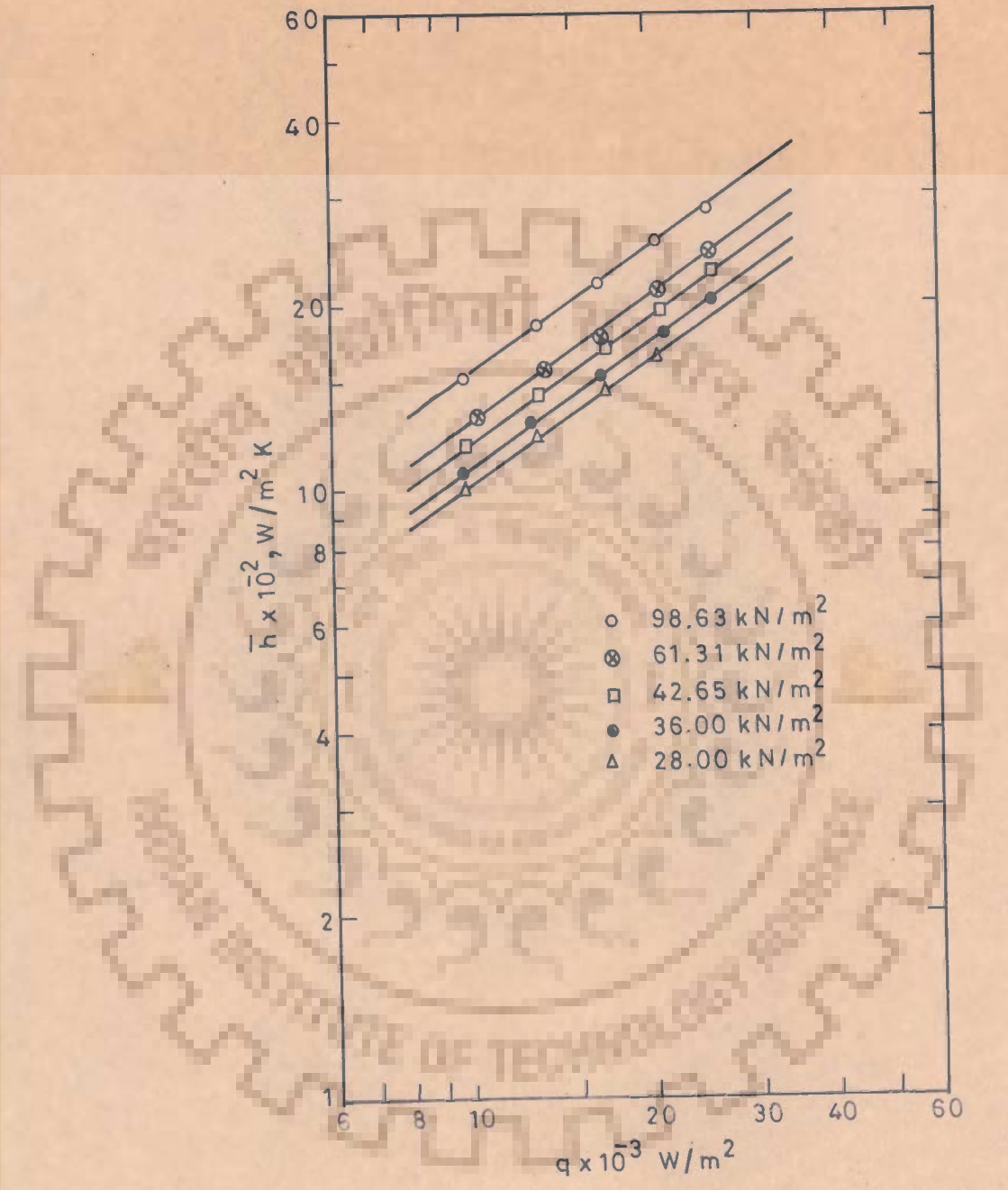


Fig 5.17- Variation of heat transfer coefficient with heat flux for 11.86 wt.% ethanol in ethanol-water mixture at atmospheric and subatmospheric pressure

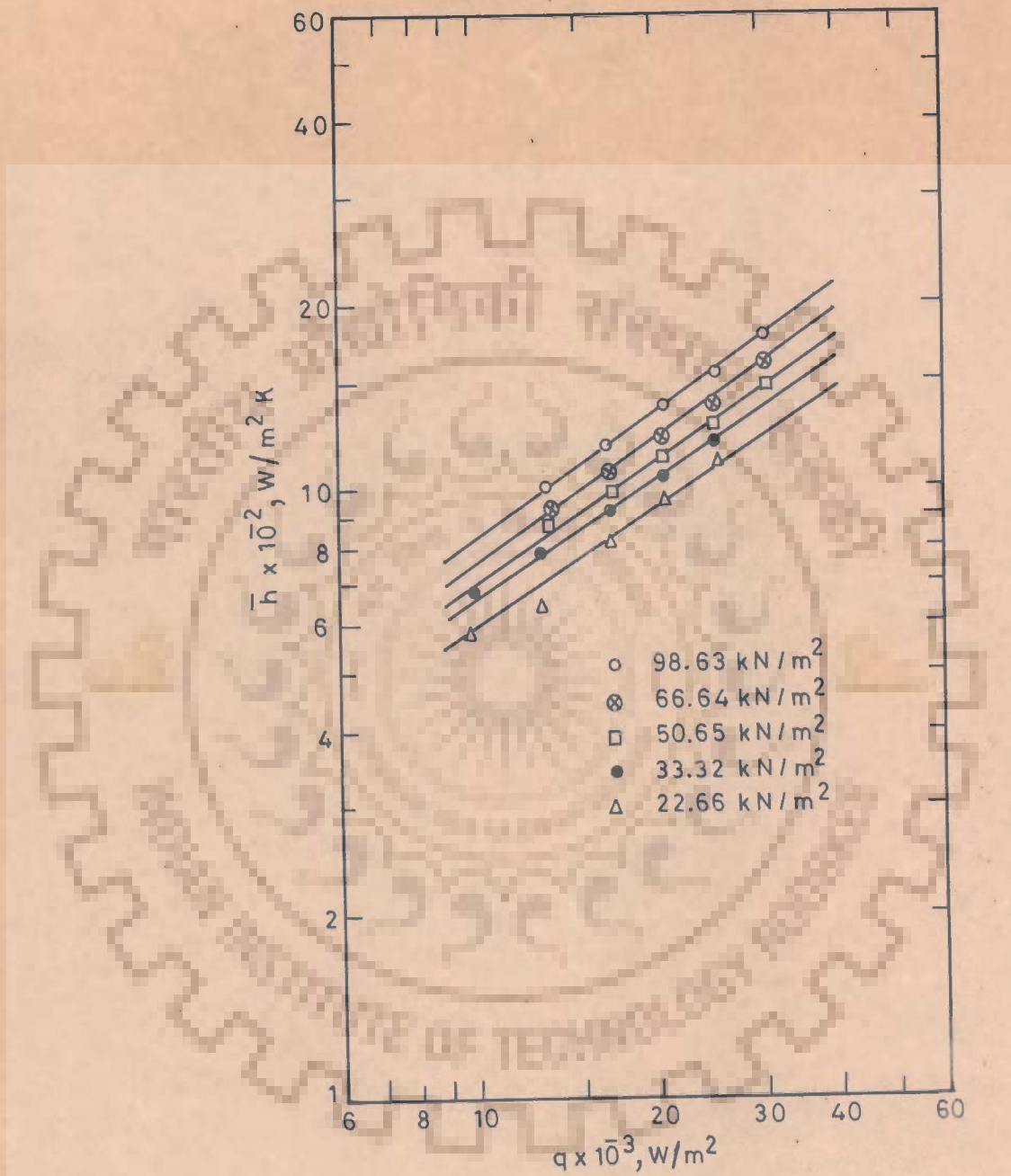


Fig.5.18-Variation of heat transfer coefficient with heat flux for 31.10 wt.% ethanol in ethanol-water mixture at atmospheric and subatmospheric pressure

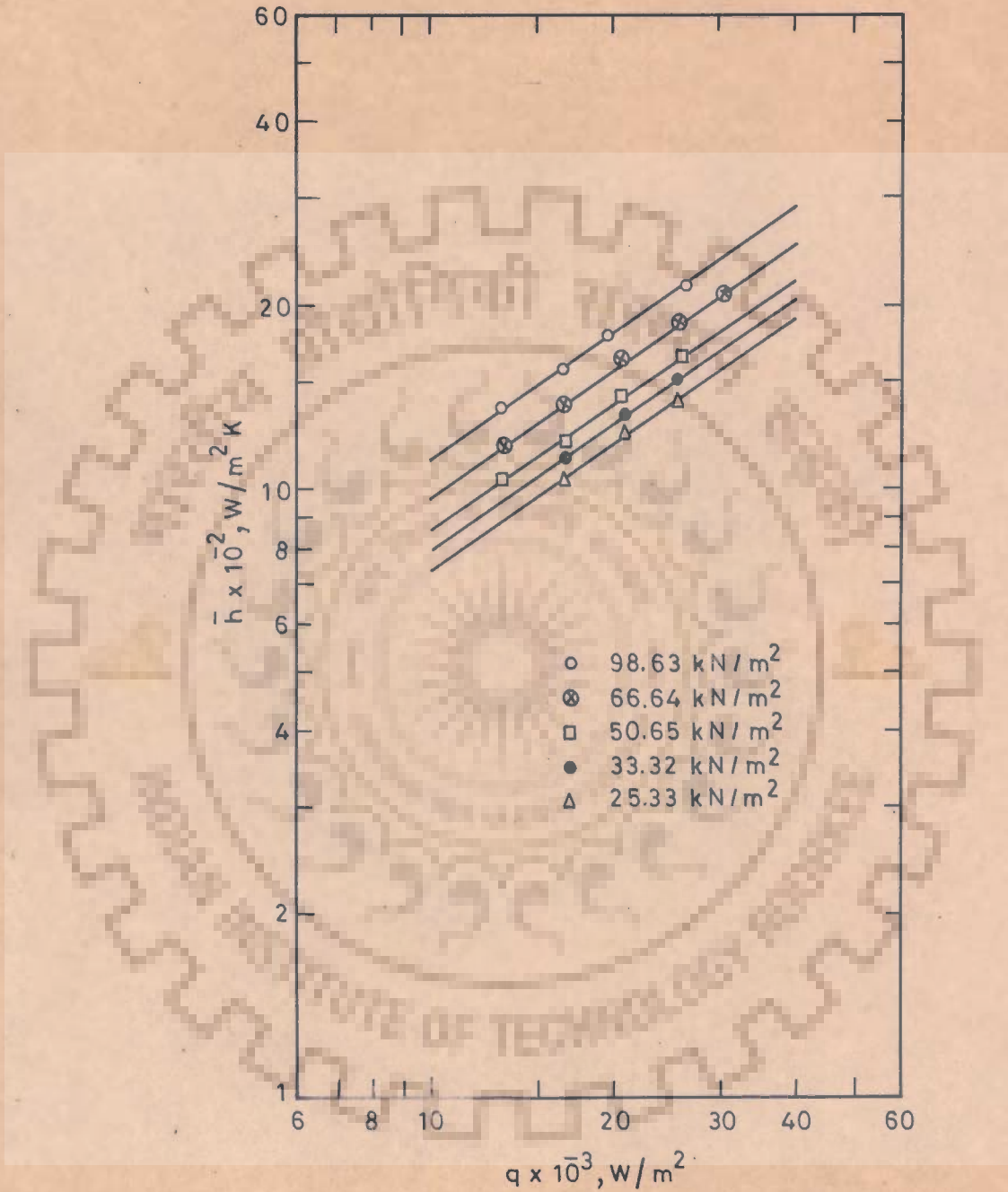


Fig.5.19-Variation of heat transfer coefficient with heat flux for 71.88 wt.% ethanol in ethanol-water mixture at atmospheric and subatmospheric pressure

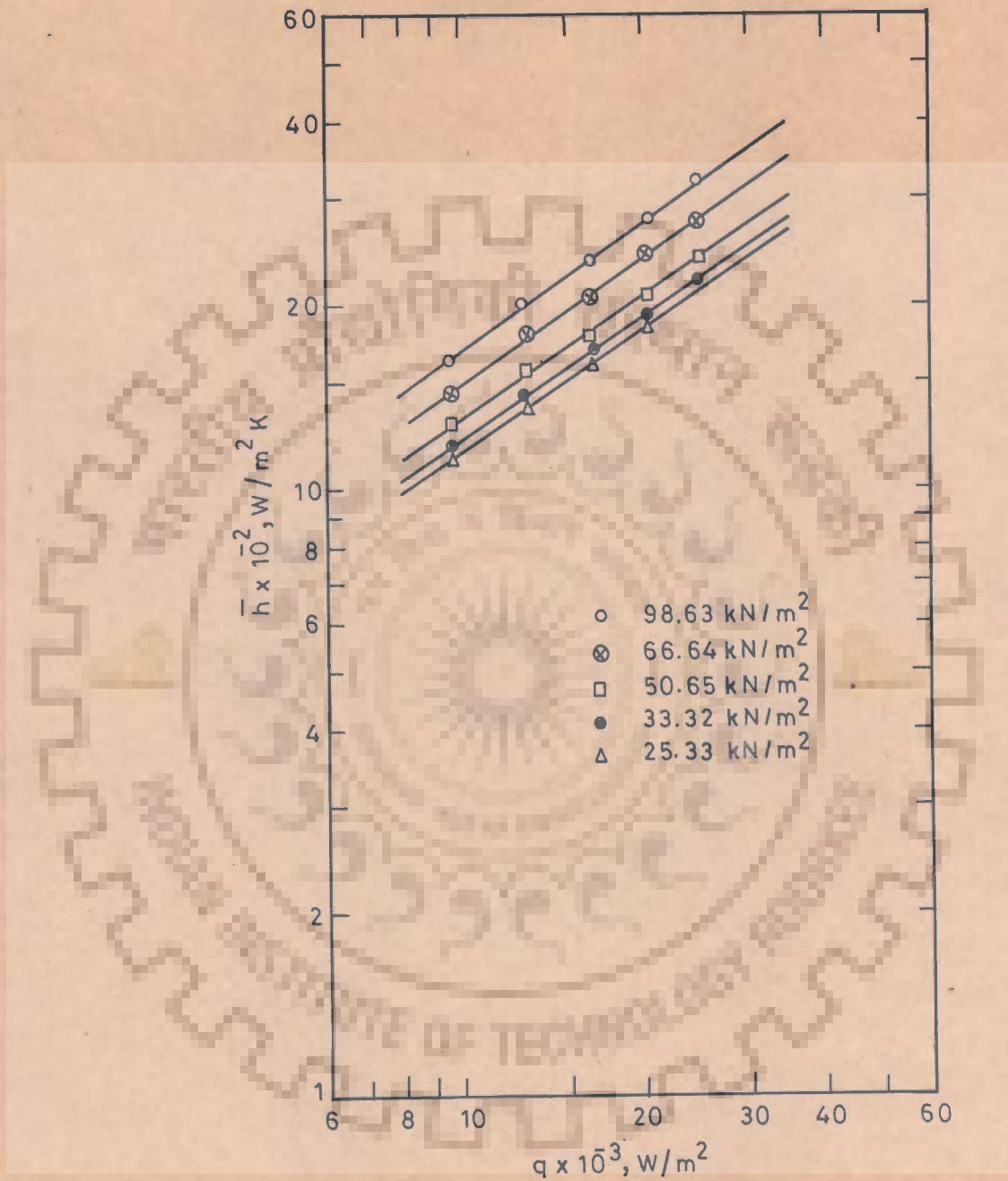


Fig.5.20-Variation of heat transfer coefficient with heat flux for 8.56 wt.% methanol in methanol-water mixture at atmospheric and subatmospheric pressure

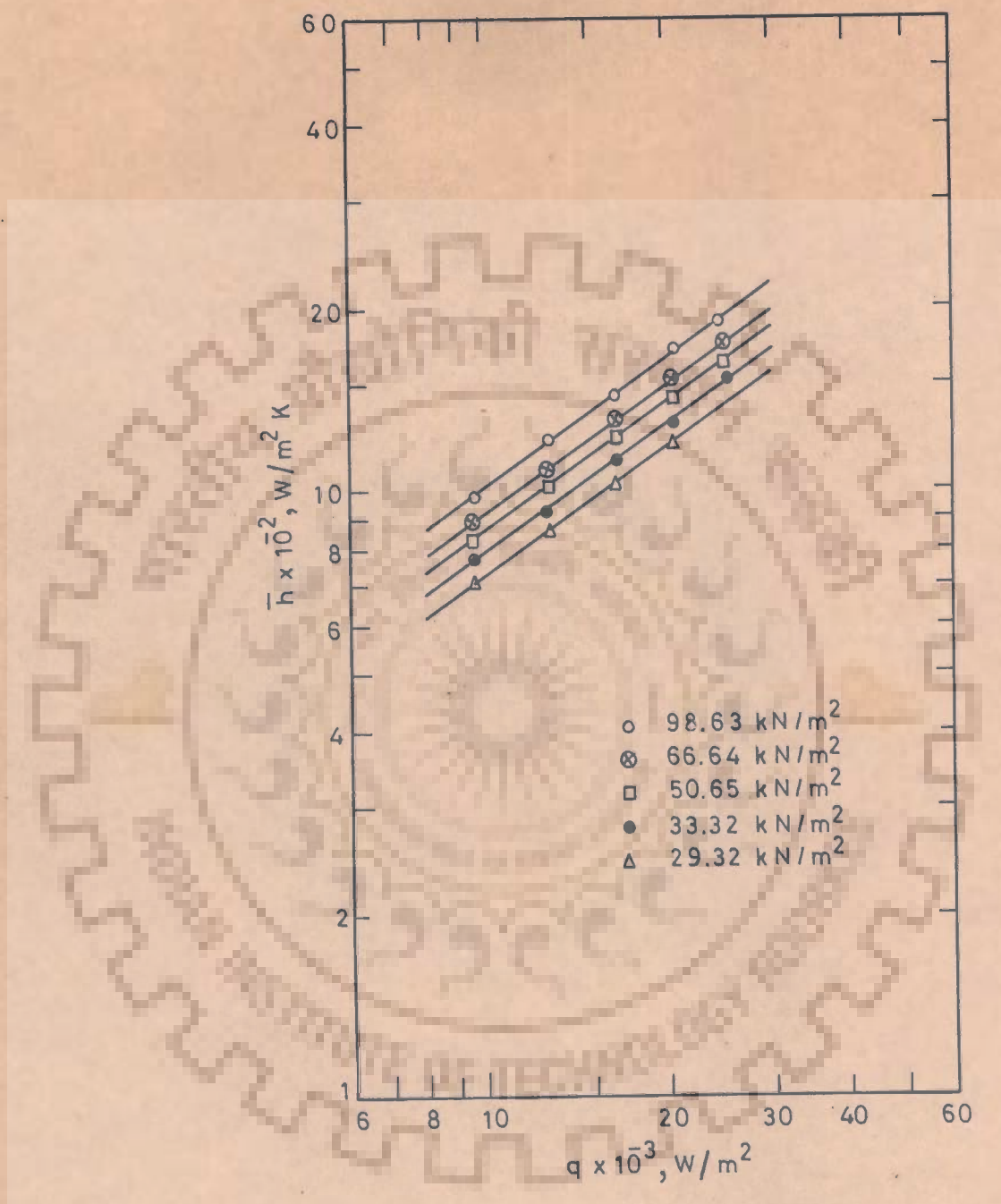


Fig.5.21-Variation of heat transfer coefficient with heat flux for 30.80 wt.% methanol in methanol-water mixture at atmospheric and subatmospheric pressure

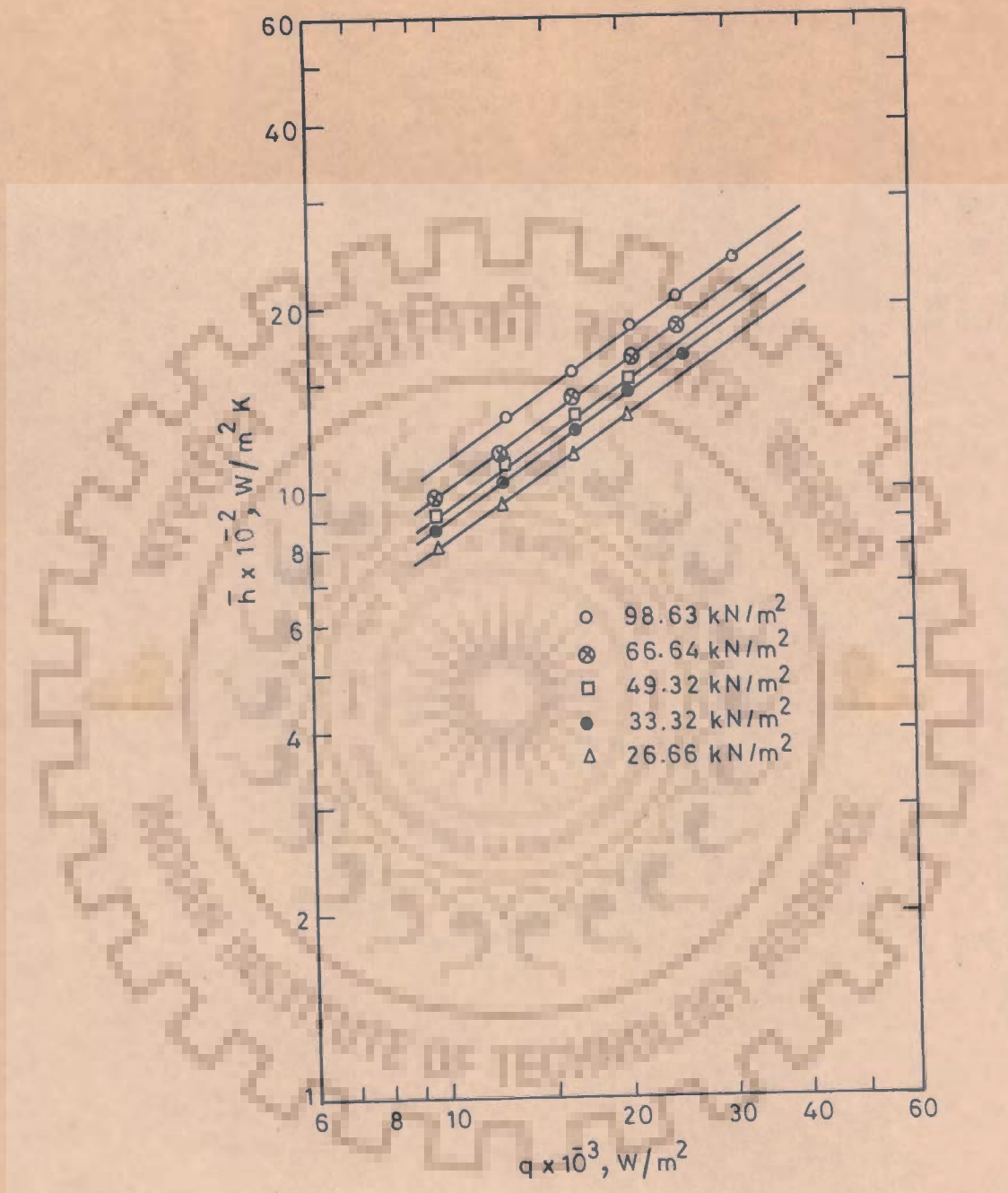


Fig.5.22—Variation of heat transfer coefficient with heat flux for 64.00 wt.% methanol in methanol-water mixture at atmospheric and subatmospheric pressure



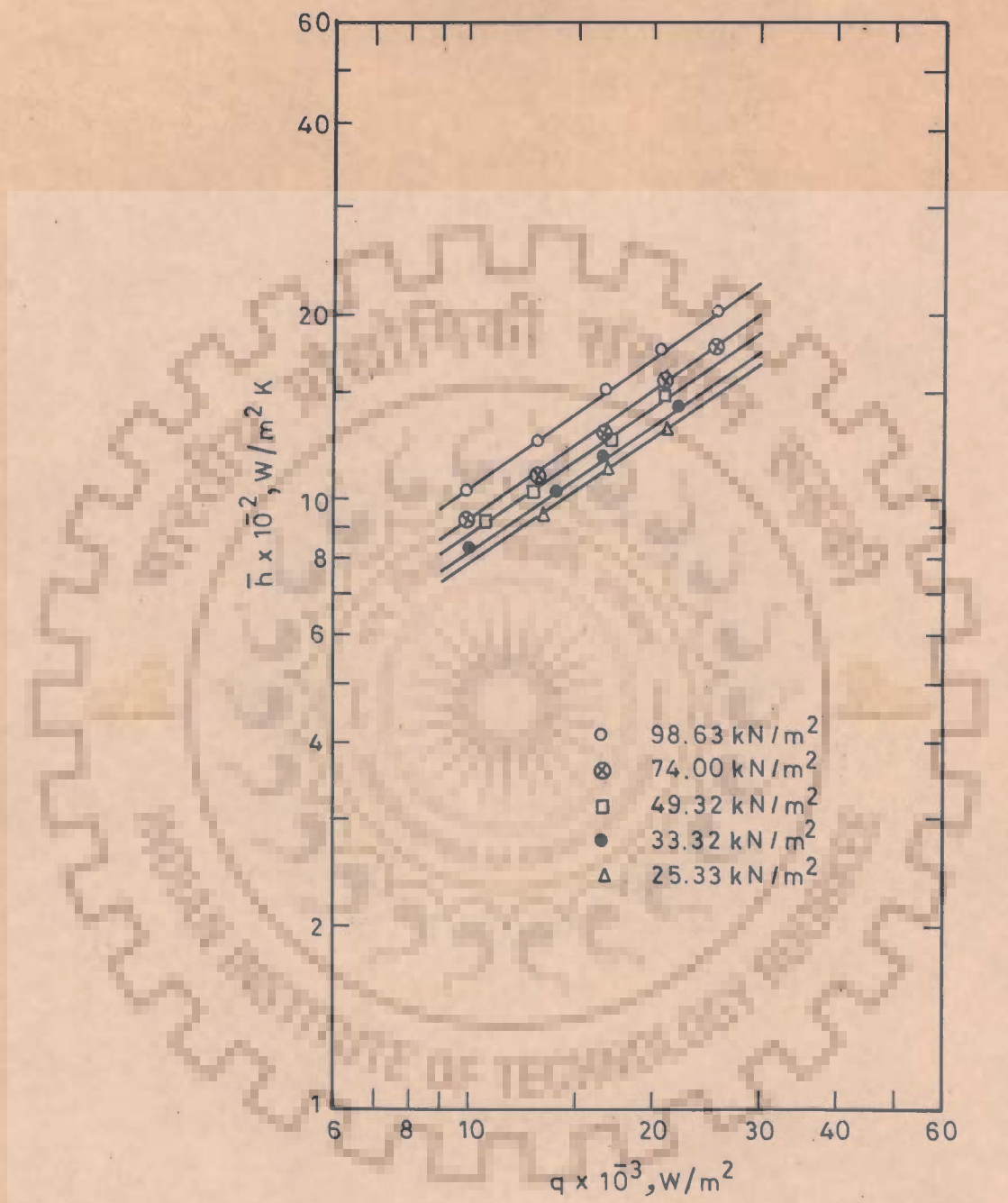


Fig.5.23-Variation of heat transfer coefficient with heat flux for 15.00 wt.% isopropanol in isopropanol-water mixture at atmospheric and subatmospheric pressure

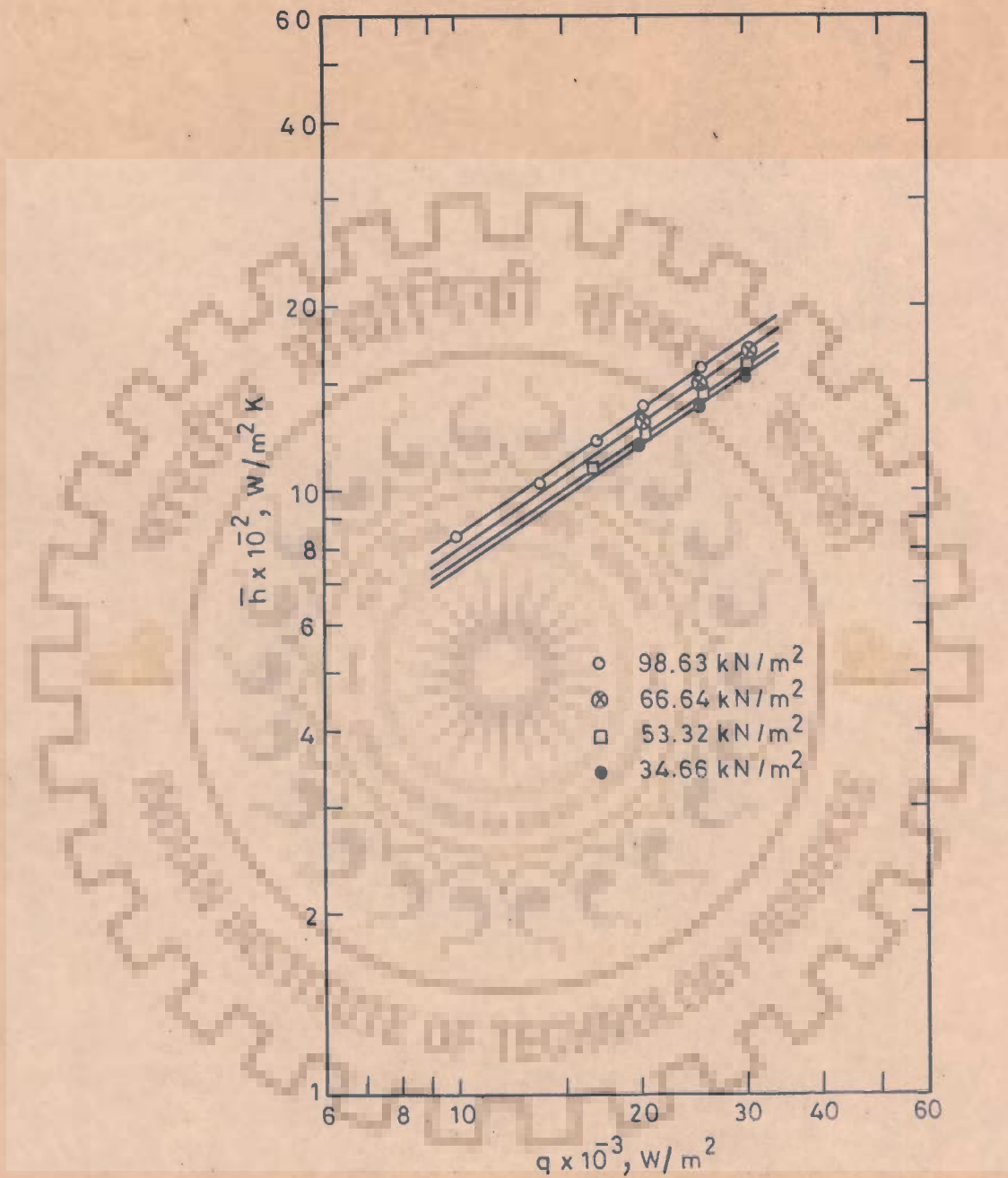


Fig.5.24-Variation of heat transfer coefficient with heat flux for 22.50 wt% isopropanol in isopropanol-water mixture at atmospheric and subatmospheric pressure

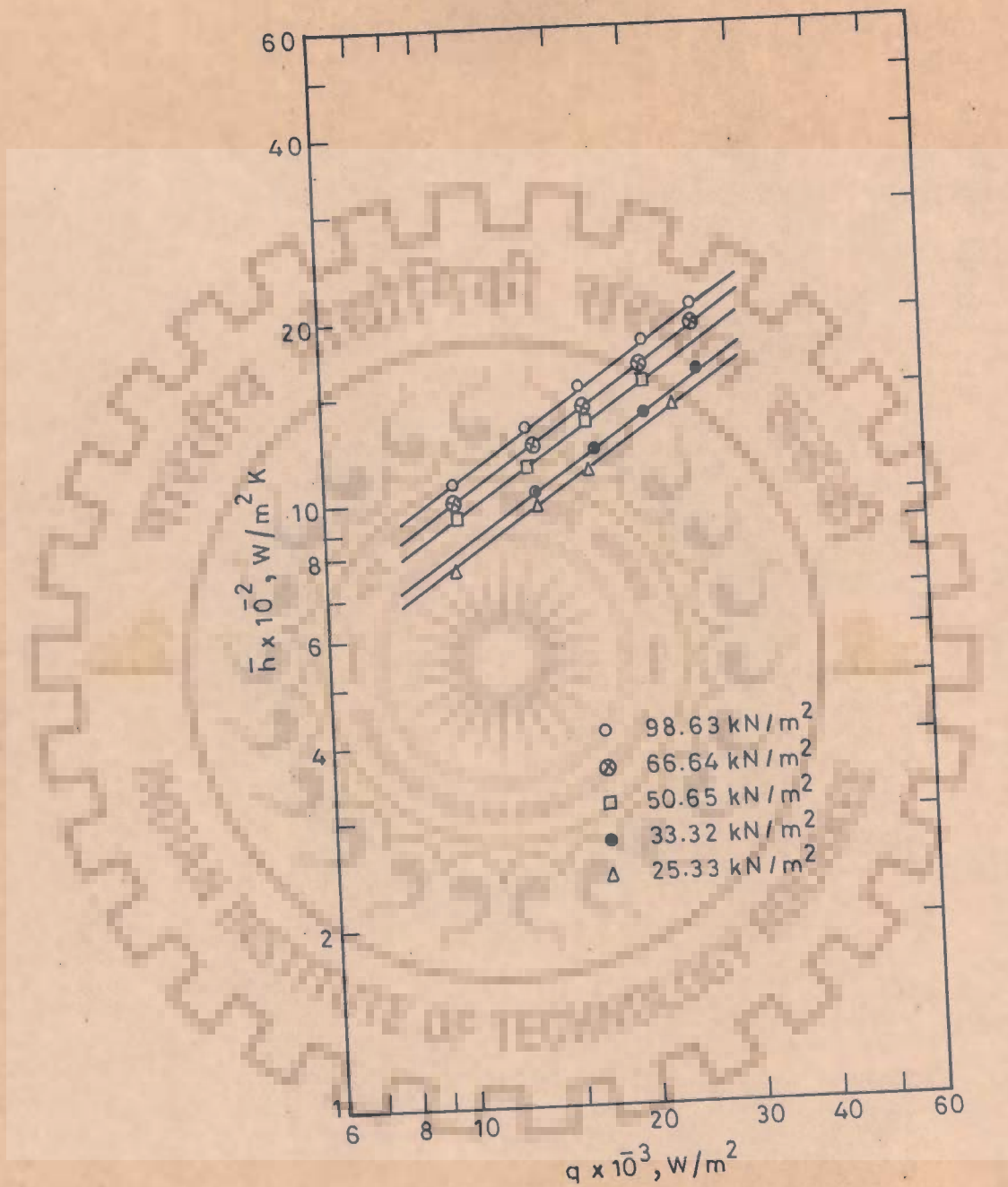


Fig.5.25- Variation of heat transfer coefficient with heat flux for 77.00 wt.% isopropanol in isopropanol-water mixture at atmospheric and subatmospheric pressure

The increase in the value of heat transfer coefficient with the heat flux is an expected behaviour for the reasons given in Section 5.2.1.

The term,  $C_m$ , in Equation (5.5) is, in fact, the constant of proportionality like constant,  $C$ , in Equation (5.2).

- b. Higher values of the system pressure shift the straight lines to higher values of heat transfer coefficient. However, qualitatively, all the lines are alike and represent a family of straight lines.

The above behaviour of the data points, obviously, is for the reasons given in Section 5.2.1 and can also be explained by the consideration of the following expression for minimum radius of curvature,  $R_{min}$ , of nucleation site for the bubble formation :

$$R_{min} = \frac{2 \sigma}{\left(\frac{dP}{dT}\right)_s (T_w - T_s)}$$

As per this expression, a reduction in surface tension, which takes place as the pressure is raised, lowers the value of  $R_{min}$  and thereby larger number of nucleation sites on the heating surface becomes active, giving rise to increased induced turbulence. This, in turn, enhances the value of heat transfer coefficient.

### 5.5.2 Effect of Surface Characteristics on Heat Transfer Coefficient

To demonstrate this, a typical log-log plot is shown in Figure 5.26. This plot represents the data of Sternling and Tichacek [18] and of Alam [126] conducted for the boiling of 19.3 wt. per cent water-ethylene glycol mixture at atmospheric pressure on two differing heating surfaces. In fact, Sternling and Tichacek [18] employed stainless steel, whereas Alam [126] used silver plated brass tube.

The above plot,  $h$  vs  $q$ , clearly shows that these two data differ widely amongst themselves. In fact, they fall on two distinct straight lines represented by the following relationship :

$$\bar{h} = \text{const. } q^{0.7}$$

where the constant for the data of Sternling and Tichacek [18] is smaller than for the data of Alam [126]. This is attributed to the differing heating surface characteristics. Consequently, it is concluded that the constant of above equation depends on the heating surface characteristics.

### 5.5.3 Effect of Composition of Liquid Mixture on Heat Transfer Coefficient

Figures 5.27 through 5.29 represent the typical variation of heat transfer coefficient as a function of heat flux to show the effect of concentration of

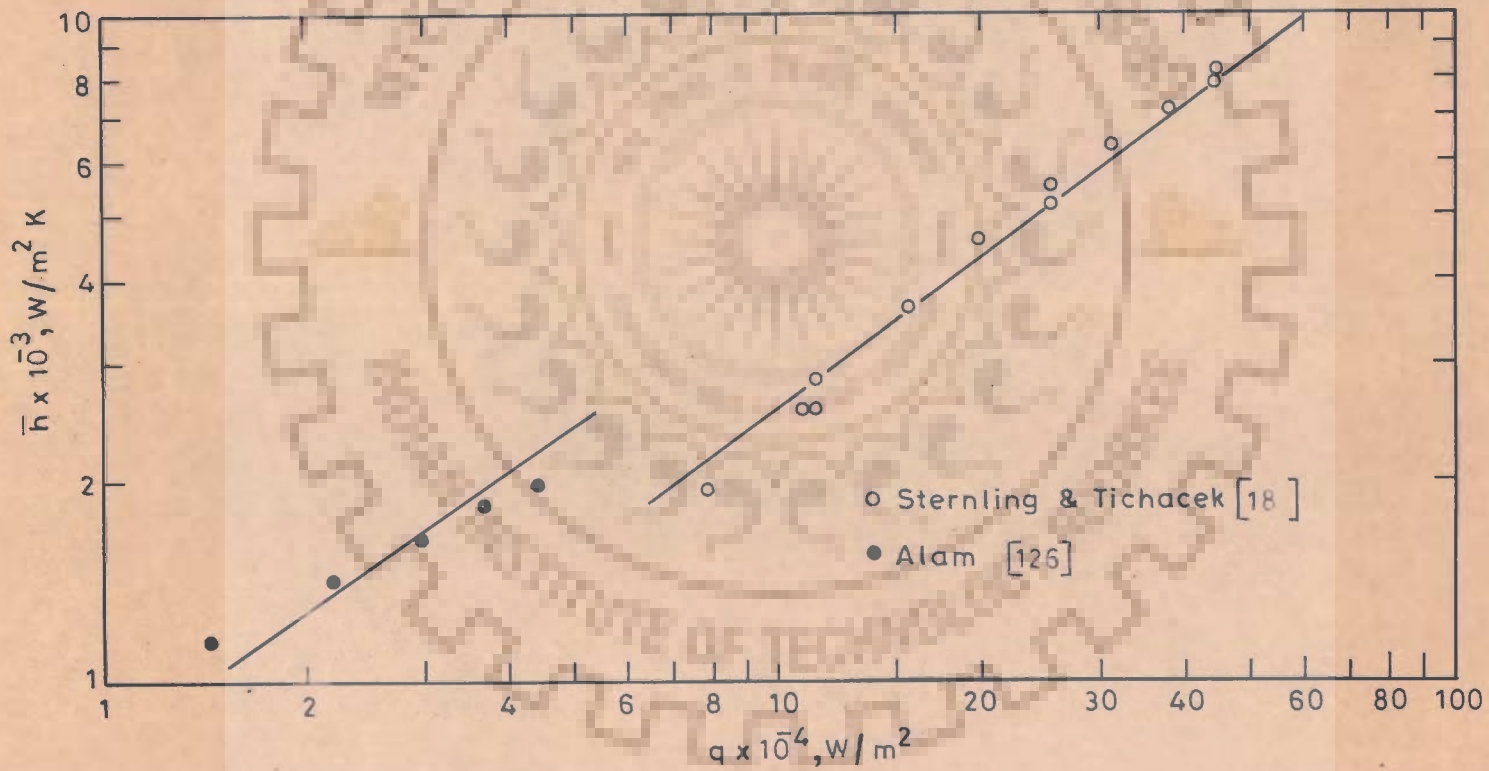


Fig.5.26-Heat transfer coefficient-heat flux relationship for 19.3 wt.% water in water-ethylene glycol mixture on different heating surfaces at  $98.63 \text{ kN/m}^2$

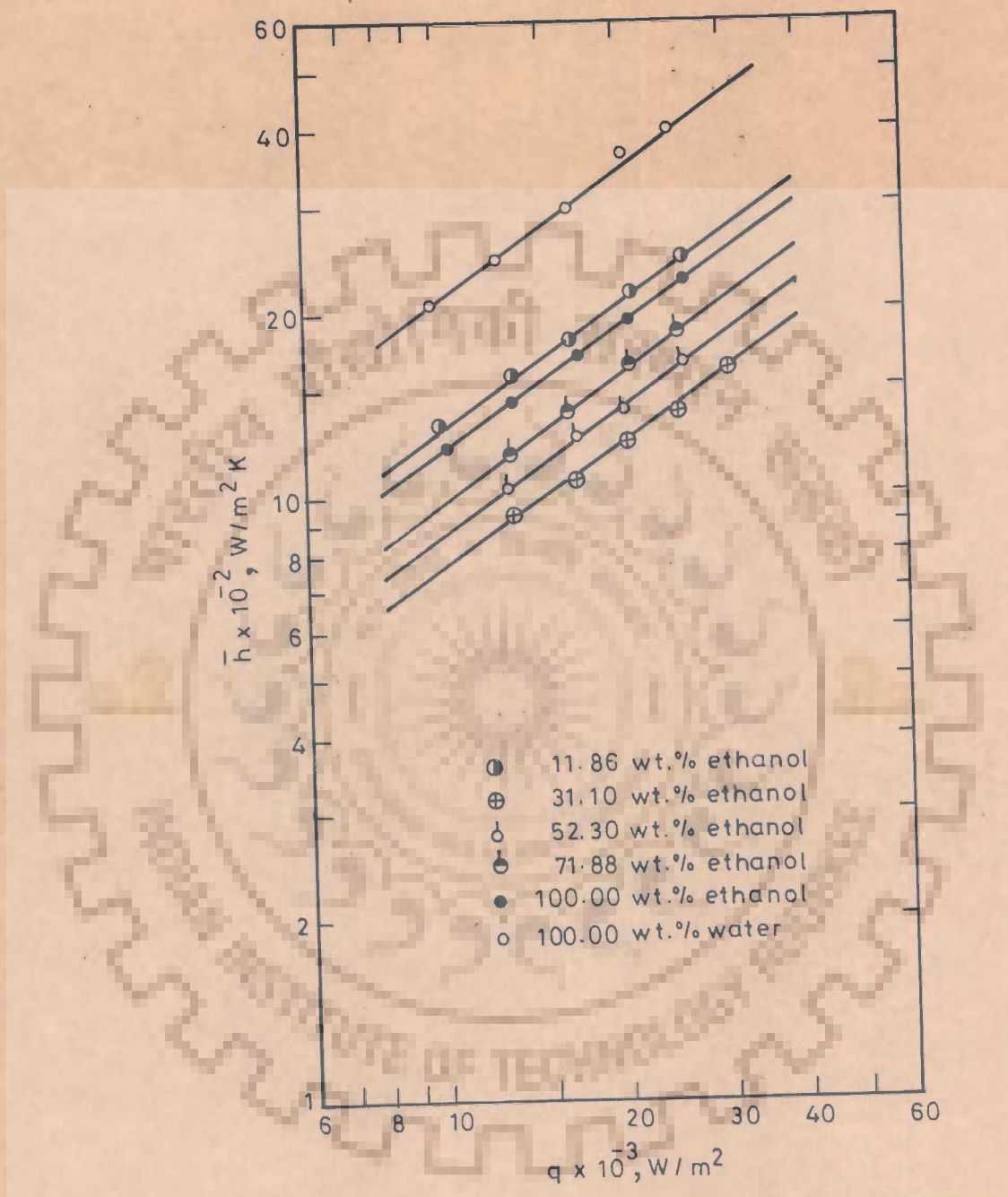


Fig.5.27-Variation of heat transfer coefficient with heat flux for ethanol-water mixtures at  $66.64 \text{ kN/m}^2$

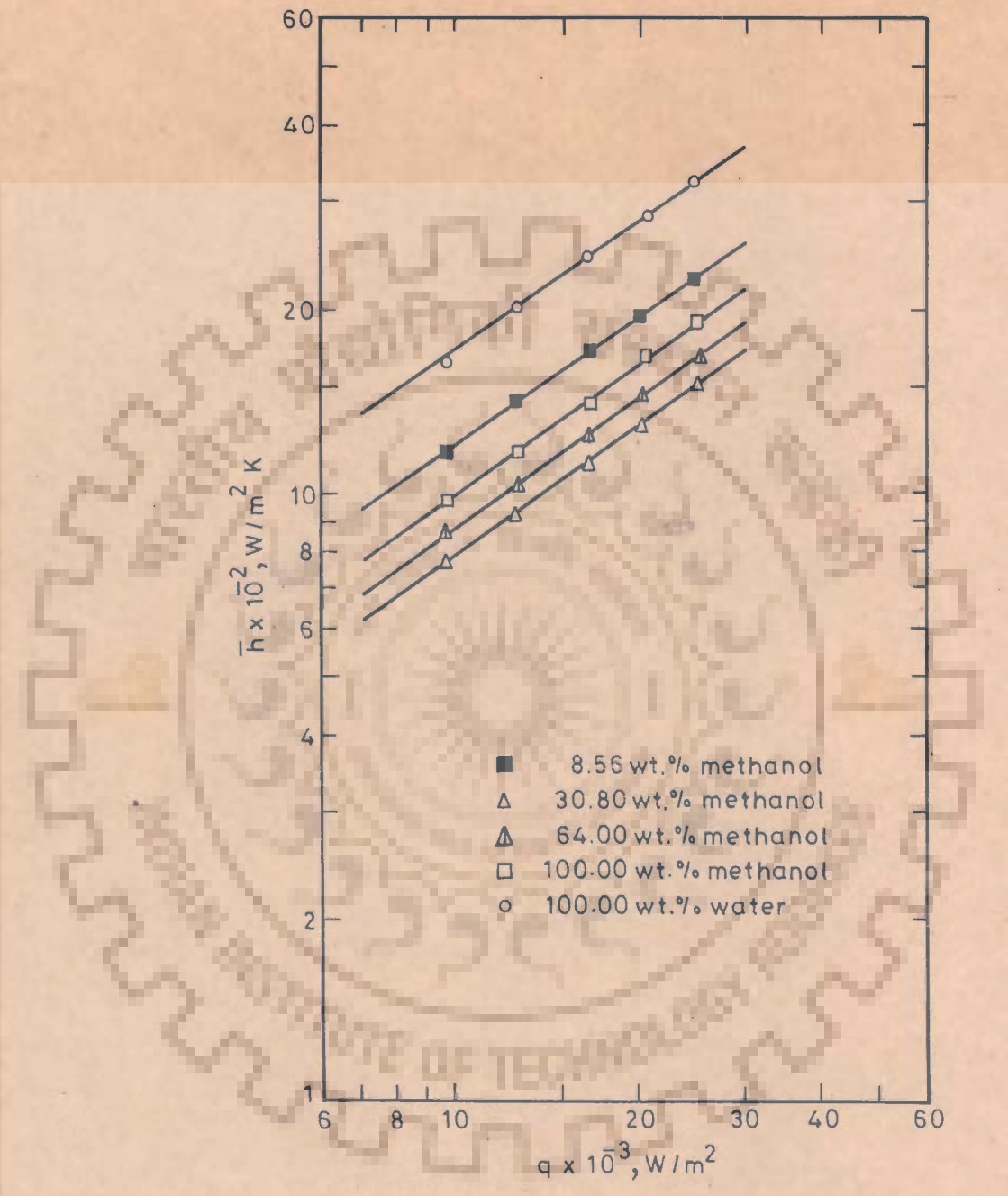


Fig.5.28-Variation of heat transfer coefficient with heat flux for methanol-water mixtures at  $33.32 \text{ kN/m}^2$



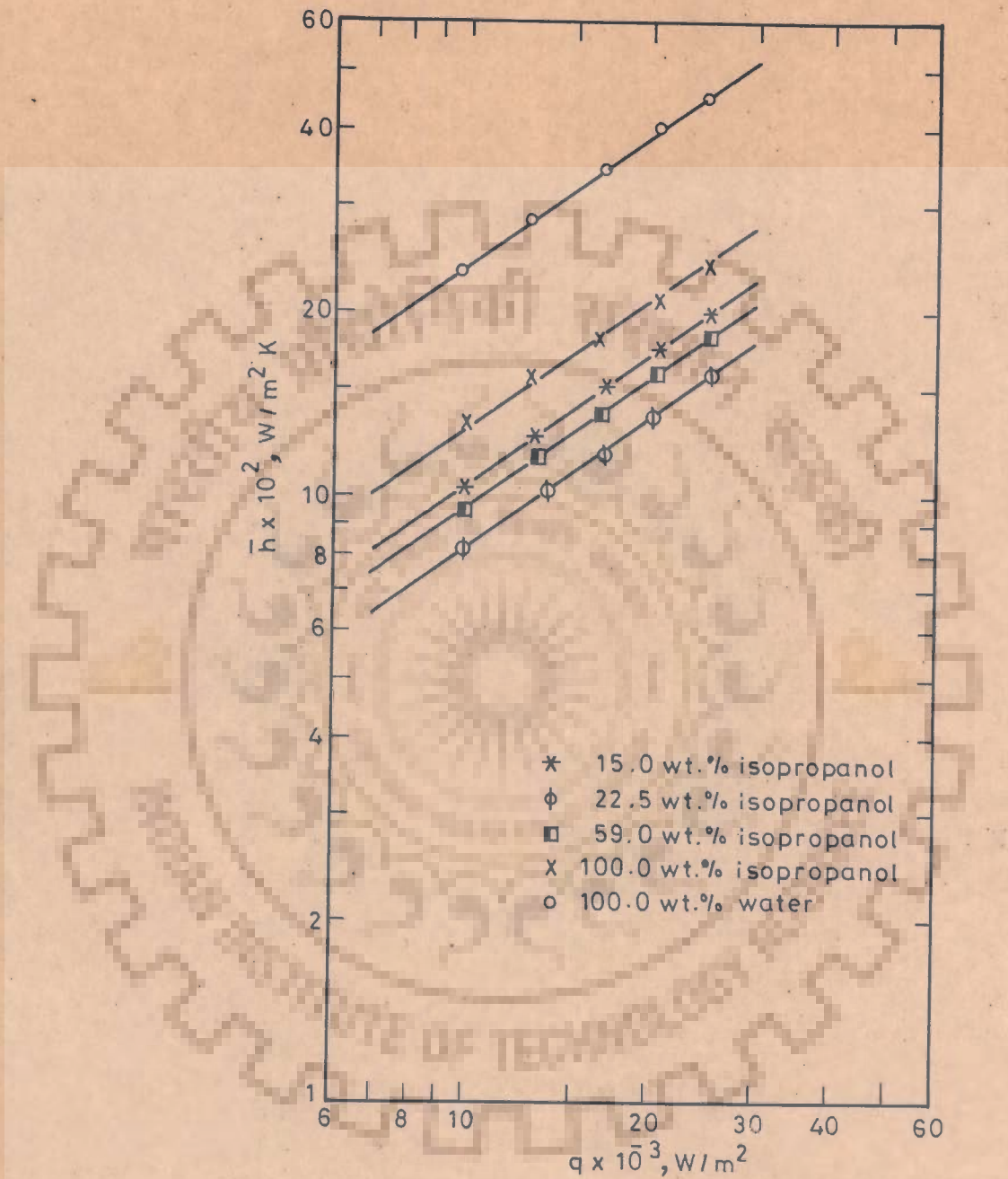


Fig.5.29-Variation of heat transfer coefficient with heat flux for isopropanol-water mixtures at 98.63 kN/m<sup>2</sup>

ethanol, methanol, and isopropanol in their aqueous mixtures, respectively. These figures reveal the following characteristic features :

- a. Heat transfer coefficient changes linearly with heat flux having the same functional relationship as represented by Equation (5.5). Further, from Figure 5.27, it is observed that an addition of ethanol to pure distilled water lowers the boiling heat transfer coefficient. This trend takes place till the concentration of ethanol reaches 31.10 wt. per cent. Further addition of ethanol results in a 'turnaround' and heat transfer coefficient continues to increase.

Figures 5.28 and 5.29 also reveal the same results as those of Figure 5.27 and show their respective 'turnaround' at the definite concentrations of the mixtures.

The concentration representing the 'turnaround' in heat transfer coefficient is 31.10 wt. per cent ethanol in ethanol-water, 30.80 wt. per cent methanol in methanol-water, and 22.50 wt. per cent isopropanol in isopropanol-water mixtures.

- b. The reduction in heat transfer coefficient is appreciable for all the liquid mixtures at their respective 'turnaround' concentration

To have better appreciation of the effect of concentration on heat transfer coefficient,  $\bar{h}^*$  is plotted against wt. per cent ethanol, wt. per cent methanol, and wt. per cent isopropanol in Figures 5.30, 5.31 and 5.32, respectively with system pressure as parameter. On examining these figures, the following characteristic points can be noted :

- a. Referring to Figure 5.30, it is observed that the parameter,  $\bar{h}^*$  decreases with the addition of ethanol till a definite concentration of ethanol, beyond which it begins to increase. The concentration at which this 'turnaround' occurs is 31.10 wt. per cent ethanol.
- b. Higher values of system pressure shift the curves to higher values of heat transfer coefficient. However, this does not change the concentration of ethanol i.e. 31.10 wt. per cent ethanol, for which the heat transfer coefficient is minimum representing the 'turnaround' point.
- c. The actual heat transfer coefficient for any concentration of the ethanol-water mixture investigated is less than the

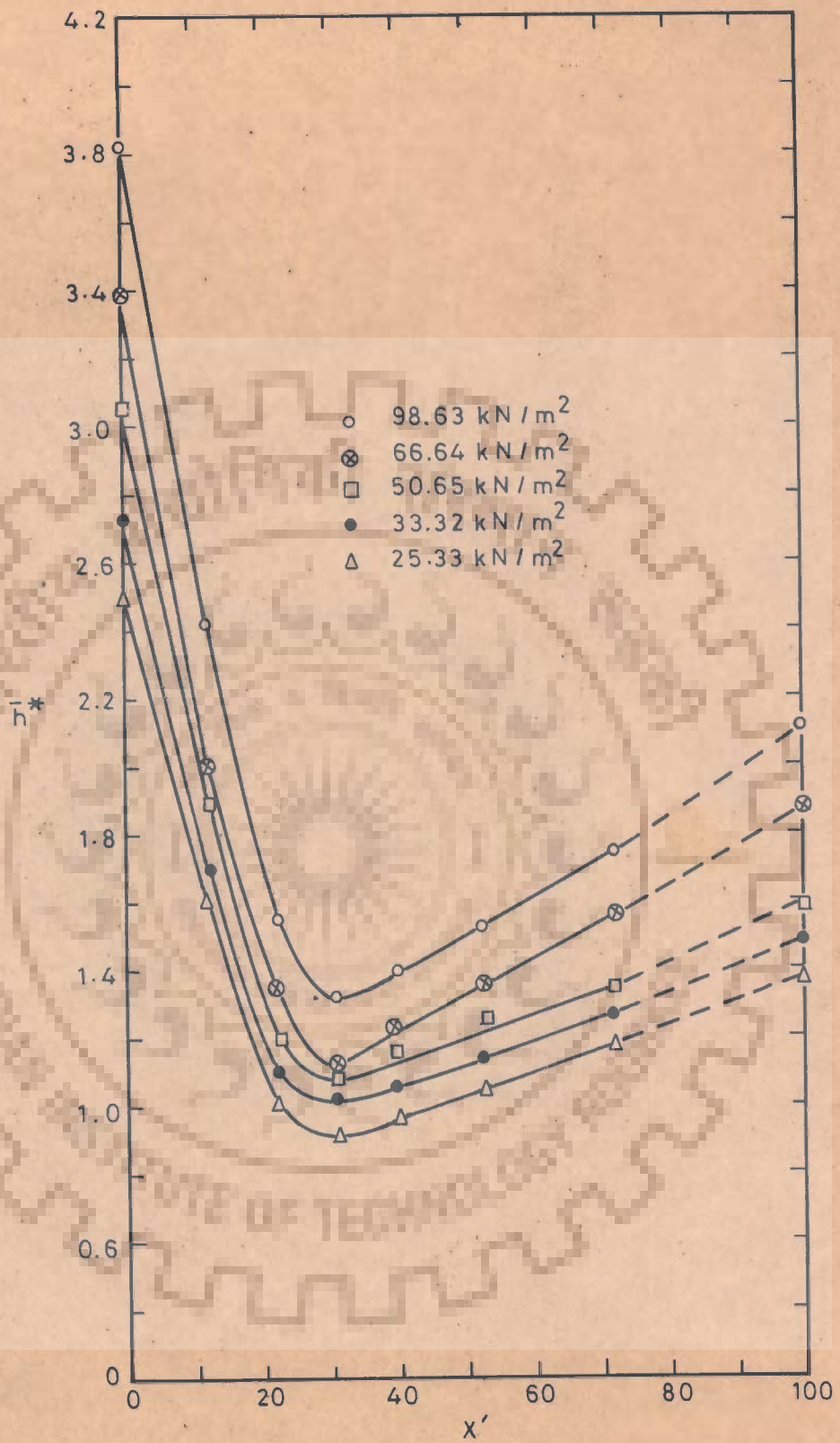


Fig.5.30-Variation of normalised heat transfer coefficient with wt.% of ethanol for ethanol-water mixtures

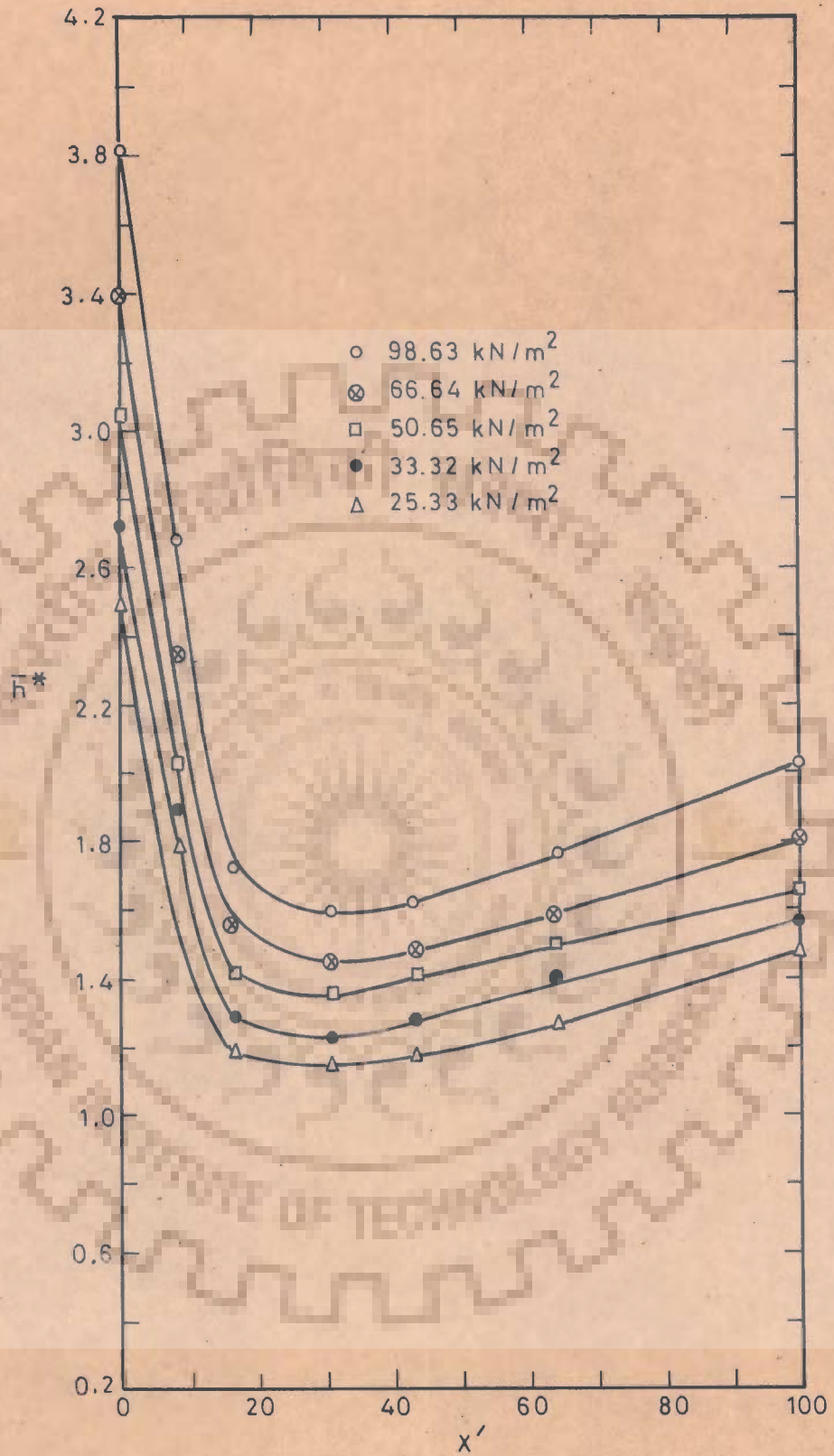


Fig.5.31-Variation of normalised heat transfer coefficient with wt.% of methanol for methanol-water mixtures

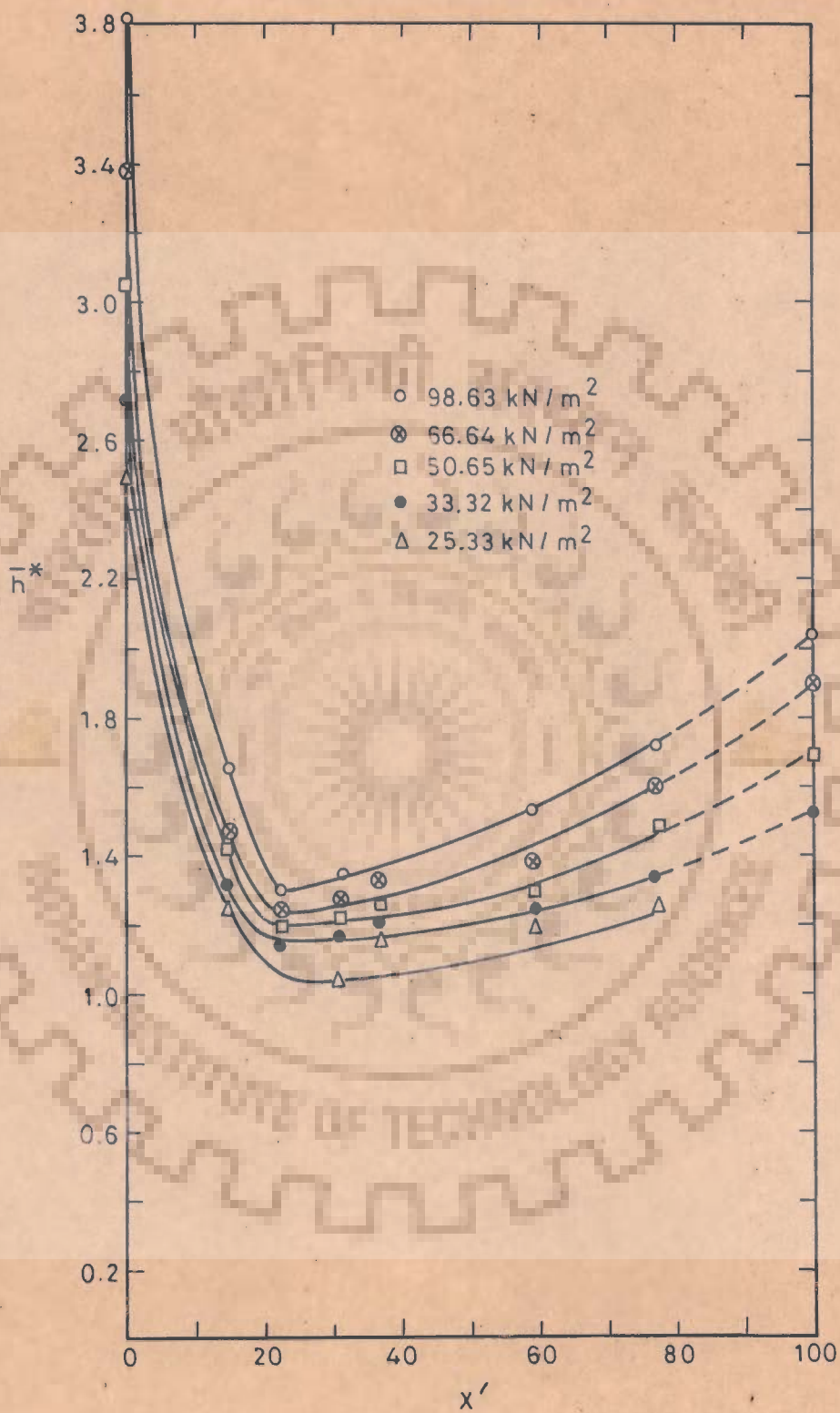


Fig.5.32 - Variation of normalised heat transfer coefficient with wt.% of isopropanol for isopropanol-water mixtures

weighted heat transfer coefficient. The weighted heat transfer coefficient is calculated by the following equation :

$$h_{\text{wtd.}} = h_1 X_1'' + h_2 (1 - X_1'')$$

where  $h_1$  and  $h_2$  are the respective heat transfer coefficients of components 1 and 2 in their pure state and  $X_1''$  is the wt. fraction of component 1 in the binary liquid mixture.

- d. The dotted line on this figure is the region in which the azeotropic composition lies. Therefore, the interpolation has not been done.

Figures 5.31 and 5.32 have similar characteristic features as those possessed by Figure 5.30. The concentration at which the turnaround occurs is 30.80 wt. per cent methanol and 22.50 wt. per cent isopropanol respectively. Methanol-water mixture does not form azeotrope whereas isopropanol-water does and hence the dotted lines have been drawn for the region for which the data were not conducted.

Figure 5.33 shows a comparative behaviour of all the three binary liquid mixtures investigated for a system pressure of  $33.32 \text{ kN/m}^2$ . The data do not deviate appreciably. This plot is a typical one.

The typical behaviour of Figures 5.30 through 5.32 can be explained as follows :

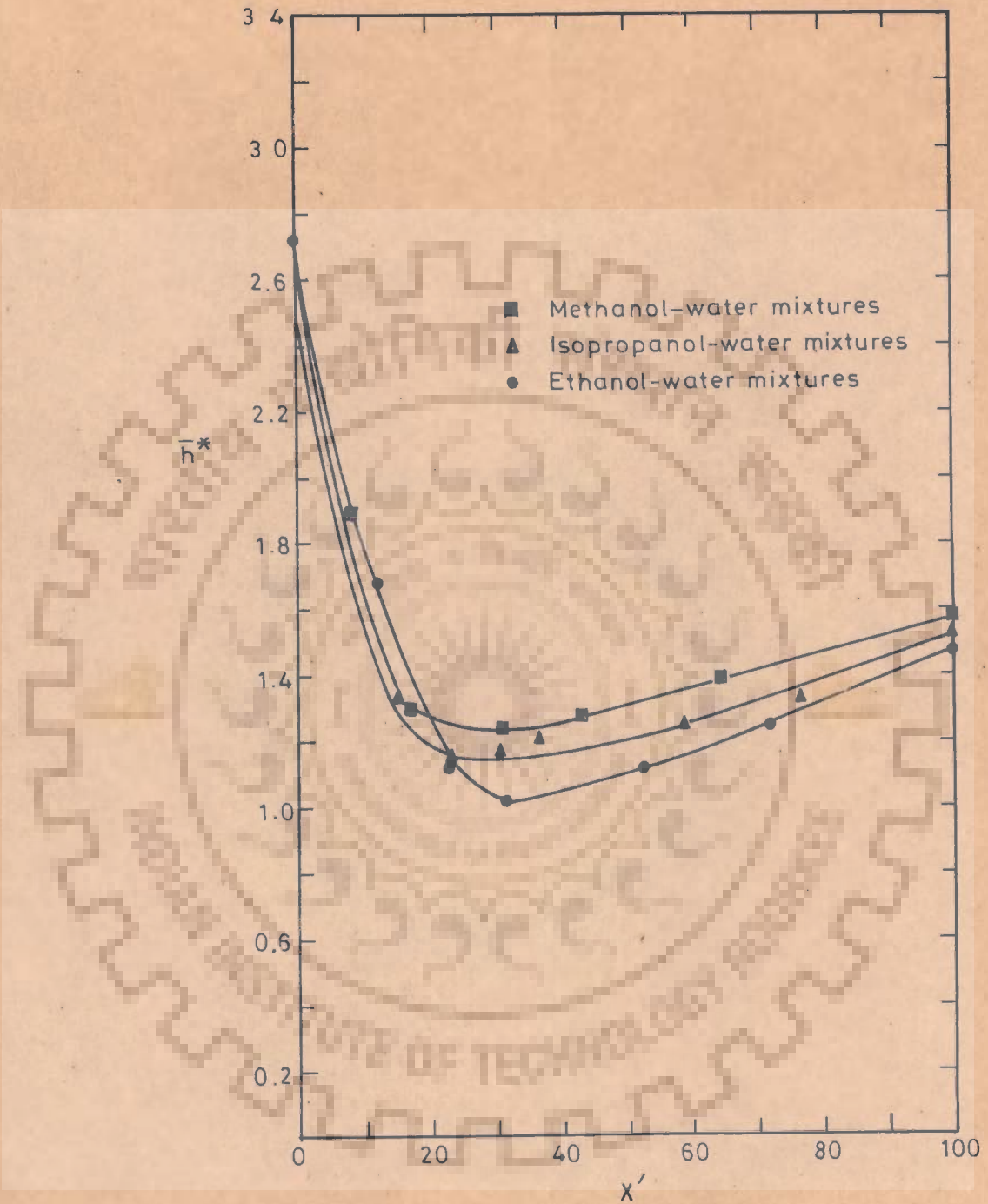


Fig.5.33-Variation of normalised heat transfer coefficient with wt.% of more volatile component for binary liquid mixtures at  $33.32 \text{ kN/m}^2$



Tolubinskii et al [103] have carried out the photographic study to calculate the growth rate of vapour bubbles in a superheated liquid mixture layer over a heated surface. They conclude that the liquid concentration at which the rate of bubble growth is minimum corresponds to a maximum value of  $(Y-X)$ . In other words, the liquid concentration at which  $(Y-X)$  attains a maximum value represents the 'turnaround' point, signifying the minimum value of heat transfer coefficient.

With the above in view, the plots between  $(Y-X)$  and  $X$  for ethanol-water, methanol-water, and isopropanol-water are drawn in Figures 5.34, 5.35 and 5.36, respectively for different pressures. These Figures reveal that the value of  $(Y-X)$  is maximum for ethanol concentration in the liquid phase of 31.10 wt. per cent, for methanol concentration of 30.80 wt. per cent, and for isopropanol concentration of 22.50 wt. per cent.

It may be noted that for these concentrations the value of heat transfer coefficient, as found in the present investigation is minimum for their respective liquid mixtures.

The above results are in conformity with the findings of Happel [60] who has reported the experimental data for the pool boiling of benzene-toluene mixtures conducted for the pressures; 0.5, 1.0, and 2.0 bar and heat flux of  $10^5 \text{ W/m}^2$ .

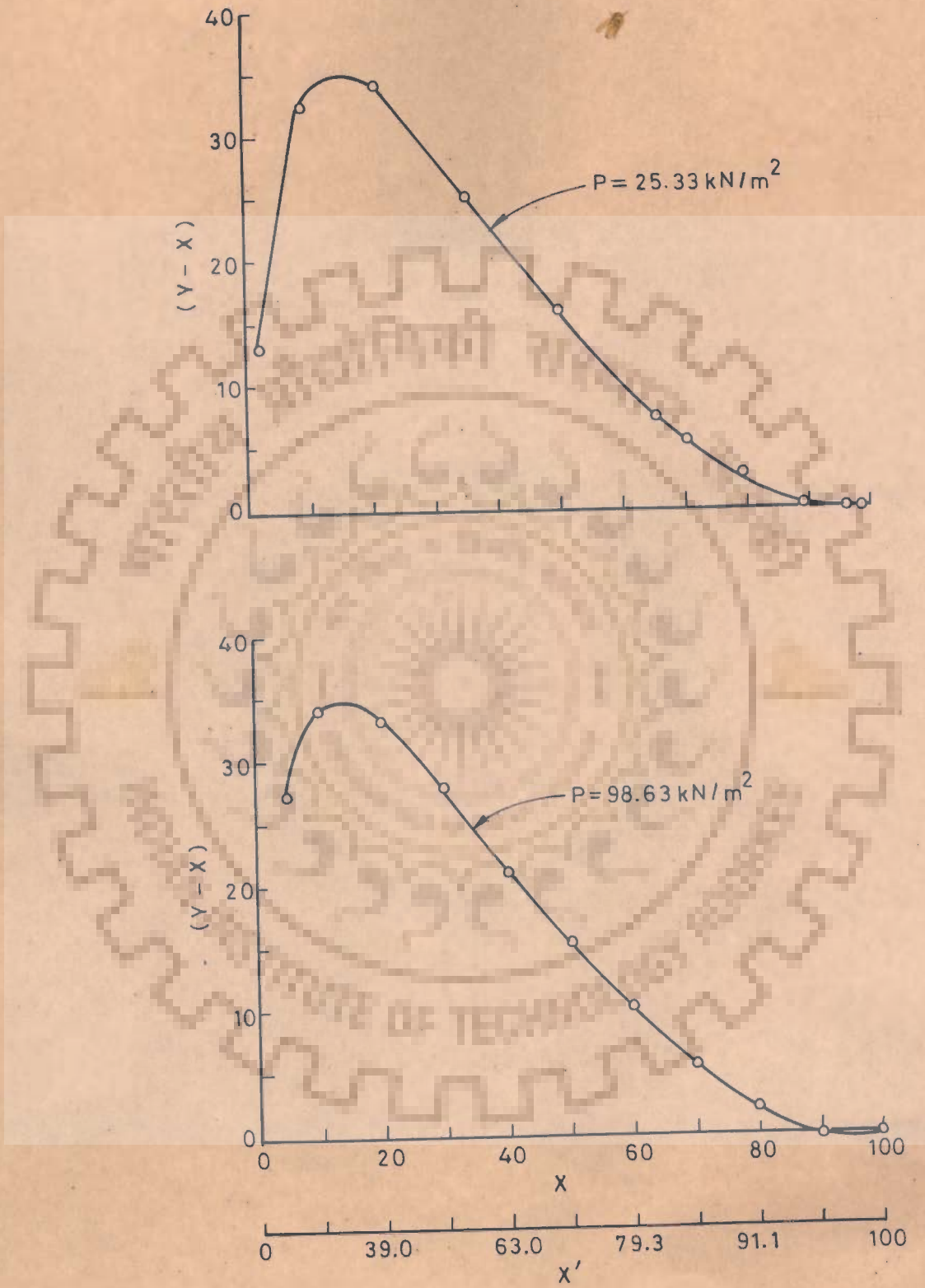


Fig.5.34-Plot of  $(Y-X)$  vs  $X$  or  $X'$  for ethanol-water mixtures

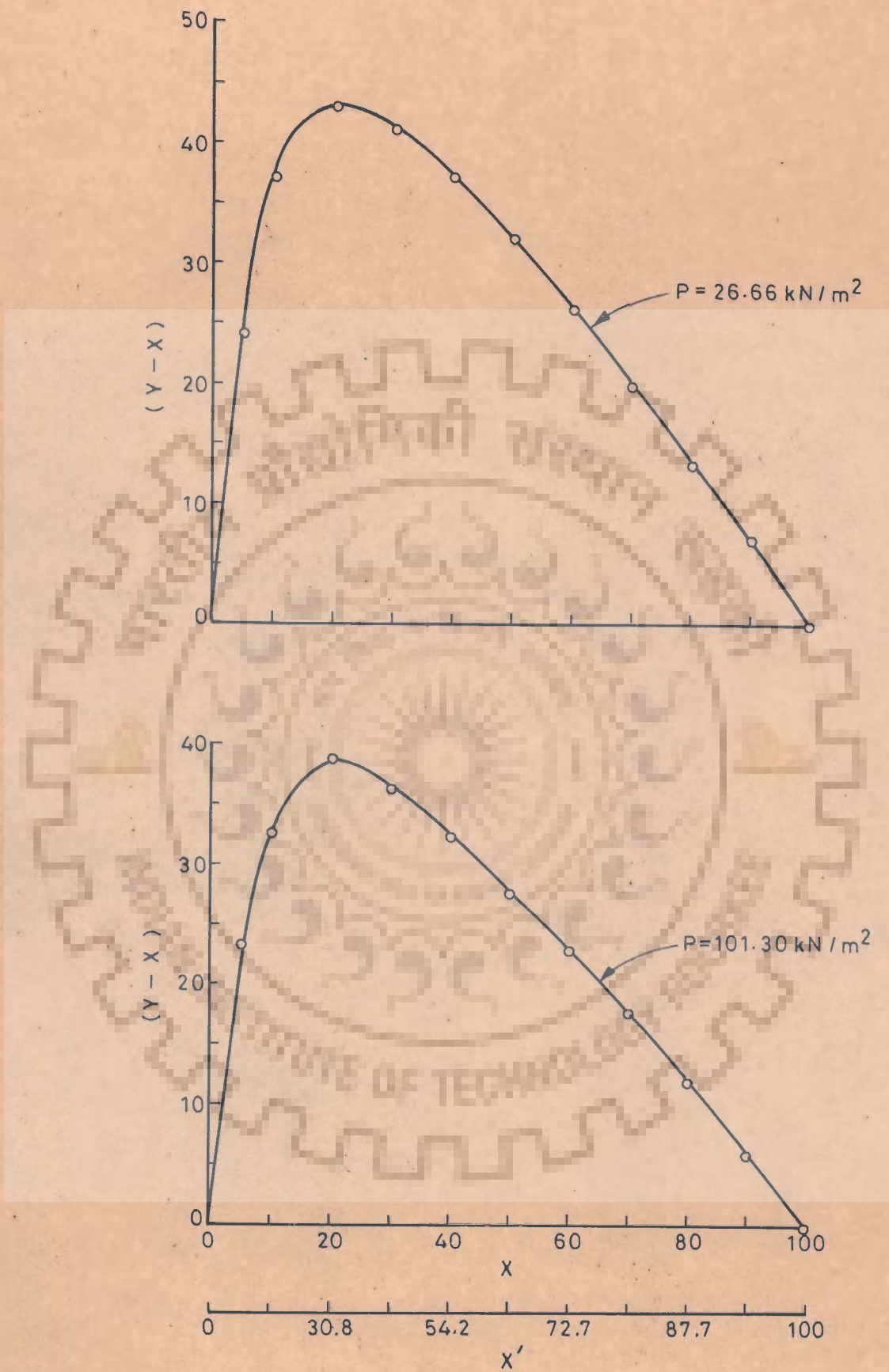


Fig.5.35 - Plot of  $(Y-X)$  vs  $X$  or  $X'$  for methanol-water mixtures

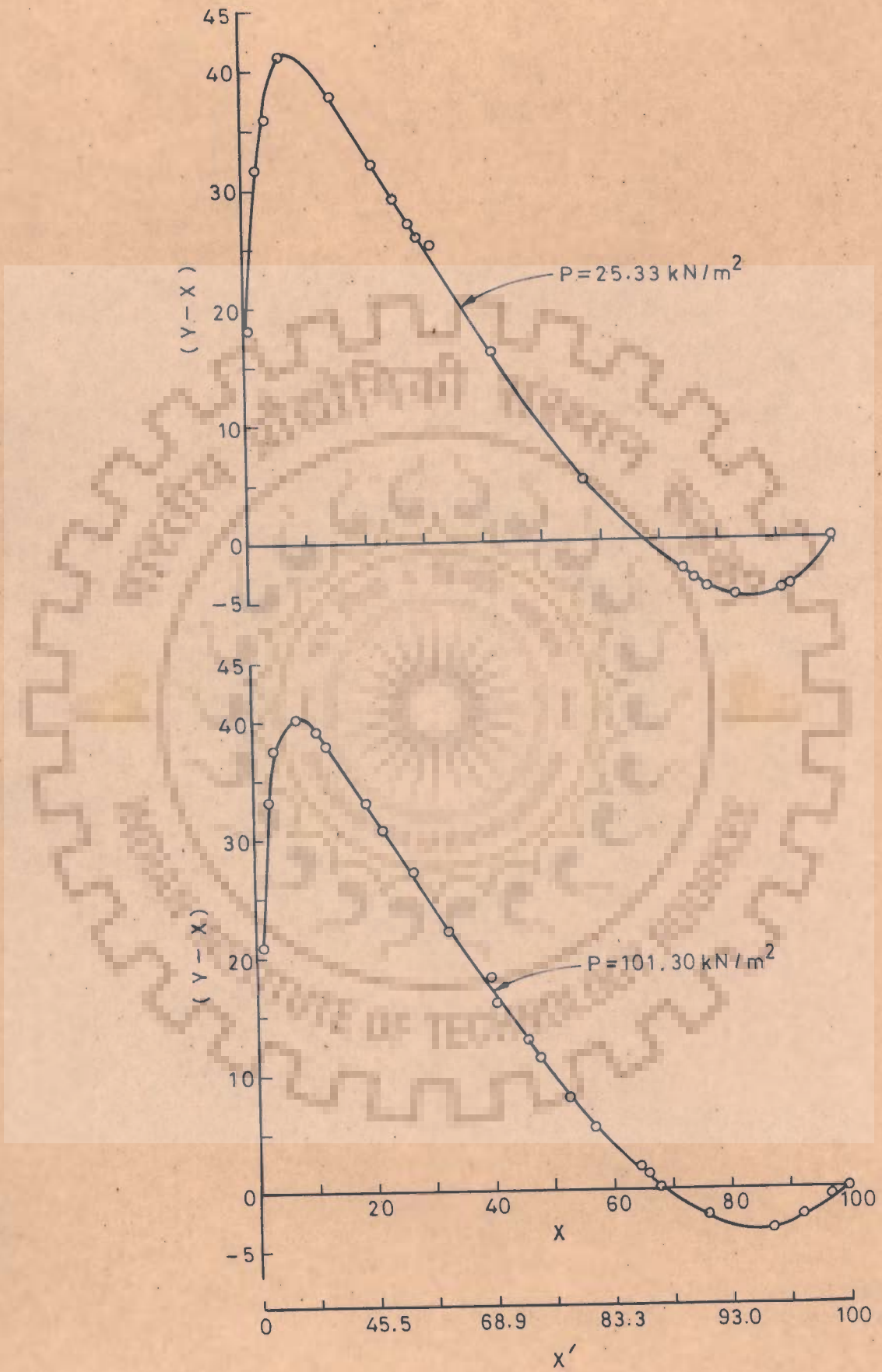


Fig.5.36-Plot of  $(Y-X)$  vs  $X$  or  $X'$  for isopropanol-water mixtures

Figure 5.37 further illustrates the heat transfer coefficient versus concentration relationship for saturated pool boiling of water-acetic acid, water-acetone, water-glycerine and water-ethylene glycol mixtures at  $22,450 \text{ W/m}^2$ . These studies were carried out by Alam [126] at atmospheric pressure and the author has reported the concentrations corresponding to minimum heat transfer coefficients as 17 wt. per cent water in water-acetic acid, 7 wt. per cent water in water-ethylene glycol, and 65 wt. per cent water in acetone-water mixtures.

The characteristic features of the curves obtained for various liquid mixtures in Figure 5.37 are similar to those of Figures 5.30 through 5.33. Each system of binary liquid mixture possesses a 'turnaround' point as found in the present investigation.

#### 5.5.4 Effect of Pressure on Heat Transfer Coefficient

Figures 5.38 through 5.43 represent the variation of heat transfer coefficient with pressure for all the concentrations of aqueous binary mixtures used in the present investigation. The effect of heat flux has been eliminated by taking  $\bar{h}^*$  on Y-axis and pressure on X-axis, as done for the pure liquids in Section 5.2.4. The data of distilled water, ethanol and ethanol-water mixtures are shown in Figures 5.38 and 5.39, whereas those of distilled water, methanol and

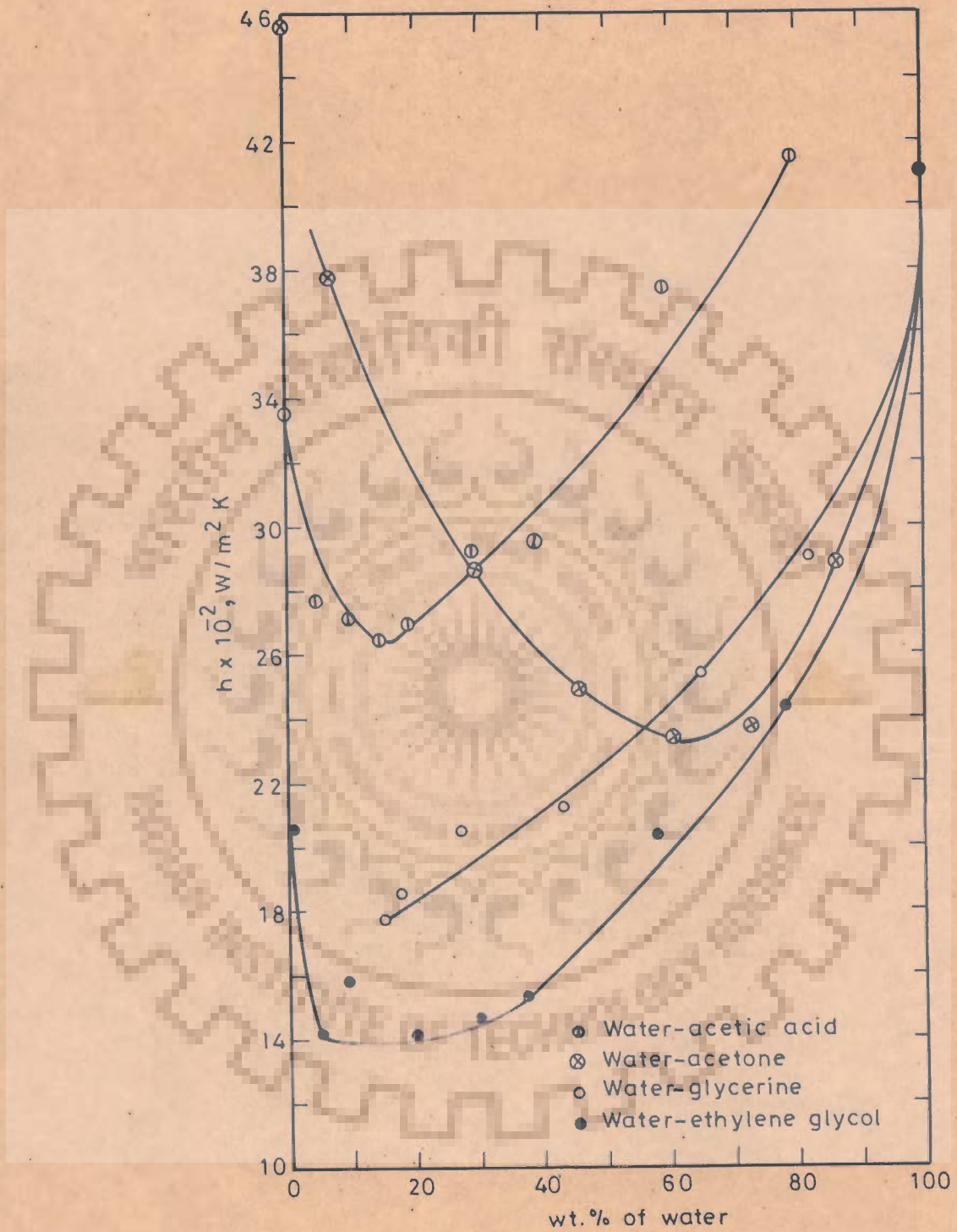


Fig.5.37—Variation of heat transfer coefficient with wt.% of water in binary liquid mixtures at  $22.45 \times 10^3 W/m^2$  [126]

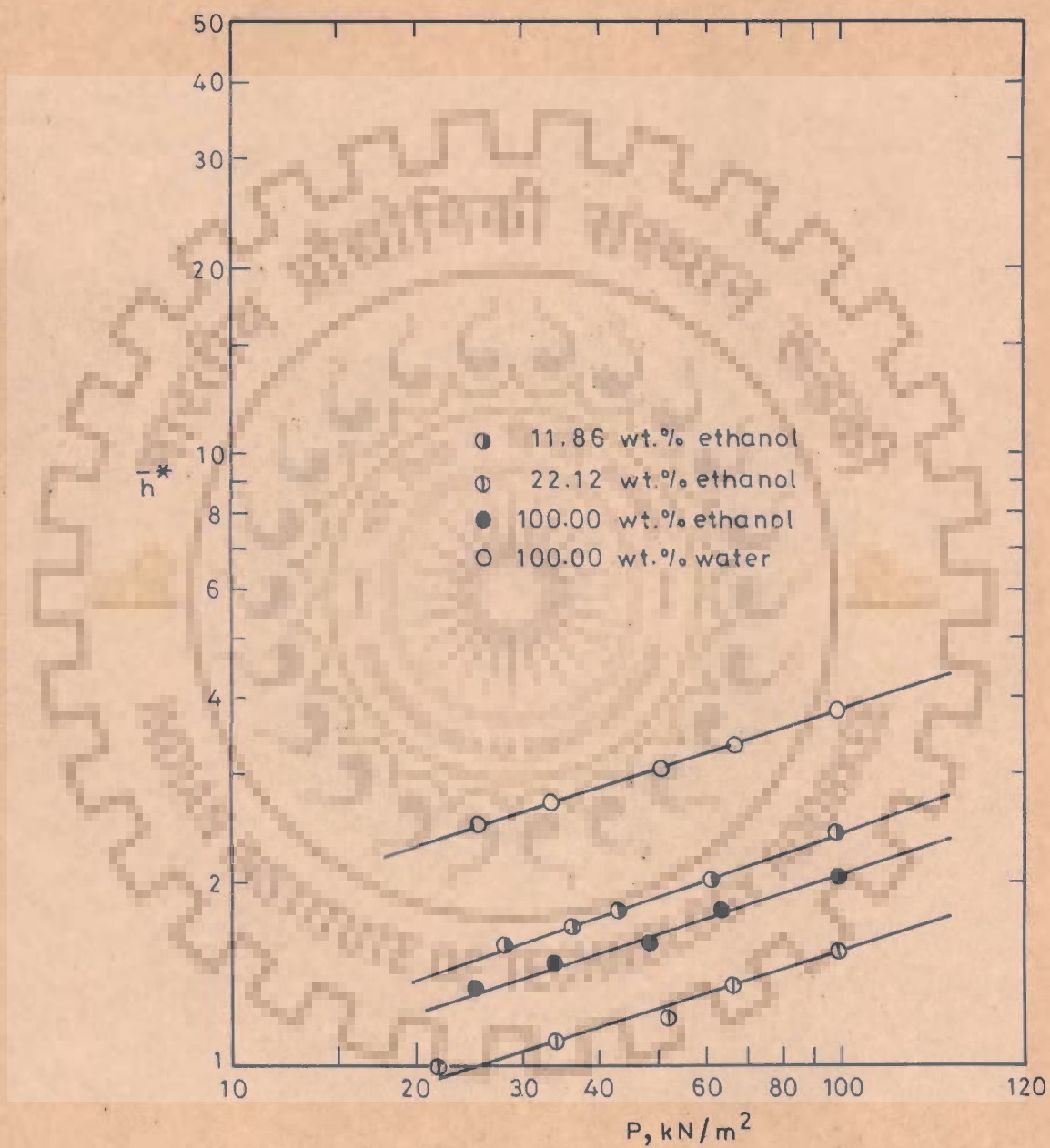


Fig.5.38-Variation of normalised heat transfer coefficient with pressure for water, ethanol & ethanol-water mixtures

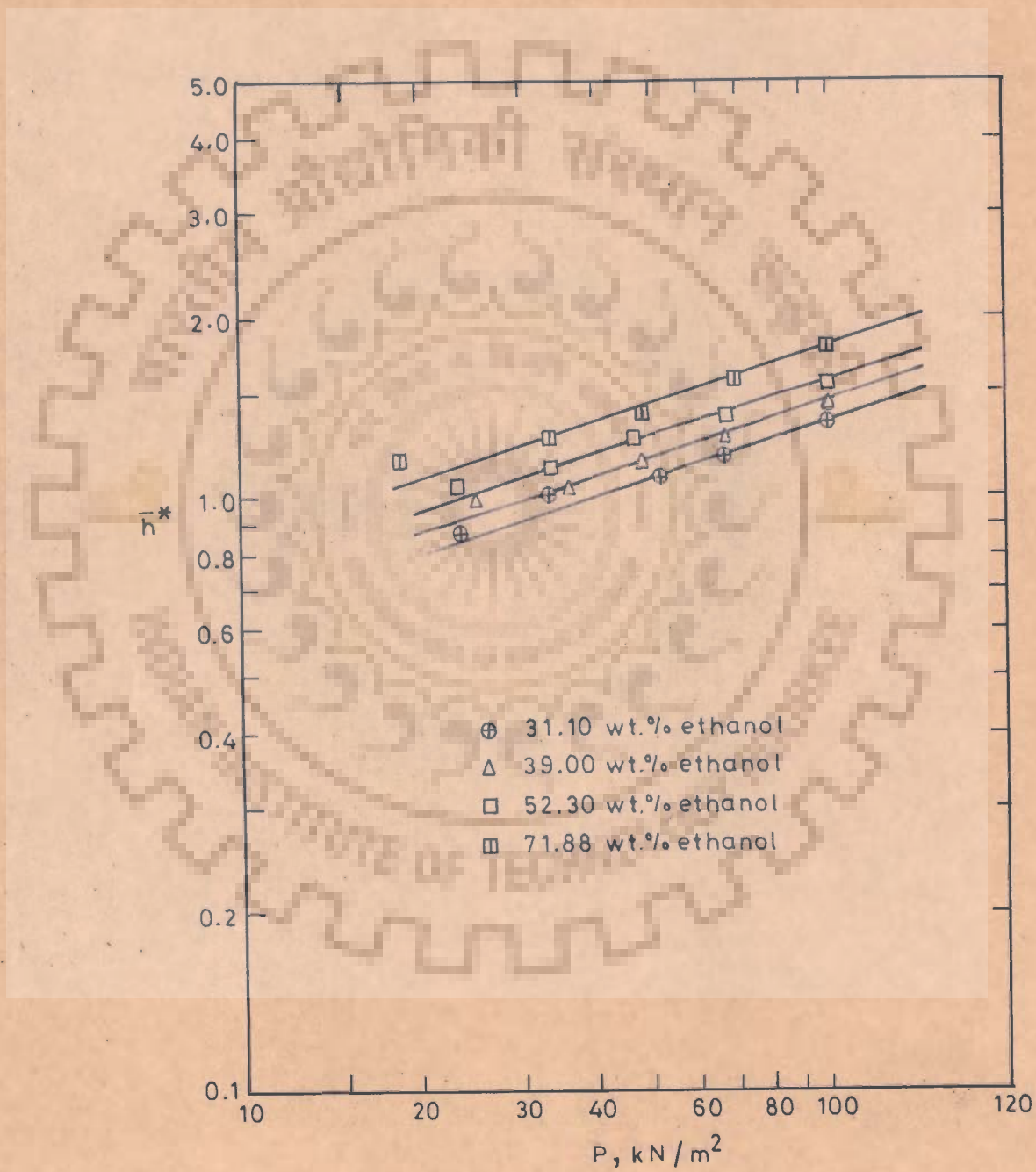


Fig.5.39-Variation of normalised heat transfer coefficient with pressure for ethanol-water mixtures



methanol-water mixtures in Figures 5.40 and 5.41, and of distilled water, isopropanol and isopropanol-water mixtures in Figures 5.42 and 5.43. The parallel lines obtained for various compositions of ethanol-water, methanol-water and isopropanol-water are mathematically expressed by the following expression :

$$\bar{h}^* = C_{m_1} P^{0.32} \quad \dots(5.7)$$

where  $C_{m_1}$  is constant of proportionality. The experimental data correlated by Equation (5.7) were conducted on a given heating surface made of stainless steel. The parallel lines obtained for the boiling of pure liquids as well as their binaries with a slope of 0.32 indicate that the constant  $C_{m_1}$  depends upon the physico-thermal properties of the boiling liquids for a given heating surface. It may be mentioned here that the value of exponent over pressure in Equation (5.7) for binary mixtures remains the same as for their constituents in pure liquid states.

The experimental values of constant,  $C_{m_1}$ , are given in Table 5.5. The statistical parameters of the values of constant,  $C_{m_1}$  were calculated. They are listed in Table 5.5. The maximum value of Coefficient of Variation is 8.87 per cent which is well within the experimental error. Hence, it is concluded that the constant,  $C_{m_1}$  is independent of pressure for a given boiling liquid mixture and heating surface.

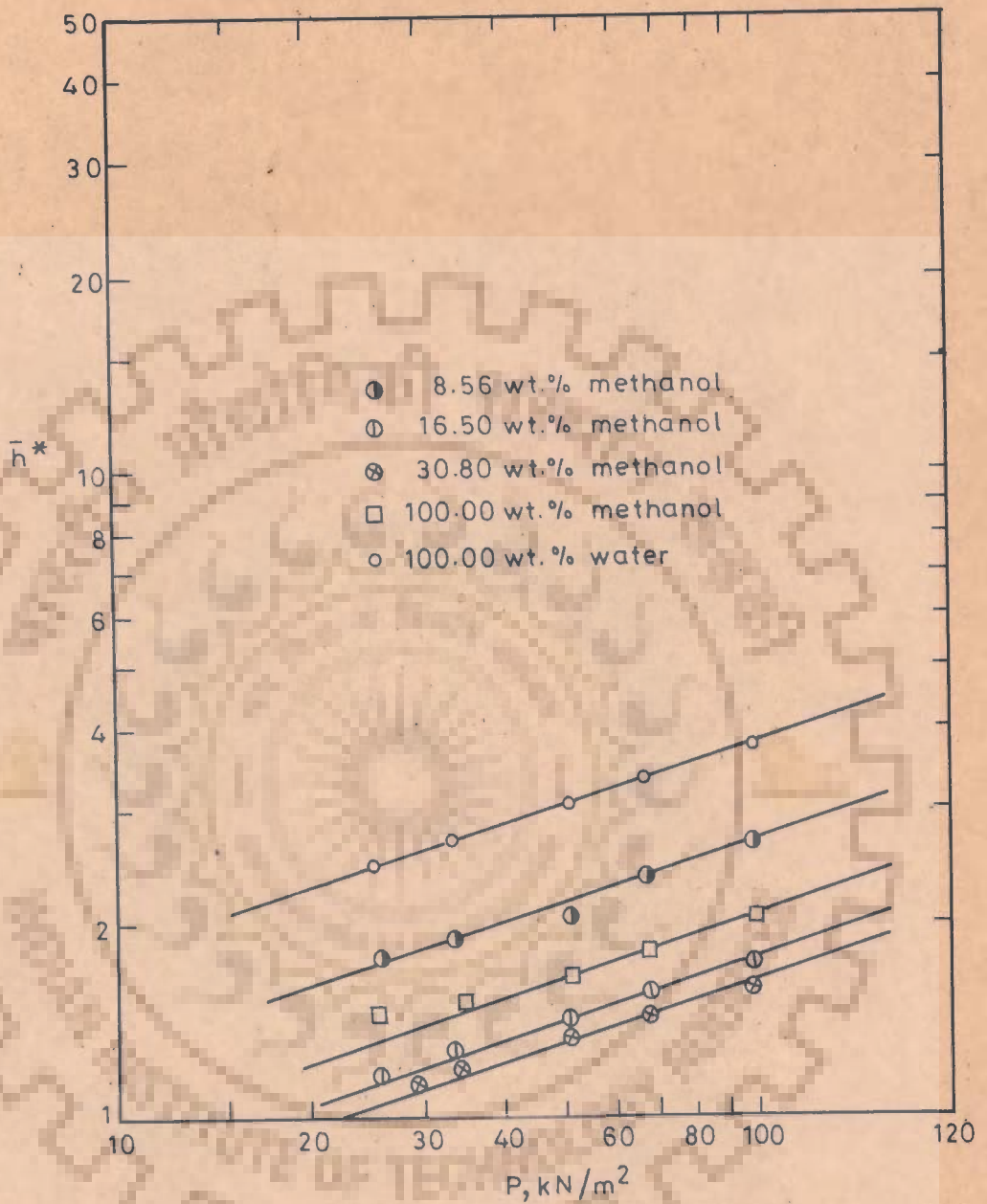


Fig.5.40-Variation of normalised heat transfer coefficient with pressure for distilled water, methanol and methanol-water mixtures.

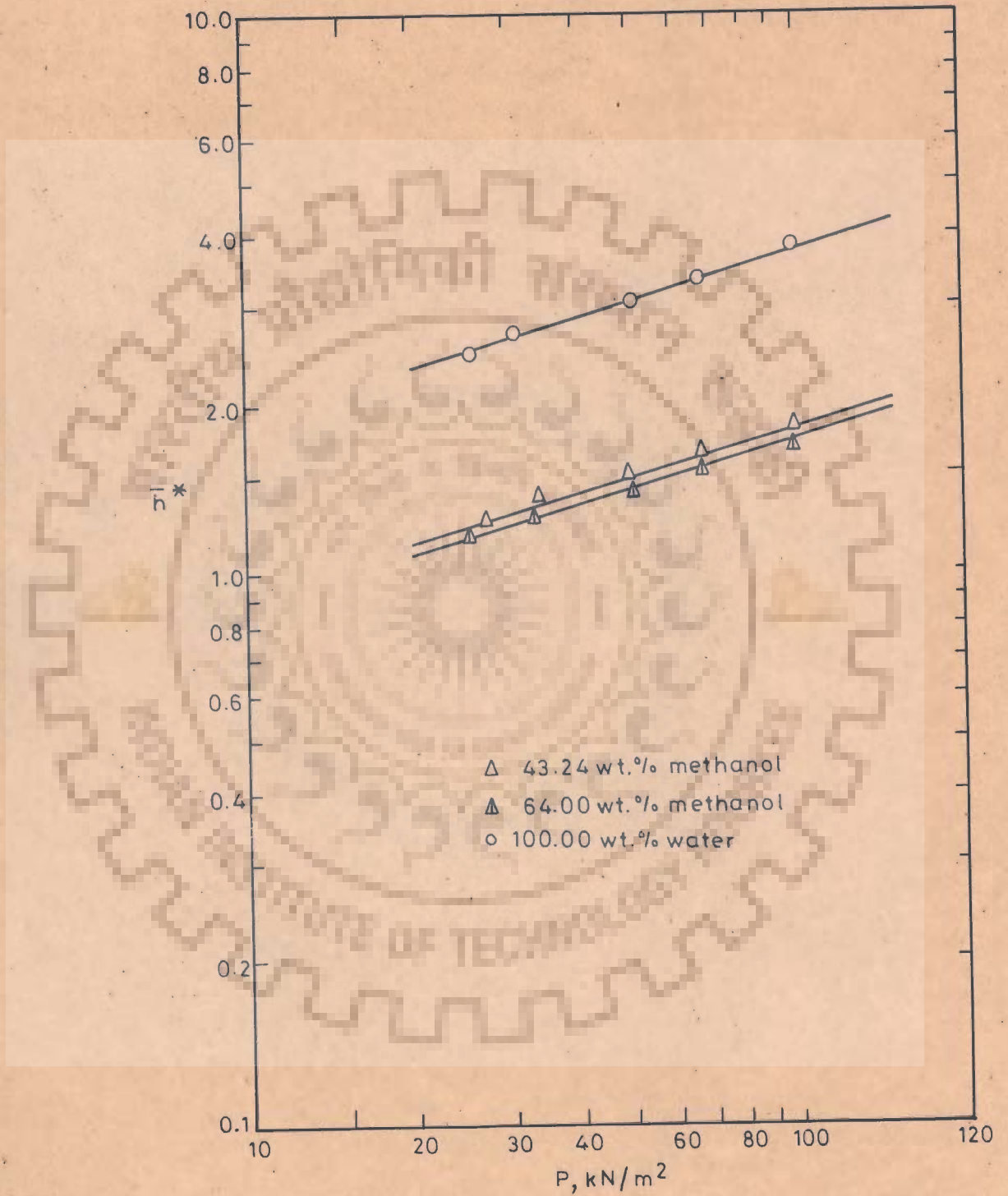


Fig.5.41-Variation of normalised heat transfer coefficient with pressure for methanol-water mixtures & distilled water

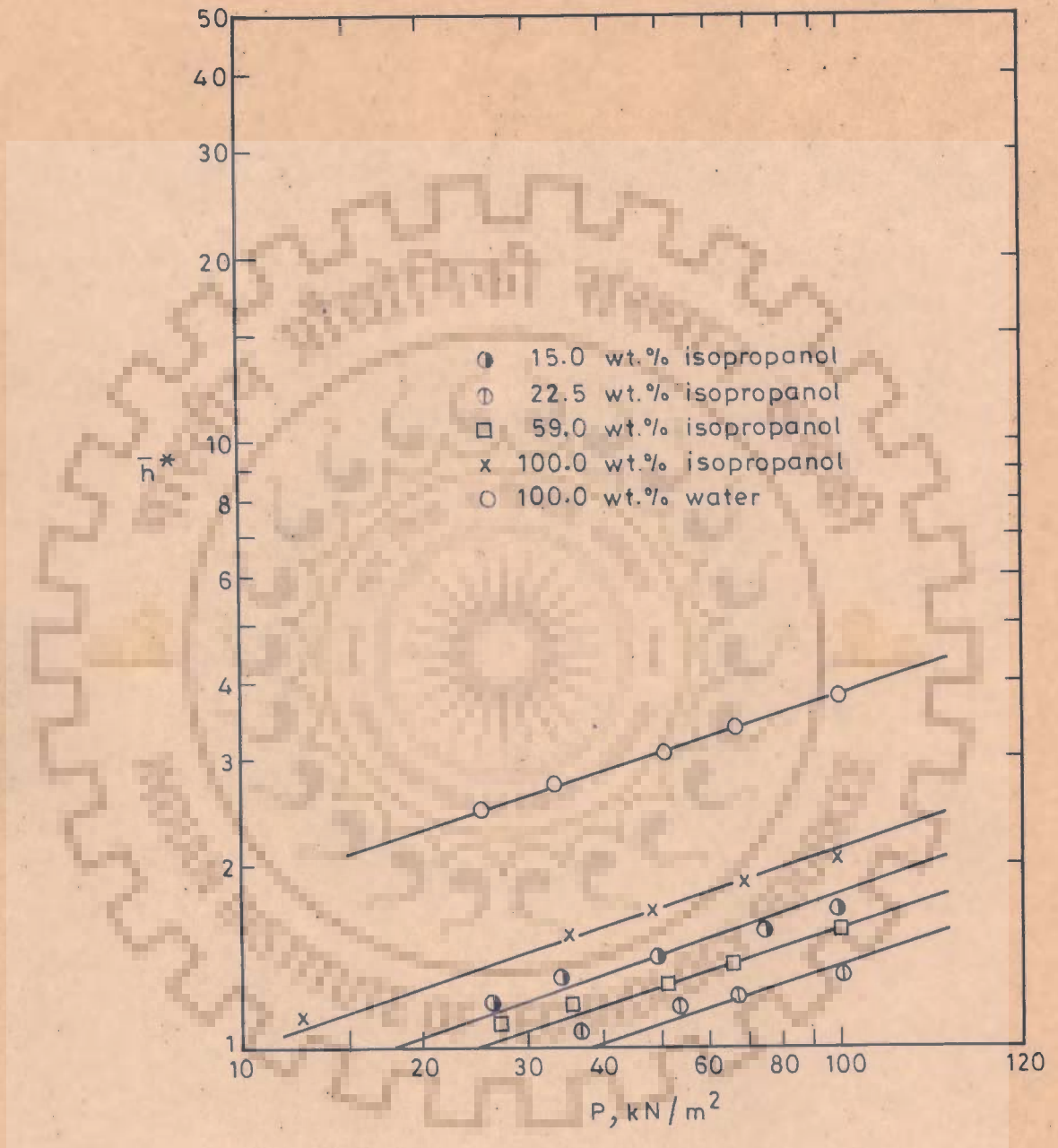


Fig.5.42 - Variation of normalised heat transfer coefficient with pressure for distilled water, isopropanol and isopropanol-water mixtures

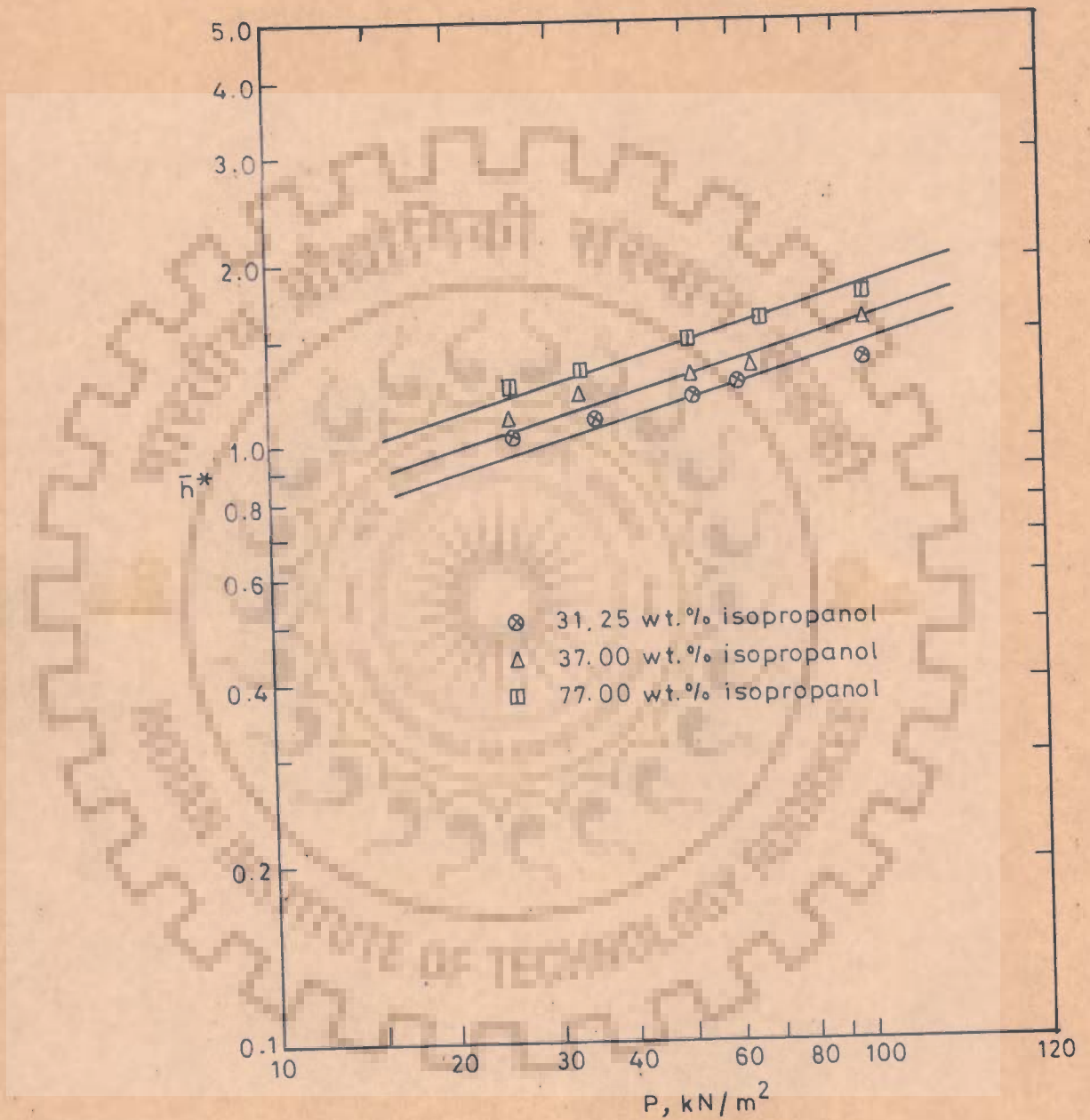


Fig.5.43-Variation of normalised heat transfer coefficient with pressure for isopropanol-water mixtures

Table 5.5 : Values of Constant,  $C_{m1}$  in Equation (5.7) for Binary Liquid Mixtures at Subatmospheric Pressures

Boiling Liquid	Pressure kN/m <sup>2</sup>	Constant $C_{m1}$	Heating Surface	Investigator	Statistical Parameter for Constant $C_{m1}$
Ethanol-Water Mixtures					
11.86 wt.% ethanol	98.63	0.556	410 ASIS Grade Stainless Steel Cylinder	Present Investigation	$\bar{X} = 0.5504$ $\sigma = 0.011$ COV = 2.01%
	61.31	0.540			
	42.65	0.566			
	36.00	0.540			
	28.00	0.550			
31.10 wt.% Ethanol	98.63	0.302	-do-	-do-	$\bar{X} = 0.3156$ $\sigma = 0.0151$ COV = 4.79%
	66.64	0.304			
	50.65	0.308			
	33.32	0.332			
	22.66	0.332			
52.30 wt.% Ethanol	98.63	0.350	-do-	-do-	$\bar{X} = 0.3656$ $\sigma = 0.0151$ COV = 4.15%
	66.64	0.353			
	46.65	0.369			
	33.32	0.368			
	22.66	0.388			
71.88 wt.% Ethanol	98.63	0.399	-do-	-do-	$\bar{X} = 0.411$ $\sigma = 0.0292$ COV = 7.11%
	69.31	0.401			
	47.98	0.385			
	33.32	0.409			
	18.66	0.461			

Boiling Liquid	Pressure kN/m <sup>2</sup>	Constant C <sub>m1</sub>	Heating Surface	Investigator	Statistical Parameters for Constant C <sub>m1</sub>
Methanol- Water Mixtures					
8.56 wt.% Methanol	98.63	0.616	410 ASIS Grade Stainless Steel Cylinder	Present Investigation	$\bar{X} = 0.6126$ $\sigma = 0.0208$ COV = 3.4%
	66.64	0.612			
	50.65	0.580			
	33.32	0.617			
	25.33	0.638			
16.50 wt.% Methanol	98.63	0.400	-do-	-do-	$\bar{X} = 0.4102$ $\sigma = 0.0094$ COV = 2.28%
	66.64	0.408			
	50.65	0.403			
	33.32	0.420			
	25.33	0.420			
30.80 wt.% Methanol	98.63	0.370	-do-	-do-	$\bar{X} = 0.3868$ $\sigma = 0.013$ COV = 3.36 %
	66.64	0.380			
	50.65	0.388			
	33.32	0.405			
	29.32	0.391			
64.00 wt.% Methanol	98.63	0.410	-do-	-do-	$\bar{X} = 0.4328$ $\sigma = 0.0214$ COV = 4.93 %
	66.64	0.415			
	49.32	0.430			
	33.32	0.459			
	26.66	0.450			
Isopropanol- Water Mixtures					
15.00 wt.% Isopropanol	98.63	0.381			$\bar{X} = 0.4088$ $\sigma = 0.029$ COV = 7.09 %
	74.00	0.380			
	49.32	0.408			
	33.32	0.430			
	25.33	0.445			

Boiling Liquid	Pressure kN/m <sup>2</sup>	Constant C <sub>m1</sub>	Heating Surface	Investigator	Statistical Parameters for Constant C <sub>m1</sub>
22.50 wt.% Isopropanol	98.63	0.300	410 ASIS	Present Investigation	$\bar{X} = 0.331$ $\sigma = 0.0293$ COV = 8.87 %
	66.64	0.321	Grade		
	53.32	0.333	Stainless		
	34.66	0.370	Steel Cylinder		
37.00 wt.% Isopropanol	98.63	0.370	-do-	-do-	$\bar{X} = 0.376$ $\sigma = 0.0237$ COV = 6.30 %
	64.00	0.350			
	50.65	0.360			
	33.32	0.392			
	25.33	0.408			
77.00 wt.% Isopropanol	98.63	0.400	-do-	-do-	$\bar{X} = 0.4248$ $\sigma = 0.018$ COV = 4.24 %
	66.64	0.420			
	50.65	0.424			
	33.32	0.430			
	25.33	0.450			

$\bar{X}$  = Mean  
 $\sigma$  = Standard Deviation  
 COV = Coefficient of Variation

### 5.6 VARIATION OF $\bar{h}^*/\bar{h}_1^*$ WITH $P/P_1$ FOR SUBATMOSPHERIC PRESSURE

Keeping in view that the constant,  $C_{m1}$  depends on the nature of binary liquid mixture and the heating surface characteristics, an attempt was made to plot  $\bar{h}^*/\bar{h}_1^*$  against  $P/P_1$  as done for pure liquids in Section 5.3.



Figure 5.44 is a log-log plot for distilled water, ethanol and ethanol-water mixtures of varying concentrations. Similar logarithmic plots are shown for water, methanol and methanol-water mixtures and water, isopropanol and isopropanol-water mixtures in Figures 5.45 and 5.46 respectively. All the data points are represented by a straight line. Further, Figure 5.47 represents all the data points of Figures 5.44 through 5.46. An examination of Figure 5.47 shows that all the data points are well-correlated by a single straight line within  $\pm 15$  per cent deviation by the following equation :

$$\bar{h}^*/\bar{h}_1^* = (P/P_1)^{0.32} \quad \dots(5.8)$$

The significance of subscript '1' has already been explained in Section 5.3. The reference pressure chosen was atmospheric pressure.

It may be noted that the correlation, Equation (5.8) offers a procedure for predicting the boiling heat transfer coefficients at atmospheric and subatmospheric pressures and for checking the consistency of boiling heat transfer data for binary liquid mixtures similar to correlation represented by Equation (5.4) in Section 5.3.



Fig.5.44-Variation of  $\bar{h}/\bar{h}_1^*$  with  $P/P_1$  for ethanol and ethanol-water mixtures

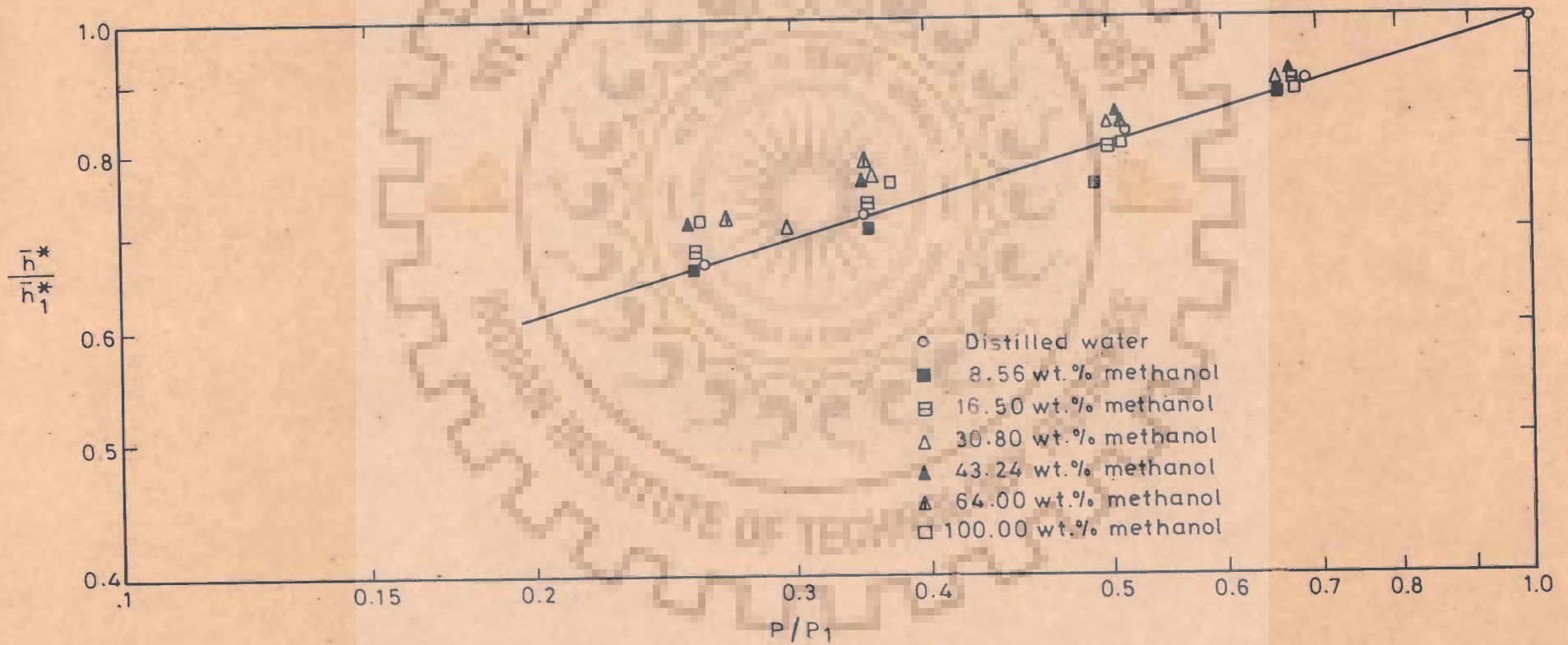


Fig.5.45-Variation of  $\bar{h}/\bar{h}_1^*$  with  $P/P_1$  for methanol and methanol-water mixtures

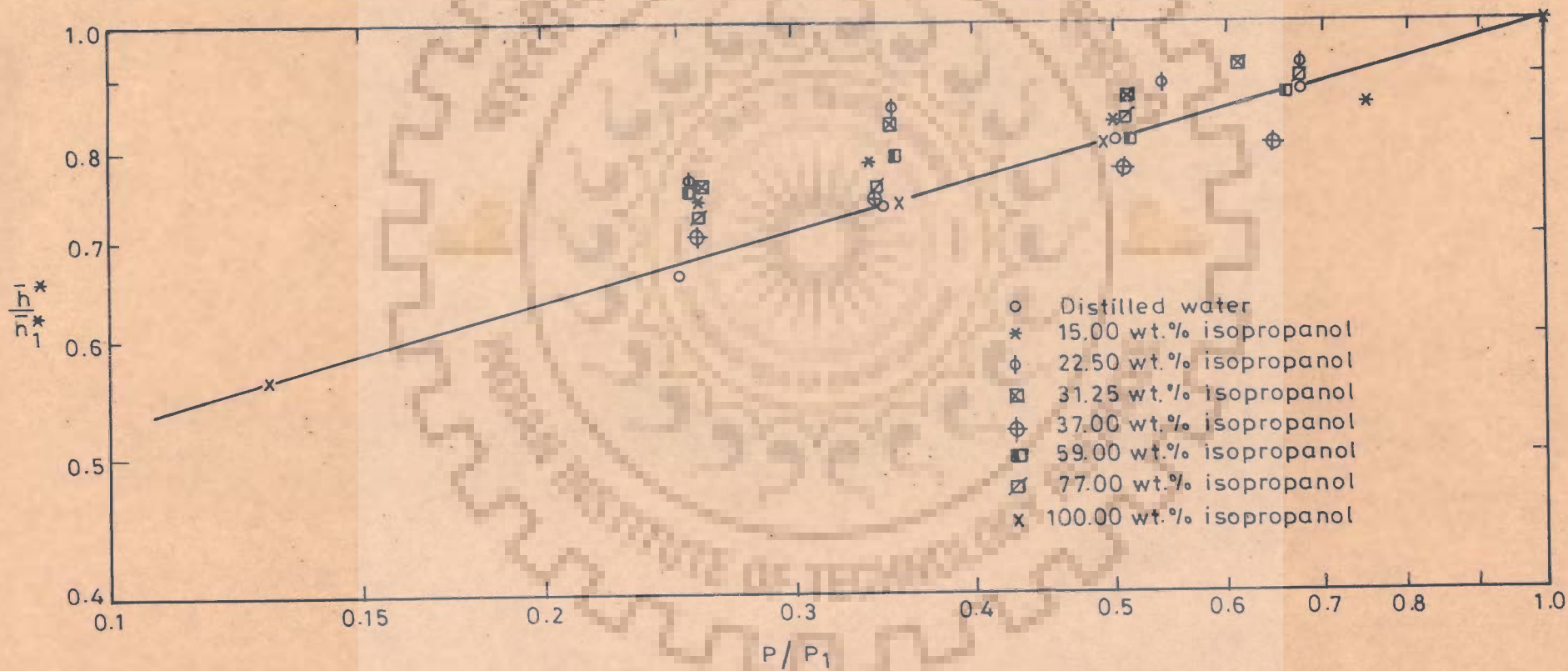


Fig.5.46-Variation of  $\bar{h}^*/\bar{h}_1^*$  with  $P/P_1$  for isopropanol and isopropanol-water mixtures

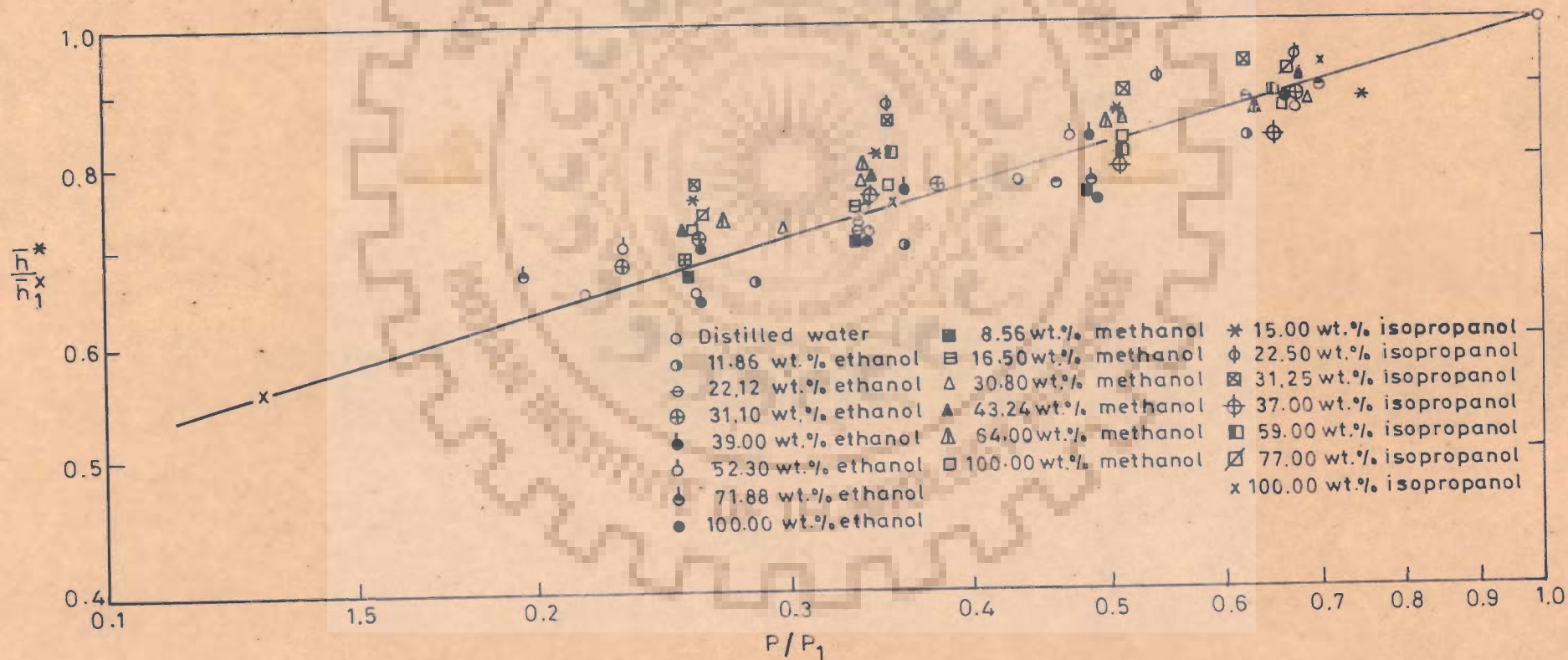


Fig.5.47-Variation of  $\bar{h}^*/\bar{h}_1^*$  with  $P/P_1$  for pure liquids and alcohol-water mixtures

## 5.7 GENERALISED CORRELATION

Figures 5.30 through 5.32 show that the heat transfer coefficient is influenced considerably by the concentration of binary liquid mixtures, in addition to the system pressure and the physico-thermal properties of the boiling liquids.

A scrutiny of the correlation given by Equation (5.8) shows that the correlation can be used to predict the values of heat transfer coefficient at any subatmospheric pressure for a given liquid concentration and heating surface only when one knows the value of heat transfer coefficient at the 'reference' pressure for the same liquid concentration and the heating surface. In fact, in a way it is the shortcoming of the correlation Equation (5.8), unlike the generally available correlation proposed for boiling heat transfer.

Keeping the above two factors into consideration, a generalised correlation was attempted as follows :

Plots were drawn to represent the data of ethanol-water, methanol-water, and isopropanol-water mixtures in Figures 5.48, 5.49 and 5.50 respectively. Y-axis represents  $\bar{N}_u^*(P_1/P)^{0.32}$ , whereas x-axis contains  $X'$ . Fortunately, such an attempt succeeded in correlating all the experimental data of the present investigation within  $\pm 15$  per cent. Figure 5.51 correlates almost all the data points of Figures 5.48 through 5.50 within  $\pm 15$  per cent. From this Figure it is seen that the

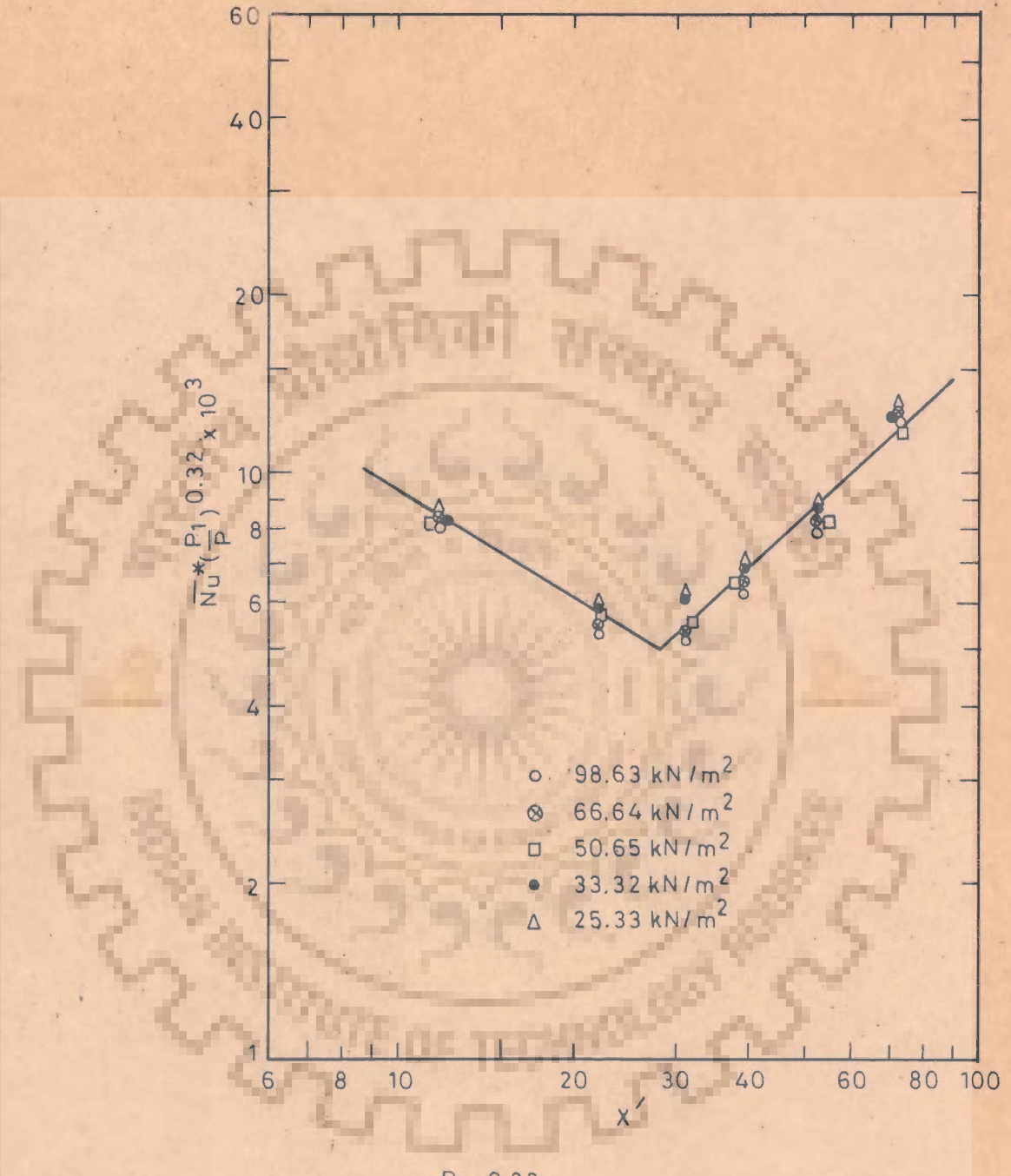


Fig.5.48-Plot of  $\bar{Nu}^* \left(\frac{P_1}{P}\right)^{0.32}$  vs  $X'$  for ethanol-water mixtures

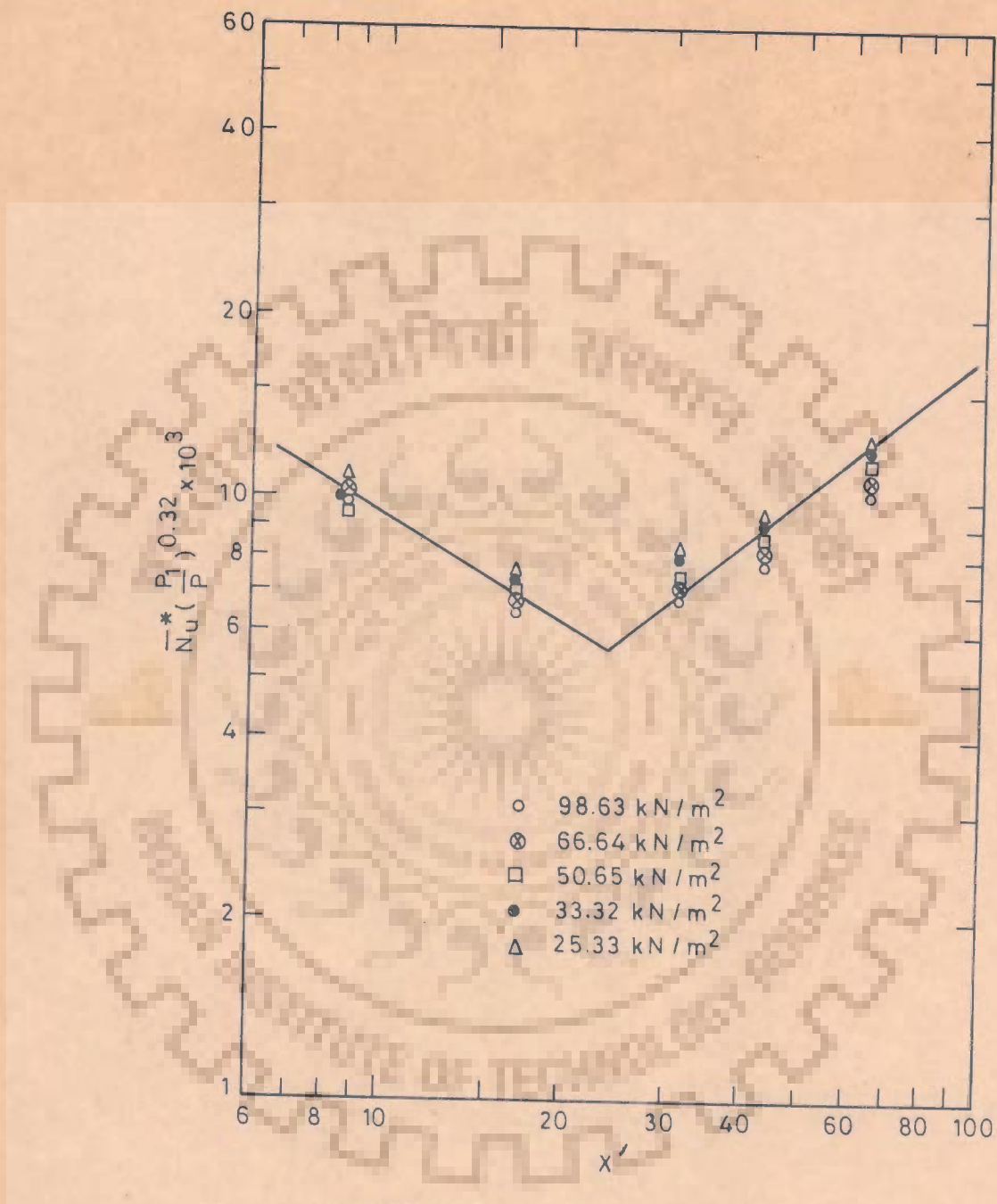


Fig.5.49-Plot of  $\bar{Nu}^* (\frac{P_1}{P})^{0.32}$  vs  $X'$  for methanol-water mixtures



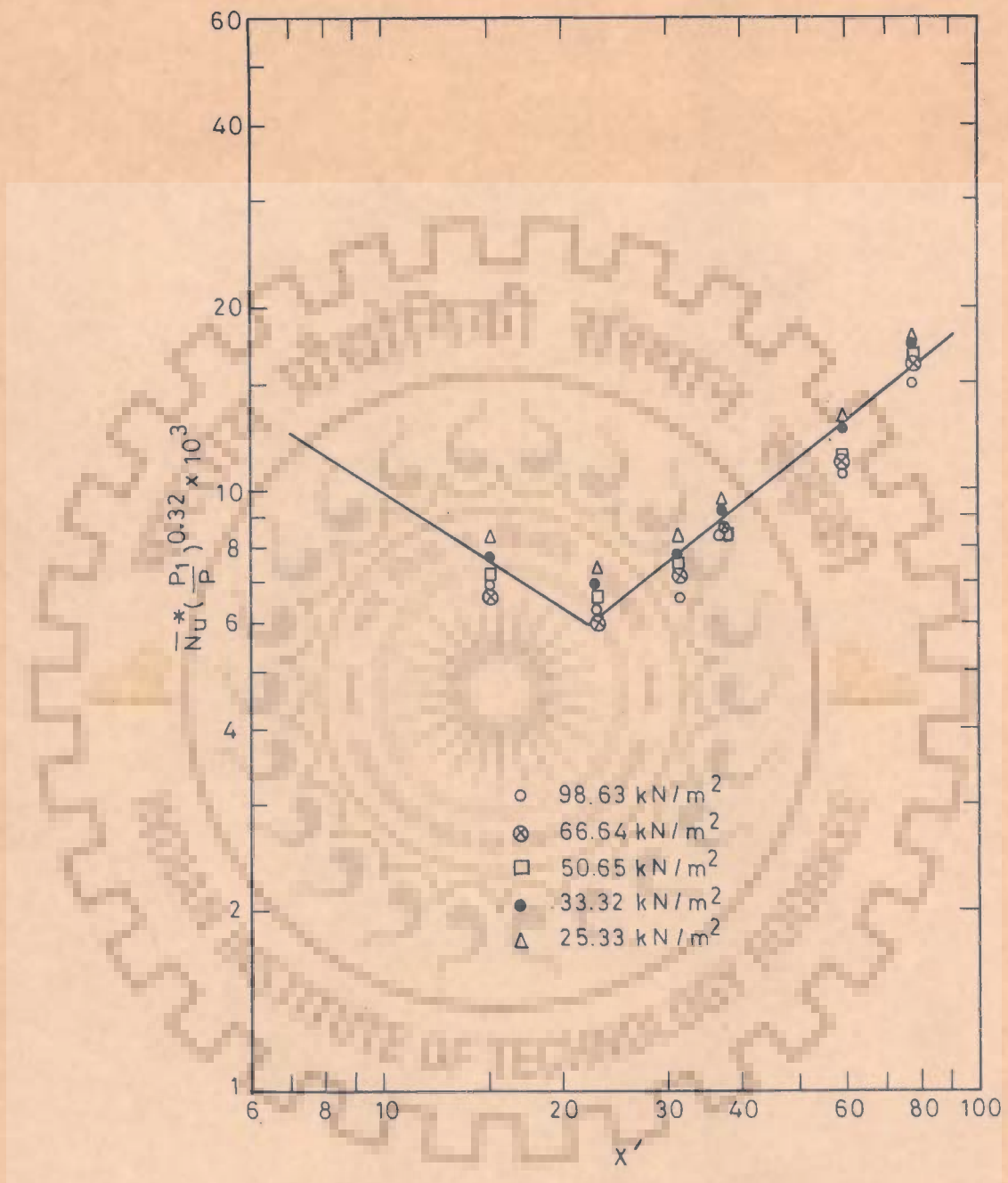


Fig.5.50-Plot of  $\bar{Nu}^* (\frac{P_1}{P})^{0.32}$  vs  $X'$  for isopropanol-water mixtures

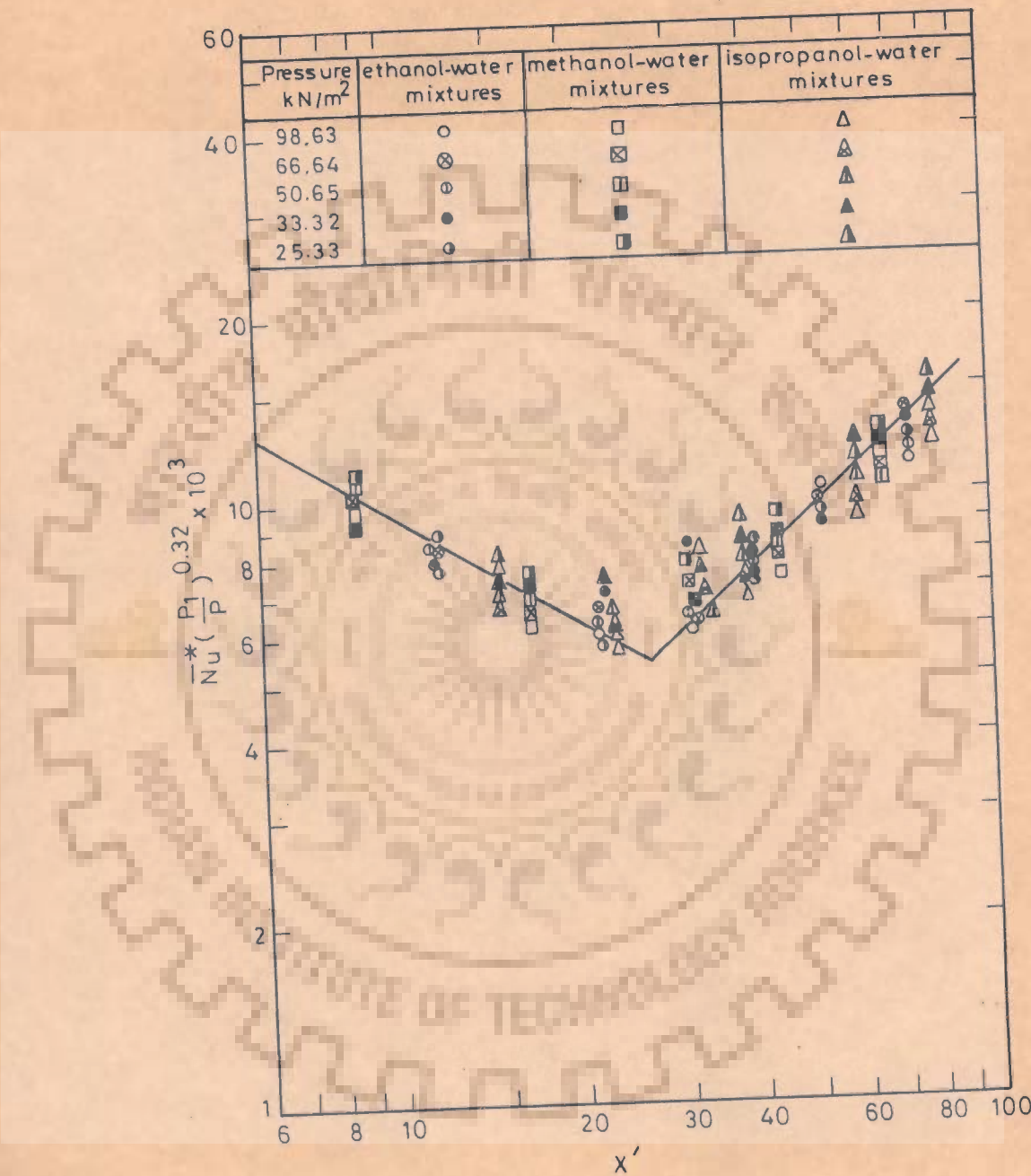


Fig.5.51-Plot of  $\bar{Nu}^* \left( \frac{P_1}{P} \right)^{0.32}$  vs  $X'$  for alcohol-water mixtures

data points are correlated by the following two equations :

(a) For the values of  $X'$  ;  $0 < X' \leq 22.0$

$$\bar{Nu} \left( \frac{P_1}{P} \right)^{0.32} = 3.70 \times 10^{-2} (X')^{-0.60} \quad \dots(5.9)$$

(b) For the values of  $X'$  ;  $30 \leq X' \leq 78.0$

$$\bar{Nu} \left( \frac{P_1}{P} \right)^{0.32} = 2.51 \times 10^{-4} (X')^{0.90} \quad \dots(5.10)$$

In Equations (5.9 and 5.10) the term  $\bar{Nu}^*$  represents

$\bar{h}^*/k \sqrt{\frac{\sigma}{(\rho_l - \rho_v)g}}$ ,  $P_1$  stands for one atmospheric pressure and  $P$  for subatmospheric pressures. The remaining terms have their usual meaning as given in Nomenclature. It may be noted that the physical properties of the boiling liquids are to be calculated at their saturation temperatures corresponding to the pressures at which the boiling takes place.

The above correlations, given by Equations (5.9 and 5.10), are capable to predict the values of boiling heat transfer coefficient for atmospheric as well as subatmospheric pressures for any binary liquid concentration of the systems investigated for a given heating surface.

## CHAPTER - 6

### CONCLUSIONS AND RECOMMENDATIONS

The main conclusions drawn from the present study are as follows :

1. New experimental data have been generated for both atmospheric and subatmospheric pressures for the nucleate pool boiling of distilled water, ethanol, methanol and isopropanol and their aqueous binary liquid mixtures for the heat flux ranging from  $9618 \text{ W/m}^2$  to  $31354 \text{ W/m}^2$  and pressure from  $25.33 \text{ kN/m}^2$  to  $98.63 \text{ kN/m}^2$ .
2. The experimental data for the pool boiling of saturated liquids; distilled water, ethanol, methanol and isopropanol and their binary mixtures, corroborates the well-established law for the variation of heat transfer coefficient with heat flux, i.e.  $h \propto q^{0.7}$  for the heat flux ranging from  $9618 \text{ W/m}^2$  to  $31354 \text{ W/m}^2$ .

Further, data points establish that the heat transfer coefficient is directly proportional to the pressure raised to the power of 0.32 for the pressure range from  $25.33 \text{ kN/m}^2$  to  $98.63 \text{ kN/m}^2$ .

3. The experimental data of pool boiling of saturated ethanol, methanol and isopropanol, conducted on a given heating surface, when plotted as heat transfer coefficient vs heat flux are represented by a single straight line for both atmospheric and subatmospheric pressures. However, the experimental data for the saturated distilled water differ significantly from those of ethanol, methanol and isopropanol.
4. The experimental data points of this investigation and those of earlier investigations [9,125] for pure liquids, conducted on differing heating surfaces, for both atmospheric and subatmospheric pressures are well-correlated by the following equation within  $\pm 15$  per cent.

$$\left( \bar{h}^*/\bar{h}_1^* \right) = \left( P/P_1 \right)^{0.32}$$

The subscript '1' denotes a reference pressure for which the value of boiling heat transfer coefficient is known for a given heating surface and the liquid. In other words, the above correlation is capable to predict the value of boiling heat transfer coefficient at pressures other than the reference pressure for a given heating surface and the liquid from the knowledge of heat transfer coefficient for the same heating surface and the liquid at the reference pressure.

For the present investigation the reference pressure has been chosen as atmospheric pressure, though it may be any pressure lying between atmospheric and subatmospheric pressures.

However, the above correlation fails to correlate the experimental data for pressures exceeding atmospheric pressure.

An implication of this finding is that the constant,  $C_1$  in Equation (5.3), which is analogous to surface-liquid combination factor,  $C_{sf}$ , in the literature [20,21] does not depend upon the pressure for the data conducted at subatmospheric pressures, whereas it depends upon the pressure for the data obtained at superatmospheric pressures. This is clearly shown from the statistical parameters, namely; Mean, Standard Deviation and Coefficient of Variation, for the constant  $C_1$  for both subatmospheric and superatmospheric pressures.

For subatmospheric pressures the maximum Coefficient of Variation in the values of  $C_1$  for the data of present investigation is 4.55 per cent, that for the data of Cryder and Finalborgo [9] is 7.57 per cent and for Raben et al [125] is 9.66 %. In fact, these variations are negligible, and are acceptable keeping in view the errors involved in conducting the heat transfer data especially for boiling heat transfer.

For superatmospheric pressures the Coefficient of Variation is as large of 67.09 per cent indicating that the values of  $C_1$  are not independent of pressure.

5. The experimental data for the pool boiling of binary liquid mixtures showed a peculiar behaviour: the addition of any of the alcohols investigated into the distilled water keeps on lowering the boiling heat transfer coefficient till such a concentration of the alcohol added for which the coefficient attains a minimum value. Beyond this concentration the heat transfer coefficient begins to increase. The concentration for which the transfer coefficient is minimum has been termed as 'turnaround - concentration', being 31.10 wt. per cent ethanol, 30.80 wt. per cent methanol, and 22.50 wt. per cent isopropanol for ethanol-water, methanol-water, and isopropanol-water mixtures, respectively ; irrespective of the system pressure.

The concentration for which the heat transfer coefficient is minimum corresponds to a value of  $X$  for which  $(Y-X)$  is maximum.

It is also noted that the value of the actual heat transfer coefficient, for all the alcohol liquid mixtures investigated, is less than the weighted heat transfer coefficient. This phenomena is observed at all the pressures studied. This

observation, thus, provides a caution that taking 'weighted heat transfer coefficient value' in the design of boiling heat transfer equipment like vapourisers, evaporators or reboilers is a gross mistake which may lead to failure of the equipment.

6. Like the data of pure liquids, all the experimental data of the saturated pool boiling of binary liquid mixtures, obtained for both the atmospheric and the subatmospheric pressures, satisfy the following correlation within  $\pm 15$  per cent :

$$\frac{\bar{h}^*}{h_1^*} = \left( \frac{P}{P_1} \right)^{0.32}$$

where subscript '1' denotes the reference pressure as discussed under conclusion 4. It may be noted that the above correlation, like for pure liquids, is capable to predict the value of boiling heat transfer at pressures other than the reference pressure for a given heating surface and binary liquid composition from the knowledge of heat transfer coefficient for the same heating surface and the liquid composition at the reference pressure.

This may also be noted that the constant,  $C_{m1}$ , in Equation (5.7) has a value which is independent of pressure for a given boiling liquid mixture and heating surface as is evident from its values enlisted in Table 5.5 where the maximum value of Coefficient of Variation is



8.87 per cent which is, of course, well within the experimental error for the data of boiling heat transfer.

7. For the binary liquid mixtures, the following generalised correlations are recommended based on the data obtained in the present investigation within  $\pm 15$  per cent :

- (a) For the values of  $X'$  ;  $0 < X' \leq 22.0$

$$\frac{\overline{Nu}^*}{P} \left(\frac{P_1}{P}\right)^{0.32} = 3.70 \times 10^{-2} (X')^{-0.60}$$

- (b) For the values of  $X'$  ;  $30 \leq X' \leq 78.0$

$$\frac{\overline{Nu}^*}{P} \left(\frac{P_1}{P}\right)^{0.32} = 2.51 \times 10^{-4} (X')^{0.90}$$

These correlations can predict the values of boiling heat transfer coefficient of binary liquid mixtures investigated for 1 atmosphere and subatmospheric pressures for a given heating surface.

The present investigation can be extended to cover the following :

1. The experimental data should be conducted for the concentration of ethanol-water and isopropanol-water mixtures representing their azeotropic composition and also in the neighbourhood of these concentrations.

2. Keeping in view the fact that the experimental data of ethanol, methanol and isopropanol are represented by a straight line on  $\bar{h}$  vs  $q$  and  $\bar{h}^*$  vs  $P$  plots, it is necessary to investigate other alcohols also for their thermal behaviour for the pool boiling heat transfer.
3. There is a need to determine the extent of pressure greater than 1 atmosphere for which correlation, given by Equation (5.4) is valid.
4. There is a need to obtain experimental data for the pool boiling of binary liquid mixtures on differing heating surfaces, since the literature does not possess enough of them.

## A P P E N D I X - A

### ANALYSIS OF ERRORS

Errors in evaluation of the average heat transfer coefficient are caused due to the inaccuracies in measuring the current, voltage, dimensions of the heating surface and the e.m.f. of thermocouples. To determine the accuracy of the experimental data, error analysis was carried out for several experimental runs. This Appendix presents a typical sample calculation of error analysis for Run No. 14 of Appendix-B.

The experimental error for the average heat transfer coefficient can be defined mathematically [141] as follows :

$$e_{\bar{h}} = \left[ \sum_{i=1}^n \left( \frac{\partial \bar{h}}{\partial z_i} \cdot e_{z_i} \right)^2 \right]^{0.5} \quad \dots(A.1)$$

where  $e$  represents the error and  $z_i$  any of the  $n$  parameters affecting average heat transfer coefficient. In the present investigation, the average value of heat transfer coefficient has been defined as

$$\bar{h} = \frac{Q}{A(\bar{T}_w - \bar{T}_f)} \quad \dots(A.2)$$

where

$Q$  Power input, W

$A$  Area

$\bar{T}_w$  Average wall temperature

$\bar{T}_f$  Average liquid temperature

$$\text{Further, } Q = VI \quad \dots(A.3)$$

$$A = \pi d_o \ell \quad \dots(A.4)$$

From Equations (A.1) and (A.2) the error in average heat transfer coefficient becomes :

$$e_{\bar{h}} = \left[ \left( \frac{e_Q}{A(\bar{T}_w - \bar{T}_\ell)} \right)^2 + \left( - \frac{Q e_A}{A^2(\bar{T}_w - \bar{T}_\ell)} \right)^2 + \left( - \frac{Q e_{\bar{T}_w}}{A(\bar{T}_w - \bar{T}_\ell)^2} \right)^2 + \left( \frac{Q e_{\bar{T}_\ell}}{A(\bar{T}_w - \bar{T}_\ell)^2} \right)^2 \right]^{0.5} \quad \dots(A.5)$$

The above Equation requires evaluation of  $e_Q$ ,  $e_A$ ,  $e_{\bar{T}_w}$  and  $e_{\bar{T}_\ell}$  which will be discussed in the following Sections :

#### A.1 ERROR IN POWER INPUT, $e_Q$

$$\text{Since } Q = V I$$

$$\text{Therefore, } e_Q = [(V.e_I)^2 + (I.e_V)^2]^{0.5} \quad \dots(A.6)$$

where  $e_I$  and  $e_V$  are the errors in the measurement of current and voltage supplied to the heater.

Run No. 14 corresponds to 80V and 10A

$$e_V = 1.0 \text{ Volt and } e_I = 0.05 \text{ Ampere}$$

Substituting the above values in Equations (A.3 and A.6)

$$Q = 10 \times 80 = 800 \text{ W}$$

$$e_Q = [(80 \times 0.05)^2 + (10 \times 1.0)^2]^{0.5}$$

$$= (16 + 100)^{0.5} = 10.77 \text{ W}$$

### A.2 ERROR IN HEAT TRANSFER AREA, $e_{\Lambda}$

$$\text{Since } \Lambda = \pi d_o \ell ,$$

$$\text{Hence, } e_{\Lambda} = [(\pi d_o e_{\ell})^2 + (\pi \ell e_{d_o})^2]^{0.5}$$

where  $e_{d_o}$  and  $e_{\ell}$  are the errors associated in the measurement of diameter and length respectively.

Since

$$d_o = 0.07 \text{ m, } e_{d_o} = 0.0001 \text{ m}$$

$$\ell = 0.179 \text{ m, } e_{\ell} = 0.0005 \text{ m}$$

$$\text{Therefore, } \Lambda = \pi \times 0.07 \times 0.179 = 3.93 \times 10^{-2} \text{ m}^2$$

$$e_{\Lambda} = [(\pi \times 0.07 \times 0.0005)^2 + (\pi \times 0.179 \times 0.0001)^2]^{0.5}$$

$$e_{\Lambda} = 1.235 \times 10^{-4} \text{ m}^2$$

### A.3 ERROR IN AVERAGE WALL TEMPERATURE, $e_{\bar{T}_w}$

Average wall temperature of the heat transfer surface has been obtained by using the following Equation:

$$\bar{T}_w = \left( \frac{T_{w1} + T_{w2} + T_{w3}}{3} \right) \quad \dots(\text{A.7})$$

where subscripts 1, 2 and 3 refer to the wall temperature of the top-, the side- and the bottom-position of the heating surface.

The value of local temperatures, as obtained corresponding to the measured thermocouple e.m.f., were corrected by subtracting the temperature drop in the

wall thickness of the heating surface,  $\delta T_w$ .

Thus, corrected wall temperature is given by

$$T_w = T_{w_m} - \delta T_w \quad \dots(A.8)$$

where  $T_{w_m}$  is the measured wall temperature. The value of  $\delta T_w$  was calculated as follows :

$$\delta T_w = \frac{q d_o}{2 k_w} \ln \frac{d_o}{d_h} \quad \dots(A.9)$$

The error associated with temperature drop is calculated as follows :

$$e_{\delta T_w} = \left[ \left( e_q \frac{d_o}{2k_w} \ln \frac{d_o}{d_h} \right)^2 + \left\{ \left( \frac{q}{2k_w} \ln \frac{d_o}{d_h} + \frac{q}{2k_w} \right) e_{d_o} \right\}^2 + \left\{ - \frac{q d_o}{2k_w^2} \ln \left( \frac{d_o}{d_h} \right) e_{k_w} \right\}^2 + \left\{ - \frac{q d_o}{2k_w} \frac{1}{d_h} e_{d_h} \right\}^2 \right]^{0.5} \quad \dots(A.10)$$

where  $e_q$ ,  $e_{d_h}$  and  $e_{k_w}$  are the errors associated with heat flux, thermocouple circle diameter and the thermal conductivity respectively.

$$\text{Since, } q = \frac{Q}{A} = \frac{Q}{\pi d_o \ell} = \frac{800}{3.93 \times 10^{-2}} = 20356.20 \text{ W/m}^2$$

$$\begin{aligned} \therefore e_q &= \left[ \left( \frac{e_Q}{\pi d_o \ell} \right)^2 + \left( - \frac{Q}{\pi \ell d_o^2} e_{d_o} \right)^2 + \left( - \frac{Q}{\pi d_o \ell^2} e_{\ell} \right)^2 \right]^{0.5} \\ &+ \left[ \left( \frac{10.77}{3.93 \times 10^{-2}} \right)^2 + \left( - \frac{800 \times 0.0001}{3.93 \times 10^{-2} \times 0.07} \right)^2 \right. \\ &\left. + \left( - \frac{800 \times 0.0005}{3.93 \times 10^{-2} \times 0.179} \right)^2 \right]^{0.5} = 281.389 \text{ W/m}^2 \end{aligned}$$

Thermal conductivity,  $k_w = 25.76 \text{ W/m K}$ ,  $e_{k_w} = 0$ .

$$\text{Since, } d_h = \frac{d_i + d_o}{2} = \frac{0.062 + 0.07}{2} = 0.066 \text{ m}$$

$$\text{Therefore, } e_{d_h} = \left[ \left( \frac{1}{2} e_{d_o} \right)^2 + \left( \frac{1}{2} e_{d_i} \right)^2 \right]^{0.5}$$

$$\text{Since } e_{d_i} = e_{d_o}$$

$$\therefore e_{d_h} = \left[ 2 \left( \frac{1}{2} e_{d_o} \right)^2 \right]^{0.5}$$

$$= \left[ 2 \left( \frac{1}{2} \times 0.0001 \right)^2 \right]^{0.5}$$

$$\therefore e_{d_h} = 7.071 \times 10^{-5} \text{ m}$$

On substituting the values of  $e_q$ ,  $e_{d_h}$  and  $e_{k_w}$  in Equation (A.10), the value of  $e_{\delta T_w}$  is calculated as follows :

$$\begin{aligned} e_{\delta T_w} = & \left[ \left\{ \frac{281.389 \times 0.07}{2 \times 25.76} \ln \left( \frac{0.07}{0.066} \right) \right\}^2 \right. \\ & + \left\{ \left( \frac{20356.20}{2 \times 25.76} \ln \left( \frac{0.07}{0.066} \right) + \frac{20356.20}{2 \times 25.76} \right) 0.0001 \right\}^2 \\ & + \left\{ - \frac{20356.20 \times 0.07}{2 \times (25.76)^2} \ln \left( \frac{0.07}{0.066} \right) \times 0 \right\}^2 \\ & \left. + \left\{ - \frac{20356.20 \times 0.07}{2 \times 25.76 \times 0.066} \times 7.071 \times 10^{-5} \right\}^2 \right]^{0.5} \end{aligned}$$

$$\therefore e_{\delta T_w} = 0.0558^\circ\text{C}$$

From Equation (A.8),  $e_{T_w}$  is calculated as :

$$e_{T_w} = \left[ \left( e_{T_{w_m}} \right)^2 + \left( - e_{\delta T_w} \right)^2 \right]^{0.5}$$

$$\text{Since } e_{T_{w_m}} = 0.01^\circ\text{C}$$

$$\begin{aligned}\text{Therefore, } e_{T_w} &= [(0.01)^2 + (-0.0558)^2]^{0.5} \\ &= 0.0567^\circ\text{C}\end{aligned}$$

By using Equation (A.7), the value of  $e_{\bar{T}_w}$  is calculated as given below :

$$\begin{aligned}e_{\bar{T}_w} &= \left[ 3 \times \left( \frac{e_{T_w}}{3} \right)^2 \right]^{0.5} \\ &= \left[ 3 \times \left( \frac{0.0567}{3} \right)^2 \right]^{0.5} \\ &= 0.0327^\circ\text{C}\end{aligned}$$

#### A.4 ERROR IN AVERAGE LIQUID TEMPERATURE

Average liquid temperature has been defined as follows :

$$\bar{T}_\ell = \frac{T_{\ell_1} + T_{\ell_2} + T_{\ell_3}}{3}$$

$$\text{Therefore, } e_{\bar{T}_\ell} = \left[ 3 \left( \frac{e_{T_\ell}}{3} \right)^2 \right]^{0.5} \quad \dots(\text{A.11})$$

$$\text{Since } e_{T_\ell} = e_{T_{w_m}} = 0.01^\circ\text{C}$$

Thus, substituting the value of  $e_{T_\ell}$  in Equation (A.11):

$$e_{\bar{T}_\ell} = \left[ 3 \left( \frac{0.01}{3} \right)^2 \right]^{0.5} = 0.0058^\circ\text{C}$$



### A.5 ERROR IN AVERAGE HEAT TRANSFER COEFFICIENT, $e_{\bar{h}}$

Equation (A.5) is used to compute  $e_{\bar{h}}$ . On substituting the values of  $Q$ ,  $A$ ,  $\bar{T}_w$ ,  $\bar{T}_f$ ,  $e_Q$ ,  $e_A$ ,  $e_{\bar{T}_w}$  and  $e_{\bar{T}_f}$  in Equation (A.5), the value of  $e_{\bar{h}}$  is calculated as follows:

$$\begin{aligned}
 e_{\bar{h}} &= \left[ \left\{ \frac{10.77}{3.93 \times 10^{-2} (90.306 - 84.117)} \right\}^2 \right. \\
 &+ \left\{ \frac{800 \times 1.235 \times 10^{-4}}{(3.93 \times 10^{-2})^2 (90.306 - 84.117)} \right\}^2 \\
 &+ \left\{ \frac{-800 \times 0.0327}{3.93 \times 10^{-2} (90.306 - 84.117)^2} \right\}^2 \\
 &+ \left. \left\{ \frac{800 \times 0.0058}{3.93 \times 10^{-2} (90.306 - 84.117)^2} \right\}^2 \right]^{0.5} \\
 &= 48.77 \text{ W/m}^2 \text{ K}
 \end{aligned}$$

Since the average experimental value of the heat transfer coefficient is  $3289 \text{ W/m}^2 \text{ K}$ , the actual value of the average heat transfer coefficient as obtained by this error analysis is  $3289 \pm 48.77 \text{ W/m}^2 \text{ K}$ . Thus the expected error in the reported data of heat transfer coefficient is within  $\pm 15$  per cent.

A P P E N D I X - B

TABULATION OF EXPERIMENTAL DATA

	Page
Table B-1 Experimental Data of Heat Transfer to Saturated Pool Boiling of Distilled Water	203
Table B-2 Experimental Data of Heat Transfer to Saturated Pool Boiling of Ethanol	208
Table B-3 Experimental Data of Heat Transfer to Saturated Pool Boiling of 11.86 wt. % Ethanol in Ethanol-Water Mixture	213
Table B-4 Experimental Data of Heat Transfer to Saturated Pool Boiling of 22.12 wt. % Ethanol in Ethanol-Water Mixture	218
Table B-5 Experimental Data of Heat Transfer to Saturated Pool Boiling of 31.1 wt. % Ethanol in Ethanol-Water Mixture	223
Table B-6 Experimental Data of Heat Transfer to Saturated Pool Boiling of 39.0 wt. % Ethanol in Ethanol-Water Mixture	228
Table B-7 Experimental Data of Heat Transfer to Saturated Pool Boiling of 52.3 wt. % Ethanol in Ethanol-Water Mixture	233
Table B-8 Experimental Data of Heat Transfer to Saturated Pool Boiling of 71.88 wt. % Ethanol in Ethanol-Water Mixture	238
Table B-9 Experimental Data of Heat Transfer to Saturated Pool Boiling of Methanol	243
Table B-10 Experimental Data of Heat Transfer to Saturated Pool Boiling of 8.56 wt. % Methanol in Methanol-Water Mixture	248

		Page
Table B-11	Experimental Data of Heat Transfer to Saturated Pool Boiling of 16.5 wt. % Methanol in Methanol-Water Mixture	253
Table B-12	Experimental Data of Heat Transfer to Saturated Pool Boiling of 30.8 wt. % Methanol in Methanol - Water Mixture	258
Table B-13	Experimental Data of Heat Transfer to Saturated Pool Boiling of 43.24wt. % Methanol in Methanol - Water Mixture	263
Table B-14	Experimental Data of Heat Transfer to Saturated Pool Boiling of 64.0 wt. % Methanol in Methanol-Water Mixture	268
Table B-15	Experimental Data of Heat Transfer to Saturated Pool Boiling of Isopropanol	273
Table B-16	Experimental Data of Heat Transfer to Saturated Pool Boiling of 15.0 wt. % Isopropanol in Isopropanol - Water Mixture	278
Table B-17	Experimental Data of Heat Transfer to Saturated Pool Boiling of 22.5 wt. % Isopropanol in Isopropanol - Water Mixture	283
Table B-18	Experimental Data of Heat Transfer to Saturated Pool Boiling of 31.25 wt. % Isopropanol in Isopropanol - Water Mixture	287
Table B-19	Experimental Data of Heat Transfer to Saturated Pool Boiling of 37.0 wt. % Isopropanol in Isopropanol - Water Mixture	292
Table B-20	Experimental Data of Heat Transfer to Saturated Pool Boiling of 59.0 wt. % Isopropanol in Isopropanol - Water Mixture	297
Table B-21	Experimental Data of Heat Transfer to Saturated Pool Boiling of 77.0 wt. % Isopropanol in Isopropanol - Water Mixture	302

Table B-1 : Experimental Data of Heat Transfer to Saturated Pool  
Boiling of Distilled Water at  $98.63 \text{ kN/m}^2$  ( $T_s=99.0^\circ\text{C}$ )

Run No.	Heat Flux $\text{W/m}^2$	Conduction Correction $^\circ\text{C}$	Recorded Wall Temp. $^\circ\text{C}$	Corrected Wall Temp. $^\circ\text{C}$	Liquid Temp. $^\circ\text{C}$	Wall Superheat $^\circ\text{C}$	Heat Transfer Coefficient $\text{W/m}^2\text{K}$
1	9618.32	0.769	105.00	104.231	100.25	3.981	2416
			103.95	103.182	99.90	3.282	2931
			106.30	105.531	100.40	5.131	1875
						AVG = 4.131	AVG = 2329
2	12620.90	1.009	106.05	105.041	100.90	4.141	3048
			105.50	104.491	100.45	4.041	3123
			107.25	106.241	100.92	5.321	2372
						AVG = 4.501	AVG = 2804
3	16488.55	1.320	106.90	105.580	101.20	4.380	3765
			106.20	104.880	100.60	4.280	3852
			107.95	106.630	101.00	5.630	2929
						AVG = 4.763	AVG = 3462
4	20356.23	1.627	107.65	106.023	101.45	4.573	4451
			107.20	105.573	100.85	4.723	4310
			108.65	107.023	101.15	5.873	3466
						AVG = 5.056	AVG = 4026
5	24631.04	1.969	108.90	106.931	101.85	5.081	4848
			108.35	106.381	101.00	5.381	4577
			109.25	107.281	101.35	5.931	4153
						AVG = 5.464	AVG = 4508

Table B-1 : Experimental Data of Heat Transfer to Saturated Pool  
Boiling of Distilled Water at  $66.64 \text{ kN/m}^2 (T_s=88.5^\circ\text{C})$

Run No.	Heat Flux $\text{W/m}^2$	Conduction Correction $^\circ\text{C}$	Recorded Wall Temp. $^\circ\text{C}$	Corrected Wall Temp. $^\circ\text{C}$	Liquid Temp. $^\circ\text{C}$	Wall Superheat $^\circ\text{C}$	Heat Transfer Coefficient $\text{W/m}^2\text{K}$
6	9618.32	0.769	95.35	94.581	90.40	4.181	2301
			94.85	94.081	89.50	4.581	2100
			96.00	95.231	90.15	5.081	1893
					AVG = 4.614	AVG = 2085	
7	12620.90	1.009	96.30	95.291	90.65	4.641	2720
			96.05	95.041	89.65	5.391	2341
			97.15	96.141	90.60	5.541	2278
					AVG = 5.191	AVG = 2431	
8	16488.55	1.320	97.75	96.430	91.25	5.180	3183
			97.15	95.830	90.40	5.430	3037
			98.30	96.980	91.10	5.880	2804
					AVG = 5.497	AVG = 3000	
9	20356.20	1.627	98.30	96.673	91.40	5.273	3861
			97.75	96.123	90.65	5.473	3719
			99.00	97.373	91.30	6.073	3352
					AVG = 5.606	AVG = 3631	
10	24631.00	1.969	99.15	97.181	91.75	5.431	4535
			99.10	97.131	90.90	6.231	3953
			99.80	97.831	91.10	6.731	3659
					AVG = 6.131	AVG = 4018	

Table B-1 : Experimental Data of Heat Transfer to Saturated Pool  
Boiling of Distilled Water at  $50.65 \text{ kN/m}^2 (T_s=81.5^\circ\text{C})$

Run No.	Heat Flux $\text{W/m}^2$	Conduction Correction $^\circ\text{C}$	Recorded Wall Temp. $^\circ\text{C}$	Corrected Wall Temp. $^\circ\text{C}$	Liquid Temp. $^\circ\text{C}$	Wall Superheat $^\circ\text{C}$	Heat Transfer Coefficient $\text{W/m}^2\text{K}$
11	9618.32	0.769	87.55	86.781	82.45	4.331	2221
			87.50	86.731	81.60	5.131	1875
			88.40	87.631	81.60	6.031	1595
						AVG = 5.164	AVG = 1863
12	12620.90	1.009	88.90	87.891	82.90	4.991	2529
			88.45	87.450	82.00	5.450	2316
			90.00	88.991	82.45	6.541	1930
						AVG = 5.660	AVG = 2230
13	16259.50	1.299	90.20	88.901	83.55	5.351	3039
			90.20	88.901	83.00	5.901	2755
			91.00	89.701	83.35	6.351	2560
						AVG = 5.870	AVG = 2770
14	20356.20	1.627	91.55	89.923	84.25	5.673	3588
			91.95	90.323	84.00	6.323	3219
			92.30	90.673	84.10	6.573	3097
						AVG = 6.190	AVG = 3289
15	24631.00	1.969	92.85	90.881	94.45	6.431	3830
			93.30	91.331	84.00	7.331	3360
			93.70	91.731	84.00	7.731	3186
						AVG = 7.164	AVG = 3438

Table B-1 : Experimental Data of Heat Transfer to Saturated Pool  
Boiling of Distilled Water at  $33.32 \text{ kN/m}^2$  ( $T_s=71.33^\circ\text{C}$ )

Run No.	Heat Flux $\text{W/m}^2$	Conduction Correction $^\circ\text{C}$	Recorded Wall Temp. $^\circ\text{C}$	Corrected Wall Temp. $^\circ\text{C}$	Liquid Temp. $^\circ\text{C}$	Wall Superheat $^\circ\text{C}$	Heat Transfer Coefficient $\text{W/m}^2\text{K}$
16	9618.32	0.769	78.60	77.831	72.40	5.431	1771
			78.15	77.381	71.70	5.681	1693
			79.20	78.431	71.90	6.531	1473
					AVG = 5.881	AVG = 1636	
17	12620.90	1.009	79.35	78.341	72.65	5.691	2218
			79.55	78.541	72.35	6.191	2039
			80.50	79.491	72.50	6.991	1805
					AVG = 6.291	AVG = 2006	
18	16259.50	1.300	80.45	79.150	73.15	6.000	2710
			80.70	79.400	72.90	6.500	2501
			81.70	80.400	73.10	7.300	2227
					AVG = 6.593	AVG = 2466	
19	20356.20	1.627	82.00	80.373	73.95	6.423	3169
			82.50	80.873	73.40	7.473	2724
			83.10	81.473	73.90	7.573	2688
					AVG = 7.156	AVG = 2845	
20	24631.04	1.969	83.80	81.831	74.65	7.181	3430
			83.80	81.831	74.40	7.431	3315
			85.00	83.030	74.65	8.381	2939
					AVG = 7.664	AVG = 3214	

Table B-1 : Experimental Data of Heat Transfer to Saturated Pool Boiling of Distilled Water at  $25.33 \text{ kN/m}^2 (T_g = 65.3^\circ\text{C})$

Run No.	Heat Flux $\text{W/m}^2$	Conduction Correction $^\circ\text{C}$	Recorded Wall Temp. $^\circ\text{C}$	Corrected Wall Temp. $^\circ\text{C}$	Liquid Temp. $^\circ\text{C}$	Wall Superheat $^\circ\text{C}$	Heat Transfer Coefficient $\text{W/m}^2\text{K}$
21	9618.32	0.769	75.12	74.351	68.45	5.901	1630
			74.60	73.831	68.00	5.831	1650
			75.80	75.031	68.15	6.881	1398
					AVG = 6.204	AVG = 1550	
22	12620.90	1.009	75.37	74.361	68.50	5.861	2153
			75.20	74.191	68.15	6.041	2089
			77.25	76.241	68.45	7.791	1620
					AVG = 6.564	AVG = 1923	
23	16259.50	1.299	77.60	76.301	68.97	7.331	2218
			77.50	76.201	68.59	7.611	2136
			78.55	77.250	68.97	8.281	1963
					AVG = 7.741	AVG = 2100	
24	20356.20	1.627	79.35	77.723	70.35	7.373	2761
			79.35	77.723	70.00	7.723	2636
			80.25	78.623	70.05	8.573	2374
					AVG = 7.890	AVG = 2580	
25	24910.94	1.991	80.45	78.459	70.65	7.809	3190
			80.45	78.459	70.25	8.209	3035
			81.70	79.709	70.55	9.159	2720
					AVG = 8.392	AVG = 2968	



Table B-2 : Experimental Data of Heat Transfer to Saturated Pool  
Boiling of Ethanol at  $98.63 \text{ kN/m}^2$  ( $T_s = 78.0^\circ\text{C}$ )

Run No.	Heat Flux $\text{W/m}^2$	Conduction Correction $^\circ\text{C}$	Recorded Wall Temp. $^\circ\text{C}$	Corrected Wall Temp. $^\circ\text{C}$	Liquid Temp. $^\circ\text{C}$	Wall Superheat $^\circ\text{C}$	Heat Transfer Coefficient $\text{W/m}^2\text{K}$
26	9974.56	0.798	85.98	85.182	78.45	6.732	1482
			87.80	87.000	78.25	8.750	1140
			85.98	85.182	78.45	6.732	1482
					AVG = 7.405	AVG = 1347	
27	12865.14	1.029	87.55	86.521	78.85	7.671	1677
			89.25	88.221	78.70	9.521	1351
			86.70	85.671	78.85	6.821	1886
					AVG = 8.004	AVG = 1607	
28	16946.56	1.355	89.60	88.245	79.53	8.715	1944
			91.15	89.795	79.35	10.445	1622
			88.00	86.645	79.55	7.095	2388
					AVG = 8.752	AVG = 1936	
29	20610.70	1.648	91.75	90.102	80.60	9.502	2169
			93.30	91.652	80.50	11.152	1848
			89.62	87.972	80.55	7.422	2777
					AVG = 9.359	AVG = 2202	
30	25190.84	2.014	93.25	91.236	81.70	9.536	2642
			96.15	94.136	81.70	12.436	2026
			91.85	89.836	81.85	7.986	3154
					AVG = 9.986	AVG = 2523	

Table B-2 : Experimental Data of Heat Transfer to Saturated Pool  
 Boiling of Ethanol at  $61.31 \text{ kN/m}^2 (T_s=65.3^\circ\text{C})$

Run No.	Heat Flux $\text{W/m}^2$	Conduction correction $^\circ\text{C}$	Recorded Wall Temp. $^\circ\text{C}$	Corrected Wall Temp. $^\circ\text{C}$	Liquid Temp. $^\circ\text{C}$	Wall Superheat $^\circ\text{C}$	Heat Transfer Coefficient $\text{W/m}^2\text{K}$
31	10117.05	0.809	75.50	74.691	67.20	7.491	1351
			77.35	76.541	66.90	9.641	1049
			75.90	75.091	67.20	7.891	1282
					AVG = 8.341	AVG = 1213	
32	13027.99	1.042	76.68	75.638	67.05	8.588	1517
			77.65	76.608	66.70	9.908	1315
			76.80	75.758	67.00	8.758	1438
					AVG = 9.085	AVG = 1488	
33	16946.56	1.355	78.15	76.795	67.20	9.595	1766
			79.55	78.195	67.00	11.195	1514
			77.25	75.895	67.05	8.845	1916
					AVG = 9.878	AVG = 1716	
34	20814.25	1.664	80.00	78.336	67.52	10.816	1924
			81.65	79.986	67.35	12.636	1647
			78.50	76.836	67.50	9.336	2229
					AVG = 10.929	AVG = 1905	
35	25470.74	2.036	82.25	80.214	69.35	10.864	2344
			84.35	82.314	69.20	13.114	1942
			80.80	78.764	69.35	9.414	2706
					AVG = 11.131	AVG = 2288	

Table B-2 : Experimental Data of Heat Transfer to Saturated Pool  
 Boiling of Ethanol at  $47.98 \text{ kN/m}^2$  ( $T_s = 60.25^\circ\text{C}$ )

Run No.	Heat Flux $\text{W/m}^2$	Conduction Correction $^\circ\text{C}$	Recorded Wall Temp. $^\circ\text{C}$	Corrected Wall Temp. $^\circ\text{C}$	Liquid Temp. $^\circ\text{C}$	Wall Superheat $^\circ\text{C}$	Heat Transfer Coefficient $\text{W/m}^2\text{K}$
36	9974.55	0.797	70.50	69.703	61.88	7.823	1275
			74.30	73.503	61.55	11.953	834
			73.13	72.333	61.70	10.633	938
						AVG = 10.136	AVG = 984
37	12946.56	1.035	72.40	71.365	61.80	9.565	1354
			74.40	73.365	61.55	11.815	1096
			73.50	72.465	61.55	10.915	1186
						AVG = 10.765	AVG = 1203
38	17984.73	1.438	74.45	73.012	62.03	10.982	1638
			76.25	74.812	61.80	13.012	1382
			74.45	73.012	61.80	11.212	1604
						AVG = 11.735	AVG = 1533
39	21671.76	1.733	76.85	75.117	62.73	12.387	1750
			78.70	76.967	62.60	14.367	1508
			75.68	73.947	62.73	11.217	1932
						AVG = 12.657	AVG = 1712
40	26740.46	2.138	79.55	77.412	63.95	13.462	1986
			81.25	79.112	63.50	15.612	1713
			77.48	75.342	63.50	11.842	2258
						AVG = 13.640	AVG = 1960

Table B-2 : Experimental Data of Heat Transfer to Saturated Pool  
Boiling of Ethanol at  $33.32 \text{ kN/m}^2 (T_s=52.2^\circ\text{C})$

Run No.	Heat Flux $\text{W/m}^2$	Conduction Correction $^\circ\text{C}$	Recorded Wall Temp. $^\circ\text{C}$	Corrected Wall Temp. $^\circ\text{C}$	Liquid Temp. $^\circ\text{C}$	Wall Superheat $^\circ\text{C}$	Heat Transfer Coefficient $\text{W/m}^2\text{K}$
41	9974.55	0.797	64.53	63.733	54.80	8.933	1117
			68.70	67.903	54.58	13.323	749
			66.85	66.053	54.80	11.253	886
					AVG = 11.170	AVG = 893	
42	13027.99	1.042	66.10	65.058	54.83	10.228	1274
			70.48	69.438	54.45	14.988	869
			68.85	67.808	54.70	13.108	994
					AVG = 12.775	AVG = 1020	
43	16717.56	1.336	68.32	66.984	54.95	12.034	1389
			70.95	69.614	54.80	14.814	1128
			69.65	68.314	54.90	13.414	1246
					AVG = 13.420	AVG = 1246	
44	20404.60	1.631	68.90	67.269	55.15	12.119	1684
			71.70	70.069	55.15	14.919	1368
			70.10	68.469	54.95	13.519	1509
					AVG = 13.519	AVG = 1509	
45	25190.84	2.014	70.23	68.216	55.65	12.566	2005
			73.30	71.286	55.45	15.836	1591
			71.75	69.736	55.60	14.136	1782
					AVG = 14.180	AVG = 1777	

Table B-2 : Experimental Data of Heat Transfer to Saturated Pool  
Boiling of Ethanol at 25.33 kN/m<sup>2</sup> (T<sub>s</sub>=46.13°C)

Run No.	Heat Flux W/m <sup>2</sup>	Conduction Correction °C	Recorded Wall Temp. °C	Corrected Wall Temp. °C	Liquid Temp. °C	Wall Superheat °C	Heat Transfer Coefficient W/m <sup>2</sup> K
46	9974.55	0.797	53.53	52.733	43.70	9.033	1104
			58.23	57.433	43.60	13.833	721
			58.23	57.433	43.83	13.603	733
					AVG = 12.156	AVG = 821	
47	12946.56	1.035	53.75	54.715	45.15	9.565	1353
			60.40	59.365	44.85	14.515	892
			61.10	60.065	45.10	14.965	865
					AVG = 13.015	AVG = 995	
48	16717.60	1.340	58.68	57.340	46.90	10.440	1601
			63.25	61.910	46.90	15.010	1114
			63.15	61.810	46.80	15.010	1114
					AVG = 13.490	AVG = 1239	
49	20610.70	1.648	60.73	59.082	47.50	11.582	1780
			64.05	62.402	47.15	15.252	1351
			64.30	62.562	47.15	15.502	1330
					AVG = 14.112	AVG = 1461	

Table B-3 : Experimental Data of Heat Transfer to Saturated Pool Boiling of 11.86 wt.% Ethanol in Ethanol - Water Mixture at  $98.63 \text{ kN/m}^2 (T_s=89.75^\circ\text{C})$

Run No.	Heat Flux $\text{W/m}^2$	Conduction Correction $^\circ\text{C}$	Recorded Wall Temp. $^\circ\text{C}$	Corrected Wall Temp. $^\circ\text{C}$	Liquid Temp. $^\circ\text{C}$	Wall Superheat $^\circ\text{C}$	Heat Transfer Coefficient $\text{W/m}^2\text{K}$
50	9974.55	0.797	95.58	94.783	90.20	4.583	2176
			97.65	96.853	89.65	7.203	1385
			98.65	97.853	90.05	7.803	1278
					AVG = 6.530	AVG = 1528	
51	13027.99	1.042	97.15	96.108	91.15	4.958	2628
			99.20	98.158	90.80	7.358	1771
			100.58	99.538	91.20	8.338	1562
					AVG = 6.885	AVG = 1892	
52	16531.80	1.322	99.80	98.478	92.85	5.628	2937
			101.20	99.878	92.20	7.678	2153
			103.60	102.280	92.85	9.430	1753
					AVG = 7.580	AVG = 2181	
53	20865.14	1.670	102.00	100.33	93.25	7.080	2947
			102.85	101.18	92.90	8.280	2520
			104.80	103.13	93.55	9.580	2178
					AVG = 8.313	AVG = 2510	
54	25190.84	2.014	103.60	101.586	94.15	7.436	3388
			104.65	102.636	93.80	8.836	2851
			106.50	104.486	94.10	10.386	2425
					AVG = 8.886	AVG = 2835	

Table B-3 : Experimental Data of Heat Transfer to Saturated Pool Boiling of 11.86 wt.% Ethanol in Ethanol - Water Mixture at  $61.31 \text{ kN/m}^2 (T_s = 77.5^\circ\text{C})$

Run No.	Heat Flux $\text{W/m}^2$	Conduction Correction $^\circ\text{C}$	Recorded Wall Temp. $^\circ\text{C}$	Corrected Wall Temp. $^\circ\text{C}$	Liquid Temp. $^\circ\text{C}$	Wall Superheat $^\circ\text{C}$	Heat Transfer Coefficient $\text{W/m}^2\text{K}$
55	10297.71	0.823	86.00	85.177	79.56	5.617	1833
			90.43	89.607	79.35	10.260	1004
			88.50	87.677	79.80	7.877	1307
					AVG = 7.918	AVG = 1301	
56	13435.10	1.074	86.70	85.626	79.80	5.826	2306
			91.20	90.126	79.52	10.606	1267
			89.80	88.726	79.90	8.826	1522
					AVG = 8.420	AVG = 1596	
57	16946.60	1.355	87.35	85.995	80.00	5.995	2827
			92.85	91.495	79.75	11.745	1443
			92.50	91.145	80.10	11.045	1534
					AVG = 9.595	AVG = 1766	
58	20865.14	1.670	88.90	87.230	81.18	6.050	3449
			94.52	92.850	80.83	12.020	1376
			94.52	92.850	81.15	11.700	1783
					AVG = 9.923	AVG = 2103	
59	25076.34	2.000	90.75	88.750	82.70	6.050	4145
			96.65	94.650	82.35	12.300	2039
			97.10	95.100	82.55	12.550	1998
					AVG = 10.300	AVG = 2435	

Table B-3 : Experimental Data of Heat Transfer to Saturated Pool Boiling of 11.86 wt.% Ethanol in Ethanol - Water Mixture at  $42.65 \text{ kN/m}^2 (T_s = 69.1^\circ\text{C})$

Run No.	Heat Flux $\text{W/m}^2$	Conduction Correction $^\circ\text{C}$	Recorded Wall Temp. $^\circ\text{C}$	Corrected Wall Temp. $^\circ\text{C}$	Liquid Temp. $^\circ\text{C}$	Wall Superheat $^\circ\text{C}$	Heat Transfer Coefficient $\text{W/m}^2\text{K}$
60	9974.55	0.797	79.15	78.353	72.40	5.953	1675
			83.02	82.223	71.78	10.443	955
			81.70	80.903	72.27	8.633	1155
					AVG = 8.343	AVG = 1196	
61	13027.99	1.042	79.55	78.508	72.40	6.108	2133
			83.45	82.408	71.80	10.608	1228
			83.45	82.408	72.35	10.058	1295
					AVG = 8.925	AVG = 1460	
62	16946.56	1.355	80.80	79.445	72.70	6.745	2512
			84.35	82.995	72.20	10.795	1570
			85.60	84.245	72.40	11.845	1431
					AVG = 9.795	AVG = 1730	
63	20865.14	1.670	82.70	81.030	73.25	7.780	2682
			85.65	83.980	72.60	11.380	1833
			87.15	85.480	73.25	12.230	1706
					AVG = 10.463	AVG = 1994	
64	25190.84	2.014	84.45	82.440	73.90	8.540	2950
			87.55	85.550	73.75	11.800	2135
			88.95	86.950	73.95	13.000	1938
					AVG = 11.113	AVG = 2267	



Table B-3 : Experimental Data of Heat Transfer to Saturated Pool Boiling of 11.86 wt.% Ethanol in Ethanol - Water Mixture at  $36.0 \text{ kN/m}^2 (T_s = 65.4^\circ\text{C})$

Run No.	Heat Flux $\text{W/m}^2$	Conduction Correction $^\circ\text{C}$	Recorded Wall Temp. $^\circ\text{C}$	Corrected Wall Temp. $^\circ\text{C}$	Liquid Temp. $^\circ\text{C}$	Wall Superheat $^\circ\text{C}$	Heat Transfer Coefficient $\text{W/m}^2\text{K}$
65	9974.55	0.797	72.50	71.703	64.65	7.053	1414
			74.87	74.073	63.50	10.573	943
			75.20	74.403	64.65	9.753	1023
					AVG = 9.126	AVG = 1093	
66	12946.56	1.035	73.75	72.715	64.75	7.965	1625
			76.00	74.965	64.22	10.745	1205
			76.60	75.565	64.90	10.665	1214
					AVG = 9.792	AVG = 1322	
67	16946.56	1.355	74.90	73.545	65.33	8.215	2063
			78.25	76.895	65.15	11.745	1443
			79.70	78.345	65.50	12.845	1319
					AVG = 10.935	AVG = 1550	
68	21119.60	1.690	77.25	75.560	66.50	9.060	2331
			80.50	78.810	66.20	12.610	1675
			82.10	80.410	66.40	14.010	1507
					AVG = 11.893	AVG = 1775	
69	25470.74	2.036	79.05	77.014	68.00	9.014	2826
			83.25	81.214	67.40	13.814	1844
			84.90	82.864	68.00	14.864	1714
					AVG = 12.564	AVG = 2027	

Table B-3 : Experimental Data of Heat Transfer to Saturated Pool Boiling of 11.86 wt.% Ethanol in Ethanol - Water Mixture at 28.0 kN/m<sup>2</sup> (T<sub>s</sub>=60.8°C)

Run No.	Heat Flux W/m <sup>2</sup>	Conduction Correction °C	Recorded Wall Temp. °C	Corrected Wall Temp. °C	Liquid Temp. °C	Wall Superheat °C	Heat Transfer Coefficient W/m <sup>2</sup> K
70	9974.55	0.797	68.90	68.103	60.95	7.153	1394
			71.35	70.553	59.35	11.203	890
			72.30	71.503	60.75	10.753	928
					AVG = 9.703	AVG = 1028	
71	13027.99	1.042	70.10	69.058	60.98	8.078	1613
			72.95	71.908	60.75	11.158	1168
			74.50	73.458	60.90	12.558	1037
					AVG = 10.598	AVG = 1229	
72	16832.06	1.346	72.85	71.504	62.00	9.504	1771
			75.20	73.854	61.45	12.404	1357
			75.70	74.354	61.45	12.904	1304
					AVG = 11.604	AVG = 1451	
73	20865.14	1.670	76.35	74.680	62.50	12.180	1713
			76.35	74.680	62.25	12.430	1679
			77.93	76.260	62.50	13.760	1516
					AVG = 12.800	AVG = 1630	

Table B-4 : Experimental Data of Heat Transfer to Saturated Pool Boiling of 22.12 wt.% Ethanol in Ethanol - Water Mixture at 98.63 kN/m<sup>2</sup> (T<sub>s</sub>=85.3°C)

Run No.	Heat Flux W/m <sup>2</sup>	Conduction Correction °C	Recorded Wall Temp. °C	Corrected Wall Temp. °C	Liquid Temp. °C	Wall Superheat °C	Heat Transfer Coefficient W/m <sup>2</sup> K
74	10063.61	0.804	94.35	93.546	85.50	8.046	1251
			96.30	95.496	85.15	10.346	973
			98.40	97.596	85.25	12.346	815
					AVG =10.246	AVG = 982	
75	13231.55	1.058	95.90	94.842	85.70	9.142	1447
			97.65	96.592	85.50	11.092	1193
			99.90	98.842	85.70	13.142	1007
					AVG =11.125	AVG =1189	
76	16418.60	1.313	96.85	95.537	86.00	9.537	1722
			98.70	97.387	85.80	11.587	1417
			100.75	99.437	85.85	13.587	1208
					AVG =11.570	AVG =1419	
77	20865.14	1.670	98.20	96.530	86.25	10.280	2030
			100.25	98.580	86.00	12.580	1659
			102.85	101.180	86.25	14.930	1398
					AVG =12.600	AVG =1656	
78	26503.82	2.120	100.15	98.030	86.55	11.480	2309
			102.30	100.180	86.45	13.730	1930
			105.55	103.430	86.50	16.930	1566
					AVG =14.050	AVG =1886	

Table B-4 : Experimental Data of Heat Transfer to Saturated Pool Boiling of 22.12 wt.% Ethanol in Ethanol - Water Mixture at  $66.64 \text{ kN/m}^2 (T_s=75.7^\circ\text{C})$

Run No.	Heat Flux $\text{W/m}^2$	Conduction Correction $^\circ\text{C}$	Recorded Wall Temp. $^\circ\text{C}$	Corrected Wall Temp. $^\circ\text{C}$	Liquid Temp. $^\circ\text{C}$	Wall Superheat $^\circ\text{C}$	Heat Transfer Coefficient $\text{W/m}^2\text{K}$
79	9974.55	0.797	87.00	86.203	76.20	10.003	997
			89.50	88.703	75.85	12.853	776
			88.00	87.203	76.23	10.973	909
					AVG = 11.276	AVG = 885	
80	13027.99	1.042	88.90	87.860	76.25	11.610	1122
			92.10	91.060	76.00	15.058	865
			89.18	88.138	76.30	11.838	1101
					AVG = 12.835	AVG = 1015	
81	16946.60	1.355	90.55	89.195	76.45	12.745	1330
			93.15	91.795	76.45	15.345	1104
			91.40	90.045	76.50	13.545	1251
					AVG = 13.878	AVG = 1221	
82	20610.70	1.648	90.95	89.595	76.60	12.995	1586
			95.25	93.602	76.55	17.052	1209
			92.45	90.802	76.60	14.202	1451
					AVG = 14.750	AVG = 1397	
83	26218.83	2.096	93.00	90.904	76.75	14.154	1852
			97.10	95.004	76.60	18.404	1425
			93.05	90.954	76.70	14.254	1839
					AVG = 15.604	AVG = 1680	

Table B-4 : Experimental Data of Heat Transfer to Saturated Pool Boiling of 22.12 wt.% Ethanol in Ethanol - Water Mixture at  $53.32 \text{ kN/m}^2$  ( $T_s=70.0^\circ\text{C}$ )

Run No.	Heat Flux $\text{W/m}^2$	Conduction Correction $^\circ\text{C}$	Recorded Wall Temp. $^\circ\text{C}$	Corrected Wall Temp. $^\circ\text{C}$	Liquid Temp. $^\circ\text{C}$	Wall Superheat $^\circ\text{C}$	Heat Transfer Coefficient $\text{W/m}^2\text{K}$
84	13333.33	1.066	83.80	82.734	70.60	12.054	1106
			87.35	86.284	70.50	15.784	845
			85.70	84.634	70.68	13.954	956
						AVG = 13.931	AVG = 957
85	16717.56	1.336	86.58	85.244	70.80	14.444	1157
			89.43	88.094	70.73	17.194	972
			87.25	85.914	70.90	15.014	1113
						AVG = 15.551	AVG = 1075
86	20865.14	1.670	88.55	86.880	71.15	15.730	1326
			90.43	88.760	70.90	17.860	1168
			90.55	88.880	71.15	17.730	1177
						AVG = 17.107	AVG = 1220
87	25190.84	2.014	89.30	87.286	71.30	15.986	1576
			91.30	89.286	71.30	17.986	1401
			91.70	89.686	71.35	18.336	1374
						AVG = 17.436	AVG = 1445
88	30229.00	2.417	90.33	87.913	71.55	16.363	1847
			93.00	90.583	71.30	19.283	1568
			94.95	92.533	71.50	21.033	1437
						AVG = 18.893	AVG = 1600

Table B-4 : Experimental Data of Heat Transfer to Saturated Pool Boiling of 22.12 wt.% Ethanol in Ethanol - Water Mixture at  $33.32 \text{ kN/m}^2 (T_s = 60.0^\circ\text{C})$

Run No.	Heat Flux $\text{W/m}^2$	Conduction Correction $^\circ\text{C}$	Recorded Wall Temp. $^\circ\text{C}$	Corrected Wall Temp. $^\circ\text{C}$	Liquid Temp. $^\circ\text{C}$	Wall Superheat $^\circ\text{C}$	Heat Transfer Coefficient $\text{W/m}^2\text{K}$
89	13333.33	1.066	73.67	72.604	60.30	12.304	1084
			77.05	75.984	60.15	15.834	842
			77.70	76.634	60.30	16.334	816
					AVG = 14.824	AVG = 899	
90	16832.06	1.346	76.35	75.004	60.30	14.704	1145
			79.13	77.784	60.30	17.484	963
			79.50	78.154	60.35	17.804	945
					AVG = 16.664	AVG = 1010	
91	20865.14	1.670	77.25	75.580	60.45	15.130	1379
			81.25	79.580	60.30	19.280	1082
			82.20	80.530	60.50	20.030	1042
					AVG = 18.147	AVG = 1150	
92	25470.74	2.036	79.03	76.994	60.70	16.294	1563
			82.63	80.594	60.50	20.094	1268
			84.10	82.064	60.75	21.314	1195
					AVG = 19.234	AVG = 1324	
93	30229.00	2.417	80.80	78.383	60.95	17.433	1734
			84.70	82.283	60.80	21.483	1407
			86.75	84.333	61.00	23.333	1296
					AVG = 20.750	AVG = 1457	

Table B-4 : Experimental Data of Heat Transfer to Saturated Pool Boiling of 22.12 wt.% Ethanol in Ethanol - Water Mixture at  $21.33 \text{ kN/m}^2 (T_s=50.6^\circ\text{C})$

Run No.	Heat Flux $\text{W/m}^2$	Conduction Correction $^\circ\text{C}$	Recorded Wall Temp. $^\circ\text{C}$	Corrected Wall Temp. $^\circ\text{C}$	Liquid Temp. $^\circ\text{C}$	Wall Superheat $^\circ\text{C}$	Heat Transfer Coefficient $\text{W/m}^2\text{K}$
94	9974.55	0.797	63.15	62.353	49.80	12.553	795
			65.60	64.803	49.50	15.303	652
			66.60	65.803	49.65	16.153	618
					AVG = 14.670	AVG = 680	
95	13027.99	1.042	65.10	64.058	50.15	13.908	937
			68.30	67.258	50.00	17.258	755
			69.78	68.738	50.15	18.588	701
					AVG = 16.585	AVG = 786	
96	16946.56	1.355	67.05	65.695	50.55	15.145	1119
			70.58	69.225	50.40	18.825	900
			72.38	71.025	50.50	20.525	826
					AVG = 18.165	AVG = 933	
97	20865.14	1.670	69.25	67.580	50.80	16.780	1243
			72.72	71.050	50.55	20.500	1018
			75.10	73.430	50.70	22.730	918
					AVG = 20.000	AVG = 1043	
98	25190.84	2.014	71.05	69.036	51.00	18.036	1397
			75.90	73.886	50.85	23.036	1094
			75.90	73.886	51.00	22.886	1101
					AVG = 21.320	AVG = 1182	

Table B-5 : Experimental Data of Heat Transfer to Saturated Pool Boiling of 31.1 wt.% Ethanol in Ethanol - Water Mixture at  $98.63 \text{ kN/m}^2$  ( $T_g = 83.7^\circ\text{C}$ )

Run No.	Heat Flux $\text{W/m}^2$	Conduction Correction $^\circ\text{C}$	Recorded Wall Temp. $^\circ\text{C}$	Corrected Wall Temp. $^\circ\text{C}$	Liquid Temp. $^\circ\text{C}$	Wall Superheat $^\circ\text{C}$	Heat Transfer Coefficient $\text{W/m}^2\text{K}$
99	13027.99	1.042	97.10	96.058	85.25	10.808	1205
			100.95	99.908	85.15	14.758	883
			98.60	99.758	85.15	13.450	969
						AVG = 13.000	AVG = 1002
100	16717.56	1.337	98.70	97.363	85.40	11.963	1397
			103.50	102.163	85.25	16.913	988
			99.95	98.613	85.40	13.213	1265
						AVG = 14.030	AVG = 1192
101	20865.14	1.668	100.10	98.432	85.80	12.632	1652
			104.60	102.932	85.65	17.282	1207
			102.85	101.182	85.70	15.482	1348
						AVG = 15.132	AVG = 1379
102	25190.84	2.014	101.75	99.736	86.10	13.636	1847
			105.80	103.786	85.90	17.886	1408
			105.00	102.986	86.20	16.786	1501
						AVG = 16.103	AVG = 1564
103	30534.35	2.441	103.65	101.210	86.65	14.559	2097
			108.00	105.560	86.45	19.109	1598
			106.25	103.809	86.65	17.159	1779
						AVG = 16.942	AVG = 1802



Table B-5 : Experimental Data of Heat Transfer to Saturated Pool Boiling of 31.1 wt.% Ethanol in Ethanol - Water Mixture at  $66.64 \text{ kN/m}^2 (T_s=74.1^\circ\text{C})$

Run No.	Heat Flux $\text{W/m}^2$	Conduction Correction $^\circ\text{C}$	Recorded Wall Temp. $^\circ\text{C}$	Corrected Wall Temp. $^\circ\text{C}$	Liquid Temp. $^\circ\text{C}$	Wall Superheat $^\circ\text{C}$	Heat Transfer Coefficient $\text{W/m}^2\text{K}$
104	13027.99	1.042	86.70	85.658	74.10	11.558	1127
			90.90	89.858	73.95	15.908	819
			89.50	88.458	74.10	14.358	907
					AVG = 13.941	AVG = 935	
105	16946.56	1.355	88.60	87.245	74.40	12.845	1319
			93.80	92.445	74.30	18.145	934
			92.85	91.495	74.40	17.095	991
					AVG = 16.028	AVG = 1057	
106	20865.14	1.668	90.73	89.062	75.00	14.062	1484
			96.00	94.332	74.85	19.482	1071
			94.90	93.232	75.15	18.082	1154
					AVG = 17.209	AVG = 1212	
107	25190.84	2.014	92.60	90.586	75.40	15.186	1659
			98.20	96.186	75.40	20.786	1212
			97.10	95.086	75.45	19.636	1283
					AVG = 18.536	AVG = 1359	
108	30534.35	2.441	93.80	91.359	76.00	15.360	1988
			99.30	96.860	75.90	20.959	1457
			99.30	96.860	76.05	20.809	1467
					AVG = 19.043	AVG = 1603	

Table B-5 : Experimental Data of Heat Transfer to Saturated Pool Boiling of 31.1 wt.% Ethanol in Ethanol - Water Mixture at  $50.65 \text{ kN/m}^2 (T_s=67.7^\circ\text{C})$

Run No.	Heat Flux $\text{W/m}^2$	Conduction Correction $^\circ\text{C}$	Recorded Wall Temp. $^\circ\text{C}$	Corrected Wall Temp. $^\circ\text{C}$	Liquid Temp. $^\circ\text{C}$	Wall Superheat $^\circ\text{C}$	Heat Transfer Coefficient $\text{W/m}^2\text{K}$
109	13027.99	1.042	80.85	79.808	67.70	12.108	1076
			86.00	84.958	67.58	17.378	750
			83.45	82.408	67.85	14.558	895
						AVG =14.681	AVG = 887
110	16946.56	1.355	83.50	82.145	68.20	13.945	1215
			89.25	87.895	68.20	19.695	860
			87.50	86.145	68.40	17.745	955
						AVG =17.130	AVG = 989
111	20865.14	1.668	86.58	84.912	68.65	16.262	1283
			91.08	89.412	68.65	20.762	1005
			90.00	88.332	68.88	19.452	1073
						AVG =18.825	AVG = 1108
112	25190.84	2.014	88.10	86.086	69.00	17.086	1474
			93.50	91.486	69.10	22.386	1125
			92.30	90.286	69.10	21.186	1189
						AVG =20.219	AVG = 1246
113	30534.35	2.441	89.85	87.409	69.85	17.559	1739
			94.45	92.009	69.68	22.329	1367
			94.25	91.809	69.85	21.959	1390
						AVG =20.616	AVG = 1481

Table B-5 : Experimental Data of Heat Transfer to Saturated Pool Boiling of 31.1 wt.% Ethanol in Ethanol - Water Mixture at  $33.32 \text{ kN/m}^2$  ( $T_s = 58.3^\circ\text{C}$ )

Run No.	Heat Flux $\text{W/m}^2$	Conduction Correction $^\circ\text{C}$	Recorded Wall Temp. $^\circ\text{C}$	Corrected Wall Temp. $^\circ\text{C}$	Liquid Temp. $^\circ\text{C}$	Wall Superheat $^\circ\text{C}$	Heat Transfer Coefficient $\text{W/m}^2\text{K}$
114	9974.55	0.797	71.25	70.453	58.55	11.903	838
			74.83	74.033	58.35	15.683	636
			74.83	74.033	58.63	15.402	648
					AVG = 14.335	AVG = 696	
115	12865.14	1.028	74.45	73.422	59.00	14.422	892
			78.05	77.022	59.00	18.022	714
			76.75	75.722	59.10	16.622	774
					AVG = 16.355	AVG = 787	
116	16946.56	1.355	76.80	75.455	59.48	15.965	1061
			81.60	80.245	59.48	20.765	816
			80.50	79.145	59.58	19.565	866
					AVG = 18.765	AVG = 903	
117	20610.69	1.648	78.90	77.252	59.83	17.422	1183
			82.03	80.382	59.70	20.682	997
			83.20	81.552	59.70	21.852	943
					AVG = 19.985	AVG = 1031	
118	25190.84	2.014	81.70	79.686	59.92	19.766	1274
			83.75	81.740	59.80	21.940	1148
			84.45	82.440	59.92	22.516	1119
					AVG = 21.410	AVG = 1177	

Table B-5 : Experimental Data of Heat Transfer to Saturated Pool Boiling of 31.1 wt.% Ethanol in Ethanol - Water Mixture at  $22.66 \text{ kN/m}^2 (T_g=51.0^\circ\text{C})$

Run No.	Heat Flux $\text{W/m}^2$	Conduction Correction $^\circ\text{C}$	Recorded Wall Temp. $^\circ\text{C}$	Corrected Wall Temp. $^\circ\text{C}$	Liquid Temp. $^\circ\text{C}$	Wall Superheat $^\circ\text{C}$	Heat Transfer Coefficient $\text{W/m}^2\text{K}$
119	9974.55	0.798	65.55	64.752	50.50	14.252	700
			70.45	69.652	50.50	19.152	521
			70.22	69.422	50.58	18.842	529
					AVG = 17.420	AVG = 573	
120	13027.99	1.042	67.70	66.658	50.75	15.908	819
			73.40	72.360	50.70	21.700	600
			75.10	74.060	50.98	23.078	564
					AVG = 20.230	AVG = 644	
121	16946.60	1.355	70.20	68.845	50.93	17.915	946
			74.45	73.095	50.83	22.265	761
			75.15	73.795	50.98	22.815	743
					AVG = 21.000	AVG = 807	
122	20865.14	1.668	72.75	71.082	51.05	20.032	1042
			75.00	73.332	50.93	22.402	931
			75.15	73.482	51.20	22.282	936
					AVG = 21.572	AVG = 967	
123	25190.84	2.014	74.55	72.536	51.35	21.180	1189
			76.10	74.086	51.35	22.736	1108
			76.10	74.086	51.40	22.686	1110
					AVG = 22.203	AVG = 1135	

Table B-6 : Experimental Data of Heat Transfer to Saturated Pool Boiling of 39.0 wt.% Ethanol in Ethanol - Water Mixture at  $98.63 \text{ kN/m}^2 (T_s = 32.1^\circ\text{C})$

Run No.	Heat Flux $\text{W/m}^2$	Conduction Correction $^\circ\text{C}$	Recorded Wall Temp. $^\circ\text{C}$	Corrected Wall Temp. $^\circ\text{C}$	Liquid Temp. $^\circ\text{C}$	Wall Superheat $^\circ\text{C}$	Heat Transfer Coefficient $\text{W/m}^2\text{K}$
124	10152.67	0.812	92.93	92.118	83.55	8.570	1185
			97.10	96.288	83.35	12.940	785
			97.80	96.988	83.45	13.538	750
					AVG = 11.683	AVG = 869	
125	13027.99	1.042	93.70	92.658	83.68	8.978	1451
			98.90	97.858	83.50	14.358	907
			98.90	97.858	83.60	14.258	914
					AVG = 12.530	AVG = 1040	
126	16717.56	1.337	94.80	93.463	84.30	9.363	1785
			99.95	98.613	84.10	14.513	1152
			100.80	99.463	84.45	15.013	1114
					AVG = 12.963	AVG = 1290	
127	20865.14	1.668	96.15	94.482	84.80	9.682	2155
			101.75	100.082	84.70	14.382	1451
			101.75	100.082	84.75	15.332	1361
					AVG = 13.465	AVG = 1550	
128	24961.83	1.996	97.90	95.904	85.10	10.804	2310
			103.00	101.004	84.90	16.104	1550
			104.20	102.204	85.15	17.054	1464
					AVG = 14.654	AVG = 1703	

Table B-6 : Experimental Data of Heat Transfer to Saturated Pool Boiling of 39.0 wt.% Ethanol in Ethanol - Water Mixture at  $66.64 \text{ kN/m}^2$  ( $T_s=72.6^\circ\text{C}$ )

Run No.	Heat Flux $\text{W/m}^2$	Conduction Correction $^\circ\text{C}$	Recorded Wall Temp. $^\circ\text{C}$	Corrected Wall Temp. $^\circ\text{C}$	Liquid Temp. $^\circ\text{C}$	Wall Superheat $^\circ\text{C}$	Heat Transfer Coefficient $\text{W/m}^2\text{K}$
129	13231.55	1.058	85.20	84.142	72.95	11.192	1182
			88.80	87.742	72.83	14.912	887
			88.60	87.542	72.95	14.592	907
					AVG =13.565	AVG = 975	
130	16946.56	1.355	87.85	86.495	73.45	13.045	1299
			90.73	89.375	73.30	16.075	1054
			90.20	88.845	73.50	15.345	1104
					AVG =14.822	AVG = 1143	
131	20610.70	1.648	88.65	87.002	73.65	13.352	1543
			92.73	91.082	73.60	17.482	1179
			91.20	89.552	73.70	15.952	1292
					AVG =15.600	AVG = 1321	
132	25190.83	2.014	90.65	88.636	74.30	14.336	1757
			95.90	93.886	74.20	19.686	1279
			93.70	91.686	74.40	17.286	1457
					AVG =17.103	AVG = 1473	
133	30534.35	2.441	93.10	90.659	74.95	15.709	1944
			97.35	94.909	74.85	20.059	1522
			97.35	94.909	75.10	19.809	1541
					AVG =18.525	AVG = 1648	

Table B-6 : Experimental Data of Heat Transfer to Saturated Pool Boiling of 39.0 wt.% Ethanol in Ethanol - Water Mixture at 48.0 kN/m<sup>2</sup> (T<sub>s</sub>=65.8°C)

Run No.	Heat Flux W/m <sup>2</sup>	Conduction Correction °C	Recorded Wall Temp. °C	Corrected Wall Temp. °C	Liquid Temp. °C	Wall Superheat °C	Heat Transfer Coefficient W/m <sup>2</sup> K
134	10152.67	0.812	78.98	78.168	66.83	11.338	895
			82.60	81.788	66.83	15.158	670
			81.90	81.088	66.95	14.138	718
						AVG =13.545	AVG = 750
135	13027.99	1.042	80.25	79.208	67.00	12.208	1067
			84.35	83.308	66.83	16.478	791
			83.60	82.558	67.00	15.558	837
						AVG =14.750	AVG = 883
136	16717.56	1.337	81.55	80.213	67.30	12.913	1295
			86.45	85.113	67.15	17.963	931
			84.80	83.463	67.55	15.913	1051
						AVG =15.600	AVG = 1072
137	20865.14	1.668	83.15	81.482	67.85	13.632	1531
			88.60	86.932	67.75	19.182	1088
			87.15	85.482	68.00	17.482	1194
						AVG =16.765	AVG = 1245
138	25750.64	2.059	86.20	84.141	68.20	15.941	1615
			91.08	89.021	68.20	20.821	1237
			88.10	86.041	68.35	17.691	1456
						AVG =18.151	AVG = 1419

Table B-6 : Experimental Data of Heat Transfer to Saturated Pool Boiling of 39.0 wt.% Ethanol in Ethanol - Water Mixture at  $36.0 \text{ kN/m}^2$  ( $T_s = 58.4^\circ\text{C}$ )

Run No.	Heat Flux $\text{W/m}^2$	Conduction Correction $^\circ\text{C}$	Recorded Wall Temp. $^\circ\text{C}$	Corrected Wall Temp. $^\circ\text{C}$	Liquid Temp. $^\circ\text{C}$	Wall Superheat $^\circ\text{C}$	Heat Transfer Coefficient $\text{W/m}^2\text{K}$
139	12946.56	1.035	74.60	73.565	59.50	14.065	920
			77.25	76.215	59.25	16.965	763
			77.85	76.815	59.40	17.415	743
						AVG = 16.150	AVG = 802
140	16946.56	1.355	76.00	74.645	59.62	15.025	1128
			78.60	77.245	59.62	17.625	961
			79.40	78.045	59.80	18.245	929
						AVG = 16.965	AVG = 999
141	20865.14	1.668	77.95	76.282	60.10	16.182	1290
			80.80	79.132	60.10	19.032	1096
			81.70	80.032	60.15	19.882	1049
						AVG = 18.360	AVG = 1136
142	25190.84	2.014	79.45	77.436	60.40	17.036	1478
			82.60	80.586	60.28	20.306	1240
			82.60	80.586	60.40	20.186	1248
						AVG = 19.180	AVG = 1313
143	30534.35	2.441	81.85	79.409	61.00	18.409	1659
			84.35	81.909	60.85	21.059	1450
			85.90	83.460	61.10	22.360	1366
						AVG = 20.610	AVG = 1482



Table B-6 : Experimental Data of Heat Transfer to Saturated Pool Boiling of 39.0 wt.% Ethanol in Ethanol - Water Mixture at  $25.33 \text{ kN/m}^2 (T_s=53.2^\circ\text{C})$

Run No.	Heat Flux $\text{W/m}^2$	Conduction Correction $^\circ\text{C}$	Recorded Wall Temp. $^\circ\text{C}$	Corrected Wall Temp. $^\circ\text{C}$	Liquid Temp. $^\circ\text{C}$	Wall Superheat $^\circ\text{C}$	Heat Transfer Coefficient $\text{W/m}^2\text{K}$
144	12946.60	1.035	67.15	66.115	51.60	14.520	892
			71.70	70.915	51.40	19.270	672
			70.95	69.915	51.65	18.265	709
					AVG = 17.350	AVG = 746	
145	16717.56	1.337	68.40	67.063	51.95	15.113	1106
			73.70	72.363	51.90	20.463	817
			73.70	72.363	52.00	20.363	821
					AVG = 18.650	AVG = 896	
146	20865.14	1.668	70.15	68.482	52.40	16.082	1297
			75.87	74.202	52.40	21.802	957
			76.40	74.732	52.50	22.232	939
					AVG = 20.040	AVG = 1041	
147	25190.84	2.014	73.15	71.136	52.85	18.286	1377
			77.00	74.986	52.65	22.336	1128
			77.20	75.186	52.85	22.336	1128
					AVG = 20.986	AVG = 1200	

Table B-7 : Experimental Data of Heat Transfer to Saturated Pool Boiling of 52.3 wt.% Ethanol in Ethanol - Water Mixture at 98.63 kN/m<sup>2</sup> (T<sub>s</sub>=80.7°C)

Run No.	Heat Flux W/m <sup>2</sup>	Conduction Correction °C	Recorded Wall Temp. °C	Corrected Wall Temp. °C	Liquid Temp. °C	Wall Superheat °C	Heat Transfer Coefficient W/m <sup>2</sup> K
148	10152.67	0.812	91.25	90.438	82.35	8.088	1255
			94.90	94.088	82.05	12.038	843
			95.55	94.738	82.35	12.388	819
						AVG =10.838	AVG = 937
149	12865.14	1.030	92.30	91.270	82.75	8.520	1510
			96.10	95.070	82.35	12.720	1011
			97.25	96.220	82.70	13.520	952
						AVG =11.590	AVG = 1110
150	17674.30	1.413	93.25	91.837	82.90	8.937	1978
			97.40	95.987	82.60	13.387	1320
			98.20	96.787	82.60	14.187	1245
						AVG =12.170	AVG = 1452
151	21119.59	1.690	95.00	93.310	83.50	9.810	2153
			98.65	96.960	83.35	13.610	1552
			99.90	98.210	83.55	14.660	1441
						AVG =12.690	AVG = 1664
152	25610.70	2.048	97.50	95.452	83.90	11.552	2217
			100.30	98.252	83.80	14.452	1772
			101.05	99.002	83.90	15.102	1696
						AVG =13.702	AVG = 1869

Table B-7 : Experimental Data of Heat Transfer to Saturated Pool Boiling of 52.3 wt.% Ethanol in Ethanol - Water Mixture at  $66.64 \text{ kN/m}^2 (T_s = 71.1^\circ\text{C})$

Run No.	Heat Flux $\text{W/m}^2$	Conduction Correction $^\circ\text{C}$	Recorded Wall Temp. $^\circ\text{C}$	Corrected Wall Temp. $^\circ\text{C}$	Liquid Temp. $^\circ\text{C}$	Wall Superheat $^\circ\text{C}$	Heat Transfer Coefficient $\text{W/m}^2\text{K}$
153	12946.56	1.035	83.90	82.865	72.00	10.865	1192
			87.80	86.765	71.90	14.865	871
			85.50	84.465	72.20	12.265	1056
					AVG = 12.665	AVG = 1022	
154	16946.60	1.355	85.95	84.595	72.20	12.395	1367
			88.45	87.095	72.05	15.045	1126
			86.80	85.445	72.25	13.195	1284
					AVG = 13.545	AVG = 1251	
155	20610.70	1.648	87.25	85.602	72.70	12.902	1597
			91.30	89.652	72.28	17.372	1186
			88.70	87.052	72.83	14.222	1449
					AVG = 14.832	AVG = 1390	
156	25470.73	2.036	88.10	86.064	72.83	13.234	1925
			92.20	90.164	72.70	17.464	1458
			90.05	88.014	72.83	15.184	1677
					AVG = 15.294	AVG = 1665	
157	30229.00	2.417	89.35	86.933	73.10	13.833	2185
			93.10	90.683	72.95	17.733	1705
			93.10	90.683	73.18	17.503	1727
					AVG = 16.356	AVG = 1848	

Table B-7 : Experimental Data of Heat Transfer to Saturated Pool Boiling of 52.3 wt.% Ethanol in Ethanol - Water Mixture at  $46.65 \text{ kN/m}^2 (T_s = 63.6^\circ\text{C})$

Run No.	Heat Flux $\text{W/m}^2$	Conduction Correction $^\circ\text{C}$	Recorded Wall Temp. $^\circ\text{C}$	Corrected Wall Temp. $^\circ\text{C}$	Liquid Temp. $^\circ\text{C}$	Wall Superheat $^\circ\text{C}$	Heat Transfer Coefficient $\text{W/m}^2\text{K}$
158	13129.77	1.050	76.90	75.850	64.90	10.950	1199
			81.60	80.550	64.70	15.850	828
			80.50	79.450	64.90	14.550	902
					AVG = 13.783	AVG = 953	
159	16946.56	1.355	77.95	76.595	65.13	11.465	1477
			82.92	81.565	65.13	16.435	1031
			82.63	81.275	65.23	16.045	1056
					AVG = 14.650	AVG = 1157	
160	20865.14	1.668	79.70	78.032	65.90	12.132	1720
			84.00	82.332	65.80	16.532	1262
			84.85	83.182	66.10	17.082	1221
					AVG = 15.250	AVG = 1368	
161	25190.83	2.014	81.50	79.486	66.50	12.986	1939
			86.25	84.236	66.10	18.136	1389
			87.00	84.986	66.25	18.736	1344
					AVG = 16.620	AVG = 1516	
162	30534.35	2.441	83.25	80.809	66.98	13.829	2208
			88.88	86.439	66.83	19.609	1557
			89.00	86.559	67.10	19.459	1569
					AVG = 17.632	AVG = 1732	

Table B-7 : Experimental Data of Heat Transfer to Saturated Pool Boiling of 52.3 wt.% Ethanol in Ethanol - Water Mixture at  $33.32 \text{ kN/m}^2 (T_s=55.2^\circ\text{C})$

Run No.	Heat Flux $\text{W/m}^2$	Conduction Correction $^\circ\text{C}$	Recorded Wall Temp. $^\circ\text{C}$	Corrected Wall Temp. $^\circ\text{C}$	Liquid Temp. $^\circ\text{C}$	Wall Superheat $^\circ\text{C}$	Heat Transfer Coefficient $\text{W/m}^2\text{K}$
163	13435.11	1.074	68.20	67.126	55.68	11.446	1174
			73.05	71.976	55.68	16.296	824
			73.05	71.976	55.78	16.196	829
						AVG =14.650	AVG = 917
164	16946.56	1.355	70.20	68.845	56.00	12.845	1319
			75.55	74.195	55.78	18.415	920
			76.00	74.645	55.88	18.765	903
						AVG =16.675	AVG = 1016
165	20865.14	1.668	71.68	70.012	56.40	13.612	1533
			77.40	75.732	56.25	19.482	1071
			78.60	76.932	56.50	20.432	1021
						AVG =17.842	AVG = 1169
166	25190.83	2.014	74.43	72.416	56.85	15.566	1618
			78.57	76.556	56.50	20.056	1256
			79.55	77.536	56.80	20.736	1215
						AVG =18.786	AVG = 1341
167	30534.35	2.441	75.90	73.460	57.15	16.310	1872
			80.30	77.860	57.03	20.830	1466
			81.60	79.160	57.28	22.130	1380
						AVG =19.757	AVG = 1546

Table B-7 : Experimental Data of Heat Transfer to Saturated Pool Boiling of 52.3 wt.% Ethanol in Ethanol - Water Mixture at  $22.66 \text{ kN/m}^2 (T_s=48.1^\circ\text{C})$

Run No.	Heat Flux $\text{W/m}^2$	Conduction Correction $^\circ\text{C}$	Recorded Wall Temp. $^\circ\text{C}$	Corrected Wall Temp. $^\circ\text{C}$	Liquid Temp. $^\circ\text{C}$	Wall Superheat $^\circ\text{C}$	Heat Transfer Coefficient $\text{W/m}^2\text{K}$
168	13027.98	1.042	64.15	63.108	50.47	12.640	1031
			68.10	67.058	50.23	16.828	774
			68.10	67.058	50.58	16.478	761
					AVG = 15.315	AVG = 851	
169	16946.56	1.355	67.40	66.045	51.05	14.995	1130
			72.50	71.145	50.93	20.215	838
			70.55	69.195	51.22	17.975	943
					AVG = 17.730	AVG = 956	
170	20865.13	1.668	68.43	66.762	51.35	15.412	1354
			75.43	73.762	51.18	22.582	924
			73.68	72.012	51.35	20.662	1010
					AVG = 19.552	AVG = 1067	
171	25190.83	2.014	70.00	67.986	52.00	15.986	1576
			76.60	74.586	51.90	22.686	1110
			75.10	73.086	52.13	20.956	1202
					AVG = 19.880	AVG = 1267	

Table B-8 : Experimental Data of Heat Transfer to Saturated Pool Boiling of 71.88 wt.% Ethanol in Ethanol - Water Mixture at  $98.63 \text{ kN/m}^2 (T_s=78.9^\circ)$

Run No.	Heat Flux $\text{W/m}^2$	Conduction Correction $^\circ\text{C}$	Recorded Wall Temp. $^\circ\text{C}$	Corrected Wall Temp. $^\circ\text{C}$	Liquid Temp. $^\circ\text{C}$	Wall Superheat $^\circ\text{C}$	Heat Transfer Coefficient $\text{W/m}^2\text{K}$
172	13027.99	1.042	88.55	87.508	79.70	7.808	1669
			92.20	91.160	79.58	11.578	1125
			90.70	89.658	79.80	9.858	1322
					AVG = 9.750	AVG = 1336	
173	16488.55	1.320	90.55	89.230	79.90	9.330	1767
			93.05	91.730	79.65	12.080	1365
			91.75	90.430	79.95	10.480	1573
					AVG = 10.630	AVG = 1551	
174	19824.42	1.585	91.30	89.715	80.30	9.415	2106
			94.80	93.215	80.05	13.165	1506
			92.93	91.345	80.40	10.945	1811
					AVG = 11.175	AVG = 1774	
175	26218.83	2.096	92.65	90.554	80.60	9.954	2634
			97.10	95.004	80.50	14.504	1808
			95.30	93.204	80.60	12.604	2080
					AVG = 12.354	AVG = 2122	

Table B-8 : Experimental Data of Heat Transfer to Saturated Pool Boiling of 71.88 wt.% Ethanol in Ethanol - Water Mixture at  $69.31 \text{ kN/m}^2 (T_s=70.4^\circ\text{C})$

Run No.	Heat Flux $\text{W/m}^2$	Conduction Correction $^\circ\text{C}$	Recorded Wall Temp. $^\circ\text{C}$	Corrected Wall Temp. $^\circ\text{C}$	Liquid Temp. $^\circ\text{C}$	Wall Superheat $^\circ\text{C}$	Heat Transfer Coefficient $\text{W/m}^2\text{K}$
176	13231.56	1.058	82.40	81.342	71.40	9.942	1331
			85.30	84.242	71.20	13.042	1015
			83.30	82.242	71.47	10.772	1228
					AVG = 11.252	AVG = 1176	
177	16488.55	1.320	83.45	82.130	71.47	10.660	1547
			86.10	84.780	71.35	13.430	1228
			84.25	82.930	71.47	11.460	1439
					AVG = 11.850	AVG = 1391	
178	20865.13	1.668	84.90	83.232	72.00	11.232	1858
			87.25	85.582	72.00	13.582	1536
			86.30	84.632	72.15	12.482	1672
					AVG = 12.432	AVG = 1678	
179	25190.83	2.014	86.40	84.386	72.25	12.136	2076
			88.45	86.436	72.15	14.286	1763
			87.85	85.836	72.30	13.536	1861
					AVG = 13.320	AVG = 1891	
180	30534.35	2.441	87.60	85.160	72.70	12.460	2451
			90.55	88.110	72.60	15.510	1969
			90.25	87.810	72.70	15.110	2021
					AVG = 14.360	AVG = 2126	



Table B-8 : Experimental Data of Heat Transfer to Saturated Pool Boiling of 71.88 wt.% Ethanol in Ethanol - Water Mixture at  $48.0 \text{ kN/m}^2 (T_s=62.7^\circ\text{C})$

Run No.	Heat Flux $\text{W/m}^2$	Conduction Correction $^\circ\text{C}$	Recorded Wall Temp. $^\circ\text{C}$	Corrected Wall Temp. $^\circ\text{C}$	Liquid Temp. $^\circ\text{C}$	Wall Superheat $^\circ\text{C}$	Heat Transfer coefficient $\text{W/m}^2\text{K}$
181	13027.99	1.042	76.50	75.458	63.72	11.738	1110
			79.03	77.988	63.50	14.488	899
			76.90	75.858	63.83	12.028	1083
					AVG =12.752		AVG = 1022
182	16717.55	1.337	78.05	76.713	63.83	12.883	1298
			80.50	79.163	63.58	15.583	1073
			78.68	77.343	63.83	13.513	1237
					AVG =13.993		AVG = 1195
183	20865.14	1.668	79.45	77.782	64.10	13.682	1525
			81.85	80.182	63.90	16.282	1281
			80.60	78.932	64.18	14.752	1414
					AVG =14.905		AVG = 1400
184	26218.83	2.096	81.20	79.104	64.50	14.604	1795
			83.30	81.204	64.30	16.904	1551
			83.30	81.204	64.65	16.554	1584
					AVG =16.021		AVG = 1637

Table B-8 : Experimental Data of Heat Transfer to Saturated Pool Boiling of 71.88 wt.% Ethanol in Ethanol - Water Mixture at  $33.32 \text{ kN/m}^2$  ( $T_s = 54.0^\circ\text{C}$ )

Run No.	Heat Flux $\text{W/m}^2$	Conduction Correction	Recorded Wall Temp. $^\circ\text{C}$	Corrected Wall Temp. $^\circ\text{C}$	Liquid Temp. $^\circ\text{C}$	Wall Superheat $^\circ\text{C}$	Heat Transfer Coefficient $\text{W/m}^2\text{K}$
185	16717.55	1.337	68.50	67.163	54.53	12.633	1323
			72.60	71.263	54.53	16.733	999
			70.50	69.163	54.65	14.513	1152
					AVG = 14.626	AVG = 1143	
186	20865.14	1.670	70.65	68.980	54.70	14.300	1459
			74.00	72.330	54.58	17.750	1176
			71.80	70.130	54.70	15.430	1352
					AVG = 15.830	AVG = 1318	
187	25190.83	2.014	72.25	70.236	54.95	15.286	1648
			75.40	73.386	54.95	18.436	1366
			73.58	71.566	55.10	16.466	1530
					AVG = 16.730	AVG = 1506	

Table B-8 : Experimental Data of Heat Transfer to Saturated Pool Boiling of 71.88 wt.% Ethanol in Ethanol - Water Mixture at  $18.66 \text{ kN/m}^2 (T_s=41.7^\circ\text{C})$

Run No.	Heat Flux $\text{W/m}^2$	Conduction Correction $^\circ\text{C}$	Recorded Wall Temp. $^\circ\text{C}$	Corrected Wall Temp. $^\circ\text{C}$	Liquid Temp. $^\circ\text{C}$	Wall Superheat $^\circ\text{C}$	Heat Transfer Coefficient $\text{W/m}^2\text{K}$
188	16531.80	1.322	60.88	59.558	46.43	13.128	1259
			63.85	62.528	45.98	16.548	999
			64.90	63.578	45.98	17.598	939
					AVG =15.760	AVG = 1049	
189	20865.13	1.668	62.93	61.262	47.27	13.992	1491
			66.27	64.602	47.15	17.452	1196
			67.10	65.432	47.27	18.162	1149
					AVG =16.535	AVG = 1262	
190	25190.83	2.014	64.70	62.686	47.75	14.936	1687
			68.45	66.436	47.60	18.836	1337
			69.90	67.886	47.85	20.036	1257
					AVG =17.936	AVG = 1405	

Table B-9 : Experimental Data of Heat Transfer to Saturated Pool  
 Boiling of Methanol at  $98.63 \text{ kN/m}^2 (T_s=64.0^\circ\text{C})$

Run No.	Heat Flux $\text{W/m}^2$	Conduction Correction $^\circ\text{C}$	Recorded Wall Temp. $^\circ\text{C}$	Corrected Wall Temp. $^\circ\text{C}$	Liquid Temp. $^\circ\text{C}$	Wall Superheat $^\circ\text{C}$	Heat Transfer Coefficient $\text{W/m}^2\text{K}$
191	9618.32	0.769	76.00	75.231	66.50	8.731	1102
			75.10	74.331	66.10	8.231	1169
			73.35	72.581	66.45	6.131	1569
					AVG = 7.698	AVG = 1249	
192	12620.90	1.009	77.60	76.600	66.85	10.750	1174
			75.25	74.250	66.25	8.000	1578
			74.10	73.100	66.85	6.250	2019
					AVG = 8.333	AVG = 1515	
193	16259.50	1.300	79.35	78.050	66.95	11.100	1465
			76.45	75.150	66.25	8.900	1827
			74.65	73.350	66.85	6.500	2501
					AVG = 8.833	AVG = 1841	
194	20356.20	1.627	81.90	80.273	67.40	12.873	1581
			77.55	75.923	66.80	9.123	2231
			75.85	74.223	67.30	6.923	2940
					AVG = 9.640	AVG = 2112	
195	24910.90	1.990	83.50	81.510	67.70	13.810	1804
			79.00	77.010	66.85	10.160	2452
			77.25	75.260	67.45	7.810	3190
					AVG = 10.593	AVG = 2352	

Table B-9 : Experimental Data of Heat Transfer to Saturated Pool  
 Boiling of Methanol at  $66.64 \text{ kN/m}^2$  ( $T_s=55.2^\circ\text{C}$ )

Run No.	Heat Flux $\text{W/m}^2$	Conduction Correction $^\circ\text{C}$	Recorded Wall Temp. $^\circ\text{C}$	Corrected Wall Temp. $^\circ\text{C}$	Liquid Temp. $^\circ\text{C}$	Wall Superheat $^\circ\text{C}$	Heat Transfer Coefficient $\text{W/m}^2\text{K}$
196	9618.32	0.769	66.80	66.031	55.83	10.201	943
			64.50	63.731	55.10	8.631	1114
			64.62	63.851	55.75	8.101	1187
					AVG = 8.978	AVG = 1071	
197	12824.43	1.025	67.20	66.175	55.90	10.275	1248
			65.10	64.075	55.15	8.925	1437
			65.70	64.675	55.75	8.925	1437
					AVG = 9.375	AVG = 1368	
198	16488.55	1.320	68.90	67.580	55.95	11.630	1418
			65.80	64.480	55.20	9.280	1777
			65.80	64.480	55.65	8.830	1867
					AVG = 9.913	AVG = 1663	
199	20356.23	1.627	69.60	67.973	56.05	11.923	1707
			68.10	66.473	55.65	10.823	1881
			67.55	65.923	55.85	10.073	2021
					AVG = 10.940	AVG = 1861	
200	24910.94	1.990	71.60	69.610	56.10	13.510	1844
			68.55	66.560	55.65	10.910	2283
			67.65	65.660	55.85	9.810	2539
					AVG = 11.410	AVG = 2183	

Table B-9 : Experimental Data of Heat Transfer to Saturated Pool  
Boiling of Methanol at  $50.65 \text{ kN/m}^2 (T_s=49.1^\circ\text{C})$

Run No.	Heat Flux $\text{W/m}^2$	Conduction Correction $^\circ\text{C}$	Recorded Wall Temp. $^\circ\text{C}$	Corrected Wall Temp. $^\circ\text{C}$	Liquid Temp. $^\circ\text{C}$	Wall Superheat $^\circ\text{C}$	Heat Transfer Coefficient $\text{W/m}^2\text{K}$
201	9618.32	0.769	59.45	58.681	49.40	9.281	1036
			58.80	58.031	49.05	8.981	1071
			58.70	57.931	49.25	8.681	1108
			AVG = 8.981		AVG = 1071		
202	12620.86	1.009	61.25	60.250	49.45	10.800	1169
			60.15	59.150	49.05	10.100	1250
			60.25	59.250	49.30	9.950	1268
			AVG = 10.280		AVG = 1228		
203	16259.50	1.300	62.50	61.200	49.40	11.800	1378
			61.15	59.850	49.05	10.800	1506
			60.85	59.550	49.25	10.300	1579
			AVG = 10.970		AVG = 1482		
204	20356.20	1.627	64.75	63.123	49.50	13.623	1494
			62.70	61.073	49.25	11.823	1722
			61.85	60.223	49.35	10.873	1872
			AVG = 12.106		AVG = 1682		
205	24631.00	1.970	67.90	65.930	50.65	15.280	1612
			64.85	62.880	50.70	12.180	2022
			63.60	61.630	50.70	10.930	2254
			AVG = 12.800		AVG = 1924		

Table B-9 : Experimental Data of Heat Transfer to Saturated Pool  
 Boiling of Methanol at  $34.65 \text{ kN/m}^2 (T_s=40.0^\circ\text{C})$

Run No.	Heat Flux $\text{W/m}^2$	Conduction Correction $^\circ\text{C}$	Recorded Wall Temp. $^\circ\text{C}$	Corrected Wall Temp. $^\circ\text{C}$	Liquid Temp. $^\circ\text{C}$	Wall Superheat $^\circ\text{C}$	Heat Transfer Coefficient $\text{W/m}^2\text{K}$
206	9618.32	0.769	50.75	49.981	40.95	9.031	1065
			51.40	50.631	40.70	9.931	969
			52.70	51.931	40.95	10.981	876
			AVG = 9.981		AVG = 964		
207	12824.43	1.025	53.55	52.525	42.20	10.325	1242
			54.25	53.225	41.95	11.275	1137
			54.35	53.325	42.10	11.225	1142
			AVG = 10.942		AVG = 1172		
208	16259.54	1.300	54.85	53.550	41.95	11.600	1402
			55.30	54.000	41.95	12.050	1349
			54.98	53.680	42.20	11.480	1416
			AVG = 11.710		AVG = 1389		
209	20356.20	1.627	55.90	54.273	42.25	12.023	1693
			56.65	55.023	42.20	12.823	1587
			55.90	54.273	42.30	11.973	1700
			AVG = 12.273		AVG = 1659		
210	24631.00	1.970	56.95	54.980	42.30	12.680	1943
			57.90	55.930	42.28	13.650	1804
			57.70	55.730	42.30	13.450	1831
			AVG = 13.260		AVG = 1858		

Table B-9 : Experimental Data of Heat Transfer to Saturated Pool  
 Boiling of Methanol at  $25.33 \text{ kN/m}^2 (T_s=32.8^\circ\text{C})$

Run No.	Heat Flux $\text{W/m}^2$	Conduction Correction $^\circ\text{C}$	Recorded Wall Temp. $^\circ\text{C}$	Corrected Wall Temp. $^\circ\text{C}$	Liquid Temp. $^\circ\text{C}$	Wall Superheat $^\circ\text{C}$	Heat Transfer Coefficient $\text{W/m}^2\text{K}$
211	9618.32	0.769	45.75	44.981	35.65	9.331	1031
			47.15	46.381	35.55	10.831	888
			47.95	47.181	35.55	11.631	827
					AVG =10.600	AVG = 907	
212	12824.43	1.025	47.15	46.125	35.70	10.425	1230
			48.20	47.175	35.40	11.775	1089
			48.80	47.775	35.60	12.175	1053
					AVG =11.460	AVG = 1119	
213	16259.50	1.300	49.50	48.200	36.40	11.800	1378
			50.35	49.050	36.35	12.700	1280
			50.35	49.050	36.35	12.700	1280
					AVG =12.400	AVG = 1311	
214	20101.80	1.610	50.95	49.340	36.60	12.740	1578
			51.45	49.840	36.50	13.340	1507
			51.85	50.240	36.50	13.740	1463
					AVG =13.273	AVG = 1515	



Table B-10 : Experimental Data of Heat Transfer to Saturated Pool Boiling of 8.56 wt. % Methanol in Methanol - Water Mixture at  $98.63 \text{ kN/m}^2 (T_s = 92.3^\circ\text{C})$

Run No.	Heat Flux $\text{W/m}^2$	Conduction Correction $^\circ\text{C}$	Recorded Wall Temp. $^\circ\text{C}$	Corrected Wall Temp. $^\circ\text{C}$	Liquid Temp. $^\circ\text{C}$	Wall Superheat $^\circ\text{C}$	Heat Transfer Coefficient $\text{W/m}^2\text{K}$
215	9618.32	0.769	98.10	97.331	92.15	5.181	1856
			97.25	96.481	91.30	5.181	1856
			99.70	98.931	91.55	7.381	1303
					AVG = 5.914	AVG = 1626	
216	12620.90	1.009	99.25	98.241	92.65	5.591	2257
			99.25	98.241	92.25	5.991	2107
			101.00	99.991	92.80	7.191	1755
					AVG = 6.260	AVG = 2016	
217	16488.55	1.320	100.90	99.580	92.90	6.680	2468
			100.15	98.830	92.30	6.530	2525
			101.85	100.530	92.60	7.930	2079
					AVG = 7.047	AVG = 2340	
218	20356.20	1.627	101.45	99.823	93.15	6.673	3051
			101.30	99.673	92.70	6.973	2919
			102.70	101.073	92.85	8.223	2476
					AVG = 7.290	AVG = 2792	
219	24631.00	1.969	102.80	100.831	93.50	7.331	3360
			102.40	100.431	93.30	7.131	3454
			103.90	101.931	93.50	8.431	2921
					AVG = 7.631	AVG = 3228	

Table B-10 : Experimental Data of Heat Transfer to Saturated Pool Boiling of 8.56 wt. % Methanol in Methanol - Water Mixture at  $66.64 \text{ kN/m}^2 (T_s = 81.2^\circ\text{C})$

Run No.	Heat Flux $\text{W/m}^2$	Conduction Correction $^\circ\text{C}$	Recorded Wall Temp. $^\circ\text{C}$	Corrected Wall Temp. $^\circ\text{C}$	Liquid Temp. $^\circ\text{C}$	Wall Superheat $^\circ\text{C}$	Heat Transfer Coefficient $\text{W/m}^2\text{K}$
220	9618.32	0.769	90.20	89.431	84.10	5.331	1804
			90.90	90.131	83.35	6.781	1418
			92.70	91.931	84.00	7.931	1213
					AVG = 6.681	AVG = 1440	
221	12824.40	1.025	90.65	89.625	84.25	5.375	2386
			91.95	90.925	83.90	7.025	1826
			93.95	92.925	84.10	8.825	1453
					AVG = 7.075	AVG = 1813	
222	16488.55	1.320	92.40	91.08	84.90	6.180	2668
			93.20	91.88	83.80	8.080	2041
			95.25	93.93	84.45	9.480	1739
					AVG = 7.913	AVG = 2084	
223	20356.23	1.627	93.35	91.723	85.15	6.573	3097
			93.90	92.273	84.00	8.273	2461
			96.10	94.473	84.45	10.023	2031
					AVG = 8.290	AVG = 2456	
224	24910.94	1.990	94.75	92.760	85.40	7.360	3385
			95.90	93.910	84.25	9.660	2579
			97.20	95.210	84.70	10.510	2370
					AVG = 9.177	AVG = 2715	

Table B-10 : Experimental Data of Heat Transfer to Saturated Pool Boiling of 8.56 wt. % Methanol in Methanol - Water Mixture at  $50.65 \text{ kN/m}^2 (T_s = 74.7^\circ\text{C})$

Run No.	Heat Flux $\text{W/m}^2$	Conduction Correction $^\circ\text{C}$	Recorded Wall Temp. $^\circ\text{C}$	Corrected Wall Temp. $^\circ\text{C}$	Liquid Temp. $^\circ\text{C}$	Wall Superheat $^\circ\text{C}$	Heat Transfer Coefficient $\text{W/m}^2\text{K}$
225	9618.32	0.769	82.35	81.581	75.00	6.581	1462
			82.15	81.381	74.40	6.981	1378
			84.50	83.731	74.70	9.031	1065
					AVG = 7.531	AVG = 1277	
226	12824.43	1.025	83.65	82.625	75.33	7.295	1758
			83.35	82.325	74.90	7.425	1727
			86.10	85.075	75.20	9.875	1299
					AVG = 8.198	AVG = 1564	
227	16488.55	1.320	85.20	83.880	75.55	8.330	1979
			84.90	83.580	75.00	8.580	1921
			87.40	86.080	75.35	10.730	1537
					AVG = 9.213	AVG = 1790	
228	20356.23	1.627	86.50	84.973	75.80	9.173	2219
			86.25	84.623	75.20	9.423	2160
			87.85	86.223	75.35	10.873	1872
					AVG = 9.823	AVG = 2072	
229	25050.00	2.000	88.35	86.350	76.50	9.850	2543
			87.90	85.900	75.90	10.000	2505
			89.80	87.800	76.25	11.550	2169
					AVG = 10.470	AVG = 2393	

Table B-10 : Experimental Data of Heat Transfer to Saturated Pool Boiling of 8.56 wt. % Methanol in Methanol - Water Mixture at  $33.32 \text{ kN/m}^2 (T_s=65.0^\circ\text{C})$

Run No.	Heat Flux $\text{W/m}^2$	Conduction Correction $^\circ\text{C}$	Recorded Wall Temp. $^\circ\text{C}$	Corrected Wall Temp. $^\circ\text{C}$	Liquid Temp. $^\circ\text{C}$	Wall Superheat $^\circ\text{C}$	Heat Transfer Coefficient $\text{W/m}^2\text{K}$
230	9618.32	0.769	74.40	73.631	66.40	7.231	1330
			74.00	73.231	65.80	7.431	1294
			76.90	76.131	66.15	9.981	964
					AVG = 8.214	AVG = 1171	
231	12620.87	1.009	75.25	74.250	66.55	7.700	1639
			75.00	74.000	66.20	7.800	1618
			78.25	77.250	66.35	10.900	1158
					AVG = 8.800	AVG = 1434	
232	16488.55	1.320	76.78	75.460	66.90	8.560	1926
			76.70	75.380	66.62	8.760	1882
			79.55	78.230	66.75	11.480	1436
					AVG = 9.600	AVG = 1718	
233	20356.23	1.627	78.55	76.923	67.10	9.823	2072
			78.55	76.923	66.80	10.123	2011
			80.40	78.773	66.95	11.823	1722
					AVG = 10.589	AVG = 1922	
234	24631.00	1.970	80.00	78.030	67.45	10.580	2328
			79.85	77.880	67.20	10.680	2306
			81.70	79.730	67.45	12.280	2006
					AVG = 11.180	AVG = 2203	

Table B-10 : Experimental Data of Heat Transfer to Saturated Pool Boiling of 8.56 wt. % Methanol in Methanol - Water Mixture at  $25.33 \text{ kN/m}^2 (T_s = 59.0^\circ\text{C})$

Run No.	Heat Flux $\text{W/m}^2$	Conduction Correction $^\circ\text{C}$	Recorded Wall Temp. $^\circ\text{C}$	Corrected Wall Temp. $^\circ\text{C}$	Liquid Temp. $^\circ\text{C}$	Wall Superheat $^\circ\text{C}$	Heat Transfer Coefficient $\text{W/m}^2\text{K}$
235	9618.32	0.769	69.48	68.711	61.20	7.511	1281
			69.10	68.331	60.40	7.931	1213
			72.20	71.431	60.90	10.531	913
					AVG = 8.658	AVG = 1111	
236	12926.20	1.033	70.80	69.767	61.55	8.217	1573
			71.20	70.167	61.22	8.947	1445
			73.45	72.417	61.40	11.017	1173
					AVG = 9.394	AVG = 1376	
237	16488.55	1.320	72.40	71.080	61.85	9.230	1786
			72.70	71.380	61.65	9.730	1695
			75.03	73.710	61.85	11.860	1390
					AVG = 10.273	AVG = 1605	
238	20356.23	1.627	74.25	72.623	62.20	10.423	1953
			74.25	72.623	62.10	10.533	1933
			76.65	75.023	62.40	12.623	1613
					AVG = 11.200	AVG = 1818	

Table B-11 : Experimental Data of Heat Transfer to Saturated Pool Boiling of 16.5 wt.% Methanol in Methanol - Water Mixture at  $98.63 \text{ kN/m}^2 (T_s=87.7^\circ\text{C})$

Run No.	Heat Flux $\text{W/m}^2$	Conduction Correction $^\circ\text{C}$	Recorded Wall Temp. $^\circ\text{C}$	Corrected Wall Temp. $^\circ\text{C}$	Liquid Temp. $^\circ\text{C}$	Wall Superheat $^\circ\text{C}$	Heat Transfer Coefficient $\text{W/m}^2 \text{ K}$
239	9618.32	0.769	97.85	97.081	87.85	9.231	1042
			96.00	95.231	86.70	8.531	1127
			98.20	97.431	87.80	9.631	999
					AVG = 9.131	AVG = 1053	
240	12926.20	1.033	99.05	98.017	88.30	9.717	1330
			97.75	96.717	87.40	9.317	1387
			99.30	98.267	88.00	10.267	1259
					AVG = 9.767	AVG = 1323	
241	16488.55	1.320	100.25	98.930	88.40	10.530	1566
			99.35	98.030	88.25	9.780	1686
			101.05	99.730	88.40	11.330	1455
					AVG = 10.550	AVG = 1563	
242	20356.20	1.627	101.40	99.773	88.55	11.223	1814
			100.58	98.953	88.35	10.603	1920
			102.25	100.623	88.45	12.173	1672
					AVG = 11.330	AVG = 1797	
243	24910.24	1.990	102.95	100.960	89.00	11.960	2083
			101.80	99.810	88.45	11.360	2193
			103.70	101.710	88.70	13.010	1915
					AVG = 12.110	AVG = 2057	

Table B-11 : Experimental Data of Heat Transfer to Saturated Pool Boiling of 16.5 wt.% Methanol in Methanol - Water Mixture at  $66.64 \text{ kN/m}^2 (T_s=76.0^\circ\text{C})$

Run No.	Heat Flux $\text{W/m}^2$	Conduction Correction $^\circ\text{C}$	Recorded Wall Temp. $^\circ\text{C}$	Corrected Wall Temp. $^\circ\text{C}$	Liquid Temp. $^\circ\text{C}$	Wall Superheat $^\circ\text{C}$	Heat Transfer Coefficient $\text{W/m}^2\text{K}$
244	9618.32	0.769	88.20	87.431	77.20	10.231	940
			86.90	86.131	76.80	9.331	1031
			88.50	87.731	76.95	10.781	892
			AVG =10.114		AVG = 951		
245	12824.43	1.025	89.80	88.775	77.55	11.225	1142
			88.55	87.525	77.13	10.395	1234
			90.50	89.475	77.55	11.925	1075
			AVG =11.180		AVG = 1147		
246	16488.55	1.320	91.10	89.780	78.00	11.780	1400
			89.25	87.930	77.50	10.430	1581
			92.50	91.180	77.75	13.430	1228
			AVG =11.880		AVG = 1388		
247	20356.20	1.627	92.15	90.523	78.15	12.373	1645
			91.35	89.723	77.80	11.923	1707
			92.95	91.323	78.00	13.323	1528
			AVG =12.540		AVG = 1623		
248	24910.90	1.990	93.30	91.310	78.45	12.860	1937
			92.10	90.110	78.28	11.830	2106
			94.20	92.210	78.45	13.760	1810
			AVG =12.820		AVG = 1943		

Table B-11 : Experimental Data of Heat Transfer to Saturated Pool Boiling of 16.5 wt. % Methanol in Methanol - Water Mixture at 50.65 kN/m<sup>2</sup> (T<sub>s</sub>=70.0°C)

Run No.	Heat Flux W/m <sup>2</sup>	Conduction Correction °C	Recorded Wall Temp. °C	Corrected Wall Temp. °C	Liquid Temp. °C	Wall Superheat °C	Heat Transfer Coefficient W/m <sup>2</sup> K
249	9618.32	0.769	82.90	82.131	70.78	11.351	847
			81.70	80.931	70.60	10.331	931
			83.30	82.531	70.68	11.851	812
					AVG =11.180	AVG = 860	
250	12824.43	1.025	84.15	83.125	71.10	12.025	1066
			83.75	82.725	70.90	11.825	1085
			84.45	83.425	71.03	12.395	1035
					AVG =12.082	AVG = 1061	
251	16488.55	1.320	85.65	84.330	71.35	12.980	1270
			84.85	83.530	71.25	12.280	1343
			86.55	85.230	71.35	13.890	1187
					AVG =13.050	AVG = 1264	
252	20356.23	1.627	86.70	85.073	71.65	13.423	1517
			86.70	85.073	71.50	13.573	1500
			87.40	85.773	71.55	14.223	1431
					AVG =13.740	AVG = 1482	
253	24910.90	1.990	88.30	86.310	72.00	14.310	1741
			88.00	86.010	71.75	14.260	1747
			89.20	87.210	71.90	15.310	1627
					AVG =14.630	AVG = 1703	



Table B-11 : Experimental Data of Heat Transfer to Saturated Pool Boiling of 16.5 wt.% Methanol in Methanol - Water Mixture at  $33.32 \text{ kN/m}^2 (T_s=60.0^\circ\text{C})$

Run No.	Heat Flux $\text{W/m}^2$	Conduction Correction $^\circ\text{C}$	Recorded Wall Temp. $^\circ\text{C}$	Corrected Wall Temp. $^\circ\text{C}$	Liquid Temp. $^\circ\text{C}$	Wall Superheat $^\circ\text{C}$	Heat Transfer Coefficient $\text{W/m}^2\text{K}$
254	9618.32	0.769	73.35	72.581	60.60	11.981	803
			72.80	72.031	60.05	11.981	803
			73.65	72.881	60.35	12.531	768
			AVG =12.164		AVG = 791		
255	12620.90	1.009	74.70	73.700	60.75	12.950	975
			74.70	73.700	60.65	13.050	967
			75.15	74.150	60.75	13.400	942
			AVG =13.130		AVG = 961		
256	16488.55	1.320	76.15	75.330	61.55	13.780	1197
			76.80	75.480	61.25	14.230	1159
			76.95	75.630	61.50	14.380	1147
			AVG =14.130		AVG = 1167		
257	20356.23	1.627	78.10	76.473	61.80	14.673	1387
			78.60	76.973	61.67	15.303	1330
			79.35	77.723	61.80	15.923	1278
			AVG =15.300		AVG = 1331		

Table B-11 : Experimental Data of Heat Transfer to Saturated Pool Boiling of 16.5 wt.% Methanol in Methanol - Water Mixture at  $25.33 \text{ kN/m}^2 (T_s = 54.0^\circ\text{C})$

Run No.	Heat Flux $\text{W/m}^2$	Conduction Correction $^\circ\text{C}$	Recorded Wall Temp. $^\circ\text{C}$	Corrected Wall Temp. $^\circ\text{C}$	Liquid Temp. $^\circ\text{C}$	Wall Superheat $^\circ\text{C}$	Heat Transfer Coefficient $\text{W/m}^2\text{K}$
258	12620.90	1.009	69.55	68.550	55.05	13.500	935
			70.28	69.280	54.92	14.360	879
			71.85	70.850	54.92	15.930	792
					AVG = 14.600	AVG = 864	
259	16488.55	1.320	71.05	69.730	55.45	14.280	1155
			71.90	70.580	55.25	15.330	1076
			73.10	71.780	55.40	16.380	1007
					AVG = 15.330	AVG = 1076	
260	20356.23	1.627	72.65	71.023	55.53	15.493	1314
			73.50	71.873	55.28	16.593	1227
			74.50	72.873	55.53	17.343	1174
					AVG = 16.480	AVG = 1235	

Table B-12 : Experimental Data of Heat Transfer to Saturated Pool Boiling of 30.8 wt. % Methanol in Methanol - Water Mixture at  $98.63 \text{ kN/m}^2$  ( $T_s = 81.6^\circ\text{C}$ )

Run No.	Heat Flux $\text{W/m}^2$	Conduction Correction $^\circ\text{C}$	Recorded Wall Temp. $^\circ\text{C}$	Corrected Wall Temp. $^\circ\text{C}$	Liquid Temp. $^\circ\text{C}$	Wall Superheat $^\circ\text{C}$	Heat Transfer Coefficient $\text{W/m}^2 \text{K}$
261	9618.32	0.769	92.50	91.731	82.35	9.381	1025
			91.75	90.981	82.00	8.981	1071
			93.95	93.181	82.15	11.031	872
			AVG = 9.798		AVG = 982		
262	12824.43	1.025	93.80	92.775	82.70	10.075	1273
			92.40	91.375	82.30	9.075	1413
			95.90	94.875	82.50	12.375	1036
			AVG = 10.510		AVG = 1220		
263	16488.55	1.320	95.35	94.030	82.95	11.080	1488
			94.75	93.430	82.60	10.830	1522
			97.10	95.780	82.80	12.980	1270
			AVG = 11.630		AVG = 1418		
264	20610.70	1.648	96.50	94.852	83.23	11.622	1773
			96.05	94.402	82.90	11.502	1792
			98.05	96.402	83.23	13.172	1565
			AVG = 12.100		AVG = 1703		
265	24910.94	1.992	98.25	96.258	83.65	12.608	1976
			97.90	95.908	83.35	12.558	1984
			99.70	97.708	83.45	14.258	1747
			AVG = 13.141		AVG = 1896		

Table B-12 : Experimental Data of Heat Transfer to Saturated Pool Boiling of 30.8 wt. % Methanol in Methanol - Water Mixture at  $66.64 \text{ kN/m}^2 (T_s=70.4^\circ\text{C})$

Run No.	Heat Flux $\text{W/m}^2$	Conduction Correction $^\circ\text{C}$	Recorded Wall Temp. $^\circ\text{C}$	Corrected Wall Temp. $^\circ\text{C}$	Liquid Temp. $^\circ\text{C}$	Wall Superheat $^\circ\text{C}$	Heat Transfer Coefficient $\text{W/m}^2 \text{ K}$
266	9618.32	0.769	82.25	81.481	70.95	10.531	913
			81.85	81.081	70.65	10.431	922
			83.45	82.681	70.80	11.881	810
					AVG =10.950	AVG = 878	
267	12824.43	1.025	83.80	82.775	71.28	11.495	1116
			83.50	82.475	70.85	11.625	1103
			84.50	83.475	71.05	12.425	1032
					AVG =11.850	AVG = 1082	
268	16488.55	1.320	85.45	84.130	71.50	12.630	1305
			84.20	82.880	70.90	11.980	1376
			86.00	84.680	71.25	13.430	1228
					AVG =12.680	AVG = 1300	
269	20356.23	1.627	86.70	85.073	71.80	13.273	1534
			86.10	84.473	71.45	13.023	1563
			87.30	85.673	71.45	14.223	1431
					AVG =13.510	AVG = 1507	
270	25190.84	2.014	88.23	86.216	71.95	14.266	1766
			87.60	85.586	71.75	13.836	1821
			88.70	86.686	71.85	14.836	1698
					AVG =14.313	AVG = 1760	

Table B-12 : Experimental Data of Heat Transfer to Saturated Pool Boiling of 30.8 wt. % Methanol in Methanol - Water Mixture at  $50.65 \text{ kN/m}^2 (T_s=64.0^\circ\text{C})$

Run No.	Heat Flux $\text{W/m}^2$	Conduction Correction $^\circ\text{C}$	Recorded Wall Temp. $^\circ\text{C}$	Corrected Wall Temp. $^\circ\text{C}$	Liquid Temp. $^\circ\text{C}$	Wall Superheat $^\circ\text{C}$	Heat Transfer Coefficient $\text{W/m}^2 \text{ K}$
271	9618.32	0.769	76.75	75.981	64.90	11.081	868
			76.75	75.981	64.70	11.281	853
			77.85	77.081	64.70	12.381	777
					AVG =11.581	AVG =	831
272	12824.43	1.025	78.55	77.525	65.15	12.375	1036
			78.25	77.225	64.90	12.325	1041
			78.75	77.725	64.95	12.775	1004
					AVG =12.492	AVG =	1027
273	16488.55	1.320	80.15	78.830	65.40	13.430	1228
			79.60	78.280	65.25	13.030	1265
			80.50	79.180	65.30	13.880	1188
					AVG =13.450	AVG =	1226
274	20356.23	1.627	81.50	79.873	65.65	14.223	1431
			80.60	78.973	65.15	13.823	1473
			82.10	80.473	65.35	15.123	1346
					AVG =14.390	AVG =	1415
275	24910.94	1.992	82.90	80.908	65.80	15.108	1649
			82.15	80.158	65.35	14.808	1682
			83.45	81.458	65.45	16.008	1556
					AVG =15.308	AVG =	1627

Table B-12 : Experimental Data of Heat Transfer to Saturated Pool Boiling of 30.8 wt. % Methanol in Methanol - Water Mixture at  $33.32 \text{ kN/m}^2 (T_s = 54.3^\circ\text{C})$

Run No.	Heat Flux $\text{W/m}^2$	Conduction Correction $^\circ\text{C}$	Recorded Wall Temp. $^\circ\text{C}$	Corrected Wall Temp. $^\circ\text{C}$	Liquid Temp. $^\circ\text{C}$	Wall Superheat $^\circ\text{C}$	Heat Transfer Coefficient $\text{W/m}^2 \text{ K}$
276	9618.32	0.769	67.95	67.181	54.45	12.731	756
			66.85	66.081	54.25	11.831	813
			68.20	67.431	54.35	13.081	735
					AVG = 12.550	AVG = 766	
277	12620.90	1.009	69.55	68.55	54.80	13.750	918
			69.00	68.00	54.65	13.350	945
			70.45	69.45	54.80	14.650	862
					AVG = 13.920	AVG = 907	
278	16488.55	1.320	71.03	69.710	55.00	14.710	1121
			70.55	69.230	54.92	14.310	1152
			72.33	71.010	55.15	15.860	1040
					AVG = 14.960	AVG = 1102	
279	20356.23	1.627	72.55	70.923	55.40	15.523	1311
			72.20	70.573	55.20	15.373	1324
			73.10	71.473	55.40	16.073	1266
					AVG = 15.660	AVG = 1300	
280	25239.19	2.020	74.10	72.080	55.80	16.280	1550
			73.70	71.680	55.45	16.230	1555
			75.00	72.980	55.75	17.230	1465
					AVG = 16.580	AVG = 1522	

Table B-12 : Experimental Data of Heat Transfer to Saturated Pool Boiling of 30.8 wt. % Methanol in Methanol - Water Mixture at  $29.32 \text{ kN/m}^2 (T_s = 51.4^\circ\text{C})$

Run No.	Heat Flux $\text{W/m}^2$	Conduction Correction $^\circ\text{C}$	Recorded Wall Temp. $^\circ\text{C}$	Corrected Wall Temp. $^\circ\text{C}$	Liquid Temp. $^\circ\text{C}$	Wall Superheat $^\circ\text{C}$	Heat Transfer Coefficient $\text{W/m}^2 \text{ K}$
281	9796.44	0.783	64.55	63.767	50.30	13.470	727
			64.20	63.417	50.10	13.317	736
			65.45	64.667	50.25	14.417	680
					AVG = 13.735	AVG = 713	
282	12824.43	1.025	66.30	65.275	50.55	14.725	871
			65.35	64.325	50.25	14.075	911
			66.75	65.725	50.25	15.475	829
					AVG = 14.760	AVG = 869	
283	16488.55	1.320	68.30	66.980	50.85	16.130	1022
			67.45	66.130	50.85	15.280	1079
			68.80	67.480	50.90	16.580	994
					AVG = 16.000	AVG = 1031	
284	20356.23	1.627	69.45	67.823	51.10	16.723	1217
			69.40	67.773	50.93	16.843	1209
			69.90	68.273	51.17	17.103	1190
					AVG = 16.890	AVG = 1205	

Table B-13 : Experimental Data of Heat Transfer to Saturated Pool Boiling of 43.24 wt. % Methanol in Methanol - Water Mixture at  $98.63 \text{ kN/m}^2 (T_s=78.1^\circ\text{C})$

Run No.	Heat Flux $\text{W/m}^2$	Conduction Correction $^\circ\text{C}$	Recorded Wall Temp. $^\circ\text{C}$	Corrected Wall Temp. $^\circ\text{C}$	Liquid Temp. $^\circ\text{C}$	Wall Superheat $^\circ\text{C}$	Heat Transfer Coefficient $\text{W/m}^2 \text{ K}$
285	9618.32	0.769	89.65	88.881	79.55	9.331	1031
			89.00	88.231	79.35	8.881	1083
			90.75	89.981	79.55	10.431	922
					AVG = 9.548	AVG = 1007	
286	12417.30	0.993	90.75	89.757	80.00	9.757	1273
			90.15	89.157	79.70	9.457	1313
			92.70	91.707	79.80	11.907	1043
					AVG = 10.374	AVG = 1197	
287	16030.53	1.282	92.50	91.218	80.50	10.718	1496
			91.30	90.018	80.15	9.868	1624
			94.05	92.768	80.25	12.518	1281
					AVG = 11.035	AVG = 1453	
288	19847.33	1.587	93.80	92.213	80.80	11.413	1739
			93.05	91.463	80.65	10.813	1836
			95.60	94.013	80.75	13.263	1496
					AVG = 11.830	AVG = 1678	
289	25190.84	2.014	95.25	93.236	81.05	12.186	2067
			94.70	92.686	80.90	11.786	2137
			97.10	95.086	81.05	14.036	1795
					AVG = 12.670	AVG = 1988	



Table B-13 : Experimental Data of Heat Transfer to Saturated Pool Boiling of 43.24 wt. % Methanol in Methanol - Water Mixture at  $66.64 \text{ kN/m}^2 (T_s=67.2^\circ\text{C})$

Run No.	Heat Flux $\text{W/m}^2$	Conduction Correction $^\circ\text{C}$	Recorded Wall Temp. $^\circ\text{C}$	Corrected Wall Temp. $^\circ\text{C}$	Liquid Temp. $^\circ\text{C}$	Wall Superheat $^\circ\text{C}$	Heat Transfer Coefficient $\text{W/m}^2 \text{ K}$
290	9618.32	0.769	79.45	78.681	68.40	10.281	936
			78.35	77.581	67.95	9.681	999
			80.13	79.361	68.10	11.261	854
					AVG =10.391	AVG = 926	
291	12824.43	1.025	80.75	79.725	68.50	11.225	1142
			79.55	78.525	68.25	10.275	1248
			81.63	80.605	68.30	12.305	1042
					AVG =11.270	AVG = 1138	
292	16259.54	1.300	82.05	80.750	68.65	12.100	1344
			81.25	79.950	68.45	11.500	1414
			82.95	81.650	68.58	13.070	1244
					AVG =12.220	AVG = 1331	
293	20101.80	1.610	83.25	81.640	68.80	12.840	1566
			82.30	80.690	68.70	11.990	1677
			84.90	83.290	68.80	14.490	1387
					AVG =13.110	AVG = 1533	
294	25190.84	2.014	85.20	83.186	69.00	14.186	1776
			83.55	81.536	68.88	12.656	1990
			86.35	84.336	69.00	15.336	1643
					AVG =14.060	AVG = 1792	

Table B-13 : Experimental Data of Heat Transfer to Saturated Pool Boiling of 43.24 wt. % Methanol in Methanol - Water Mixture at  $50.65 \text{ kN/m}^2 (T_s = 60.0^\circ\text{C})$

Run No.	Heat Flux $\text{W/m}^2$	Conduction Correction $^\circ\text{C}$	Recorded Wall Temp. $^\circ\text{C}$	Corrected Wall Temp. $^\circ\text{C}$	Liquid Temp. $^\circ\text{C}$	Wall Superheat $^\circ\text{C}$	Heat Transfer Coefficient $\text{W/m}^2 \text{ K}$
295	9440.20	0.7555	72.20	71.445	60.75	10.695	883
			71.75	70.995	60.55	10.445	904
			73.10	72.345	60.85	11.495	821
					AVG = 10.880	AVG = 868	
296	12620.90	1.009	73.60	72.591	61.05	11.541	1094
			73.15	72.141	60.83	11.311	1116
			75.00	73.991	61.10	12.891	979
					AVG = 11.914	AVG = 1059	
297	16946.56	1.355	75.60	74.245	61.45	12.795	1324
			74.80	73.445	60.90	12.545	1351
			76.80	75.445	61.20	12.245	1384
					AVG = 13.200	AVG = 1284	
298	20356.23	1.627	76.95	75.323	61.70	13.623	1494
			76.30	74.673	61.55	13.123	1551
			77.85	76.223	61.68	14.543	1400
					AVG = 13.763	AVG = 1479	

Table B-13 : Experimental Data of Heat Transfer to Saturated Pool Boiling of 43.24 wt. % Methanol in Methanol - Water Mixture at 33.32 kN/m<sup>2</sup> (T<sub>s</sub>=51.0°C)

Run No.	Heat Flux W/m <sup>2</sup>	Conduction Correction °C	Recorded Wall Temp. °C	Corrected Wall Temp. °C	Liquid Temp. °C	Wall Superheat °C	Heat Transfer Coefficient W/m <sup>2</sup> K
299	9618.32	0.769	64.10	63.331	51.25	12.081	796
			63.75	62.981	50.93	12.051	798
			64.95	64.181	51.15	13.031	738
					AVG =12.390	AVG =	776
300	12824.43	1.025	65.65	64.625	51.45	13.175	973
			65.10	64.075	51.30	12.775	1004
			66.65	65.625	51.40	14.225	902
					AVG =13.392	AVG =	958
301	16488.55	1.320	67.20	65.880	51.75	14.130	1167
			67.00	65.680	51.50	14.180	1163
			68.10	66.780	51.80	14.980	1101
					AVG =14.430	AVG =	1143
302	19847.33	1.587	68.60	67.013	52.10	14.913	1331
			68.30	66.713	51.88	14.833	1338
			69.60	68.013	52.10	15.913	1247
					AVG =15.220	AVG =	1304
303	25190.84	2.014	70.40	68.386	52.30	16.086	1566
			69.55	67.536	52.13	15.406	1635
			71.30	69.286	52.20	17.086	1474
					AVG =16.193	AVG =	1556

Table B-13 : Experimental Data of Heat Transfer to Saturated Pool Boiling of 43.24 wt. % Methanol in Methanol - Water Mixture at 25.33 kN/m<sup>2</sup> (T<sub>s</sub>=45.5°C)

Run No.	Heat Flux W/m <sup>2</sup>	Conduction Correction °C	Recorded Wall Temp. °C	Corrected Wall Temp. °C	Liquid Temp. °C	Wall Superheat °C	Heat Transfer Coefficient W/m <sup>2</sup> K
304	9796.44	0.783	60.20	59.417	46.10	13.317	736
			59.75	58.967	45.85	13.117	747
			60.95	60.167	46.00	14.167	692
			AVG =13.534		AVG = 724		
305	12620.87	1.009	61.70	60.691	46.35	14.341	880
			60.95	59.941	46.15	13.791	915
			62.20	61.191	46.20	14.991	842
			AVG =14.374		AVG = 878		
306	16946.56	1.355	63.60	62.245	46.60	15.645	1083
			62.70	61.345	46.30	15.045	1126
			63.80	62.445	46.50	15.945	1063
			AVG =15.545		AVG = 1090		
307	20356.23	1.627	64.85	63.223	47.00	16.223	1255
			64.85	63.223	46.73	16.493	1234
			65.60	63.973	47.03	16.943	1201
			AVG =16.553		AVG = 1230		

Table B-14 : Experimental Data of Heat Transfer to Saturated Pool Boiling of 64.0 wt. % Methanol in Methanol - Water Mixture at  $98.63 \text{ kN/m}^2$  ( $T_s = 73.3^\circ\text{C}$ )

Run No.	Heat Flux $\text{W/m}^2$	Conduction Correction $^\circ\text{C}$	Recorded Wall Temp. $^\circ\text{C}$	Corrected Wall Temp. $^\circ\text{C}$	Liquid Temp. $^\circ\text{C}$	Wall Superheat $^\circ\text{C}$	Heat Transfer Coefficient $\text{W/m}^2 \text{ K}$
308	12824.40	1.025	83.45	82.425	73.80	8.625	1487
			85.15	84.125	73.50	10.625	1270
			84.35	83.325	73.65	9.675	1326
			AVG = 9.642		AVG = 1330		
309	16488.55	1.320	84.50	83.180	74.05	9.130	1806
			86.45	85.130	73.75	11.380	1449
			86.10	84.780	73.85	10.930	1509
			AVG = 10.480		AVG = 1573		
310	20610.70	1.648	85.85	84.202	74.30	9.902	2081
			87.60	85.952	74.13	11.822	1743
			87.25	85.602	74.20	11.402	1808
			AVG = 11.042		AVG = 1867		
311	24631.00	1.970	87.25	85.280	74.45	10.830	2274
			89.10	87.130	74.25	12.880	1912
			88.10	86.130	74.40	11.730	2100
			AVG = 11.813		AVG = 2085		
312	30534.35	2.441	88.55	86.109	74.63	11.480	2660
			90.50	88.060	74.50	13.560	2252
			90.05	87.609	74.50	13.110	2329
			AVG = 12.720		AVG = 2401		

Table B-14 : Experimental Data of Heat Transfer to Saturated Pool Boiling of 64.0 wt. % Methanol in Methanol - Water Mixture at  $66.64 \text{ kN/m}^2 (T_s=62.4^\circ\text{C})$

Run No.	Heat Flux $\text{W/m}^2$	Conduction Correction $^\circ\text{C}$	Recorded Wall Temp. $^\circ\text{C}$	Corrected Wall Temp. $^\circ\text{C}$	Liquid Temp. $^\circ\text{C}$	Wall Superheat $^\circ\text{C}$	Heat Transfer Coefficient $\text{W/m}^2 \text{ K}$
313	9618.32	0.769	72.50	71.731	63.10	8.631	1114
			74.10	73.331	62.85	10.481	918
			74.10	73.331	63.05	10.281	935
					AVG = 9.798	AVG = 982	
314	12417.30	0.993	74.20	73.207	63.30	9.907	1253
			75.65	74.657	63.15	11.507	1079
			74.85	73.857	63.25	10.607	1171
					AVG = 10.674	AVG = 1163	
315	16488.55	1.320	75.25	73.930	63.50	10.430	1581
			77.55	76.230	63.35	12.880	1280
			76.20	74.880	63.50	11.380	1449
					AVG = 11.560	AVG = 1426	
316	20610.70	1.648	76.60	74.952	63.65	11.302	1824
			78.90	77.252	63.50	13.752	1499
			77.45	75.802	63.70	12.102	1703
					AVG = 12.385	AVG = 1664	
317	24910.94	1.992	78.55	76.558	63.85	12.708	1960
			79.55	77.558	63.70	13.858	1798
			78.95	76.958	63.75	13.208	1886
					AVG = 13.260	AVG = 1879	

Table B-14 : Experimental Data of Heat Transfer to Saturated Pool Boiling of 64.0 wt.% Methanol in Methanol - Water Mixture at  $49.32 \text{ kN/m}^2 (T_s=56.1^\circ\text{C})$

Run No.	Heat Flux $\text{W/m}^2$	Conduction Correction $^\circ\text{C}$	Recorded Wall Temp. $^\circ\text{C}$	Corrected Wall Temp. $^\circ\text{C}$	Liquid Temp. $^\circ\text{C}$	Wall Superheat $^\circ\text{C}$	Heat Transfer Coefficient $\text{W/m}^2 \text{ K}$
318	9618.32	0.769	65.75	64.981	55.25	9.731	988
			66.95	66.181	54.95	11.231	856
			66.35	65.581	55.10	10.481	917
					AVG =10.481	AVG = 918	
319	12824.43	1.025	67.00	65.975	55.40	10.575	1213
			68.60	67.575	55.28	12.295	1043
			67.70	66.675	55.40	11.275	1137
					AVG =11.382	AVG = 1127	
320	16488.55	1.320	68.65	67.330	55.67	11.660	1414
			69.50	68.180	55.55	12.630	1306
			69.50	68.180	55.60	12.580	1311
					AVG =12.290	AVG = 1342	
321	20356.23	1.627	70.40	68.773	55.90	12.873	1581
			71.05	69.423	55.75	13.673	1489
			70.60	68.973	55.85	13.123	1551
					AVG =13.223	AVG = 1539	

Table : B-14 : Experimental Data of Heat Transfer to Saturated Pool Boiling of 64.0 wt. % Methanol in Methanol - Water Mixture at  $33.32 \text{ kN/m}^2 (T_s = 46.3^\circ\text{C})$

Run No.	Heat Flux $\text{W/m}^2$	Conduction Correction $^\circ\text{C}$	Recorded Wall Temp. $^\circ\text{C}$	Corrected Wall Temp. $^\circ\text{C}$	Liquid Temp. $^\circ\text{C}$	Wall Superheat $^\circ\text{C}$	Heat Transfer Coefficient $\text{W/m}^2\text{K}$
322	9618.32	0.769	57.15	56.381	46.10	10.281	936
			58.50	57.731	45.90	11.831	813
			57.80	57.031	45.98	11.051	870
			AVG = 11.054		AVG = 870		
323	12620.90	1.009	58.45	57.441	46.25	11.191	1128
			59.60	58.591	46.15	12.441	1014
			59.60	58.591	46.25	12.341	1023
			AVG = 11.991		AVG = 1053		
324	16717.55	1.337	60.15	58.813	46.52	12.293	1360
			61.30	59.963	46.40	13.563	1233
			61.10	59.763	46.45	13.313	1256
			AVG = 13.056		AVG = 1280		
325	20356.23	1.627	61.90	60.273	46.70	13.573	1500
			62.55	60.923	46.53	14.393	1414
			62.25	60.623	46.70	13.923	1462
			AVG = 13.963		AVG = 1458		
326	25190.84	2.014	63.50	61.486	46.95	14.536	1733
			64.20	62.186	46.80	15.386	1637
			64.05	62.036	46.85	15.186	1659
			AVG = 15.036		AVG = 1675		



Table B-14 : Experimental Data of Heat Transfer to Saturated Pool Boiling of 64.0 wt. % Methanol in Methanol - Water Mixture at  $26.66 \text{ kN/m}^2$  ( $T_s=42.0^\circ\text{C}$ )

Run No.	Heat Flux $\text{W/m}^2$	Conduction Correction $^\circ\text{C}$	Recorded Wall Temp. $^\circ\text{C}$	Corrected Wall Temp. $^\circ\text{C}$	Liquid Temp. $^\circ\text{C}$	Wall Superheat $^\circ\text{C}$	Heat Transfer Coefficient $\text{W/m}^2 \text{ K}$
327	9974.55	0.797	54.35	53.553	42.30	11.253	886
			55.10	54.303	42.15	12.153	821
			56.60	55.803	42.20	13.603	733
					AVG =12.340	AVG = 808	
328	12620.90	1.009	55.90	54.891	42.55	12.341	1023
			56.75	55.741	42.43	13.311	948
			57.73	56.721	42.65	14.071	897
					AVG =13.241	AVG = 953	
329	16488.55	1.320	57.60	56.280	42.80	13.480	1223
			58.55	57.230	42.65	14.580	1131
			59.50	58.180	42.85	15.330	1076
					AVG =14.463	AVG = 1140	
330	20356.23	1.627	58.65	57.023	43.15	13.873	1467
			60.15	58.523	43.00	15.523	1311
			61.22	59.593	43.25	16.343	1246
					AVG =15.250	AVG = 1335	

Table B-15 : Experimental Data of Heat Transfer to Saturated Pool  
 Boiling of Isopropanol at  $98.63 \text{ kN/m}^2 (T_s=81.6^\circ\text{C})$

Run No.	Heat Flux $\text{W/m}^2$	Conduction Correction $^\circ\text{C}$	Recorded Wall Temp. $^\circ\text{C}$	Corrected Wall Temp. $^\circ\text{C}$	Liquid Temp. $^\circ\text{C}$	Wall Superheat $^\circ\text{C}$	Heat Transfer Coefficient $\text{W/m}^2\text{K}$
331	9974.55	0.797	88.90	88.103	80.65	7.453	1338
			89.80	89.003	79.80	9.203	1084
			87.55	86.753	80.55	6.203	1608
					AVG = 7.620	AVG = 1309	
332	12783.72	1.022	90.55	89.528	81.80	7.728	1654
			91.50	90.478	81.15	9.328	1370
			90.25	89.228	81.90	7.328	1745
					AVG = 8.130	AVG = 1572	
333	16305.34	1.304	92.50	91.196	82.13	9.066	1798
			92.95	91.646	81.60	10.046	1622
			91.75	90.446	82.13	8.316	1960
					AVG = 9.143	AVG = 1783	
334	20865.14	1.668	94.20	92.532	82.48	10.052	2076
			94.80	93.132	82.10	11.032	1891
			92.70	91.032	82.35	8.682	2403
					AVG = 9.922	AVG = 2103	
335	25190.84	2.014	95.78	93.766	82.95	10.820	2328
			96.10	94.086	82.13	11.956	2107
			93.90	91.886	82.80	9.086	2772
					AVG = 10.622	AVG = 2372	

Table B-15 : Experimental Data of Heat Transfer to Saturated Pool  
 Boiling of Isopropanol at  $69.31 \text{ kN/m}^2 (T_s = 73.0^\circ\text{C})$

Run No.	Heat Flux $\text{W/m}^2$	Conduction Correction $^\circ\text{C}$	Recorded Wall Temp. $^\circ\text{C}$	Corrected Wall Temp. $^\circ\text{C}$	Liquid Temp. $^\circ\text{C}$	Wall Superheat $^\circ\text{C}$	Heat Transfer Coefficient $\text{W/m}^2\text{K}$
336	9656.50	0.772	81.13	80.358	72.18	8.178	1181
			82.00	81.228	71.55	9.678	998
			80.00	79.228	72.18	7.048	1370
					AVG = 8.301	AVG = 1163	
337	13027.99	1.042	81.90	80.858	72.28	8.578	1519
			83.38	82.338	71.70	10.638	1225
			81.03	79.988	72.28	7.708	1690
					AVG = 8.975	AVG = 1452	
338	16488.55	1.318	82.70	81.382	72.28	9.102	1812
			84.25	82.932	71.58	11.352	1452
			81.60	80.282	72.18	8.102	2035
					AVG = 9.519	AVG = 1732	
339	20610.70	1.648	84.35	82.702	72.60	10.102	2040
			86.10	84.452	72.50	11.952	1724
			83.15	81.502	72.50	9.002	2290
					AVG = 10.352	AVG = 1991	
340	25190.84	2.014	86.25	84.236	72.95	11.286	2232
			87.00	84.986	72.50	12.486	2018
			85.35	83.336	72.95	10.386	2425
					AVG = 11.384	AVG = 2210	

Table B-15 : Experimental Data of Heat Transfer to Saturated Pool  
 Boiling of Isopropanol at  $48.0 \text{ kN/m}^2 (T_s = 64.5^\circ\text{C})$

Run No.	Heat Flux $\text{W/m}^2$	Conduction Correction $^\circ\text{C}$	Recorded Wall Temp. $^\circ\text{C}$	Corrected Wall Temp. $^\circ\text{C}$	Liquid Temp. $^\circ\text{C}$	Wall Superheat $^\circ\text{C}$	Heat Transfer Coefficient $\text{W/m}^2\text{K}$
341	10297.71	0.823	72.28	71.457	62.70	8.757	1176
			73.40	72.577	62.03	10.547	976
			72.03	71.207	62.50	8.707	1183
					AVG = 9.337	AVG = 1103	
342	13027.99	1.042	74.00	72.958	63.15	9.808	1328
			75.00	73.958	62.50	11.458	1137
			72.95	71.908	63.15	8.758	1487
					AVG = 10.008	AVG = 1303	
343	16832.10	1.346	75.80	74.454	63.50	10.954	1537
			76.90	75.554	63.25	12.304	1368
			74.53	73.184	63.65	9.534	1765
					AVG = 10.930	AVG = 1540	
344	20610.70	1.648	77.28	75.632	63.90	11.732	1757
			78.25	76.602	63.50	13.102	1573
			75.78	74.132	63.90	10.232	2014
					AVG = 11.690	AVG = 1763	
345	25190.84	2.014	78.75	76.736	63.98	12.746	1974
			79.35	77.336	63.60	13.736	1833
			77.15	75.136	63.88	11.256	2237
					AVG = 12.576	AVG = 2001	

Table B-15 : Experimental Data of Heat Transfer to Saturated Pool  
 Boiling of Isopropanol at  $34.66 \text{ kN/m}^2 (T_s = 57.3^\circ\text{C})$

Run No.	Heat Flux $\text{W/m}^2$	Conduction Correction $^\circ\text{C}$	Recorded Wall Temp. $^\circ\text{C}$	Corrected Wall Temp. $^\circ\text{C}$	Liquid Temp. $^\circ\text{C}$	Wall Superheat $^\circ\text{C}$	Heat Transfer Coefficient $\text{W/m}^2\text{K}$
346	10117.05	0.809	68.10	67.291	57.35	9.941	1018
			69.15	68.341	56.70	11.641	869
			67.63	66.821	57.23	9.591	1055
					AVG = 10.391	AVG = 974	
347	13027.99	1.042	70.10	69.058	58.08	10.978	1187
			71.00	69.958	57.40	12.558	1037
			68.98	67.938	58.08	9.858	1322
					AVG = 11.131	AVG = 1170	
348	16488.55	1.318	71.30	69.982	58.20	11.782	1399
			72.60	71.282	57.55	13.732	1201
			70.45	69.132	58.15	10.982	1501
					AVG = 12.165	AVG = 1355	
349	20610.70	1.648	72.83	71.182	58.35	12.832	1606
			74.00	72.352	57.75	14.602	1412
			71.50	69.852	58.15	11.702	1761
					AVG = 13.045	AVG = 1580	
350	25190.84	2.014	74.45	72.436	58.90	13.536	1861
			76.03	74.016	58.50	15.516	1624
			73.15	71.136	58.75	12.386	2034
					AVG = 13.813	AVG = 1824	

Table B-15 : Experimental Data of Heat Transfer to Saturated Pool  
Boiling of Isopropanol at  $12.66 \text{ kN/m}^2$  ( $T_s = 38.1^\circ\text{C}$ )

Run No.	Heat Flux $\text{W/m}^2$	Conduction Correction $^\circ\text{C}$	Recorded Wall Temp. $^\circ\text{C}$	Corrected Wall Temp. $^\circ\text{C}$	Liquid Temp. $^\circ\text{C}$	Wall Superheat $^\circ\text{C}$	Heat Transfer Coefficient $\text{W/m}^2\text{K}$
351	9656.50	0.772	52.80	52.028	39.10	12.928	747
			55.15	54.378	38.95	15.428	626
			54.10	53.328	39.03	14.298	675
					AVG = 14.218	AVG = 679	
352	13027.99	1.042	54.35	53.308	39.40	13.908	937
			56.35	55.308	39.03	16.278	800
			55.63	54.588	39.40	15.188	858
					AVG = 15.125	AVG = 861	
353	16717.56	1.337	55.80	54.463	39.60	14.863	1125
			57.85	56.513	39.28	17.233	970
			57.10	55.763	39.52	16.243	1029
					AVG = 16.113	AVG = 1038	
354	20610.70	1.648	57.00	55.352	40.00	15.352	1343
			60.35	58.702	39.45	19.252	1071
			58.95	57.302	40.00	17.302	1191
					AVG = 17.302	AVG = 1191	

Table B-16 : Experimental Data of Heat Transfer to Saturated Pool Boiling of 15.0 wt. % Isopropanol in Isopropanol - Water Mixture at  $98.63 \text{ kN/m}^2 (T_s=84.6^\circ\text{C})$

Run No.	Heat Flux $\text{W/m}^2$	Conduction Correction $^\circ\text{C}$	Recorded Wall Temp. $^\circ\text{C}$	Corrected Wall Temp. $^\circ\text{C}$	Liquid Temp. $^\circ\text{C}$	Wall Superheat $^\circ\text{C}$	Heat Transfer Coefficient $\text{W/m}^2 \text{ K}$
355	9974.55	0.798	93.90	93.102	86.00	7.102	1404
			96.90	96.102	85.20	10.902	915
			97.80	97.002	85.90	11.102	898
					AVG = 9.702	AVG = 1028	
356	12946.56	1.035	95.35	94.315	86.13	8.185	1582
			98.10	97.065	85.35	11.715	1105
			98.80	97.765	86.13	11.635	1113
					AVG = 10.510	AVG = 1232	
357	16717.56	1.337	96.88	95.543	86.80	8.743	1912
			99.80	98.463	86.00	12.463	1341
			99.90	98.563	86.58	11.983	1395
					AVG = 11.063	AVG = 1511	
358	20865.14	1.668	98.10	96.432	87.13	9.302	2243
			101.25	99.582	86.15	13.432	1553
			101.50	99.832	87.03	12.802	1630
					AVG = 11.845	AVG = 1762	
359	25190.84	2.014	99.45	97.436	87.45	9.986	2523
			102.58	100.566	86.50	14.066	1791
			102.58	100.566	87.20	13.366	1885
					AVG = 12.473	AVG = 2020	

Table B-16 : Experimental Data of Heat Transfer to Saturated Pool Boiling of 15.0 wt. %  
Isopropanol in Isopropanol - Water Mixture at 74.0 kN/m<sup>2</sup> (T<sub>s</sub>=79.2°C)

Run No.	Heat Flux W/m <sup>2</sup>	Conduction Correction °C	Recorded Wall Temp. °C	Corrected Wall Temp. °C	Liquid Temp. °C	Wall Superheat °C	Heat Transfer Coefficient W/m <sup>2</sup> K
360	9974.55	0.798	88.75	87.952	79.45	8.502	1173
			91.75	90.952	78.90	12.052	828
			91.85	91.052	79.55	11.502	867
						AVG =10.685	AVG = 934
361	13027.99	1.042	90.45	89.408	79.35	10.058	1295
			93.53	92.488	78.90	13.588	959
			93.53	92.488	79.45	13.038	999
						AVG =12.228	AVG = 1065
362	16488.55	1.318	91.75	90.432	79.80	10.632	1551
			94.70	93.382	79.15	14.232	1159
			94.80	93.482	79.75	13.732	1201
						AVG =12.865	AVG = 1282
363	20865.14	1.668	93.05	91.382	80.15	11.232	1858
			95.95	94.282	79.75	14.532	1436
			96.20	94.532	80.15	14.382	1451
						AVG =13.382	AVG = 1559
364	25190.84	2.014	94.25	92.236	80.25	11.986	2102
			97.10	95.086	80.00	15.086	1670
			97.50	95.486	80.15	15.336	1643
						AVG =14.136	AVG = 1782



Table B-16 : Experimental Data of Heat Transfer to Saturated Pool Boiling of 15.0 wt. % Isopropanol in Isopropanol - Water Mixture at  $49.32 \text{ kN/m}^2 (T_s = 74.1^\circ\text{C})$

Run No.	Heat Flux $\text{W/m}^2$	Conduction Correction $^\circ\text{C}$	Recorded Wall Temp. $^\circ\text{C}$	Corrected Wall Temp. $^\circ\text{C}$	Liquid Temp. $^\circ\text{C}$	Wall Superheat $^\circ\text{C}$	Heat Transfer Coefficient $\text{W/m}^2 \text{ K}$
365	10297.71	0.823	81.70	80.877	71.70	9.177	1122
			84.70	83.877	71.15	12.727	809
			83.70	82.877	71.50	11.377	905
					AVG = 11.097	AVG = 928	
366	12783.72	1.022	83.55	82.528	72.70	9.828	1301
			87.80	86.778	72.38	14.400	888
			85.80	84.778	72.60	12.178	1050
					AVG = 12.135	AVG = 1053	
367	16832.10	1.346	84.90	83.554	72.90	10.654	1580
			89.45	88.104	72.45	15.654	1075
			87.25	85.904	72.90	13.004	1291
					AVG = 13.104	AVG = 1285	
368	20610.70	1.648	86.25	84.602	73.15	11.452	1800
			91.00	89.352	72.85	16.502	1249
			88.50	86.852	73.20	13.652	1510
					AVG = 13.869	AVG = 1486	

Table B-16 : Experimental Data of Heat Transfer to Saturated Pool Boiling of 15.0 wt. % Isopropanol in Isopropanol - Water Mixture at  $33.32 \text{ kN/m}^2 (T_s=64.4^\circ\text{C})$

Run No.	Heat Flux $\text{W/m}^2$	Conduction Correction $^\circ\text{C}$	Recorded Wall Temp. $^\circ\text{C}$	Corrected Wall Temp. $^\circ\text{C}$	Liquid Temp. $^\circ\text{C}$	Wall Superheat $^\circ\text{C}$	Heat Transfer Coefficient $\text{W/m}^2 \text{ K}$
369	9974.55	0.797	78.08	77.283	67.52	9.763	1022
			80.15	79.353	66.72	12.633	790
			81.03	80.233	67.30	12.933	771
					AVG =11.776	AVG = 847	
370	13603.05	1.088	79.60	78.512	67.70	10.812	1258
			81.05	79.962	66.72	13.242	1027
			83.55	82.462	67.75	14.912	912
					AVG =12.989	AVG = 1047	
371	16717.56	1.337	81.70	80.363	67.95	12.413	1347
			83.23	81.893	67.00	14.893	1123
			84.90	83.563	68.10	15.463	1081
					AVG =14.256	AVG = 1172	
372	21801.53	1.743	83.70	81.957	68.30	13.657	1596
			85.15	83.407	67.55	15.857	1375
			86.75	85.007	68.30	16.707	1305
					AVG =15.407	AVG = 1415	

Table B-16 : Experimental Data of Heat Transfer to Saturated Pool Boiling of 15.0 wt. % Isopropanol in Isopropanol - Water Mixture at 25.33 kN/m<sup>2</sup> (T<sub>s</sub>=59.8°C)

Run No.	Heat Flux W/m <sup>2</sup>	Conduction Correction °C	Recorded Wall Temp. °C	Corrected Wall Temp. °C	Liquid Temp. °C	Wall Superheat °C	Heat Transfer Coefficient W/m <sup>2</sup> K
373	13027.99	1.042	72.72	71.678	61.25	10.428	1249
			77.00	75.958	60.50	15.458	843
			77.00	75.958	60.65	15.308	851
			AVG =13.731		AVG = 949		
374	16717.56	1.337	74.82	73.483	61.75	11.733	1425
			78.45	77.113	61.00	16.113	1038
			79.40	78.063	61.50	16.563	1009
			AVG =14.803		AVG = 1129		
375	20610.70	1.648	76.25	74.602	61.93	12.672	1626
			79.80	78.152	61.25	16.902	1219
			80.82	79.172	61.65	17.522	1176
			AVG =15.699		AVG = 1313		

Table B-17 : Experimental Data of Heat Transfer to Saturated Pool Boiling of 22.5 wt. % Isopropanol in Isopropanol - Water Mixture at 98.63 kN/m<sup>2</sup> (T<sub>s</sub>=83.1°C)

Run No.	Heat Flux W/m <sup>2</sup>	Conduction Correction °C	Recorded Wall Temp. °C	Corrected Wall Temp. °C	Liquid Temp. °C	Wall Superheat °C	Heat Transfer Coefficient W/m <sup>2</sup> K
376	9974.55	0.798	93.05	92.252	84.15	8.102	1231
			98.20	97.402	83.13	14.272	699
			98.25	97.452	83.45	14.002	712
					AVG =12.125	AVG = 823	
377	13771.00	1.100	94.80	93.700	84.15	9.550	1442
			100.05	98.950	83.45	15.500	888
			100.70	99.600	84.33	15.270	902
					AVG =13.440	AVG = 1025	
378	17040.71	1.362	96.10	94.738	84.25	10.488	1624
			101.55	100.188	83.60	16.588	1027
			101.55	100.188	84.35	15.838	1076
					AVG =14.305	AVG = 1191	
379	20610.70	1.648	97.53	95.882	84.50	11.382	1811
			103.10	101.452	84.35	17.102	1205
			103.50	101.852	84.50	17.352	1188
					AVG =15.279	AVG = 1349	
380	25470.74	2.036	99.00	96.964	84.70	12.264	2077
			104.13	102.094	84.35	17.744	1435
			104.90	102.864	84.58	18.284	1393
					AVG =16.097	AVG = 1582	

Table B-17 : Experimental Data of Heat Transfer to Saturated Pool Boiling of 22.5 wt. % Isopropanol in Isopropanol - Water Mixture at  $66.64 \text{ kN/m}^2$  ( $T_s=74.9^\circ\text{C}$ )

Run No.	Heat Flux $\text{W/m}^2$	Conduction Correction $^\circ\text{C}$	Recorded Wall Temp. $^\circ\text{C}$	Corrected Wall Temp. $^\circ\text{C}$	Liquid Temp. $^\circ\text{C}$	Wall Superheat $^\circ\text{C}$	Heat Transfer Coefficient $\text{W/m}^2 \text{ K}$
381	20254.45	1.620	89.43	87.81	75.67	12.140	1668
			96.47	94.85	75.03	19.820	1022
			93.05	91.43	75.78	15.650	1294
					AVG = 15.870	AVG = 1276	
382	25190.84	2.014	91.32	89.306	76.05	13.256	1900
			98.60	96.586	75.75	20.836	1209
			94.80	92.786	75.90	16.886	1492
					AVG = 16.993	AVG = 1482	
383	30534.35	2.441	93.95	91.509	76.80	14.709	2076
			100.70	98.259	76.50	21.759	1403
			97.10	94.659	76.90	17.759	1719
					AVG = 18.076	AVG = 1689	

Table B-17 : Experimental Data of Heat Transfer to Saturated Pool Boiling of 22.5 wt. % Isopropanol in Isopropanol - Water Mixture at  $53.32 \text{ kN/m}^2 (T_s = 71.8^\circ\text{C})$

Run No.	Heat Flux $\text{W/m}^2$	Conduction Correction $^\circ\text{C}$	Recorded Wall Temp. $^\circ\text{C}$	Corrected Wall Temp. $^\circ\text{C}$	Liquid Temp. $^\circ\text{C}$	Wall Superheat $^\circ\text{C}$	Heat Transfer Coefficient $\text{W/m}^2 \text{ K}$
384	16717.60	1.337	84.05	82.713	70.18	12.533	1334
			89.85	88.513	69.65	18.863	886
			86.90	85.563	70.30	15.263	1095
					AVG = 15.553	AVG = 1075	
385	20278.62	1.621	85.55	83.929	70.40	13.529	1499
			91.60	89.979	70.10	19.879	1020
			88.45	86.829	70.58	16.249	1248
					AVG = 16.552	AVG = 1225	
386	25190.84	2.014	86.90	84.886	70.80	14.086	1230
			93.00	90.986	70.50	20.486	1230
			90.65	88.636	71.05	17.586	1432
					AVG = 17.386	AVG = 1449	
387	29923.66	2.392	88.55	86.158	71.35	14.808	2021
			94.35	91.958	70.85	21.108	1418
			94.35	91.958	71.45	20.508	1459
					AVG = 18.808	AVG = 1591	

Table B-17 : Experimental Data of Heat Transfer to Saturated Pool Boiling of 22.5 wt. % Isopropanol in Isopropanol - Water Mixture at  $34.66 \text{ kN/m}^2 (T_s=62.0^\circ\text{C})$

Run No.	Heat Flux $\text{W/m}^2$	Conduction Correction $^\circ\text{C}$	Recorded Wall Temp. $^\circ\text{C}$	Corrected Wall Temp. $^\circ\text{C}$	Liquid Temp. $^\circ\text{C}$	Wall Superheat $^\circ\text{C}$	Heat Transfer Coefficient $\text{W/m}^2 \text{ K}$
388	20356.23	1.627	77.90	76.273	62.43	13.843	1471
			82.70	81.073	62.03	19.043	1069
			82.30	80.673	62.43	18.243	1116
					AVG = 17.043	AVG = 1194	
389	25190.84	2.014	79.55	77.536	62.70	14.836	1698
			84.25	82.236	62.35	19.886	1267
			84.25	82.236	62.85	19.386	1299
					AVG = 18.036	AVG = 1397	
390	29923.70	2.392	82.70	80.308	63.30	17.008	1759
			86.00	83.608	62.85	20.758	1441
			85.70	83.308	63.40	19.908	1503
					AVG = 19.226	AVG = 1556	

Table B-18 : Experimental Data of Heat Transfer to Saturated Pool Boiling of 31.25 wt. % Isopropanol in Isopropanol - Water Mixture at  $98.63 \text{ kN/m}^2 (T_s=82.2^\circ\text{C})$

Run No.	Heat Flux $\text{W/m}^2$	Conduction Correction $^\circ\text{C}$	Recorded Wall Temp. $^\circ\text{C}$	Corrected Wall Temp. $^\circ\text{C}$	Liquid Temp. $^\circ\text{C}$	Wall Superheat $^\circ\text{C}$	Heat Transfer Coefficient $\text{W/m}^2 \text{ K}$
391	16717.56	1.337	94.60	93.263	82.13	11.133	1502
			98.00	96.663	81.60	15.063	1110
			97.40	96.063	82.25	13.813	1210
					AVG = 13.336	AVG = 1254	
392	20865.14	1.668	96.55	94.882	82.25	12.632	1652
			99.70	98.032	81.35	16.682	1251
			98.75	97.082	82.10	14.982	1393
					AVG = 14.765	AVG = 1413	
393	24631.00	1.969	98.00	96.031	82.58	13.451	1831
			101.45	99.481	81.85	17.631	1397
			100.30	98.331	82.58	15.751	1564
					AVG = 15.611	AVG = 1578	
394	30534.35	2.441	100.90	98.459	83.55	14.909	2048
			103.80	101.359	83.40	17.959	1700
			102.20	99.759	83.80	15.959	1913
					AVG = 16.276	AVG = 1876	



Table B-18 : Experimental Data of Heat Transfer to Saturated Pool Boiling of 31.25 wt. % Isopropanol in Isopropanol - Water Mixture at  $61.31 \text{ kN/m}^2 (T_s=70.0^\circ\text{C})$

Run No.	Heat Flux $\text{W/m}^2$	Conduction Correction $^\circ\text{C}$	Recorded Wall Temp. $^\circ\text{C}$	Corrected Wall Temp. $^\circ\text{C}$	Liquid Temp. $^\circ\text{C}$	Wall Superheat $^\circ\text{C}$	Heat Transfer Coefficient $\text{W/m}^2 \text{ K}$
395	20610.70	1.648	86.00	84.352	71.05	13.302	1549
			90.55	88.902	70.90	18.002	1145
			88.05	86.402	71.70	14.702	1402
					AVG =15.335	AVG = 1344	
396	25190.84	2.014	87.35	85.336	71.15	14.186	1776
			92.40	90.386	70.88	19.506	1291
			89.38	87.366	71.67	15.696	1605
					AVG =16.463	AVG = 1530	
397	29424.94	2.353	89.35	86.997	71.90	15.097	1941
			94.40	92.047	71.55	20.497	1436
			90.50	88.147	72.00	16.147	1822
					AVG =17.247	AVG = 1706	

Table B-18 : Experimental Data of Heat Transfer to Saturated Pool Boiling of 31.25 wt. % Isopropanol in Isopropanol - Water Mixture at 50.65 kN/m<sup>2</sup> (T<sub>s</sub>=66.8°C)

Run No.	Heat Flux W/m <sup>2</sup>	Conduction Correction °C	Recorded Wall Temp. °C	Corrected Wall Temp. °C	Liquid Temp. °C	Wall Superheat °C	Heat Transfer Coefficient W/m <sup>2</sup> K
398	16717.56	1.337	81.00	79.663	67.00	12.663	1320
			84.80	83.463	66.35	17.113	977
			84.80	83.465	66.95	16.513	1012
						AVG =15.430	AVG = 1083
399	20865.14	1.668	82.45	80.782	67.05	13.732	1519
			86.10	84.432	66.50	17.932	1164
			86.50	84.832	67.20	17.632	1183
						AVG =16.432	AVG = 1270
400	25702.30	2.055	83.90	81.845	67.40	14.445	1779
			87.13	85.075	66.75	18.325	1403
			88.05	85.995	67.50	18.495	1390
						AVG =17.088	AVG = 1504
401	30534.35	2.441	85.55	83.109	67.90	15.209	2008
			88.45	86.009	67.10	18.909	1615
			90.10	87.659	67.70	19.959	1530
						AVG =18.026	AVG = 1694

Table B-18 : Experimental Data of Heat Transfer to Saturated Pool Boiling of 31.25 wt. % Isopropanol in Isopropanol - Water Mixture at  $34.66 \text{ kN/m}^2 (T_s = 58.6^\circ\text{C})$

Run No.	Heat Flux $\text{W/m}^2$	Conduction Correction $^\circ\text{C}$	Recorded Wall Temp. $^\circ\text{C}$	Corrected Wall Temp. $^\circ\text{C}$	Liquid Temp. $^\circ\text{C}$	Wall Superheat $^\circ\text{C}$	Heat Transfer Coefficient $\text{W/m}^2 \text{K}$
402	20865.14	1.668	78.45	76.782	61.80	14.982	1393
			81.80	80.132	61.80	18.332	1138
			81.80	80.132	62.60	17.532	1190
					AVG = 16.949	AVG = 1231	
403	24183.21	1.933	79.80	77.867	62.45	15.417	1569
			83.90	81.967	62.33	19.637	1232
			82.80	80.867	62.93	17.937	1348
					AVG = 17.664	AVG = 1369	
404	31353.70	2.507	80.65	78.143	62.80	15.343	2044
			86.20	83.693	62.60	21.093	1486
			86.20	83.693	63.00	20.693	1515
					AVG = 19.043	AVG = 1647	

Table B-18 : Experimental Data of Heat Transfer to Saturated Pool Boiling of 31.25 wt. % Isopropanol in Isopropanol - Water Mixture at 25.33 kN/m<sup>2</sup> (T<sub>s</sub>=53.7°C)

Run No.	Heat Flux W/m <sup>2</sup>	Conduction Correction °C	Recorded Wall Temp. °C	Corrected Wall Temp. °C	Liquid Temp. °C	Wall Superheat °C	Heat Transfer Coefficient W/m <sup>2</sup> K
405	20865.14	1.668	70.00	68.332	53.10	15.232	1370
			75.00	73.332	52.60	20.732	1006
			75.35	73.682	53.00	20.682	1009
			AVG = 18.882		AVG = 1105		
406	25190.84	2.014	71.50	69.486	53.45	16.036	1571
			76.75	74.736	53.15	21.586	1167
			77.35	75.336	53.55	21.786	1156
			AVG = 19.800		AVG = 1272		
407	30534.35	2.441	73.10	70.659	54.00	16.659	1833
			79.40	76.959	53.80	23.159	1318
			79.55	77.109	54.00	23.109	1321
			AVG = 20.980		AVG = 1455		

Table B-19 : Experimental Data of Heat Transfer to Saturated Pool Boiling of 37.0 wt. % Isopropanol in Isopropanol - Water Mixture at 98.63 kN/m<sup>2</sup> (T<sub>s</sub>=81.5°C)

Run No.	Heat Flux W/m <sup>2</sup>	Conduction Correction °C	Recorded Wall Temp. °C	Corrected Wall Temp. °C	Liquid Temp. °C	Wall Superheat °C	Heat Transfer Coefficient W/m <sup>2</sup> K
408	16946.56	1.355	94.15	92.795	81.70	11.095	1527
			94.45	93.095	81.45	11.645	1455
			95.00	93.645	81.80	11.845	1431
			AVG =11.530		AVG = 1470		
409	20865.14	1.668	95.15	93.482	81.80	11.682	1786
			95.45	93.782	81.05	12.752	1639
			95.70	94.032	81.85	12.182	1713
			AVG =12.200		AVG = 1710		
410	25190.84	2.014	97.00	94.986	82.15	12.836	1963
			97.00	94.986	81.85	13.136	1918
			98.15	96.136	82.25	13.886	1814
			AVG =13.290		AVG = 1896		
411	30839.70	2.466	98.95	96.484	82.55	13.934	2213
			99.45	96.984	82.25	14.734	2093
			99.10	96.634	82.70	13.934	2213
			AVG =14.200		AVG = 2172		

Table B-19 : Experimental Data of Heat Transfer to Saturated Pool Boiling of 37.0 wt. % Isopropanol in Isopropanol - Water Mixture at 64.0 kN/m<sup>2</sup> (T<sub>s</sub>=69.7°C)

Run No.	Heat Flux W/m <sup>2</sup>	Conduction Correction °C	Recorded Wall Temp. °C	Corrected Wall Temp. °C	Liquid Temp. °C	Wall Superheat °C	Heat Transfer Coefficient W/m <sup>2</sup> K
412	16946.56	1.355	84.70	83.345	71.88	11.465	1478
			88.10	86.745	71.20	15.545	1090
			88.00	86.645	71.55	15.095	1123
					AVG =14.035	AVG = 1208	
413	20865.14	1.668	86.75	85.082	72.05	13.032	1601
			90.65	88.982	71.92	17.062	1223
			89.20	87.532	72.25	15.282	1365
					AVG =15.125	AVG = 1380	
414	25702.30	2.055	88.50	86.445	72.60	13.845	1856
			92.60	90.545	72.40	18.145	1417
			90.50	88.445	72.60	15.845	1622
					AVG =15.945	AVG = 1612	
415	30534.35	2.441	90.55	88.109	72.95	15.160	2014
			93.95	91.509	72.60	18.909	1615
			91.75	89.310	73.05	16.260	1878
					AVG =16.780	AVG = 1820	

Table B-19 : Experimental Data of Heat Transfer to Saturated Pool Boiling of 37.0 wt. % Isopropanol in Isopropanol - Water Mixture at 50.65 kN/m<sup>2</sup> (T<sub>s</sub>=65.5°C)

Run No.	Heat Flux W/m <sup>2</sup>	Conduction Correction °C	Recorded Wall Temp. °C	Corrected Wall Temp. °C	Liquid Temp. °C	Wall Superheat °C	Heat Transfer Coefficient W/m <sup>2</sup> K
416	17134.90	1.370	78.95	77.58	65.20	12.380	1384
			83.25	81.88	64.40	17.480	980
			80.70	79.33	64.75	14.580	1175
					AVG =14.813	AVG = 1157	
417	21541.98	1.722	80.95	79.228	65.38	13.850	1555
			84.80	83.078	64.43	18.650	1155
			81.70	79.978	64.90	15.078	1429
					AVG =15.860	AVG = 1358	
418	24961.83	1.996	82.35	80.354	65.60	14.754	1692
			86.10	84.104	64.90	19.204	1300
			83.90	81.904	65.80	16.104	1550
					AVG =16.700	AVG = 1495	
419	30534.35	2.441	84.25	81.809	66.00	15.809	1931
			88.05	85.609	65.70	19.909	1534
			85.15	82.709	66.10	16.609	1838
					AVG =17.442	AVG = 1751	

Table B-19 : Experimental Data of Heat Transfer to Saturated Pool Boiling of 37.0 wt. % Isopropanol in Isopropanol - Water Mixture at 33.32 kN/m<sup>2</sup> (T<sub>s</sub>=55.7°C)

Run No.	Heat Flux W/m <sup>2</sup>	Conduction Correction °C	Recorded Wall Temp. °C	Corrected Wall Temp. °C	Liquid Temp. °C	Wall Superheat °C	Heat Transfer Coefficient W/m <sup>2</sup> K
420	16946.56	1.355	72.15	70.795	57.68	13.115	1292
			76.75	75.395	57.25	18.145	934
			73.80	72.445	57.55	14.895	1138
					AVG =15.385	AVG = 1102	
421	21541.98	1.722	74.30	72.578	58.05	14.528	1483
			78.00	76.278	57.40	18.878	1141
			76.32	74.598	58.05	16.548	1302
					AVG =16.651	AVG = 1294	
422	25984.73	2.077	76.25	74.173	58.65	15.523	1674
			79.55	77.473	58.33	19.143	1357
			78.15	76.073	58.60	17.473	1487
					AVG =17.380	AVG = 1495	
423	30229.00	2.417	77.95	75.533	58.90	16.633	1817
			81.40	78.983	58.45	20.533	1472
			79.50	77.083	58.90	18.183	1662
					AVG =18.450	AVG = 1638	



Table B-19 : Experimental Data of Heat Transfer to Saturated Pool Boiling of 37.0 wt. % Isopropanol in Isopropanol - Water Mixture at 25.33 kN/m<sup>2</sup> (T<sub>s</sub>=51.1°C)

Run No.	Heat Flux W/m <sup>2</sup>	Conduction Correction °C	Recorded Wall Temp. °C	Corrected Wall Temp. °C	Liquid Temp. °C	Wall Superheat °C	Heat Transfer Coefficient W/m <sup>2</sup> K
424	17134.90	1.370	68.00	66.630	51.95	14.680	1167
			71.60	70.230	51.50	18.730	914
			70.20	68.830	51.80	17.030	1006
			AVG =16.813		AVG = 1019		
425	21282.44	1.702	70.15	68.448	52.83	15.618	1363
			73.90	72.198	52.60	19.598	1086
			70.80	69.098	52.95	16.148	1318
			AVG =17.121		AVG = 1243		
426	25190.84	2.014	71.75	69.736	53.05	16.686	1510
			75.55	73.536	52.85	20.686	1218
			72.60	70.586	53.15	17.436	1445
			AVG =18.270		AVG = 1379		

Table B-20 : Experimental Data of Heat Transfer to Saturated Pool Boiling of 59.0 wt. % Isopropanol in Isopropanol - Water Mixture at 98.63 kN/m<sup>2</sup> (T<sub>s</sub>=81.0°C)

Run No.	Heat Flux W/m <sup>2</sup>	Conduction Correction °C	Recorded Wall Temp. °C	Corrected Wall Temp. °C	Liquid Temp. °C	Wall Superheat °C	Heat Transfer Coefficient W/m <sup>2</sup> K
427	9974.55	0.797	90.20	89.403	80.50	8.903	1120
			90.60	89.803	79.90	9.903	1007
			93.15	92.353	80.20	12.153	821
					AVG =10.320	AVG =	967
428	13231.55	1.058	91.00	89.942	80.50	9.442	1401
			93.70	92.642	80.35	12.292	1076
			93.80	92.742	80.50	12.242	1081
					AVG =11.325	AVG =	1168
429	16717.56	1.337	92.60	91.263	80.80	10.463	1598
			95.05	93.713	80.50	13.213	1265
			95.40	94.063	80.90	13.163	1270
					AVG =12.279	AVG =	1361
430	20865.14	1.668	93.55	91.882	81.00	10.882	1917
			95.70	94.032	80.80	13.232	1577
			97.00	95.332	81.05	14.282	1461
					AVG =12.799	AVG =	1630
431	25190.84	2.014	94.90	92.886	81.15	11.736	2146
			97.20	95.186	80.95	14.236	1770
			97.75	95.736	81.15	14.586	1727
					AVG =13.519	AVG =	1863

Table B-20 : Experimental Data of Heat Transfer to Saturated Pool Boiling of 59.0 wt. % Isopropanol in Isopropanol - Water Mixture at  $65.31 \text{ kN/m}^2$  ( $T_s = 69.6^\circ\text{C}$ )

Run No.	Heat Flux $\text{W/m}^2$	Conduction Correction $^\circ\text{C}$	Recorded Wall Temp. $^\circ\text{C}$	Corrected Wall Temp. $^\circ\text{C}$	Liquid Temp. $^\circ\text{C}$	Wall Superheat $^\circ\text{C}$	Heat Transfer Coefficient $\text{W/m}^2 \text{ K}$
432	10959.30	0.876	81.75	80.874	70.90	9.974	1099
			86.30	85.424	70.32	15.104	726
			81.85	80.974	70.90	10.074	1088
					AVG = 11.717	AVG = 935	
433	13603.05	1.088	82.75	81.662	70.90	10.762	1264
			88.45	87.362	70.55	16.812	809
			83.45	82.362	71.00	11.362	1197
					AVG = 12.979	AVG = 1048	
434	16946.56	1.355	83.90	82.545	71.10	11.445	1481
			89.45	88.095	70.70	17.395	974
			84.50	83.145	71.25	11.895	1425
					AVG = 13.578	AVG = 1248	
435	20865.14	1.668	84.90	83.232	71.15	12.082	1727
			90.55	88.882	70.95	17.932	1164
			85.50	83.832	71.25	12.582	1658
					AVG = 14.199	AVG = 1469	

Table B-20 : Experimental Data of Heat Transfer to Saturated Pool Boiling of 59.0 wt. % Isopropanol in Isopropanol - Water Mixture at 50.65 kN/m<sup>2</sup> (T<sub>s</sub>=64.9°C)

Run No.	Heat Flux W/m <sup>2</sup>	Conduction Correction °C	Recorded Wall Temp. °C	Corrected Wall Temp. °C	Liquid Temp. °C	Wall Superheat °C	Heat Transfer Coefficient W/m <sup>2</sup> K
436	13027.99	1.042	76.40	75.358	64.53	10.828	1203
			82.80	81.758	64.05	17.708	736
			77.20	76.158	64.75	11.408	1142
					AVG =13.315	AVG = 978	
437	16946.56	1.355	77.48	76.125	64.65	11.475	1477
			84.00	82.645	64.30	18.345	924
			79.80	78.445	64.75	13.695	1237
					AVG =14.505	AVG = 1168	
438	20865.14	1.668	79.45	77.782	64.95	12.832	1626
			86.10	84.432	64.45	19.982	1044
			80.50	78.832	65.00	13.832	1508
					AVG =15.548	AVG = 1342	

Table B-20 : Experimental Data of Heat Transfer to Saturated Pool Boiling of 59.0 wt. % Isopropanol in Isopropanol - Water Mixture at  $34.66 \text{ kN/m}^2 (T_s = 55.7^\circ\text{C})$

Run No.	Heat Flux $\text{W/m}^2$	Conduction Correction $^\circ\text{C}$	Recorded Wall Temp. $^\circ\text{C}$	Corrected Wall Temp. $^\circ\text{C}$	Liquid Temp. $^\circ\text{C}$	Wall Superheat $^\circ\text{C}$	Heat Transfer Coefficient $\text{W/m}^2 \text{ K}$
439	9974.55	0.798	67.05	66.252	57.60	8.652	1153
			73.08	72.282	57.05	15.232	655
			72.50	71.702	57.60	14.102	707
					AVG = 12.662	AVG = 788	
440	13027.99	1.042	68.00	66.958	57.85	9.108	1430
			74.87	73.828	57.27	16.558	787
			74.15	73.108	57.60	15.508	840
					AVG = 13.725	AVG = 949	
441	16946.56	1.355	69.45	68.095	58.10	9.995	1696
			77.00	75.645	57.85	17.795	952
			76.05	74.695	58.20	16.495	1027
					AVG = 14.762	AVG = 1148	
442	20865.14	1.668	71.90	70.232	58.20	12.032	1734
			78.50	76.832	58.05	18.782	1111
			77.40	75.732	58.25	17.482	1194
					AVG = 16.099	AVG = 1296	

Table B-20 : Experimental Data of Heat Transfer to Saturated Pool Boiling of 59.0 wt. % Isopropanol in Isopropanol - Water Mixture at 25.33 kN/m<sup>2</sup> (T<sub>s</sub>=50.3°C)

Run No.	Heat Flux W/m <sup>2</sup>	Conduction Correction °C	Recorded Wall Temp. °C	Corrected Wall Temp. °C	Liquid Temp. °C	Wall Superheat °C	Heat Transfer Coefficient W/m <sup>2</sup> K
443	10297.71	0.823	59.95	59.127	50.30	8.827	1167
			66.00	65.177	50.10	15.077	683
			67.05	66.227	50.40	15.827	651
					AVG =13.244	AVG = 778	
444	13603.05	1.088	61.70	60.612	50.45	10.162	1339
			67.80	66.712	50.25	16.462	826
			68.40	67.312	50.60	16.712	814
					AVG =14.445	AVG = 942	
445	16946.56	1.355	63.95	62.595	50.80	11.795	1437
			68.90	67.545	50.50	17.045	994
			70.00	68.645	50.83	17.815	951
					AVG =15.552	AVG = 1090	
446	20865.14	1.668	65.80	64.132	51.10	13.032	1601
			70.90	69.232	50.95	18.282	1141
			70.90	69.232	51.17	18.062	1155
					AVG =16.459	AVG = 1268	

Table B-21 : Experimental Data of Heat Transfer to Saturated Pool Boiling of 77.0 wt. % Isopropanol in Isopropanol - Water Mixture at 98.63 kN/m<sup>2</sup> (T<sub>s</sub>=80.7°C)

Run No.	Heat Flux W/m <sup>2</sup>	Conduction Correction °C	Recorded Wall Temp. °C	Corrected Wall Temp. °C	Liquid Temp. °C	Wall Superheat °C	Heat Transfer Coefficient W/m <sup>2</sup> K
447	9974.55	0.797	89.40	88.603	80.20	8.403	1187
			90.75	89.953	79.55	10.403	959
			90.05	89.253	80.30	8.953	1114
					AVG = 9.253	AVG = 1078	
448	13027.99	1.042	90.55	89.508	80.50	9.008	1446
			92.65	91.608	80.15	11.458	1137
			91.15	90.108	80.60	9.508	1370
					AVG = 9.991	AVG = 1304	
449	16305.34	1.304	91.40	90.096	80.75	9.346	1745
			93.95	92.646	80.30	12.346	1321
			92.60	91.296	80.82	10.476	1556
					AVG = 10.723	AVG = 1521	
450	20865.14	1.668	92.90	91.232	80.82	10.412	2004
			95.00	93.332	80.30	13.032	1601
			93.80	92.132	80.82	11.312	1845
					AVG = 11.585	AVG = 1801	
451	25190.84	2.014	93.95	91.936	81.03	10.906	2310
			96.40	94.386	80.55	13.836	1821
			94.90	92.886	81.15	11.736	2146
					AVG = 12.159	AVG = 2072	

Table B-21 : Experimental Data of Heat Transfer to Saturated Pool Boiling of 77.0 wt. % Isopropanol in Isopropanol - Water Mixture at  $66.64 \text{ kN/m}^2 (T_g = 69.3^\circ\text{C})$

Run No.	Heat Flux $\text{W/m}^2$	Conduction Correction $^\circ\text{C}$	Recorded Wall Temp. $^\circ\text{C}$	Corrected Wall Temp. $^\circ\text{C}$	Liquid Temp. $^\circ\text{C}$	Wall Superheat $^\circ\text{C}$	Heat Transfer Coefficient $\text{W/m}^2\text{K}$
452	9974.55	0.797	79.05	78.253	69.65	8.603	1159
			79.55	78.753	69.30	9.453	1055
			82.13	81.333	69.65	11.683	854
					AVG = 9.913	AVG = 1006	
453	13603.05	1.088	80.50	79.412	69.90	9.512	1430
			81.65	80.562	69.55	11.012	1235
			83.10	82.012	69.70	12.312	1105
					AVG = 10.945	AVG = 1243	
454	16488.55	1.318	81.60	80.282	70.20	10.082	1635
			82.95	81.632	69.88	11.752	1403
			84.10	82.782	70.10	12.682	1300
					AVG = 11.505	AVG = 1433	
455	20610.70	1.648	82.80	81.152	70.55	10.602	1944
			84.00	82.352	70.20	12.152	1696
			86.00	84.352	70.55	13.802	1493
					AVG = 12.185	AVG = 1691	
456	25190.84	2.014	84.05	82.036	70.70	11.336	2222
			85.60	83.586	70.40	13.186	1910
			87.35	85.336	70.60	14.736	1709
					AVG = 13.086	AVG = 1925	



Table B-21 : Experimental Data of Heat Transfer to Saturated Pool Boiling of 77.0 wt. % Isopropanol in Isopropanol - Water Mixture at 50.65 kN/m<sup>2</sup> (T<sub>s</sub>=64.0°C)

Run No.	Heat Flux W/m <sup>2</sup>	Conduction Correction °C	Recorded Wall Temp. °C	Corrected Wall Temp. °C	Liquid Temp. °C	Wall Superheat °C	Heat Transfer Coefficient W/m <sup>2</sup> K
457	9974.55	0.797	74.10	73.303	63.55	9.753	1023
			75.75	74.953	63.55	11.403	875
			74.90	74.103	63.70	10.403	959
					AVG =10.520	AVG = 948	
458	13231.55	1.058	75.60	74.542	63.75	10.792	1226
			77.35	76.292	63.60	12.692	1043
			76.50	75.442	63.95	11.492	1151
					AVG =11.659	AVG = 1135	
459	16717.56	1.337	76.95	75.613	63.95	11.663	1433
			78.25	76.913	63.70	13.213	1265
			77.25	75.913	64.05	11.863	1409
					AVG =12.246	AVG = 1365	
460	20865.14	1.668	78.55	76.882	64.20	12.682	1645
			79.80	78.132	64.00	14.132	1476
			79.50	77.832	64.20	13.632	1531
					AVG =13.480	AVG = 1548	

Table B-21 : Experimental Data of Heat Transfer to Saturated Pool Boiling of 77.0 wt. % Isopropanol in Isopropanol - Water Mixture at  $33.32 \text{ kN/m}^2 (T_s=54.2^\circ\text{C})$

Run No.	Heat Flux $\text{W/m}^2$	Conduction Correction $^\circ\text{C}$	Recorded Wall Temp. $^\circ\text{C}$	Corrected Wall Temp. $^\circ\text{C}$	Liquid Temp. $^\circ\text{C}$	Wall Superheat $^\circ\text{C}$	Heat Transfer Coefficient $\text{W/m}^2\text{K}$
461	13603.05	1.088	69.45	68.362	56.65	11.712	1161
			73.55	72.462	56.20	16.262	837
			69.45	68.362	56.50	11.862	1147
			AVG =13.280		AVG = 1024		
462	16946.56	1.355	70.80	69.445	56.80	12.645	1340
			75.00	73.645	56.20	17.445	971
			70.20	68.845	56.70	12.145	1395
			AVG =14.078		AVG = 1204		
463	20865.14	1.668	71.50	69.832	57.10	12.732	1639
			76.25	74.582	56.58	18.002	1159
			73.15	71.482	57.10	14.382	1451
			AVG =15.038		AVG = 1388		
464	25190.84	2.014	73.10	71.086	57.50	13.586	1854
			78.10	76.086	56.90	19.186	1313
			73.50	71.486	57.27	14.216	1772
			AVG =15.663		AVG = 1608		

Table B-21 : Experimental Data of Heat Transfer to Saturated Pool Boiling of 77.0 wt. % Isopropanol in Isopropanol - Water Mixture at 25.33 kN/m<sup>2</sup> (T<sub>s</sub>=49.6°C)

Run No.	Heat Flux W/m <sup>2</sup>	Conduction Correction °C	Recorded Wall Temp. °C	Corrected Wall Temp. °C	Liquid Temp. °C	Wall Superheat °C	Heat Transfer Coefficient W/m <sup>2</sup> K
465	9974.55	0.797	60.85	60.053	49.70	10.353	963
			63.70	62.903	49.50	13.403	744
			65.60	64.803	49.75	15.053	663
					AVG =12.940	AVG =	771
466	13603.05	1.088	62.20	61.112	50.05	11.062	1230
			65.10	64.012	49.75	14.262	954
			67.00	65.912	50.05	15.862	858
					AVG =13.729	AVG =	991
467	16488.55	1.318	64.00	62.682	50.25	12.432	1326
			66.00	64.682	50.00	14.682	1123
			68.60	67.282	50.35	16.932	974
					AVG =14.682	AVG =	1123
468	22493.60	1.798	65.85	64.052	50.60	13.452	1672
			68.10	66.302	50.23	16.072	1400
			69.75	67.952	50.60	17.352	1296
					AVG =15.625	AVG =	1440

## A P P E N D I X - C

### EVALUATION OF PHYSICO-THERMAL PROPERTIES

#### C.1 PURE LIQUIDS

Physico-thermal properties of pure liquids investigated; distilled water, ethanol, methanol and isopropanol are readily available in literature [121, 127-133] in different system of units. However, they are not available in the International System of units over the entire range of temperature employed in the present investigation. Therefore, the physico-thermal properties of these pure liquids were converted to S.I. units and plotted in Figures C.1 though C.5 as a function of saturation temperature.

#### C.2 BINARY LIQUID MIXTURES

Physico-thermal properties of the aqueous binary liquid mixtures of ethanol-water, methanol-water and isopropanol-water are available in the literature [119, 129-132, 134] only over a limited range of temperature and concentration. Therefore, methods were devised to predict the physico-thermal properties of these mixtures. These methods are discussed below for evaluating physico-thermal properties used in this investigation.

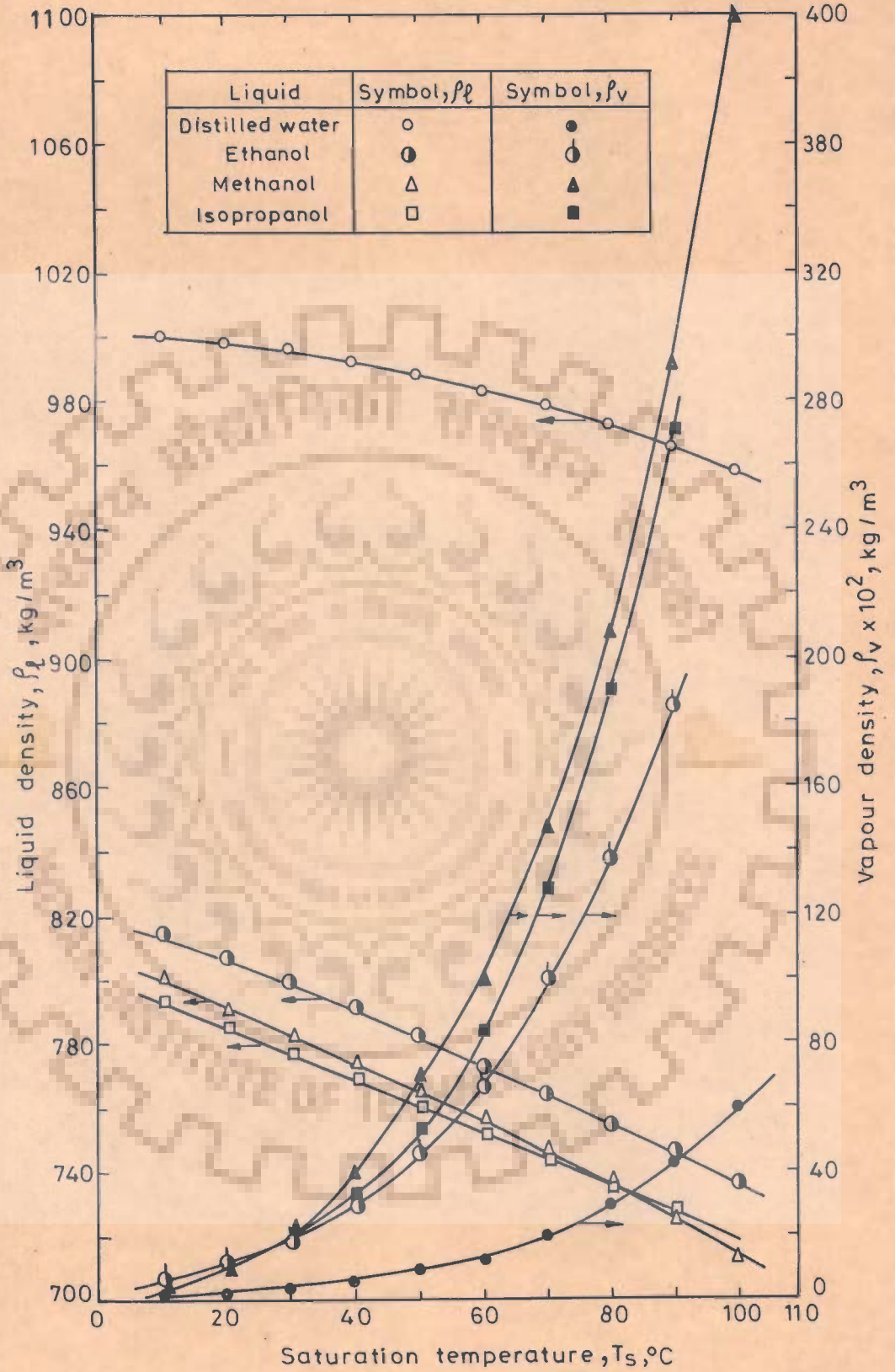


Fig.C.1 - Variation of liquid and vapour densities with saturation temperature for pure liquids

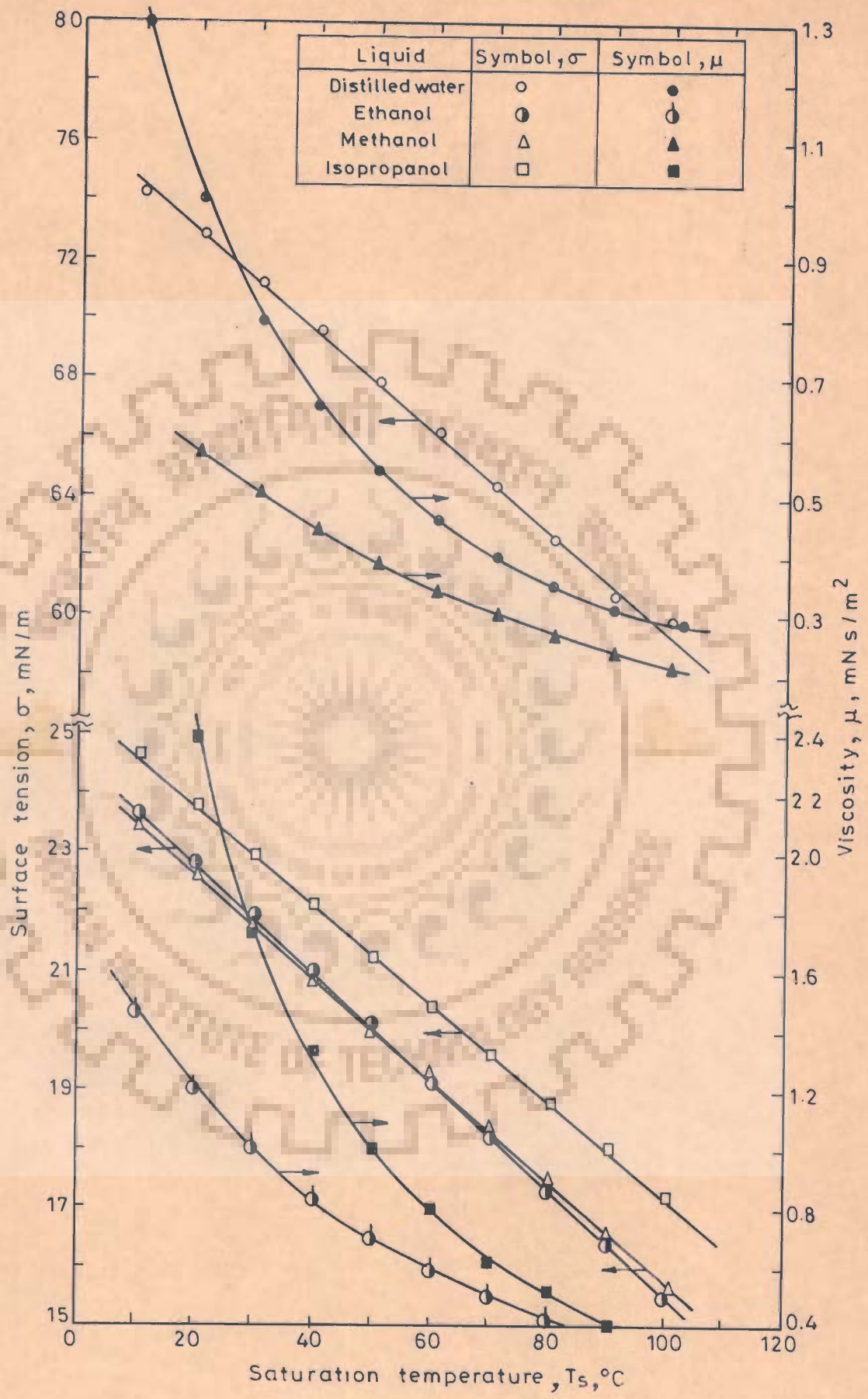


Fig.C.2-Variation of surface tension and viscosity with saturation temperature for pure liquids

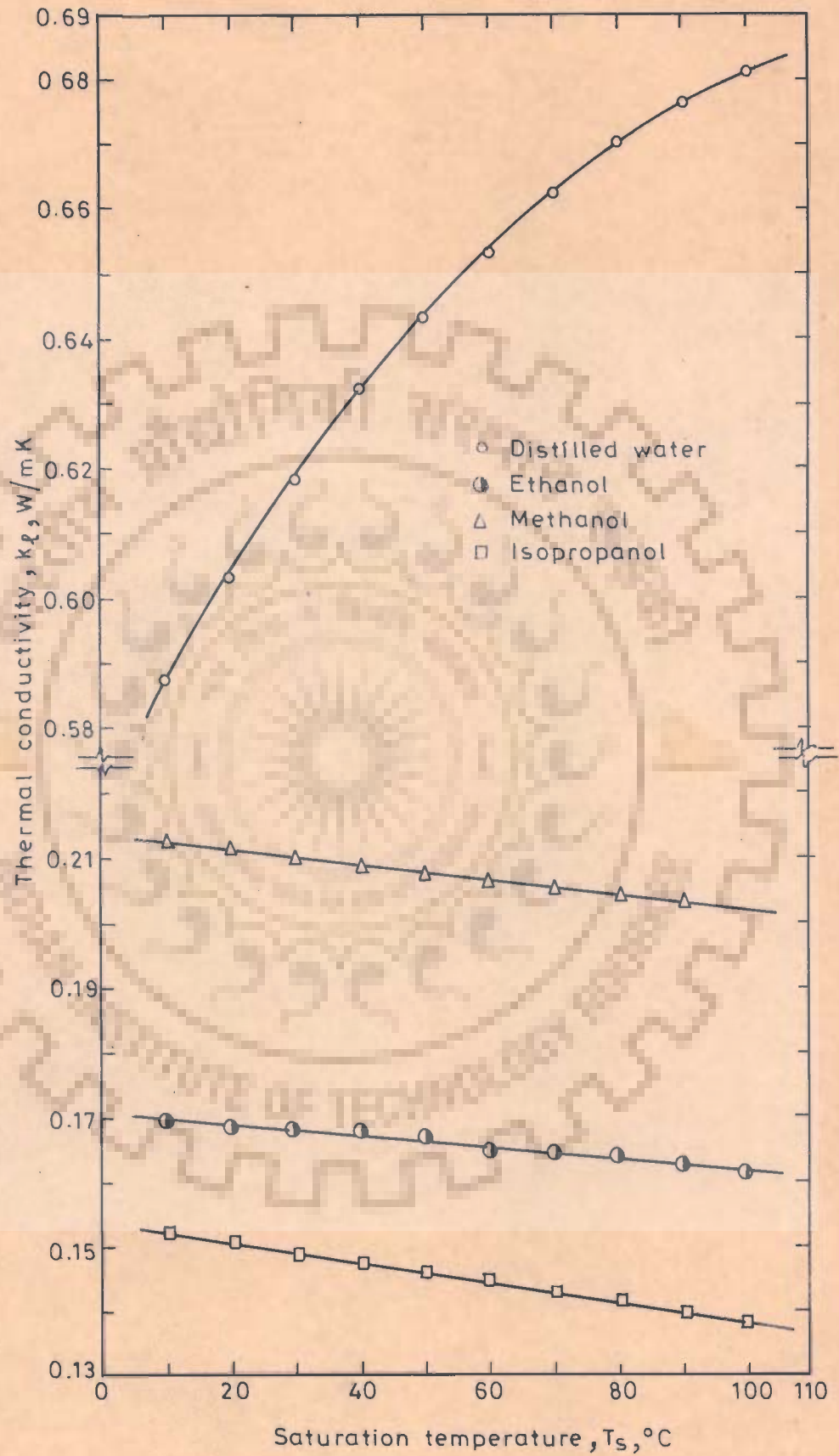


Fig.C.3-Variation of thermal conductivity with saturation temperature for pure liquids

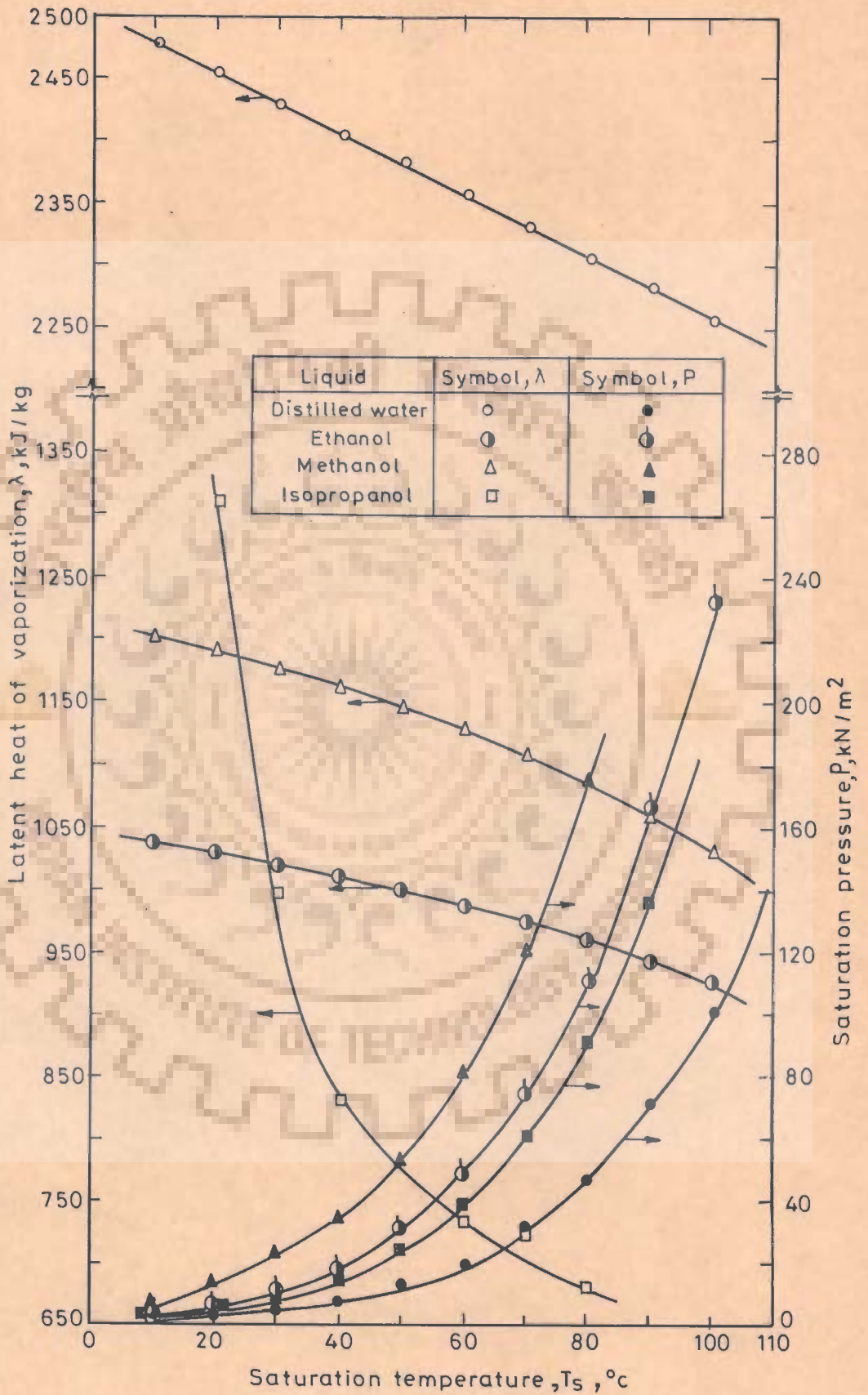


Fig.C.4-Variation of latent heat of vaporization and saturation pressure with saturation temperature for pure liquids.



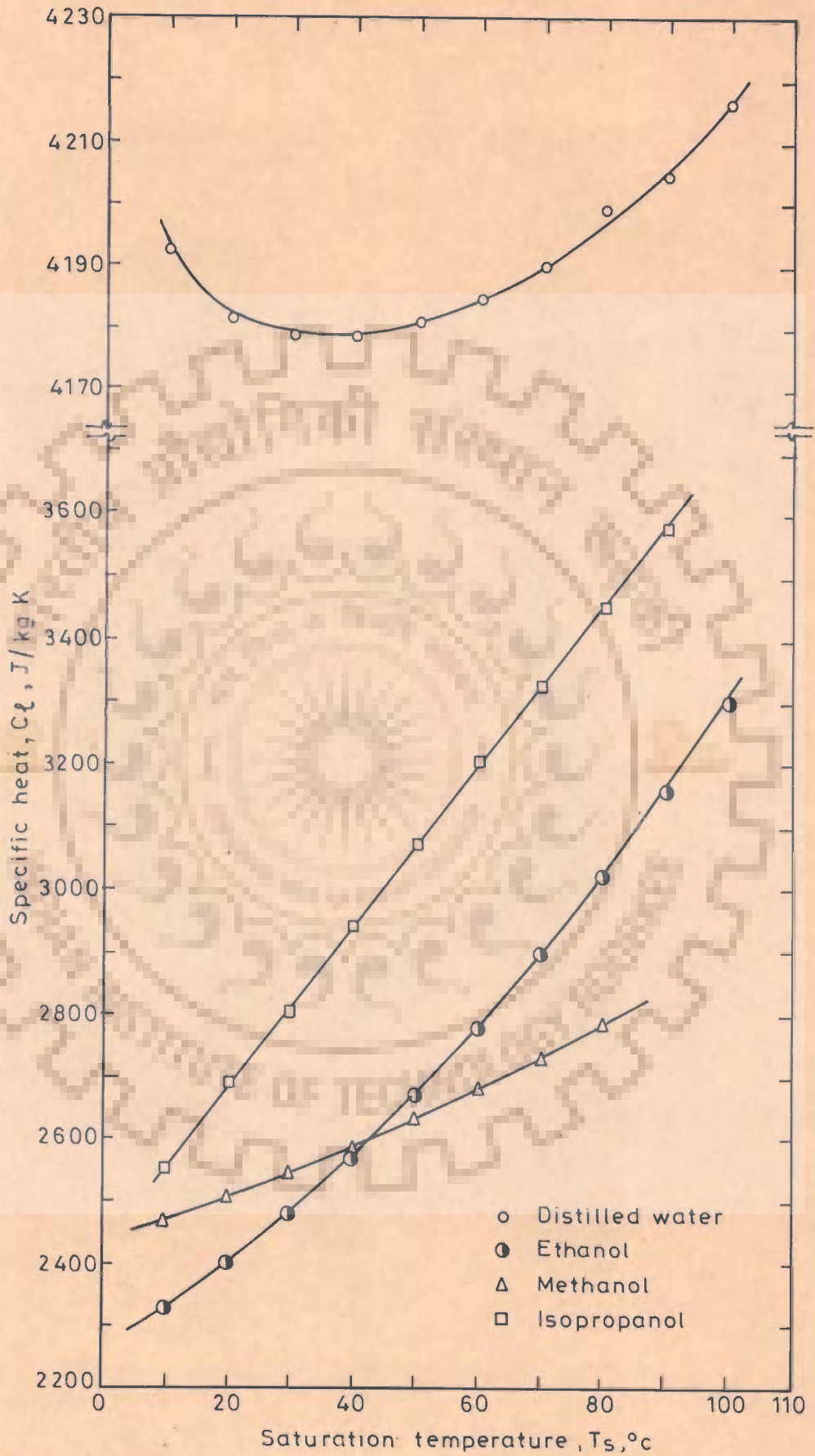


Fig.C.5-Variation of specific heat with saturation temperature for pure liquids

### C.2.1 Liquid and Vapour Densities

The liquid density was calculated at the respective saturation temperature of a given mixture with the assumption that for these mixtures the partial molar volume of each component in mixture is equal to its pure-component volume at the same temperature and pressure. The liquid densities are plotted in Figures C.8, C.12 and C.16 for these mixtures.

Vapour density was calculated by employing three different equations of state; namely, the Virial Equation, the Redlich-Kwong Equation and the ideal gas law. For the binary systems under investigation, the mixing rules proposed by Prausnitz [135] were used. A comparative study of these three equations revealed that ideal gas law predicted the vapour density for these mixtures within  $\pm 2.0$  per cent deviation as predicted by the other two equations. Therefore, keeping in view, the simplicity of the ideal gas law, this was used to predict the vapour density of mixtures.

The vapour density as a function of saturation temperature for ethanol-water, methanol-water and isopropanol-water mixtures are shown in Figures C.8, C.12 and C.16 respectively.

### C.2.2 Thermal Conductivity

For the prediction of thermal conductivity of binary liquid mixtures under investigation, the equation of Filippov and Novoselova [136] was used. The equation is as follows :

$$k_m = k_1 w_1 + k_2 w_2 - 0.72 (k_2 - k_1)(w_1 w_2) \dots (C.1)$$

where the weight fraction  $w_2$  refers to the component having the larger value of  $k$ . The values of thermal conductivity calculated by Equation (C.1) compared well with the values those available in literature [134]. The calculated values are plotted in Figures C.9, C.13 and C.17 for ethanol-water, methanol-water and isopropanol-water mixtures respectively.

### C.2.3 Surface Tension

Surface tensions of the aqueous binary liquid mixtures have been calculated using the method of Tamura et al [137]. As recommended by these investigators this method may be used to estimate surface tensions over wide concentration ranges. In the method of Tamura et al [137], the significant densities and concentrations are taken to be those characteristic of the surface layer. Tamura's method is complex and the set of relevant equations can be written as follows :

$$\Psi_w = \frac{x_w v_w}{x_w v_w + x_o v_o} \quad \dots(C.2)$$

$$\text{and } \Psi_o = \frac{x_o v_o}{x_w v_w + x_o v_o} \quad \dots(C.3)$$

where  $\Psi_w, \Psi_o$  = superficial bulk volume fractions of water and organic material

$x_w, x_o$  = bulk mole fraction of pure water and pure organic component

$v_w, v_o$  = molar volume of pure water and pure organic component

$$\beta = \log \frac{\Psi_w^q}{\Psi_o} \quad \dots(C.4)$$

where  $q$  = constant depending upon type and size of organic constituent, viz. for ethanol

$q = 2$  etc.

$$W = 0.441 \frac{q}{T} \left[ \frac{\sigma_o v_o^{0.667}}{q} - \sigma_w v_w^{0.667} \right] \quad \dots(C.5)$$

where  $\sigma_w, \sigma_o$  = surface tension of pure water and pure organic component

$T$  = absolute temperature

$$\psi = \log \frac{(\Psi_w^\sigma)^q}{\Psi_o^\sigma} = \beta + W \quad \dots(C.6)$$

$$\text{and } \Psi_w^\sigma + \Psi_o^\sigma = 1 \quad \dots(C.7)$$

Thus  $\Psi_w^\sigma$  and  $\Psi_o^\sigma$  (superficial volume fraction of water and alcohol in the surface layer, respectively) are calculated by solving Equations (C.6 and C.7) simultaneously with values of  $\beta$  and  $W$  from Equations (C.2 through C.5). These values are then inserted in

the final equation, to obtain surface tension of the mixture :

$$\sigma_m = [ \psi_w^\sigma \sigma_w^{1/4} + \psi_o^\sigma \sigma_o^{1/4} ]^4 \quad \dots(C.8)$$

The values of surface tensions for ethanol-water, methanol-water and isopropanol-water mixtures were calculated by above procedure and plotted in Figures C.9, C.13 and C.17 respectively.

#### C.2.4 Vapour-liquid Equilibria

The vapour-liquid equilibria data at atmospheric and subatmospheric pressures for the system ethanol-water were obtained from Hirata et al [138], those of methanol-water system from Othmer and Benenati [139] and of isopropanol-water system from Davaloo [140]. Figures C.6, C.10 and C.14 show the plots of equilibrium vapour-composition of the respective alcohol in the vapour phase,  $y$ , as a function of saturation pressure,  $P$ .

Variation of saturation pressures with saturation temperatures for ethanol-water, methanol-water and isopropanol-water binary mixtures are shown in Figures C.7, C.11 and C.15, respectively.

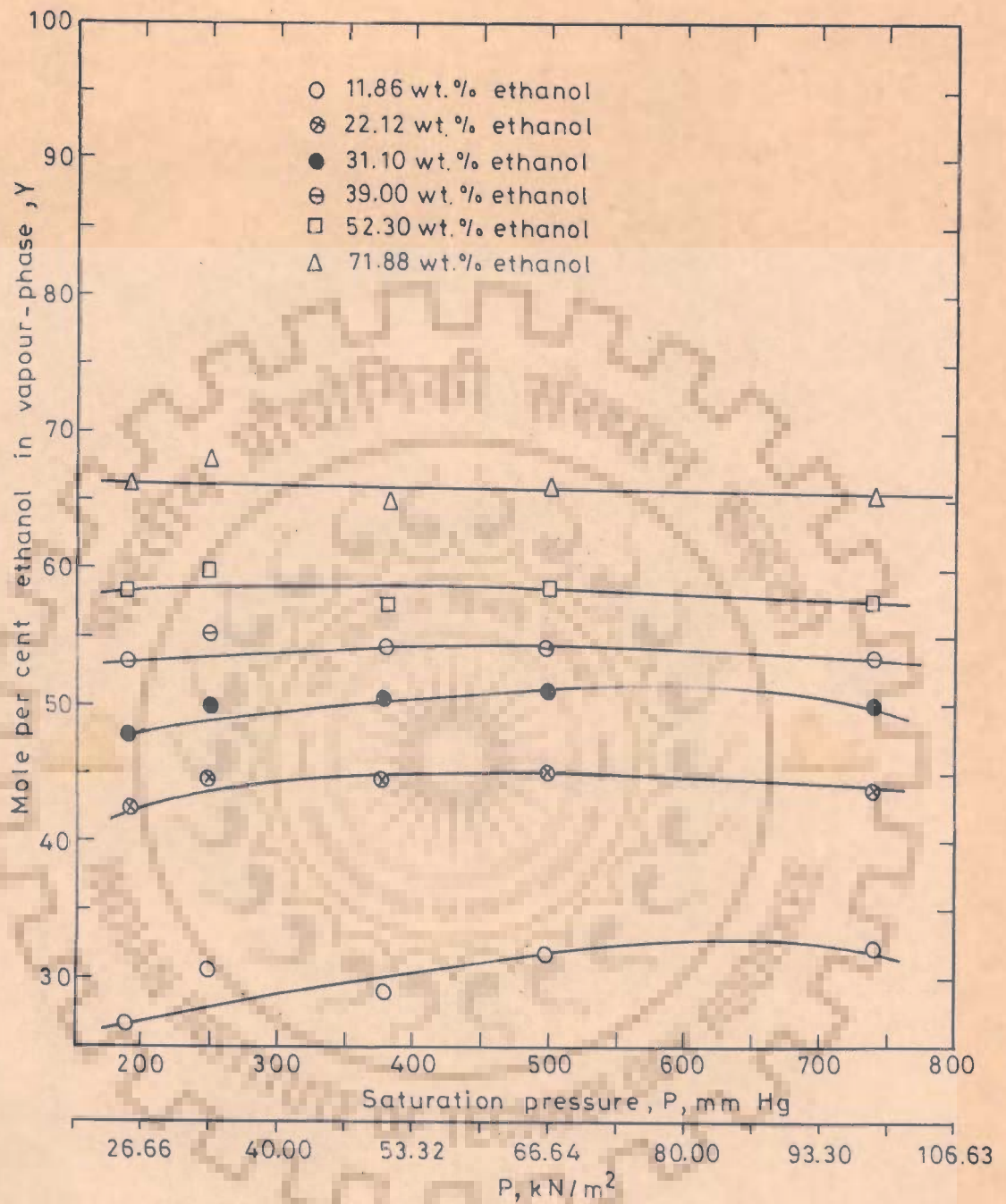


Fig.C.6-Variation of mole percent of ethanol in vapour-phase with saturation pressure for ethanol-water mixtures

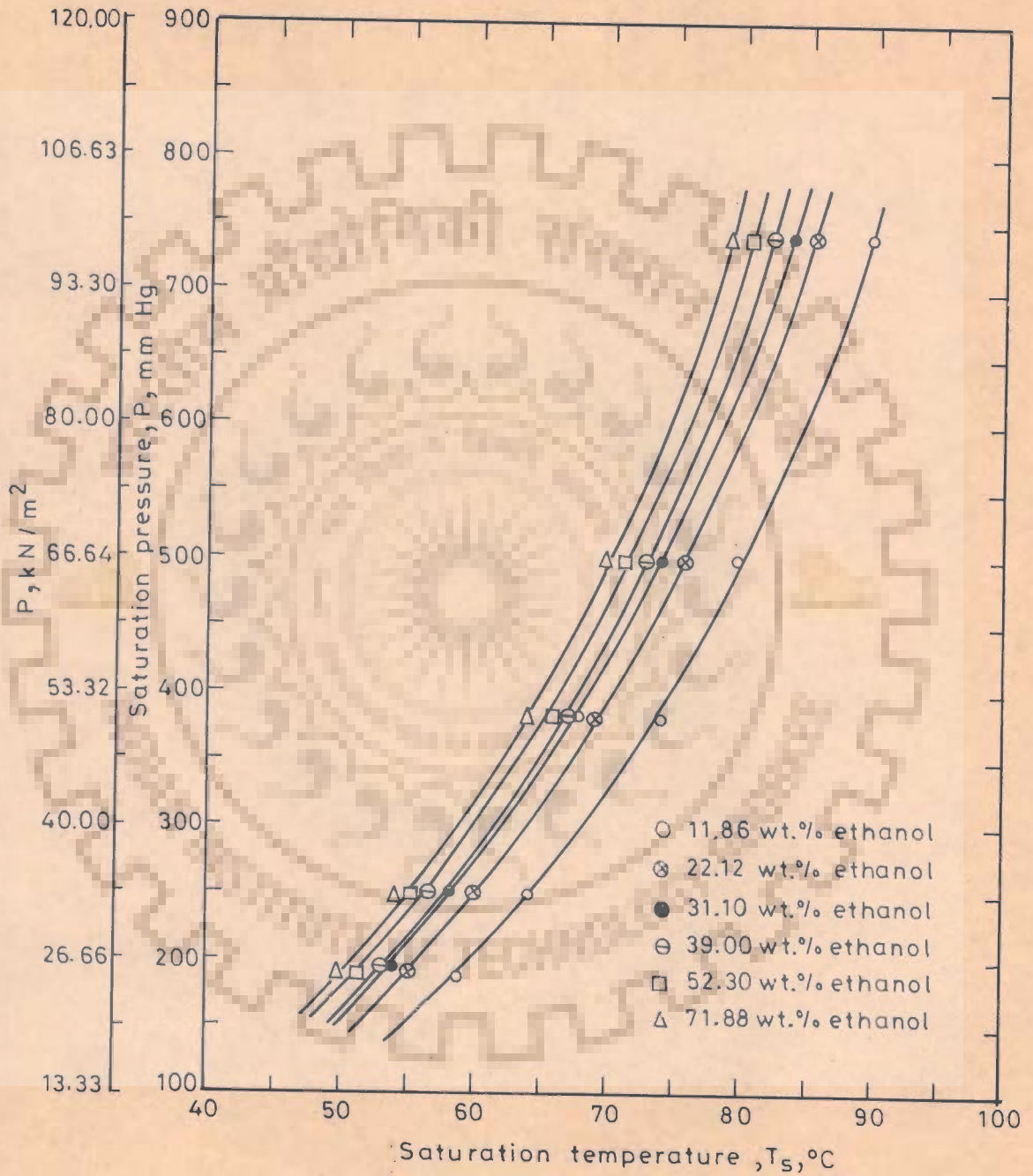


Fig.C.7-Variation of saturation pressure with saturation temperature for ethanol-water mixtures.

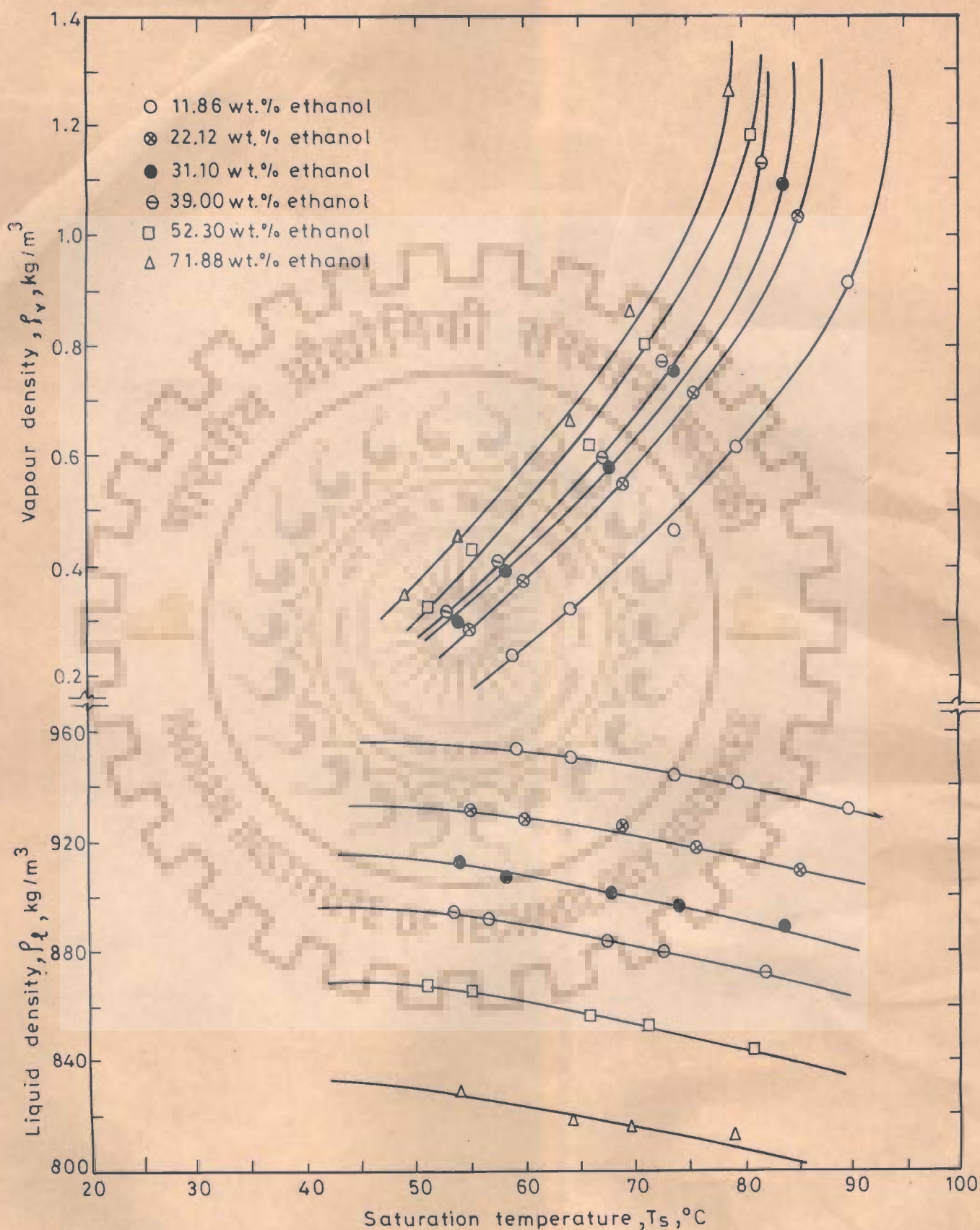


Fig.C.8-Variation of liquid and vapour densities of ethanol-water mixtures with saturation temperature



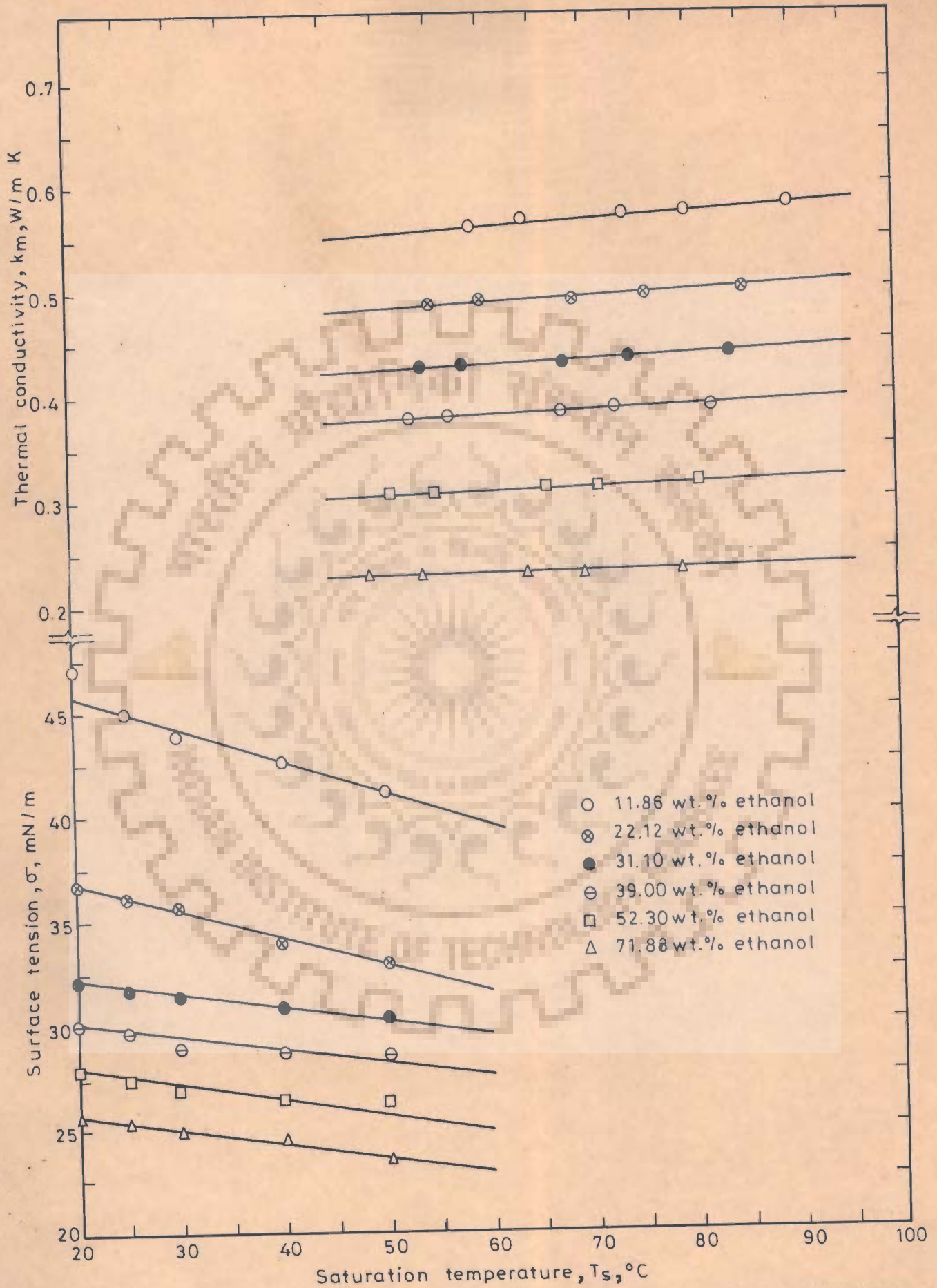


Fig.C.9-Variation of surface tension and thermal conductivity with temperature for ethanol-water mixtures.

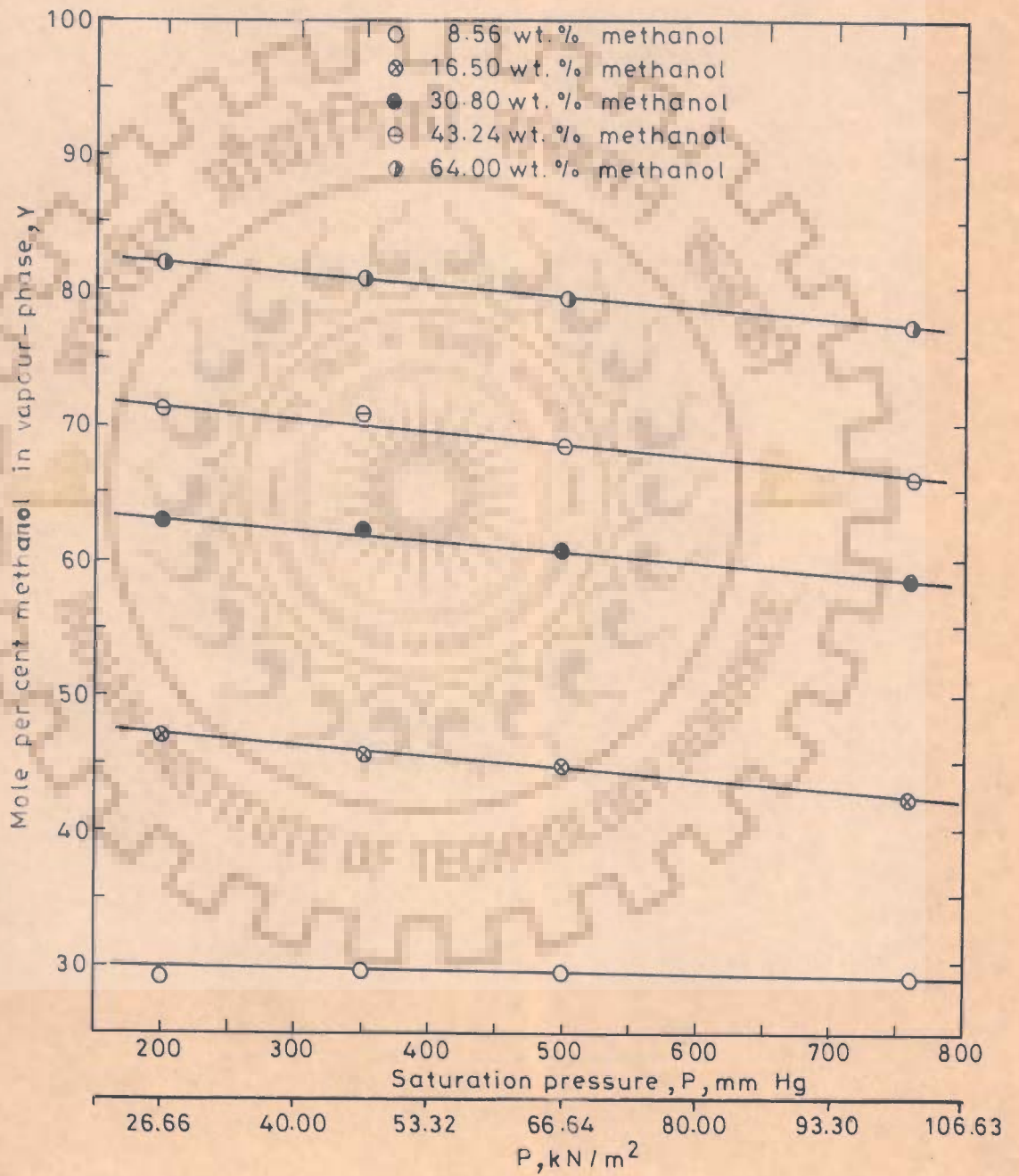


Fig.C.10-Variation of mole per cent of methanol in vapour phase with saturation pressure for methanol-water mixtures

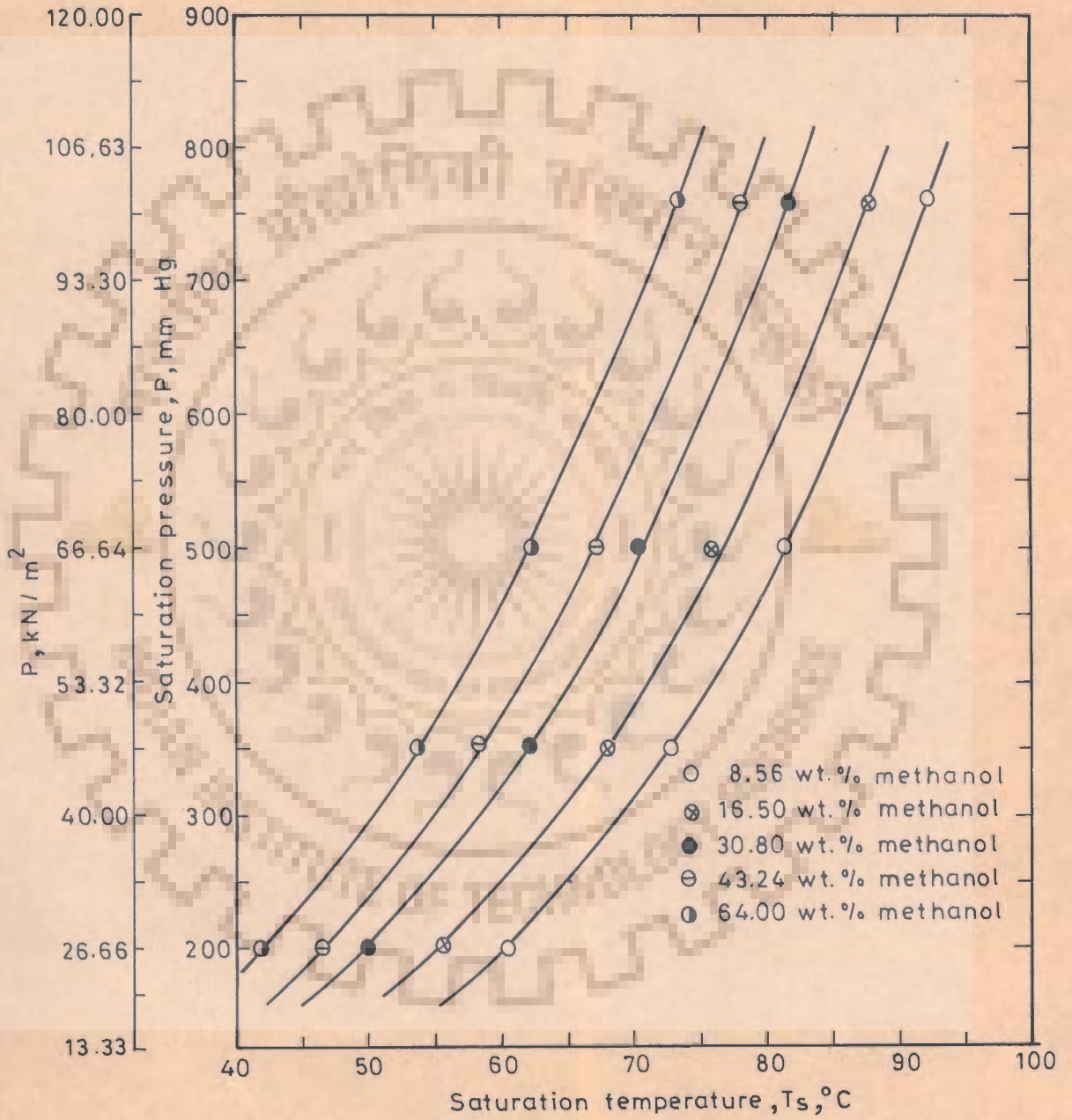


Fig.C.11-Variation of saturation pressure with saturation temperature for methanol - water mixtures

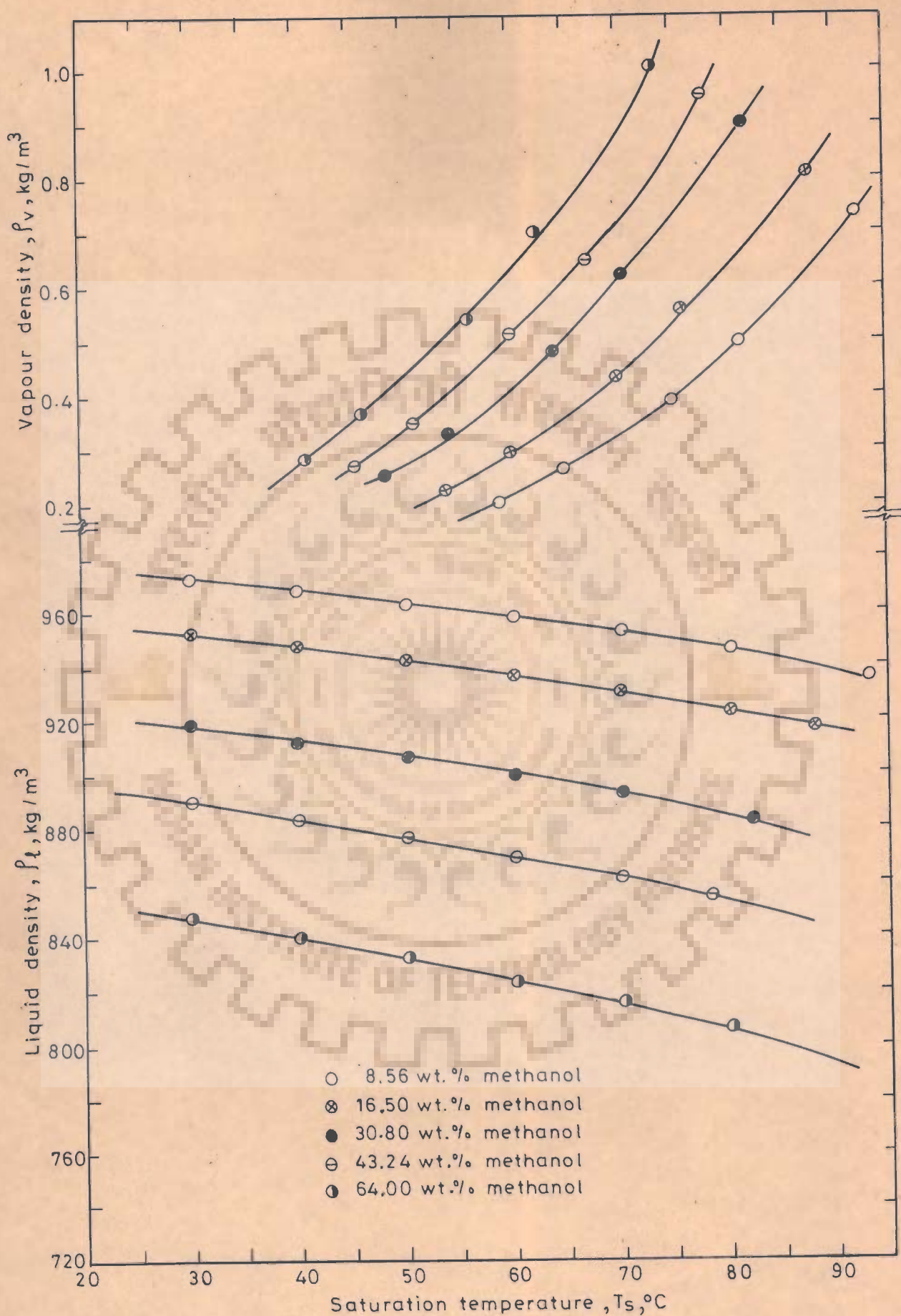


Fig.C.12-Variation of liquid and vapour densities of methanol-water mixtures with saturation temperature

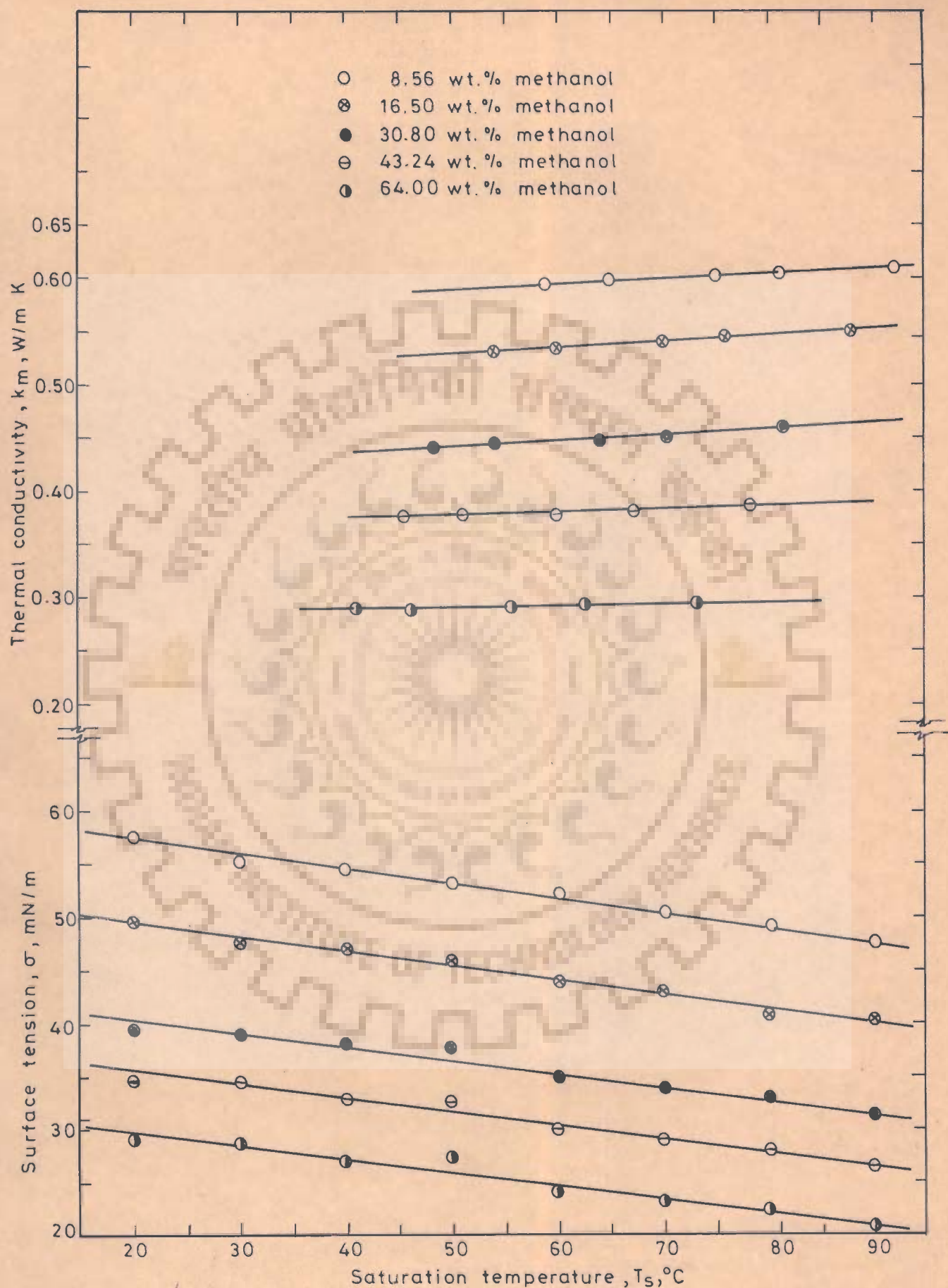


Fig.C.13-Variation of surface tension and thermal conductivity with saturation temperature for methanol-water mixtures

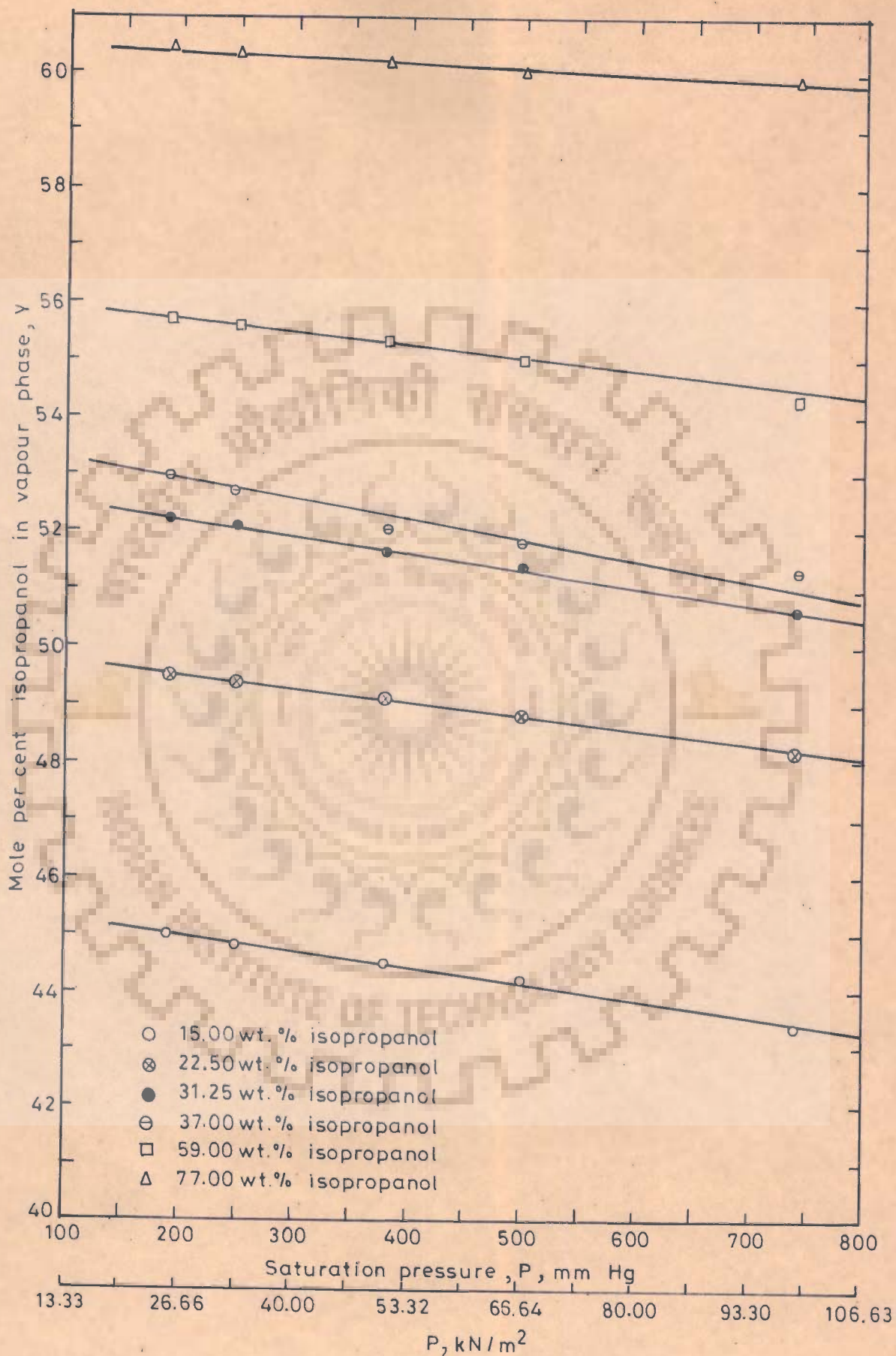


Fig.C.14-Variation of mole per cent of isopropanol in vapour phase with saturation pressure for isopropanol-water mixtures

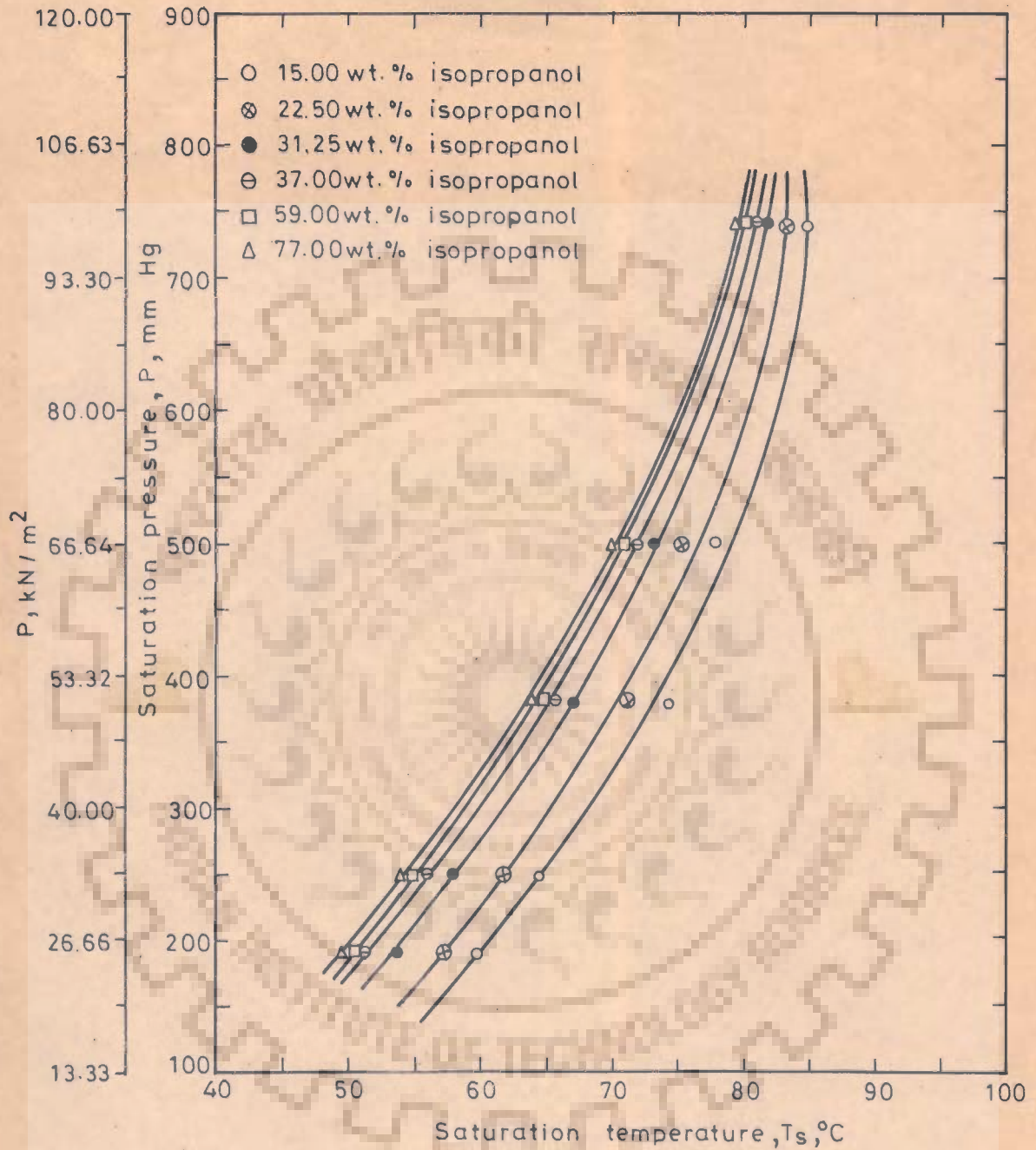


Fig.C.15-Variation of saturation pressure with saturation temperature for isopropanol water mixtures

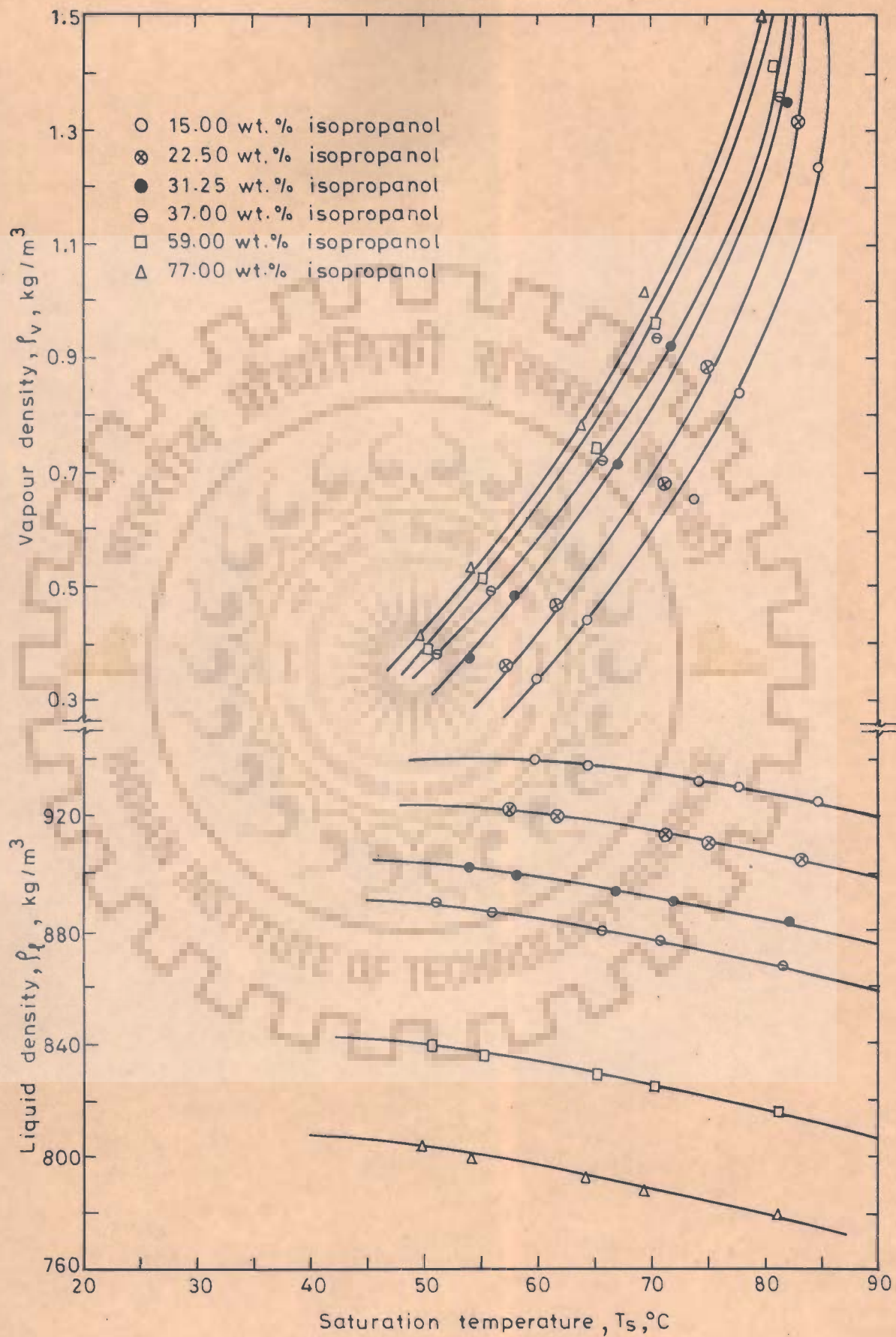


Fig.C.16-Variation of liquid and vapour densities of isopropanol-water mixtures with saturation temperature



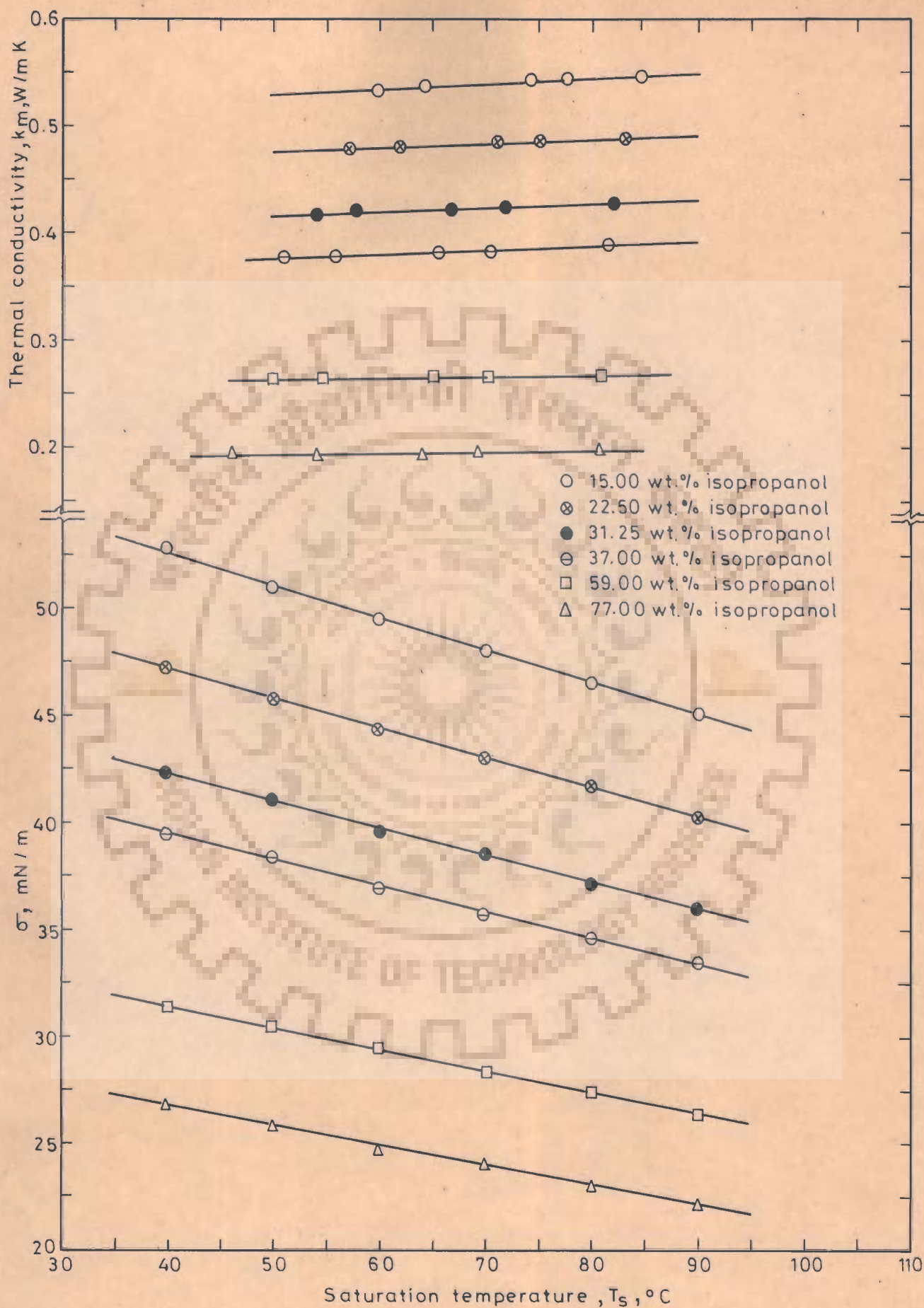


Fig.C.17-Variation of surface tension and thermal conductivity with saturation temperature for isopropanol - water mixtures

## A P P E N D I X - D

### SAMPLE CALCULATIONS

#### D.1 PURE LIQUIDS

Run No. 36 for ethanol has been selected to demonstrate the calculational procedure. The following experimental data were obtained for the above run :

System Pressure,  $P = 48.0 \text{ kN/m}^2$   
Saturation Temperature,  $T_s = 59.6^\circ\text{C}$   
Voltage,  $V = 56 \text{ Volts}$   
Current,  $I = 7.0 \text{ Amperes}$

The e.m.f. of the surface and liquid thermocouples and the corresponding temperatures under steady state conditions are reported below :

	Heating Surface			Liquid		
	Top	Side	Bottom	Top	Side	Bottom
e.m.f, millivolt	2.908	3.075	3.023	2.529	2.515	2.521
Temperature, $^\circ\text{C}$	70.50	74.30	73.13	61.88	61.55	61.70

Dimensions of the heating surface are given below :

O.D. of the heating surface,  $d_o = 70 \text{ mm}$

I.D. of the heating surface,  $d_i = 62 \text{ mm}$

Length of the heating surface,  $l = 179 \text{ mm}$

## D.1.1 Heat Transfer Area

$$\begin{aligned}
 A &= \pi d_o \ell \\
 &= \pi \times 0.07 \times 0.179 \\
 &= 3.93 \times 10^{-2} \text{ m}^2
 \end{aligned}$$

## D.1.2 Heat Flux

$$\begin{aligned}
 q &= \frac{VI}{A} \\
 &= \frac{56 \times 7}{3.93 \times 10^{-2}} = 9974.55 \text{ W/m}^2
 \end{aligned}$$

## D.1.3 Correction of Surface Temperatures

In the present investigation, heating surface is a thin walled cylinder. The temperature drop across the wall is calculated by the following equation of conductive heat transfer :

$$\delta T_w = \frac{q d_o}{2 k_w} \ln \frac{d_o}{d_h} \quad \dots(D.1)$$

where,  $d_h =$  Inside diameter of the heating surface  $+ \frac{1}{2} (d_o - d_i)$  ... (D.2)

and  $k_w =$  Thermal conductivity of the wall

$$\begin{aligned}
 \delta T_w &= \frac{q \times 70 \times 10^{-3}}{2 \times 22.15 \times 1.163} \ln \frac{70 \times 10^{-3}}{66 \times 10^{-3}} \\
 &= 7.995 \times 10^{-5} \times q
 \end{aligned}$$

$$\therefore \delta T_w = 7.995 \times 10^{-5} \times 9974.55 = 0.797^\circ\text{C}$$

Therefore, corrected surface temperatures are as follows:

$$T_{w1} = 70.50 - 0.797 = 69.703^\circ\text{C}$$

$$T_{w2} = 74.30 - 0.797 = 73.503^\circ\text{C}$$

$$T_{w3} = 73.13 - 0.797 = 72.333^\circ\text{C}$$

Subscripts 1, 2 and 3 represent the top-, side- and bottom- positions of the thermocouples respectively.

#### D.1.4 Average Temperature Difference, $\overline{\Delta T}$

$$\Delta T_1 = T_{w1} - T_{f1} = 69.703 - 61.88 = 7.823^\circ\text{C}$$

$$\Delta T_2 = T_{w2} - T_{f2} = 73.503 - 61.55 = 11.953^\circ\text{C}$$

$$\Delta T_3 = T_{w3} - T_{f3} = 72.333 - 61.70 = 10.633^\circ\text{C}$$

$$\begin{aligned} \text{Average temperature difference, } \overline{\Delta T} &= \frac{\Delta T_1 + \Delta T_2 + \Delta T_3}{3} \\ &= \frac{7.823 + 11.953 + 10.633}{3} \\ &= 10.136^\circ\text{C} \end{aligned}$$

#### D.1.5 Heat Transfer Coefficient

The point values of the experimental heat transfer coefficient at the top-, side- and bottom- positions of the heating surface are calculated in the following manner :

$$h_1 = \frac{q}{\Delta T_1} = \frac{9974.55}{7.823} = 1275.03 \frac{\text{W}}{\text{m}^2\text{K}}$$

$$h_2 = \frac{q}{\Delta T_2} = \frac{9974.55}{11.953} = 834.48 \frac{\text{W}}{\text{m}^2\text{K}}$$

$$h_3 = \frac{q}{\Delta T_3} = \frac{9974.55}{10.633} = 938.08 \frac{\text{W}}{\text{m}^2\text{K}}$$

The average value of the experimental heat transfer coefficient is calculated as follows :

$$\bar{h} = \frac{q}{(\Delta T)}$$

$$= \frac{9974.55}{10.136} = 984.072 \frac{W}{m^2 K}$$

#### D.1.6 Calculation of $\bar{h}^*/\bar{h}_1^*$ and $P/P_1$

$\bar{h}^*$  is calculated by averaging the values of  $h^*$  at  $48.0 \text{ kN/m}^2$  for all heat fluxes. The procedure is as follows :

$$\text{For Run No. 36, } h^* = \frac{984.072}{(9974.55)^{0.7}} = 1.562 \frac{W^{0.3}}{m^{0.6} K}$$

$$\text{For Run No. 37, } h^* = \frac{1202.65}{(12946.56)^{0.7}} = 1.591 \frac{W^{0.3}}{m^{0.6} K}$$

$$\text{For Run No. 38, } h^* = \frac{1532.60}{(17984.73)^{0.7}} = 1.611 \frac{W^{0.3}}{m^{0.6} K}$$

$$\text{For Run No. 39, } h^* = \frac{1712.24}{(21671.76)^{0.7}} = 1.579 \frac{W^{0.3}}{m^{0.6} K}$$

$$\text{For Run No. 40, } h^* = \frac{1960.44}{(26740.46)^{0.7}} = 1.561 \frac{W^{0.3}}{m^{0.6} K}$$

$$\text{Thus, } \bar{h}^* \text{ at } 48.0 \text{ kN/m}^2 = \frac{1}{5} [1.562 + 1.591 + 1.611 + 1.579 + 1.561]$$

$$= 1.581 \frac{W^{0.3}}{m^{0.6} K}$$

Similarly,  $\bar{h}_1^*$  is evaluated by averaging the values of  $h^*$  at  $98.63 \text{ kN/m}^2$  from Run Nos. 26 to 30. The value of  $\bar{h}_1^*$ , so obtained, is  $2.119 \frac{W^{0.3}}{m^{0.6} K}$

$$\text{Therefore, } \frac{\bar{h}^*}{\bar{h}_1^*} = \frac{1.581}{2.119} = 0.746$$

$$\text{and } \frac{P}{P_1} = \frac{48.0}{98.63} = 0.487$$

## D.2 BINARY LIQUID MIXTURES

Run No. 250 for 16.5 wt. per cent methanol in methanol-water mixture has been selected to illustrate the procedure followed in processing the experimental data for mixtures.

The following data were taken for the above run :

Mixture Composition : Methanol-water mixture containing  
16.5 wt. per cent methanol  
(10 mole per cent methanol)

System pressure,  $P = 50.65 \text{ kN/m}^2$

Barometric pressure =  $98.63 \text{ kN/m}^2$

Saturation  
Temperature,  $T_s = 70.0 \text{ }^\circ\text{C}$

Voltage,  $V = 63 \text{ Volts}$

Current,  $I = 8.0 \text{ Amperes}$

Heat flux,  $q = 8 \times 63 / 0.0393 = 12824.43 \text{ W/m}^2$

The e.m.f. of the surface and liquid thermocouples and the corresponding temperatures under steady state conditions are reported below :

	Heating Surface			Liquid		
	Top	Side	Bottom	Top	Side	Bottom
e.m.f., millivolt	3.516	3.498	3.530	2.934	2.926	2.930
Temperature, $^\circ\text{C}$	84.15	83.75	84.45	71.10	70.90	71.03

### D.2.1 Average Heat Transfer Coefficient, $\bar{h}$

$\bar{h}$  has been calculated in the similar manner as described in Sections D.1.1 to D.1.5. The value of  $\bar{h}$  is  $1061.45 \text{ W/m}^2\text{K}$ .

### D.2.2 Calculation of $\bar{h}^*/\bar{h}_1^*$ and $P/P_1$

$\bar{h}^*$  is calculated by averaging the values of  $h^*$  at  $50.65 \text{ kN/m}^2$  for all heat fluxes studied in Run Nos. 249 to 253. The procedure of calculation has already been illustrated in Section D.1.6.

$$\begin{aligned} \text{Thus, } \bar{h}^* &= \frac{1}{5} \left[ \frac{860.32}{(9618.32)^{0.7}} + \frac{1061.45}{(12824.43)^{0.7}} + \frac{1263.5}{(16488.55)^{0.7}} \right. \\ &\quad \left. + \frac{1481.53}{(20356.23)^{0.7}} + \frac{1702.73}{(24910.9)^{0.7}} \right] \\ &= 1.415 \frac{\text{W}^{0.3}}{\text{m}^{0.6}\text{K}} \end{aligned}$$

Similarly,  $\bar{h}_1^*$  has been calculated from Run Nos. 239 to 243 and the value of  $\bar{h}_1^*$  is  $1.733 \frac{\text{W}^{0.3}}{\text{m}^{0.6}\text{K}}$

$$\text{Therefore, } \frac{\bar{h}^*}{\bar{h}_1^*} = \frac{1.415}{1.733} = 0.8165$$

$$\text{and } \frac{P}{P_1} = \frac{50.65}{98.63} = 0.5135$$

### D.2.3 Evaluation of Physico-thermal Properties of the Mixture

$$(i) \rho_l = \frac{100}{\frac{16.5}{746} + \frac{83.5}{978}} = 930 \text{ Kg/m}^3$$

$$(ii) M = 0.456 \times 32 + 0.544 \times 18 = 24.4 \text{ Kg/Kg-mole}$$

$$(iii) \rho_v = \frac{100 \times 0.5 \times 24.4}{82.06 \times 343} = 0.433 \text{ Kg/m}^3$$

(iv) Thermal conductivity is calculated as follows by using equation of Fillipov and Novoselova[136]:

$$\begin{aligned} k_m &= 0.662 \times 0.835 + 0.165 \times 0.2053 \\ &\quad - [0.72(0.6620 - 0.2053) (0.835 \times 0.165)] \\ &= 0.5413 \text{ W/m K.} \end{aligned}$$

(v) Surface tension is calculated by using the method of Tamura et al [137] as discussed in Appendix-C.

The steps are as follows :

$$(a) \frac{\psi_w}{\psi_o} = \frac{0.9 \times 18.40}{0.1 \times 42.89} = 3.861$$

$$(b) \beta = \log 3.861 = 0.587$$

$$\begin{aligned} (c) W &= \frac{0.441 \times 1}{343} [18.4(42.89)^{2/3} - 64.4(18.40)^{2/3}] \\ &= -0.289 \end{aligned}$$

$$(d) \epsilon = 0.587 - 0.289 = 0.298$$

$$(e) \psi_w^\sigma = 0.665 \text{ and } \psi_o^\sigma = 0.335$$

$$\begin{aligned} (f) \sigma_m &= [0.665(64.4)^{1/4} + 0.335(18.40)^{1/4}]^4 \\ &= 44.2 \text{ dynes/cm} \end{aligned}$$



D.2.4 Evaluation of  $Nu_B$ 

$$\text{Laplace Constant, } D = \sqrt{\frac{\sigma}{g(\rho_l - \rho_v)}}$$

$$D = \sqrt{\frac{44.2 \times 10^{-3}}{9.81(930 - 0.433)}} = 2.2 \times 10^{-3} \text{ m}$$

$$\overline{Nu}_B = \frac{h}{k_m} \sqrt{\frac{\sigma}{g(\rho_l - \rho_v)}} = \frac{1061.45 \times 2.2 \times 10^{-3}}{0.5413}$$

$$\overline{Nu}_B = 4.314$$

D.2.5 Evaluation of  $\overline{Nu}_B^* \left(\frac{P_1}{P}\right)^{0.32}$ 

$$\overline{Nu}_B^* = \frac{\overline{Nu}_B}{q^{0.7}} = \frac{4.314}{(12824.43)^{0.7}} = 5.745 \times 10^{-3} \frac{m^{1.4}}{W^{0.7}}$$

$$\left(\frac{P_1}{P}\right)^{0.32} = \left(\frac{98.63}{50.65}\right)^{0.32} = 1.238$$

$$\begin{aligned} \text{Therefore, } \overline{Nu}_B^* \left(\frac{P_1}{P}\right)^{0.32} &= 5.745 \times 10^{-3} \times 1.238 \\ &= 7.11 \times 10^{-3} \frac{m^{1.4}}{W^{0.7}} \end{aligned}$$

## REFERENCES

1. Bonnet, W.E. and Gerster, J.A., "Boiling Coefficients of heat transfer - C<sub>4</sub> hydrocarbon/furfural mixtures inside vertical tubes", Chem. Eng. Prog., Vol. 47, no. 3, pp 151-158 (1951).
2. Palen, J.W. and Small, W.M., "A new way to design kettle and internal reboilers", Hydrocarbon Processing, vol. 43, no. 11, pp 199-208 (1964).
3. Hughmark, G.A., "Designing thermosiphon reboilers", Chem. Eng. Prog. Symp. Ser., Vol. 61, no. 59, pp 217-219 (1965).
4. Shellene, K.R., Sternling, C.V., Snyder, N.H. and Church, D.M., "Experimental study of a vertical thermosiphon reboiler", Chem. Eng. Prog. Symp. Ser., Vol. 64, no. 82, pp 102-113 (1968).
5. Hughmark, G.A., "Designing thermosiphon reboilers", Chem. Eng. Prog. Symp. Ser., Vol. 66, no. 102, pp 209-213 (1970).
6. Palen, J.W., Yarden, A. and Taborek, J., "Characteristics of boiling outside large-scale horizontal multitube bundles", AIChE Symp. Ser., Vol. 68, no. 118, pp 50-61 (1972).
7. Wall, K.W. and Park, Jr, E.L., "Nucleate boiling of n-pentane, n-hexane and several mixtures of the two from various tubes arrays", Int. J. Heat Mass Transfer, Vol 21, no. 1, pp 73-75 (1978).
8. Sharma, P.R., "Heat transfer studies in pool boiling of liquids", Ph.D. Thesis, University of Roorkee, Roorkee (April-1977).
9. Cryder, D.S. and Finalborgo, A.C., "Heat transmission from metal surfaces to boiling liquids: Effect of temperature of the liquid on film coefficient", Trans. AIChE, Vol. 33, pp. 346-362 (1937).

10. Bonilla, C.F. and Perry, C.W., "Heat transmission to boiling binary liquid mixtures", Trans. AIChE, Vol. 37, pp 685-705 (1941).
11. Cichelli, M.T. and Bonilla, C.F., "Heat transfer to liquid boiling under pressure", Trans. AIChE, Vol. 41, pp 755-787 (1945).
12. Bonilla, C.F. and Eisenberg, A.A., "Heat transfer to butadiene and styrene mixtures", Ind. Eng. Chem., Vol. 40, pp 1113-1122 (1948).
13. Kirschbaum, E., Angew. Chem., Vol. 20B, pp 333-335 (1948).
14. Kirschbaun, E., Chem. Ing. Techn., Vol. 24, pp 393-400 (1952).
15. Chernobylskii, I.I. and Lukach, Yu. E., "Calculation of the heat transfer coefficient during boiling of binary mixtures", Khim. Prom., pp 362-363 (1957).
16. Chi Fang Lin, Yu Che Yand and Fan Kuo Kung, "The boiling heat transfer coefficient of binary liquid mixtures", Hua Kung Hsueh Pao, no. 2, pp 137-146 (1959).
17. Averin, Ye. K. and Kruzhilin, G.N., "Generalization of experimental data for boiling heat transfer of liquids under conditions of natural convection", Izv. Akad. Nauk. SSSR, Otdel. Tekh. Nauk., no. 10 (1955).
18. Sternling, C.V. and Tichacek, L.J., "Heat transfer coefficient for boiling mixtures - Experimental data for binary mixtures of large relative volatility", Chem. Eng. Sci., Vol. 16, pp 297-337 (1961).
19. Huber, D.A. and Hoehne, J.C., "Pool boiling of benzene, diphenyl and benzene-diphenyl mixtures under pressure", J. Heat Transfer, Vol. 85, no. 3, pp 215-220 (1963).
20. Rohsenow, W.M., "A method of correlating heat transfer data for surface boiling of liquids", Trans. ASME, Vol. 74, pp 969-975 (1952).

21. Rohsenow, W.M., "Boiling heat transfer", Modern Developments in Heat Transfer, Edited by W. Ibele, Academic Press, N.Y. (1963).
22. Gilmour, C.H., "Nucleate boiling - A correlation", Chem. Eng. Prog., Vol. 54, no. 10, pp 77-79 (1958).
23. Levy, S., "Generalised correlation of boiling heat transfer", Trans. ASME, Ser. C. J. Heat Transfer, Vol. 81, pp 37-42 (1959).
24. Tolubinskiy, V.I. and Ostrovskiy, Yu. N., "Mechanism of vapour formation and rate of heat transfer during boiling of binary solutions", Akad. Nauk, Ukr. SSSR Reshul Mezhevdom, pp 7-16 (1966).
25. Afgan, N.H., "Boiling heat transfer and burnout heat flux of ethylalcohol-benzene mixtures", 3rd International Heat Transfer Conference, Chicago Ill., Paper 98, Vol. III, pp 175-185 (12th August, 1966).
26. Fritz, W. and Ende, W., Physik Z., Vol. 36, pp 379 (1935).
27. Ivanov, O.P., "Heat transfer studies in boiling of F-12 and F-22 mixtures", Kholod. Tekhnika, Vol. 43, no. 4, pp 27-29 (1966).
28. Borishanskii, V.M., "Use of thermodynamic similarity in generalizing experimental data on heat transfer", Proceedings of the International Heat Transfer Conference, pp 975 (1962).
29. Klimenko, A.P. and Kozitskii, V.I., "Calculation of heat transfer coefficient during the boiling of light hydrocarbon mixtures", Khim. Prom. Ukr., Vol. 4, pp 32-34 (1967).
30. Filatkin, V.N., "Boiling heat transfer to water-ammonia mixtures", Problems of Heat Transfer and Hydraulics of Two-Phase Media, a Symposium edited in Russian by S.S. Kutateladze and translated by O.M. Blunn, Pergamon Press, London, pp 131-136 (1969).

31. Tolubinskiy, V.I. and Ostrovskiy, Yu. N., "Mechanism of heat transfer in boiling of binary mixtures", Heat Transfer - Soviet Research, Vol. 1, no. 6, pp 6-11 (1969).
32. Stephan, K. and Körner, M., "Calculation of heat transfer in evaporating binary liquid mixtures", Chemie - Ingenieur - Technik, Vol. 41, no. 7, pp 409-417 (1969).
33. Tolubinskii, V.I., Ostrovskii, Yu. N. and Kriveshko, A.A., "Heat transfer to boiling water-glycerine mixtures", Heat Transfer - Soviet Research, Vol. 2, no. 1, pp 22-24, Jan. (1970).
34. Takeda, H., Hayakawa, T. and Fujita, S., "Boiling heat transfer coefficients of binary liquid mixtures", Kagaku Kogaku, Vol. 34, no. 7, pp 751-757 (1970).
35. Wright, R.D., Clements, L.D., and Colver, C.P., "Nucleate and film boiling of ethane-ethylene mixtures", A.I.Ch.E. J., Vol. 17, no. 3, pp 626 (1971).
36. Borishanskii, V.M., Bobrovich, G.I., and Minchenko, F.P., "Heat transfer from a tube to water and to ethanol in nucleate pool boiling", Symposium on Problems of Heat Transfer and Hydraulics of Two-Phase Media (edited by S.S. Kutateladze), Pergamon Press, London, pp 85-107 (1969).
37. Kutateladze, S.S., "Fundamentals of heat transfer" (edited by R.D. Cess), Academic Press, New York (1963).
38. McNelly, M.J., "A correlation of rates of heat transfer to nucleate boiling liquids", Journal of the Imperial College Chem. Eng. Soc., Vol. 7, pp 18-34 (1953).
39. Clements, L.D. and Colver, C.P., "Nucleate boiling of light hydrocarbons and their mixtures", Proceedings of the Heat Transfer and Fluid Mechanics Institute (edited by Landis, R.B. and Hordemann, G.J.), Stanford University Press, pp 417-430 (1972).

40. Calus, W.F. and Rice, P., " Pool boiling - binary liquid mixtures", Chem. Eng. Sci., Vol. 27, pp 1687-1697 (1972).
41. Scriven, L.E., " On the dynamics of phase growth", Chem. Eng. Sci., Vol. 10, nos. 1/2, pp 1-13 (1959).
42. van Stralen, S.J.D., " The mechanism of nucleate boiling in pure liquids and in binary mixtures - part I", Int. J. Heat Mass Transfer, Vol. 9, pp 995-1020 (1966).
43. van Stralen, S.J.D., " The mechanism of nucleate boiling in pure liquids and in binary mixtures - Part II", Int. J. Heat Mass Transfer, Vol. 9, pp 1021-1046 (1966).
44. van Stralen, S.J.D., " The mechanism of nucleate boiling in pure liquids and in binary mixtures - Part III", Int. J. Heat Mass Transfer, Vol. 10, pp 1469-1484 (1967).
45. van Stralen, S.J.D., " The mechanism of nucleate boiling in pure liquids and in binary mixtures - Part IV (surface boiling)", Int. J. Heat Mass Transfer, Vol. 10, pp 1485-1498 (1967).
46. Rice, P. and Calus, W.F., " Pool boiling - single component liquids", Chem.Eng. Sci., Vol. 27, pp 1677-1686 (1972).
47. Isshiki, N. and Nikai, I., " Boiling of binary mixtures", Heat Transfer - Japanese Research, Vol. 1, no. 4, pp. 56-66, Oct.-Dec. (1972).
48. Tolubinskiy, V.I., Kriveshko, A.A., Ostrovskiy, Yu.N., and Pisarev, V. Ye., " Effect of pressure on the boiling heat transfer rate in water-alcohol mixtures", Heat Transfer-Soviet Research, Vol. 5, no.3, pp 66-68, May-June (1973).
49. Calus, W.F. and Leonidopoulos, D.J., " Pool boiling - binary liquid mixtures", Int. J. Heat Mass Transfer, Vol. 17, pp 249-256 (1974).
50. Tolubinskiy, V.I., Ostrovskiy, Yu.N., Pisarev, V. Ye., Kriveshko, A.A. and Konstanchuk, D.M., " Boiling heat transfer rate from a benzene-ethanol mixture as a function of pressure ", Heat Transfer - Soviet Research, Vol. 7, no. 1, pp 118-121, Jan.-Feb. (1975).

51. Ohnishi, M. and Tajima, O., " Pool boiling heat transfer to lithium bromide water solution", Heat Transfer - Jap. Research, Vol. 4(4), pp 67-77, Oct.-Dec.(1975).
52. Nishikawa, K. and Yamagata, K., " On the correlation of nucleate boiling heat transfer" , Int. J. Heat Mass Transfer, Vol. 1, pp 219-235 (1960).
53. Chashchin, I.P., Shipina, L.F., Shayb, N.S. and Sobol, A.D., " Investigation of the effect of some organic additives on heat transfer during boiling", Teploenergetika, no. 8, pp 73-74 (Aug. 1975).
54. Styushin, N.G. and Astaf'ev, V.I., " Heat transfer with the boiling of solutions", Theor. Found. Chem. Eng., Vol. 9, no.4, pp 514-519 (July-Aug 1975).
55. Kravchenko, V.A., Ostrovskiy, Yu. N. and Tolubinskaya, L.F., " Boiling heat transfer to light hydrocarbons and ethylene-ethane mixtures" , Heat Transfer - Soviet Research, Vol. 8, no. 4, pp 43-46 (July-Aug 1976).
56. Yusufova, V.D. and Chernyakhovskiy, A.I., " Heat transfer with boiling mixtures" , Heat Transfer - Soviet Research, Vol. 8, no. 4, pp 57-62 (July-Aug 1976).
57. Styushin, N.G. and Astaf'ev, V.I., " Analysis of the concentration dependence of the heat transfer coefficient in the large volume boiling of binary mixtures", Teor. Osn. Khim. Tekhnol, Vol. 12, no.6, pp 856-862 (1978).
58. Thome, J.R. and Bold, W.B., " Nucleate pool boiling in cryogenic binary mixtures" , Proc. Int. Cryog. Eng. Conf., Vol. 7, pp 523-530 (1978).
59. Happle, O. and Stephan, K., " Heat transfer from nucleate to film boiling in binary mixtures" , Fifth.Int. Heat Transfer Conf. Tokyo, Paper B7.8 , AIChE, N.Y. (1974).

60. Happle, O., "Heat transfer during boiling of binary mixtures in the nucleate and film boiling ranges", Heat Transfer in Boiling (edited by E. Hahne and U. Grigull), Hemisphere Publishing Corporation, Washington, pp 207-216 (1977).
61. Grigoryev, L.N., "Study on heat transfer during the boiling of two-component mixtures", Conf. Heat and Mass Exch. Minsk (1961).
62. von Hoffman, T., "Heat transfer in nucleate boiling of liquefied gases and their binary mixtures", Wärme Stoffübertrag Thermo Fluid Dyn., Vol. 11, no. 3, pp 189-193 (1978).
63. Stephan, K. and Preusser, P., "Heat transfer in natural convection boiling of polynary mixtures", Sixth Int. Heat Transfer Conf. Ontario, Paper PB-13, pp 187-192 (Aug 7-11, 1978).
64. Stephan, K. and Preusser, P., "Heat transfer and critical heat flux in pool boiling of binary and ternary mixtures", Ger. Chem. Eng., Vol. 2, no. 3, pp 161-169 (June 1979).
65. Stephan, K. and Preusser, P., "Heat transfer and maximum heat flux density in the vessel boiling of binary and ternary liquid mixtures", Chem. Ing. Tech., Vol. 51, no. 1, pp 37 (1979).
66. Stephan, K. and Abdelsalam, M., "Heat transfer correlations for natural convection boiling", Int. J. Heat Mass Transfer, Vol. 23, no. 1, pp 73-87 (1980).
67. Plesset, M.S. and Zwick, S.A., "A nonsteady heat diffusion problem with spherical symmetry", J. Applied Physics, Vol. 23, no. 1, pp 95-98 (January-1952).
68. Forster, H.K. and Zuber, N., "Growth of a vapour bubble in a superheated liquid", J. Applied Physics, Vol. 25, no. 4, pp 474-478 (April-1954).
69. Plesset, M.S. and Zwick, S.A., "The growth of vapour bubbles in superheated liquids", J. Applied Physics, Vol. 25, no. 4, pp 493-500 (April-1954).



70. Zwick, S.A. and Plesset, M.S., " On the dynamics of small vapour bubbles in liquids" , J. Mathematics and Physics, Vol. 33, no. 4, pp 308-330 (January-1955).
71. Griffith, P., " Bubble growth rates in boiling", Trans. ASME, pp 721-727 (April-1958).
72. Forster, K.E., " Growth of vapour-filled cavity near a heating surface and some related questions", The Physics of Fluids, Vol. 4, no. 4, pp 448-455 (April-1961).
73. Zuber, N., " Dynamics of vapour bubbles in non-uniform temperature field", Int. J. Heat Mass Transfer, Vol. 2, pp 83-98 (1961).
74. Skinner, L.A. and Bankoff, S.G., " Dynamics of vapour bubbles in spherically symmetric temperature fields of general variation", The Physics of Fluids, Vol. 7, no. 1, pp 1-6 (January-1964).
75. Nishikawa, K., Kusuda, H. and Yamasaki, K., " Growth and collapse of bubbles in nucleate boiling", Bulletin of JSME, Vol. 8, no. 30, pp 205-210 (1965).
76. Han, Chi-Yeh and Griffith, P., " The mechanism of heat transfer in nucleate pool boiling - Part I, bubble initiation, growth and departure", Int. J. Heat Mass Transfer, Vol. 8, pp 887 (1965).
77. Hamberger, L.G., " On growth and rise of individual vapour bubbles", Int. J. Heat Mass Transfer, Vol. 8, pp 1369-86 (1965).
78. Cole, R. and Shulman, H.L., " Bubble growth rate at high Jakob numbers" , Int. J. Heat Mass Transfer, Vol. 9, pp 1377-1390 (1966).
79. Kotake, S., " On mechanism of nucleate boiling" , Int. J. Heat Mass Transfer, Vol. 9, pp 711 (1966).
80. van Stralen, S.J.D., " Comments on the paper - Bubble growth rates at high Jakob numbers" , Vol. 10, pp 1908-1912 (1967).

81. Mikic, B.B. and Rohsenow, W.M., " Bubble growth rates in non-uniform temperature field", Progress Heat and Mass Transfer, Pergamon - Oxford, Vol. 2, pp 283-293 (1969).
82. Sernas, V. and Hooper, F.C., " The initial bubble growth on a heated wall during nucleate boiling", Int. J. Heat Mass Transfer, Vol. 12, pp 1627-40 (1969).
83. Akiyama, M., " Dynamics of an isolated bubble in saturated boiling (Part I - bubble growth)", Bulletin JSME, Vol. 12, pp 273-282 (1969).
84. Cooper, M.G., " The microlayer and bubble growth in nucleate pool boiling", Int. J. Heat Mass Transfer, Vol. 12, pp 915-933 (1969).
85. Akiyama, M., Tachibana, F. and Ogawa, N., " Effect of pressure on bubble growth in pool boiling", Bulletin JSME, Vol. 12, pp 1121-1128 (1969).
86. Cooper, M.G. and Vijuk, R.M., " Bubble growth in nucleate pool boiling", Proceedings of Fourth International Heat Transfer Conference, Paris-Versailles, Vol. V, B-2.1 (1970).
87. Mikic, B.B., Rohsenow, W.M. and Griffith, P., " On bubble growth rates", Int. J. Heat Mass Transfer, Vol. 13, pp 657-666 (1970).
88. Dzakowic, G.S. and Frost, W., " Vapour bubble growth in saturated pool boiling by microlayer evaporation of liquid at heated surface", Proceedings of Fourth International Heat Transfer Conference, Paris-Versailles, Vol. V, B-2.2 (1970).
89. van Ouwkerk, H.J., " The rapid growth of a vapour bubble at a liquid interface", Int. J. Heat Mass Transfer, Vol. 14, pp 1415-1432 (1971).
90. Saini, J.S., Gupta, C.P., and Lal, S., " Bubble growth in nucleate pool boiling", Proceedings of First National Heat and Mass Transfer Conference, IIT Madras, pp IX-31-38 (1971).

91. Stewart, J.K. and Cole, R., " Bubble growth rates during nucleate boiling at high Jakob numbers", Int. J. Heat Mass Transfer, Vol. 15, pp 655-663 (1972).
92. van Stralen, S.J.D., Cole, R., Sluyter, W.M. and Sohal, M.S., " Bubble growth rates in nucleate boiling of water at subatmospheric pressures", Int. J. Heat Mass Transfer, Vol. 18, pp 655-669 (1975).
93. Saini, J.S., " Studies of bubble growth and departure in nucleate pool boiling" , Ph.D. Thesis, Department of Mechanical and Industrial Engineering, University of Roorkee, Roorkee (May 1975).
94. Nishikawa, K., Fujita, Y., Nawata, Y. and Nishijama, T., " Studies on nucleate pool boiling at low pressures", Heat Transfer - Jap. Research, Vol. 5, no. 2, pp 66-89 (April-June 1976).
95. Kutateladze, S.S., " Boiling and bubbling heat transfer under free convection of liquid" , Int. J. Heat Mass Transfer, Vol. 22, no. 2, pp 281-299 (1979).
96. Vos, A.S. and van Stralen, S.J.D., " Heat transfer to boiling water-methylethylketone mixtures" , Chem. Eng. Sci., Vol. 5, pp 50-56 (1956).
97. van Wijk, W.R., Vos, A.S. and van Stralen, S.J.D., " Heat transfer to boiling binary liquid mixtures" , Chem. Eng. Sci., Vol. 5, pp 68-80 (1956).
98. van Stralen, S.J.D., " Heat transfer to boiling binary liquid mixtures at atmospheric and subatmospheric pressures" , Chem. Eng. Sci., Vol.5, pp 290-296 (1956).
99. Bruijn, P.J., " On the asymptotic growth rate of vapour bubbles in superheated binary liquid mixtures", Physica, 's Grav., Vol. 26, pp 326-334 (1960).
100. Grigoryev, L.N., " Heat transfer in boiling of two component mixtures" , Teplo-i-Massoperenos (Symposium, Heat and Mass Transfer), Vol. 2, pp 120-127 (1962).

101. Steronkin, A.B., "On conclusions and limitations of the Vrevskii principle, work on theory of solutions", Izdalap'sko AN SSSR (1953).
102. Yatabe, J.M. and Westwater, J.W., "Bubble growth rates for ethanol-water and ethanol-isopropanol mixtures", Chem. Eng. Prog. Symp. Ser., Vol. 62, no. 64, pp 17-23 (1966).
103. Tolubinskiy, V.I. and Ostrovskiy, J.N., "On the mechanism of boiling heat transfer (vapour bubble growth rates in the process of boiling of liquids, solutions and binary mixtures)", Int. J. Heat Mass Transfer, Vol. 9, pp 1463-1470 (1966).
104. Hatton, A.P. and Hall, I.S., "Photographic study of boiling on prepared surfaces", 3rd International Heat Transfer Conference Chicago, Ill. Paper 115, Vol. IV, pp 24-37 (7-12th August 1966).
105. Rehm, T.H., "Bubble growth parameters in saturated and subcooled nucleate boiling", Chem. Eng. Prog. Symp. Ser., Vol. 62, no. 82, pp 88-94 (1968).
106. van Stralen, S.J.D., "The growth rate of vapour bubbles in superheated pure liquids and binary mixtures - Part I", Int. J. Heat Mass Transfer, Vol. 11, pp 1467-1490 (1968).
107. van Stralen, S.J.D., "The growth rate of vapour bubbles in superheated pure liquids and binary mixtures - Part II", Int. J. Heat Mass Transfer, Vol. 11, pp 1491-1512 (1968).
108. van Ouwkerk, H.J., "Hemispherical bubble growth in binary mixture", Chem. Eng. Sci., Vol. 27, no. 11, pp 1957-1967 (Nov. 1972).
109. van Stralen, S.J.D., Sohal, M.S., Cole, R., and Sluyter, W.M., "Bubble growth rates in pure and binary systems : combined effect of relaxation and evaporation microlayers", Int. J. Heat Mass Transfer, Vol. 18, pp 453-467 (1975).
110. Tolubinskiy, V.I., "Computation of average growth rate of vapour bubbles", Heat Transfer-Soviet Research, Vol. 7, no. 3, pp 77-83 (1975).

111. van Stralen, S.J.D., Sluyter, W.M. and Cole, R., "Bubble growth rates in nucleate boiling of aqueous binary systems at subatmospheric pressures", Int. J. Heat Mass Transfer, Vol. 19, no. 8, pp 931-941 (1976).
112. Shock, R.A.W., "Nucleate boiling in binary mixtures", Int. J. Heat Mass Transfer, Vol. 20, no.6, pp 701-709 (1977).
113. Shock, R.A.W., "The evaporation of binary mixtures in forced convection", AERE Report No. R7593 (1973).
114. Zijl, W., Moalem, D., van Stralen, S.J.D., "Inertia and diffusion controlled bubble growth and implosion in initially uniform pure and binary systems", Letters in Heat Mass Transfer, Vol. 4, no. 5, pp 331-339 (1977).
115. Zijl, W., Ramakers, F.J.M., van Stralen, S.J.D., "Global numerical solutions of growth and departure of a vapour bubble at a horizontal superheated wall in a pure liquid and a binary mixture", Int. J. Heat Mass Transfer, Vol. 22, pp 401-420 (1979).
116. Pinnes, E.L. and Mueller, W.K., "Homogeneous vapour nucleation and superheat limits of liquid mixtures", Trans. ASME, Journal of Heat Transfer, Vol. 101, pp 617 (Nov. 1979).
117. Scarborough, J.B., "Numerical Mathematical Analysis", Sixth Edition, Oxford and IBH Publishing Company, Calcutta (1966).
118. Wiebe, J.R. and Judd, R.L., "Superheat layer thickness measurements in saturated and subcooled nucleate boiling", Trans. ASME, Ser. C., J. Heat Transfer, pp 455-461 (November 1971).
119. "International Critical Tables", Vol. 7, McGraw Hill Book Company Inc. N.Y. (1928).
120. Nishikawa, K. and Urakawa, K., "An experiment of nucleate boiling under reduced pressure", Memoirs of the Faculty of Engineering, Kyushu University, Vol. 19, no. 3, pp 63-71 (1960).
121. Mikheyev, M., "Fundamentals of Heat Transfer", Mir Publishers, Moscow (1968).

122. Gaertner, R.F. and Westwater, J.W., "Population of active sites in nucleate boiling heat transfer", Chem. Eng. Prog. Symp. Ser., Vol. 56, no. 30, pp 39-48 (1960).
123. Sharma, P.R. and Varshney, B.S., "Determination of the frequency of bubble emission from a submerged heating surface to a pool of saturated liquid under subatmospheric pressure", Indian Journal of Technology, Vol. 17, pp 407-409 (November 1979).
124. Körner, W. and Photiadis, G., "Pool boiling heat transfer and bubble growth on surfaces with artificial cavities for bubble generation", Heat Transfer in Boiling, Edited by E. Hahne and U. Grigull, Hemisphere Publishing Corporation, London, pp 77-84 (1977).
125. Raben, I.A., Beaubouef, R.T. and Commerford, G.E., "A study of heat transfer in nucleate pool boiling of water at low pressure" Chem. Eng. Prog. Symp. Ser., Vol. 61, no. 57, pp 249-257(1965).
126. Alam, S.S. and Varshney, B.S., "Pool boiling of liquid mixtures", Proceedings of II National Heat and Mass Transfer Conference, Indian Institute of Technology, Kanpur, Paper No. B-6, pp 13-15 (December 1973).
127. Vargaftik, N.B., "Handbook on Physical Properties of Gases and liquids", Gasudarstvenae Isdalelstvo Physico-Matematicheskoe Literaturee, Moskava(1963).
128. Perry, J.H., "Chemical Engineers' Hand Book", Fifth Edition, McGraw-Hill Book Company Inc. (1973).
129. "International Critical Tables", Vol. 3, McGraw-Hill Book Company Inc., N.Y. (1928).
130. "International Critical Tables", Vol. 4, McGraw-Hill Book Company Inc., N.Y. (1928).
131. "International Critical Tables", Vol. 5, McGraw-Hill Book Company Inc., N.Y. (1928).
132. Hatch, L.F., "Isopropyl Alcohol", McGraw-Hill Book Company Inc., N.Y. (1961).
133. "CRC Handbook of Chemistry and Physics", 60th Edition, CRC Press Inc. Boca Raton, Florida (1980-81).

134. Chandrasekaran, K.D. and Venkateswarlu, D, " SI Units in Chemical Engineering and Technology", Chemical Engineering Education Development Centre, IIT, Madras (1979).
135. Prausnitz, J.M., " Molecular Thermodynamics of Fluid-Phase Equilibria", Chapter 5, Prentice-Hall, Englewood Cliffs, N.J. (1969).
136. Reid, R.C., Prausnitz, J.M., and Sherwood, T.K., " The properties of Gases and Liquids", Third Edition, McGraw Hill Book Co., N.Y.(1977).
137. Tamura, M., Kurata, M., and Odani, H., " Practical method for estimating surface tensions of solutions", Bull. Chem. Soc. Japan, Vol. 28, no.1, pp 83-88 (1955).
138. Hirata, M., Ohe, S. and Nagahama K., " Computer Aided Data Book of Vapour-Liquid Equilibria", Kodansha Limited Elsevier Scientific Publishing Co. N.Y. (1975).
139. Othmer, D.F. and Benenati, R.F., " Composition of vapours from boiling binary solutions", I and EC, Vol. 37, No.3, pp 299-303 (1945).
140. Davaloo, P., " Vapour-liquid equilibrium data on isopropanol-water binary system", Iranian J. Sci. and Tech., Vol. 1, No.3, pp 279-295 (December 1971).
141. Topping, J., " Errors of observation and their treatment", Chapman and Hall Ltd. London (1978).

